

**Crosstalk between cytoskeleton and
membrane components with thermosensitive
ion channels in the context of diverse
physiological functions**

**By
Somdatta Saha
LIFE11201404011
National Institute of Science Education and Research, Bhubaneswar**

*A thesis submitted to the
Board of Studies in Life Sciences
In partial fulfillment of requirements for the Degree of
DOCTOR OF PHILOSOPHY
of
HOMI BHABHA NATIONAL INSTITUTE*



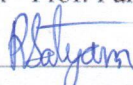
March, 2020

Homi Bhabha National Institute

Recommendations of the Viva Voce Committee

As members of the Viva Voce Committee, we certify that we have read the dissertation prepared by Ms. Somdatta Saha entitled "Crosstalk between cytoskeleton and membrane components with thermosensitive ion channels in the context of diverse physiological functions" and recommend that it may be accepted as fulfilling the thesis requirement for the award of Degree of Doctor of Philosophy.

Chairman - Prof. Parlapalli Venkata Satyam



Date:

28/7/2020

Guide / Convener - Dr. Chandan Goswami



Date:

28/07/2020

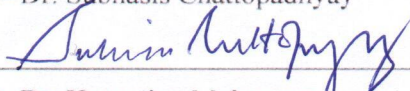
Examiner - Prof. Amitabha Chattopadhyay



Date:

28/07/2020

Member 1- Dr. Subhasis Chattopadhyay



Date:

28/07/2020

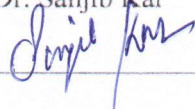
Member 2- Dr. Harapriya Mohapatra



Date:

28.07.2020

Member 3- Dr. Sanjib Kar



Date:

28.07.2020

Final approval and acceptance of this thesis is contingent upon the candidate's submission of the final copies of the thesis to HBNI.

I/We hereby certify that I/we have read this thesis prepared under my/our direction and recommend that it may be accepted as fulfilling the thesis requirement.

Date: 28/7/2020

Place: NISER, Jatni



Dr. Chandan Goswami

(Thesis Supervisor)

STATEMENT BY AUTHOR

This dissertation has been submitted in partial fulfillment of requirements for an advanced degree at Homi Bhabha National Institute (HBNI) and is deposited in the Library to be made available to borrowers under rules of the HBNI.

Brief quotations from this dissertation are allowable without special permission, provided that accurate acknowledgement of source is made. Requests for permission for extended quotation from or reproduction of this manuscript in whole or in part may be granted by the Competent Authority of HBNI when in his or her judgment the proposed use of the material is in the interests of scholarship. In all other instances, however, permission must be obtained from the author.

Somdatta Saha
Somdatta Saha

DECLARATION

I, hereby declare that the investigation presented in the thesis has been carried out by me.

The work is original and has not been submitted earlier as a whole or in part for a degree

/ diploma at this or any other Institution / University.

Somdatta Saha

Somdatta Saha

List of Publications arising from the thesis

1. TRPA1 is selected as a semi-conserved channel during vertebrate evolution due to its involvement in spermatogenesis, **Saha S**, Sucharita S, Majhi RK, Tiwari A, Ghosh A, Pradhan SK, Patra BK, Dash RR, Nayak RN, Giri SC, Routray P, Kumar A, Kumar G P, Goswami C, *Biochem Biophys Res Commun.*, 2019; 512 (2): 295-302.
2. Preferential selection of Arginine at the lipid-water-interface of TRPV1 during vertebrate evolution correlates with its snorkeling behaviour and cholesterol interaction, **Saha S**, Ghosh A, Tiwari N, Kumar A, Kumar A, Goswami C, *Scientific Reports*, 2017, 7: Article number:16808, Pages 1-21.

Other Publications

1. Transient receptor potential ankyrin1 channel is endogenously expressed in T cells and is involved in immune functions, Sahoo SS, Majhi RK, Tiwari A, Acharya T, Kumar PS, **Saha S**, Kumar A, Goswami C, Chattopadhyay S, *Bioscience Reports*, 2019, 39 (9): 1-16.
2. Plant and natural products as modulators of TRP channels, Yadav M, **Saha S**, Kumar A, Goswami C, *Biological Research and Reviews*, 2019, 1: 1-13.
3. Expression of temperature-sensitive ion channel TRPM8 in sperm cells correlates with vertebrate evolution, Majhi RK, **Saha S**, Kumar A, Ghosh A, Swain N, Goswami L, Mohapatra PP, Maity A, Sahoo V, Kumar A, Goswami C, *PeerJ*, 2015, 3: e1310, Pages 1-31.

Conference, Symposium and workshop attended

*Participated in “**International Symposium on Neuropeptide and Neurotransmitters: Role in Physiology and Pathophysiology**” held at NISER, Bhubaneswar during December 13-14,2015 and presented poster in it entitled “**Exploring the effect of N-Arachidonoyl Dopamine on TRPV1 expressing peripheral neurons and non-neuronal cells**”.

*Participated in “**Advanced Microscopy and Imaging Techniques**” held at NISER, Bhubaneswar from 4th-6th August 2016

*Participated in “**2nd meeting of Indian Immunological Society Odisha Chapter**” held in NISER, Bhubaneswar on 6th January 2017

*Participated in “**Symposium on Recent Advancement On Neuroscience**” held in NISER, Bhubaneswar on October 28th 2017

*Participated in “**Zeiss Workshop on High-End Wide-field, Confocal and SR Imaging**” organized in NISER, Bhubaneswar from November 30th-1 December 2017

*Participated in “**International Congress of Cell Biology 2018**” organised by CCMB Hyderabad from 27th-31st January 2018 and presented poster in it entitled “**Importance of Arginine residues in TRPV1 functions**”.

Somdatta Saha

Somdatta Saha

Dedicated to...

My parents

ACKNOWLEDGEMENTS

Foremost, I would like to express my gratitude to my thesis supervisor Dr. Chandan Goswami for his unprecedented support, guidance and patience. This work would have been seemingly difficult without his cooperation.

Besides my advisor, I would also like to thank my doctoral committee members Prof. P.V. Satyam (IOP, Bhubaneswar), Dr. Harapriya Mohapatra (NISER, Bhubaneswar), Dr. Subhasis Chattopadhyay (NISER, Bhubaneswar) and Dr. Sanjib Kar (NISER, Bhubaneswar) for their valuable suggestions and feedback regarding my thesis. I acknowledge the staffs, faculties and Central Instrumentation Facility of School of Biological Sciences.

This work would not have been possible without the aid of collaborative scientists who had sent constructs and helped us with samples and services. In this regard I would like to thank Dr. Soenke Cordeiro (Institute of Physiology, Christian-Albrechts-Universität zu Kiel) for providing Rat TRPV1-WT-FL in pBF1 vector, Dr. David Julius (University of California, San Francisco) for providing Human TRPA1-FL in pMO vector, Dr. Bao-Liang Song for providing Flotillin-1-RFP construct, Dr. Abhishek Kumar [German Cancer Research Center (DKFZ), Heidelberg, Germany] for his immense guidance and help in Bioinformatics.

I would also like to thank Dr. Apratim Maity (West Bengal University of Animal & Fishery Sciences) for providing bull sperm samples, Dr. S.C. Giri (Central Avian Research Institute, Bhubaneswar) for avian sperm samples, Dr. PC Routray and Dr. Asish Saha (Central Institute of Freshwater Aquaculture, Bhubaneswar) for fish sperm samples, Dr. R.C. Behera (Frozen Semen Bank, Cuttack) for bull sperm samples. I am also grateful to Prof. Ferdinand Hucho (FU, Berlin) for sharing various cell lines like F-11, SaoS and

HaCaT. I am highly obliged to all the funding agencies like DAE, ICMR, DST and DBT for all the financial assistance during this entire tenure.

My sincere thanks to all my present and past fellow lab members, namely, Dr. Ashutosh Kumar, Dr. Manoj Yadav, Dr. Rakesh Kumar Majhi, Dr. Ankit Tiwari, Dr. Pushpendu Sardar, Nirlipta Di, Divyanshi, Nikhil, Vivek, Arijit, Samikshya, Subhadra, Rashmita, Sushama, Ramprasad, Tusar, Nishant, Aniket and Ritesh and all other lab mates.

Apart from my lab members, I would like to extend my gratitude towards Dr. Charles Antony and my roommate Dr. Bushra Hayat for their endless help and support.

The motivation and encouragement provided by my mother has been the biggest strength in this journey and that provided an impetus to strive for more. I also thank our caretaker Bharati mashi for relieving me from all my familial responsibilities and allowing me to focus on my academics only. Last but not the least I would like to thank my husband Dr. Chinmoy Ghosh for his support.

I would also like to thank my thesis reviewer's Prof. Dr. Ferdinand Hucho (Freie Universität Berlin, Institut für Chemie und Biochemie), Prof. M. K. Mathew (National Centre for Biological Sciences, Bangalore) and Prof. Amitabha Chattopadhyay (Centre for Cellular & Molecular Biology, Hyderabad, India) for their critical evaluation and suggestions which have helped me enrich my thesis.

Contents

	Page number
Summary	i-ii
List of figures	iii-vi
List of tables	vii-viii
List of Abbreviations	ix-xi
Chapter 1: Introduction	
1.1. General Introduction to TRP channels	
1.1.1. Brief history of ion channels	3-6
1.1.2. Discovery of TRP channels	6-8
1.1.3. Classification of TRP channel superfamily	8-9
1.1.4. Tissue specified distribution and function of different vertebrate TRP channels	10-12
1.1.5. General architecture of TRP channels	12-15
1.2. Regulators of TRP channels	
1.2.1. Phosphoinositides	15-19
1.2.2. Post-translational modifications	19-22
1.2.3. Cytoskeletal components	23-25
1.2.4. Lipids	25-28
1.2.5. Plant and natural products	28-33
1.2.6. Animal toxins	33-34
1.2.7. Synthetic modulators	34-35
1.2.8. pH	36-37
1.2.9. Mechanical stress	37-39

1.2.10. Temperature	39-40
1.2.11. Ca ²⁺	40-43
1.3. TRP channels and disease	43-44
1.4. Specific introduction to TRPV1	
1.4.1. TRPV1 structure	45-47
1.4.2. TRPV1 expression	47-48
1.4.3. Cellular functions of TRPV1	48-49
1.4.4. Physiological functions of TRPV1	49-50
1.4.5. Regulation of TRPV1 by microtubules	50-51
1.4.6. Regulation of TRPV1 by cholesterol	52
1.5. Specific introduction to TRPA1	
1.5.1. TRPA1 structure	53-55
1.5.2. TRPA1 expression	56
1.5.3. Cellular functions of TRPA1	57-58
1.5.4. Physiological functions of TRPA1	58-59
1.5.5. Regulation of TRPA1 by cholesterol	59-60
1.6. Specific objectives of this study	60-61

Chapter 2: Results

2.1. Importance of TRPV1-tubulin complex in channel localization and cellular functions

2.1.1. TRPV1-TBS1-Ct mutants retain interaction with tubulin dimers in presence as well as absence of Ca ²⁺	66-73
2.1.2. TRPV1-TBS1-Hexamutant retain interaction with polymerized microtubules in presence as well as absence of Ca ²⁺	74-75

2.1.3. TRPV1-TBS1-Hexamutant takes subtly longer time to form high molecular weight complexes with tubulin dimer in presence of chemical cross-linker	75-77
2.1.4. TRPV1-TBS1 point mutants as well as TRPV1-TBS1-Hexamutant exhibit defects in membrane localization	77-81
2.1.5. TRPV1-TBS1-Hexamutant forms a defective channel that is insensitive to Capsaicin-induced Ca ²⁺ influx	82-85
2.1.6. TRPV1-TBS1-Hexamutant exhibits lack of surface expression	85-86

2.2. Importance of TRPV1-cholesterol complex in channel localization and cellular functions

2.2.1. Determination of the lipid-water interface amino acids of TRPV1	88
2.2.2. Amino acids present in the lipid-water interface are highly conserved	88-89
2.2.3. Amino acids present at the inner leaflet evolved under more stringent selection pressure	89-90
2.2.4. The LWI-residues have undergone different selection pressure throughout vertebrate evolution due to N- and C-terminal peptide directionality	90
2.2.5. Arg and Tyr residues are preferred in the LWI of TRPV1	91-94
2.2.6. Identification of possible cholesterol-recognition motifs within TRPV1	95-96
2.2.7. Cholesterol interacts with TRPV1 in closed conformation through highly conserved Arg 557 and Arg 575 residues	97
2.2.8. Arg557 and Arg575 of TRPV1 are essential for interaction with cholesterol in closed conformation	97-101
2.2.9. Substitution of Arg557 and Arg575 by any other amino acid alters localization of TRPV1 and presence in lipid raft	101-106

2.2.10. Analysis of molecular selection and exclusion of amino acids in the lipid-water interface regions of TRPV1 throughout vertebrate evolution	106-110
2.2.11. Changes in the Arg and/or Tyr content in the LWI of TRPV1 during Piscean to mammal evolution correlates with increasing cholesterol content and increased body temperature	110-113
2.2.12. Ratio of positive-negative amino acids in the inner LWI region remain constant in TRPV1 through-out the vertebrate evolution	113-115
2.2.13. TRPV1 retains unique combination of hydrophobic and hydrophilic amino acids in its inner lipid-water interface	115-116
2.2.14. Arg575Asp induced cellular morphology impairment can be rescued by maintaining overall positive-negative charge ratio	116-117
2.2.15. TRPV1-Arg575Asp exhibits impaired surface expression that is partly rescued by TRPV1-Arg575Asp-Asp576Arg	117-122
2.2.16. Alteration in cellular phenotype due to TRPV1-Arg575Asp can be partly rescued by long-term channel inhibition	122-123
2.2.17. TRPV1-Arg575Asp forms a Capsaicin-insensitive channel that is rescued by Arg575Asp-Asp576Arg	123-124
2.2.18. TRPV1-Arg575Asp-Asp576Arg exhibits delayed response to Capsaicin activation upon depletion of Ca ²⁺ from intracellular stores	124-128

2.3. Expression of TRPA1 in vertebrate sperm cells, its function and interaction with microtubule cytoskeleton

2.3.1. TRPA1 remain as a semi conserved protein throughout vertebrate evolution	130
2.3.2. TRPA1 syntenic locus is highly conserved in vertebrates	130-134

2.3.3. Genes retained in TRPA1-synteny are diverged in nature	134
2.3.4. TRPA1 domains and motifs are highly diverged	135
2.3.5. TRPA1 expression in mature sperm is conserved throughout vertebrate evolution	135
2.3.6. TRPA1 modulation does not alter average values of motility parameters in bull sperm	136
2.3.7. TRPA1 activation induces hyperactivation in bull sperm	136-137
2.3.8. TRPA1 doesn't affect capacitation or acrosomal reaction in bull sperm	137-139
2.3.9. TRPA1 activation or inhibition increases variability in different parameters	140
2.3.10. Localization of TRPA1 with different modified tubulin in bull sperm cells	140-145

2.4. Molecular evolution of TRPA1 during vertebrate evolution and importance of TRPA1-cholesterol complex in channel localization

2.4.1. Determination of LWI stretches in Human TRPA1 and their conservation across vertebrate evolution	148
2.4.2. Amino acids demarcating TRPA1 LWI are partially conserved	149-150
2.4.3. Frequency of occurrence of different amino acids at the LWI regions across different vertebrate phylum's in TRPA1	150-153
2.4.4. Analysis of hydrophilic, hydrophobic, positive and negatively charged residues at TRPA1 LWI across vertebrate evolution	153-154
2.4.5. TRPA1 has fairly conserved CRAC and CARC motifs	154
2.4.6. Human TRPA1 forms H-bond with cholesterol	154-156
2.4.7. Human TRPA1 localizes in lipid rafts	157

Chapter 3: Discussion

3.1. Molecular evolution of TRP channels

3.1.1. Molecular evolution of TRPV1	162
3.1.2. Critical residues involved in chemical and thermal sensitivity of TRPV1	162-163
3.1.3. TRPV1 channel gating by various components	164-165
3.1.4. Importance of membrane lipid, cytoskeleton and ion channel interaction	166

3.2. TRPV1-cholesterol interaction

3.2.1. The specific micro environment at the LWI and behaviour of Transmembrane proteins	166-169
3.2.2. Selection of amino acids at the LWI of transmembrane proteins	170-172
3.2.3. Importance of cholesterol at the LWI-regions	173-175
3.2.4. Possible importance of Arg-cholesterol interaction in channel activity of TRPV1	175-178
3.2.5. What we learn from the frequency calculation: importance of certain amino acids in channel functions	178-181
3.2.6. Importance of maintenance of ratio of positive-negative and hydrophobic-hydrophilic amino acids at inner LWI of TRPV1	182-183
3.2.7. Does Arg575Asp mutation makes it as a constitutive open ion channel	183-188

3.3. Regulation of TRP channels by microtubules 188

3.3.1. Importance of TRPV1-Microtubule interaction in channel functioning	189-196
---	---------

3.4. Molecular evolution of TRPA1 196-200

3.5. Chemical sensitivity of TRPA1 200

3.6. TRPA1 channel gating 200-201

3.7. Role of TRPA1 in sperm functions and impact on reproductive fitness 201-203

3.8. Regulation of TRPA1 by tubulin/microtubules 203-205

3.9. TRPA1-cholesterol crosstalk: implication in biological systems	205-206
3.10. TRPA1, its mutants, genetic variants and diseases	206-208
Chapter 4: Conclusion	
Future prospects and conclusion	211-212
Chapter 5: Materials and Methods	
5.1 Materials	
5.1.1. Reagents used	215-216
5.1.2. Kits, markers and enzymes	217
5.1.3. Cell lines and sperm samples	217
5.1.4. Bacterial strains	218
5.1.5. Primary antibodies	218
5.1.6. Secondary antibodies	218-219
5.1.7. Constructs used	219-221
5.2. Methods	
5.2.1. Molecular biology techniques	
5.2.1.1. Polymerase Chain Reaction (PCR)	221
5.2.1.2. Site-directed mutagenesis and construct preparation	221-225
5.2.1.3. Agarose gel electrophoresis	226
5.2.1.4. Restriction digestion	227
5.2.1.5. Ligation of insert and vector	227
5.2.1.6. Transformation	227-228
5.2.1.7. Competent cell preparation by RbCl method	228-229
5.2.1.8. Instant screening	229-230
5.2.2. Biochemical techniques	
5.2.2.1. SDS-PAGE	230-232

5.2.2.2. Coomassie staining	232
5.2.2.3. Western blot analysis	232-233
5.2.2.4. Protein expression	234
5.2.2.5. Isolation of MBP-tagged proteins	235
5.2.2.6. Protein quantification by Bradford estimation	235
5.2.2.7. Pull-down assay	235-236
5.2.2.8. Co-sedimentation assay	236-237
5.2.2.9. Cross-linking assay	237-238
5.2.2.10. Tubulin purification	238-239
5.2.3. Cell biology techniques	
5.2.3.1. Cell culture and transfection	239-240
5.2.3.2. Imaging and image analysis	240-241
5.2.3.3. Estimation of cellular dimensions of transfected F-11 cells	241-242
5.2.3.4. Ca ²⁺ -sensor based imaging	242
5.2.3.5. Quantification of Ca ²⁺ -imaging	243
5.2.3.6. Immunocytochemistry for F-11 cells	243-244
5.2.4. Sperm cell techniques	
5.2.4.1. Collection and isolation of sperm cells	244-245
5.2.4.2. Computer Assisted Sperm Analysis (CASA)	245-246
5.2.4.3. Immunofluorescence analysis and microscopy for sperm cells	246-247
5.2.5. <i>In silico</i> techniques	
5.2.5.1. Sequence retrieval, alignment and structure retrieval for TRPA1 and TRPV1	247
5.2.5.2. Embedding the TRPV1 structures in PEA or POPC membrane and determining the LWI residues	247-248

5.2.5.3. Membrane representation and SeqLogo generation for TRPV1 and TRPA1	248
5.2.5.4. Boxplot of TRPA1 and TRPV1	248-250
5.2.5.5. Statistical tests for TRPA1 and TRPV1	250
5.2.5.6. Identification of CRAC, CARC and CCM motifs for TRPA1 and TRPV1	250-251
5.2.5.7. Docking of cholesterol on closed and open structures of rTRPV1 and hTRPA1	251
5.2.5.8. Structural alignment and mutation of Arg residues in TRPV1	251-252
5.2.5.9. Frequency calculation of different amino acids at the lipid water interface of both TRPV1 and TRPA1	252
5.2.5.10. Construction of the phylogenetic tree for TRPA1	252-253
5.2.5.11. Calculation of evolutionary time for TRPA1	253
Chapter 6: Bibliography	255-283
Annexure	
Annexure 1. List of TRPV1 sequences used	286-287
Annexure 2. List of TRPA1 sequences used	287-288
Annexure 3. Schematic representation of constructs prepared in this study	288
Annexure 4. Enrichment of different snorkeling amino acids in Lipid Water Interface region of other ion channels	289
Annexure 5. Boxplot and sequence logo of lipid water interface region amino acids present in different ion channels	290

SUMMARY

Ion channels regulate various cellular events ranging from volume homeostasis to signal transduction pathways that involve influx of ions across the plasma membrane. Amongst them, the Transient Receptor Potential (TRP) family of non-selective cation channels are important and these channels are involved in the execution of a large number of cellular processes. TRP channels comprise of an intracellular N- and C-terminus, six transmembrane helices interconnected by flexible loops. Functional TRP channels are made of homo-tetramers and the functional pore region is made of 5th and 6th transmembrane region. These channels are activated by various physical and chemical stimuli, intracellular as well as extracellular ligands, temperature changes, etc. TRP channels not only play crucial roles in the regulation of cellular signalling, but also regulate the cytoskeletal dynamics and organizations and thereby cellular functions. In addition, subtle changes in the cytoskeletal dynamics can induce gross changes in the cellular morphology and specific cellular structures that are crucial for cellular functions. Eukaryotic cell membranes are heterogeneous in nature and contain microdomains that are enriched in certain specific type of glycosphingolipids, gangliosides and sterols such as cholesterol. These regions are referred to as membrane/lipid rafts (MLRs). These regions act as scaffold for a large number of molecules like signalling receptors and ion channels and hence enable transmission of extracellular information to the intracellular milieu. Often such lipid-rafts are physically and functionally associated with sub-membranous cytoskeleton. Thus, the plasma membrane lipids and submembranous cytoskeleton play an integral role in ion channel structure-function relationship.

This study is primarily focused on the cross-talk between membranous cholesterol and sub-membranous cytoskeleton with two thermosensitive ion channels, namely

TRPV1 and TRPA1 and possible involvement of such crosstalk in the gating behaviour of these channels.

Key findings from this work:

1) TRPV1-microtubule interaction ensures proper gating of the channel. Abolishing this interaction results in channel closure even in presence of prolonged exposure to various activation stimuli. Alteration of microtubule dynamics also alters the Ca^{2+} -influx through TRPV1. Thus, interaction of TRPV1 with microtubules in a dynamic equilibrium with tubulin dimers ensures normal gating of the channel in response to its specific agonists.

2) Specific amino acids are selected at the Lipid Water Interface (LWI) regions of TRPV1 that regulates its thermosensitive behaviour and mediates its interaction with specific membrane components such as cholesterol. Interaction of TRPV1 with cholesterol tends to keep it in a closed conformation and prevents spontaneous opening.

3) Activation of TRPA1 induces hyperactive motility in bovine sperm but it doesn't affect acrosomal reaction or capacitation. Its co-localization with tyrosinated tubulin in sperm tail further strengthens the possibility of this interaction in inducing hyperactivated motion in sperm.

4) The LWI of TRPA1 contains amino acids that have undergone significant changes in course of vertebrate evolution in order to adapt with its ever changing functions in different organisms of the vertebrate phyla. Docking results have identified two residues that mediate its interaction with cholesterol. Overexpression studies have shown that TRPA1 localizes in lipid rafts.

<u>List of Figures:</u>	Page number
1. Classification of TRP channels	9
2. General structure of all TRP channel members	14
3. Different plant products that modulate TRP channel activity	30
4. Structural details of Rat TRPV1 as revealed by Cryo EM at 3.4 Å resolution	46
5. Dual gate mechanism of TRPV1 activation by its specific agonists	46
6. Structural details of Human TRPA1 as revealed by Cryo EM at ~4 Å resolution	55
7. Tubulin pull down by TRPV1-Lys710Ala with tubulin dimers in presence and absence of Ca ²⁺	67
8. Tubulin pull down by TRPV1-Lys714Ala with tubulin dimers in presence and absence of Ca ²⁺	68
9. Tubulin pull down by TRPV1-Arg717Ala with tubulin dimers in presence and absence of Ca ²⁺	69
10. Tubulin pull down by TRPV1-Lys718Ala with tubulin dimers in presence and absence of Ca ²⁺	70
11. Tubulin pull down by TRPV1-Arg721Ala with tubulin dimers in presence and absence of Ca ²⁺	71
12. Tubulin pull down by TRPV1-Lys724Ala with tubulin dimers in presence and absence of Ca ²⁺	72
13. Tubulin pull down by TRPV1-TBS1-Hexamutant with tubulin dimers in presence and absence of Ca ²⁺	73
14. Co-sedimentation of TRPV1-WT and V1-TBS1-Hexamutant with polymerised microtubules in presence and absence of Ca ²⁺	74
15. Cross-linking of TRPV1-WT and TRPV1-TBS1-Hexamutant with tubulin dimers in presence of chemical cross-linker DMS	76
16. Lack of membrane localization by TRPV1-TBS1 mutants	78-81
17. Substitution of positive charges to neutral in TBS1 region results in Capsaicin-insensitive TRPV1	83-85
18. TRPV1-TBS1-Hexamutant exhibits lack of surface expression	85
19. Preferential selection of snorkeling amino acids located at the lipid-water interface of TRPV1 during vertebrate evolution	93
20. Arg and Tyr residues are enriched in the lipid-water interface of	

rTRPV1 and are preferentially selected in the lipid-water interface region	94
21. TRPV1 has conserved cholesterol-binding sequences at the lipid-water interface region	95
22. Cholesterol intercalates between CCM motif formed by TM1 and TM2 of TRPV1	96
23. The conserved cholesterol-binding motifs present in TRPV1 interacts with cholesterol through Arg557 and/or Arg575 residues in closed conformation	98
24. Closed- but not the open-conformation of TRPV1 interacts with cholesterol	99
25. Arg residues at 557th and 575th position of TRPV1 are essential for interaction with cholesterol	100
26. Arg residues at the Lipid-Water-Interface (LWI) are required for proper surface expression and membrane localization	102
27. TRPV1-WT but not the LWI mutants co-localize with endogenous lipid raft marker	103
28. TRPV1-WT but not the Lipid Water Interface (LWI) mutants co-localize with overexpressed lipid raft marker Flotillin1	104
29. TRPV1-WT but not the Lipid Water Interface (LWI) mutants co-localize with overexpressed lipid raft marker Caveolin1	105
30. “Frequency-of-occurrence” analysis for different amino acids at the Lipid-Water-Interface (LWI) of TRPV1 in different phylogenetic groups	108-109
31. Frequency of snorkeling residues present in the lipid water interface of TRPV1 share inverse relationship with body temperature and average cholesterol level throughout the vertebrate evolution	112
32. Ratio of positive/negative amino acids remain constant at the inner Lipid-Water-Interface of TRPV1	114
33. Ratio of hydrophobic/hydrophilic amino acids remain constant at the inner Lipid-Water-Interface of TRPV1	115
34. Localization of Bid- DsRed2 in TRPV1-WT and TRPV1 LWI mutants	118
35. Change in cellular morphology due to Arg575Asp mutation can be rescued by introducing another mutation	119
36. Localization of TRPV1-Arg575Asp Asp576Arg-GFP in F-11 cells and its co-localization with different lipid raft markers	120
37. TRPV1-Arg575Asp induced changes in cellular morphology in SaOS and	

HaCaT cell lines can be restored by TRPV1-Arg575Asp-Asp576Arg	121
38. TRPV1-Arg575Asp shows lack of surface expression that is partly rescued by TRPV1-Arg575Asp-Asp576Arg	122
39. Cellular morphology parameters due to Arg575Asp mutation can be rescued by TRPV1 channel blocker	123
40. Ca ²⁺ -imaging of TRPV1-WT, Arg575Asp, Arg575Asp-Asp576Arg and pmCherryC1	125-126
41. Depletion of intracellular Ca ²⁺ -stores causes significant delay in response of TRPV1-Arg575Asp-Asp576Arg towards Capsaicin activation	127-128
42. Phylogenetic tree and molecular evolution of TRPA1	131
43. TRPA1 synteny and genes are well conserved while TRPA1 protein is highly diverged	132
44. TRPA1 domains are highly diverged among both vertebrates and invertebrates	133
45. Endogenous expression of TRPA1 is conserved in all vertebrate sperm	138
46. TRPA1 activation in bull sperm results in hyper-activated motility	139
47. TRPA1 activation or inhibition doesn't have much impact on capacitation or acrosome reaction	141
48. TRPA1 activation or inhibition induce variability in motility parameters	142
49. Localization of TRPA1 with different modified tubulin in bull sperm	143-145
50. Distribution of amino acids at the lipid water interface region of Human TRPA1	149
51. Conservation of amino acids lining the TRPA1 LWI regions	150
52. Frequency-of-occurrence of different amino acids at the lipid-water-interface (LWI) of TRPA1 in different phylogenetic groups	152-153
53. Frequency of occurrence of hydrophilic, hydrophobic, positive and negatively charged amino acids at TRPA1 LWI	155
54. Conservation of different CRAC and CARC motifs in Human TRPA1	156
55. Docking of Cholesterol with Human TRPA1	156
56. Localization of TRPA1 with lipid raft markers	157
57. Pore region of TRPV1 in closed and agonist bound state	164
58. A plausible model depicting the importance of positive and negative charged amino acids in inner LWI region of TM5 in channel functions	181

59. Relative properties of TRPV1-WT, TRPV1-Arg575Asp and TRPV1-Arg575Asp/Asp576Arg channels	185
60. TRPV1-WT and TRPV1-Arg575Asp uptakes Ca ²⁺ -sensor Rhod-3-AM dye in different extent	186
61. A plausible model depicting the importance of positive and negative charged amino acids in inner LWI region of TM5 in channel functions	187
62. Relative properties of TRPV1 and TRPV1-TBS1-Hexamutant channels	193
63. A tentative model: TRPV1 channel gating in response to tubulin, microtubule and cholesterol	195
64. Endogenous expression of TRPA1 in butterfly sperm cells	203
65. Human TRPA1-Ct interacts with various modified tubulin	204
66. Possible molecular evolution of TRPV1 and TRPA1	207

<u>List of tables:</u>	Page number
1. Tissue specific distribution and function of different vertebrate TRP channel members	10-12
2. Regulation of various TRP channel members by phosphoinositides	16-19
3. Enrichment of snorkeling amino acids in the lipid water interface of TRPV1	91
4. Comparative analysis of TRPV1 and TRPA1 from this study	208
5. Reagents used	215-216
6. Kits, markers and enzymes	217
7. Cell lines and sperm samples used	217
8. Bacterial strains	218
9. Primary antibodies	218
10. Secondary antibodies	218-219
11. Constructs used	219-221
12. List of primers used for Site Directed Mutagenesis (SDM)	222-223
13. PCR for Site-Directed Mutagenesis (SDM)	223-224
14. PCR reaction conditions for SDM	224
15. List of primers used for cloning into pSGFP2C1, pmCherryC1 and MBP-LacZ vector	224-225
16. PCR reaction for Cloning	225
17. PCR Cycle for Cloning into pSGFP2C1 and pmCherryC1 vector	225
18. PCR Cycle for Cloning into pMAL-c2X vector	225
19. 50X TAE buffer recipe	226
20. LB Media composition	228
21. Composition of TFB I buffer	229
22. Composition of TFB II buffer	229
23. Composition of 1X Lysis buffer for Instant Screening	230
24. 12% SDS-PAGE gel composition	231
25. Composition of 10X SDS running buffer	232
26. Composition of staining solution	232
27. Composition of de-staining solution	232
28. Composition of TBS (5X)	233
29. Composition of Western Blot Transfer Buffer	233
30. Composition of Lysis buffer (50 ml)	234

31. PEMS buffer composition	235
32. Domains and motifs of TRPV1	249
33. Domains and motifs of TRPA1	249-250

ABBREVIATIONS

2-APB	2-minoethoxydiphenyl borate
4 α PDD	4 α -Phorbol 12,13-didecanoate
5'-IRTX	5'-iodoresiniferatoxin
a.u.	Arbitrary Unit
AA	Arachidonic Acid
ACA	N-(p-amylcinnamoyl) anthranilic acid
ADP	Adenosine diphosphate
ADPKD	Autosomal dominant polycystic kidney disease
AF	Alexa Flour
AITC	Allyl Isothiocyanate
ALH	Amplitude of Lateral Head displacement
ALS-G	Guamanian amyotrophic lateral sclerosis
APS	Ammonium persulphate
ARD	Ankyrin Repeat Domain
ASIC	Acid Sensing Ion Channels
ATP	Adenosine triphosphate
BAA	Bisandrographolide A
BCF	Beat Cross Frequency
bp	Base Pair
BSA	Bovine Serum Albumin
CaM	Calmodulin
CaMKII	Calmodulin-dependent kinase II
cAMP	Cyclic adenosine monophosphate
CASA	Computer Assisted Sperm Analysis
CBB	Coomassie Brilliant Blue
CBD	Cannabidiol
CCE	Capacitative Calcium Entry
CCM	Cholesterol Consensus Motif
CGRP	Calcitonin Gene Related Peptide
CNS	Central Nervous System
CRAC	Cholesterol recognition amino acid consensus
Cryo-EM	Cryo Electron Microscope
Ct	C-terminus
CTXB	Cholera Toxin-B
DAG	Diacyl Glycerol
DAPI	4',6-diamidino-2-phenylindole
DMS	Dimethyl Suberimidate
DMSO	Dimethyl Sulfoxide
DNA	Deoxyribonucleic acid
dNTP	Deoxynucleoside triphosphate
DRG	Dorsal Root Ganglia
dsDNA	Double Stranded DNA
EDTA	Ethylenediaminetetraacetic acid
EGTA	Ethylene glycol bis(2-aminoethyl ether)tetraacetic acid
ER	Endoplasmic Reticulum
ERG	Electroretinogram
EtBr	Ethidium Bromide
FBS	Fetal Bovine Serum

FITC	Fluorescein isothiocyanate
FSGS	Focal and Segmental Glomerulosclerosis
GFP	Green Fluorescent Protein
GTP	Guanosine-5'-triphosphate
HEPES	4-(2-Hydroxyethyl)piperazine-1-ethanesulfonic acid
HF	High Fidelity
HRP	Horseradish Peroxidase
InsP6	inositol hexakisphosphate
IP3	Inositol trisphosphate
Kb	Kilobase
kDa	Kilo Dalton
LB	Luria Bertani
LIN	Linearity of a curvilinear path
LPA	Lysophosphatidic Acid
LPC	Lysophosphatidylcholine
LWI	Lipid Water Interface
MAD	Mean angular displacement
MAP	Microtubule Associated Protein
MAPK	Mitogen-Activated Protein Kinase
MBP	Maltose Binding Protein
MHR	TRPM Homology Regions
MIA	Monosodium iodoacetate
MLRs	Membrane/lipid rafts
MOPS	3-(N-Morpholino)propanesulfonic acid
MT	Microtubule
M β CD	Methyl- β -Cyclodextrin
NCBI	National Centre for Biotechnology Information
NG	Nodose Ganglia
NMDG	N-methyl-D-glucamine
NO	Nitric Oxide
PAGE	Polyacrylamide Gel Electrophoresis
PBS	Phosphate Buffer Saline
PCR	Polymerase Chain Reaction
PDB	Protein Data Bank
PD-G	parkinsonism-dementia complex of Guam
PEA	Phosphatidylethanolamine
PFA	Paraformaldehyde
PIP ₂	Phosphatidylinositol 4,5-bisphosphate
PIP ₃	Phosphatidylinositol (3,4,5)-trisphosphate
PKC	Protein kinase C
PLC	Phospholipase C
PMSF	Phenylmethanesulfonyl fluoride
PNA	Peanut agglutinin
PNS	Peripheral Nervous System
POPC	Phosphatidylcholine
PTM	Post-translational Modification
PUFA	Poly Unsaturated Fatty Acid
PVDF	Polyvinylidene difluoride
RCS	Reactive Carbonyl Species
RFP	Red Fluorescent Protein

RNS	Reactive Nitrogen Species
ROS	Reactive Oxygen Species
RPM	Revolutions per minute
RTX	Resiniferatoxin
SDM	Site Directed Mutagenesis
SDS	Sodium Dodecyl Sulphate
SGK1	Serum and Glucocorticoid Inducible Kinase
SMDK	Spondylometaphyseal dysplasia (SMD) Kozlowski type
SOC	Store Operated Calcium
SOCE	Store Operated Calcium Entry
STR	Straightness
TAE	Tris-Acetic Acid-EDTA
TBS	Tris-buffered saline
TBS-1	Tubulin Binding Sequence-1
TBS-2	Tubulin Binding Sequence-2
TEMED	N,N,N',N'-Tetramethylethylenediamine
TG	Trigeminal Ganglia
THC	Δ^9 -tetrahydrocannabinol
TM	Transmembrane
TRP	Transient Receptor Potential
V1	TRPV1
UCP	Uncoupling Protein
UV	Ultraviolet
VAP	Average Path Velocity
VaTx	Vanillotoxins
VCL	Curvilinear Velocity
VDAC	Voltage-dependent Anion Channel
VNO	Vomeronasal organ
VSL	Straight-line (rectilinear) velocity
VSM	Vascular Smooth Muscle
WOB	Wobble
WT	Wild type

Chapter 1

Introduction

1.1. General introduction to TRP channels

1.1.1. Brief history of ion channels

Occurrence of electrical activity within the human body is a prerequisite for sustenance of life. Such activities are a consequence of distribution and movement of electrically charged ions through pore forming units present in membranes of almost all cells known as ion channels. Cardiac cells in heart, neurons in brain, β -cells in pancreas, sperm cells are examples of electrically excitable cells (1).. Transmembrane potential is primarily determined by three factors: a) relative distribution or concentration of ions across the membrane (both inside and outside the cell). b) relative permeability of the cell membrane to these ions via specific ion channels embedded in them and c) activity of ion pumps that maintain a concentration gradient across the membrane.

Ion channels and transporters embedded in cell membranes are responsible for maintaining this charge difference (2). The methods for studying these ion channels and how they regulate the electrical properties of cells were a matter of intrigue since 1930s. Techniques like voltage clamp to study the membrane potential of large cells began developing in 1940 by Cole and Mormont (3). It was only in 1970 that biologists were capable of studying ionic influxes at single channel level with the advent of Patch Clamp technique for which Neher and Sakmann received Noble Prize. In this technique the cell membrane is tightly sealed with a thin glass pipette of appropriate shape and then a patch of it containing ion channel is excised out. Various properties of ion channels including their role in regulation of membrane voltage and several cellular processes can be studied (4).

Electrodes placed on surface of nerves enable recording of changes in membrane potential that are occurring between its external and internal environment. These changes are recorded as electrical impulses and they form the basis by which nerve cells transmit

information from one place to another. Inside of the cell is relatively negative to that of the outside. When a nerve cell is impaled with a microelectrode the voltage recorded in absence of any stimulus is known as resting potential. This value for resting potential is generally -60mV for a nerve cell but it varies with cell type. Hyperpolarization is referred to that state of the membrane potential when it becomes more negative than the resting potential. Depolarization is the event when the membrane potential becomes more positive than the resting potential. The magnitude of responses exhibited during depolarization and hyperpolarization are proportional to the magnitude of the stimulus applied. However, when the magnitude of depolarization reaches a particular level of membrane potential, referred to as threshold, then the signal that is generated is referred to as Action Potential. Unlike the other events, a further increase in magnitude of threshold stimulus does not further amplify the size of the action potential. Its persistence is proportional to the time of stimulus application. There are several features of an action potential:

- * It has a short lifetime of ~ 1 millisecond.

- * They are elicited in an all-or-none fashion i.e. once the membrane potential attains the threshold value it will occur and if the stimulus is not capable of raising the value to the threshold limit then even longer application duration won't be sufficient for its occurrence. The depolarizing phase or upstroke refers to the rising phase of the action potential. Return of the membrane potential to its resting value is referred to as repolarization phase. The phase of the action potential when it becomes more negative than the resting membrane potential is referred to as hyperpolarizing after potential or undershoot.

- * Intensity of the stimulus is proportional to the number and occurrence of action potential. Augmented stimulus intensity does not increase the size of the action potential;

rather it increases its frequency or number. Hence, greater the intensity of the applied stimulus e.g. mechanical stimulus to the skin or light stimulus to photoreceptor, the greater the number of action potentials that will develop. Consequently, in the motor system, the greater the number of action potentials generated in a motor neuron, the greater will be the intensity of muscle contraction that is innervated by it (5).

Precise movement of ions into and out of cells and organelles are crucial for normal physiological functions. Movement of ions across membranes regulate miscellaneous processes like signal transduction, volume and pH regulation, immune functions, fertilization, electrical signals in muscles and nerves, etc. Integral membrane proteins involved in such ion transport can be broadly classified into ion channels and pumps. Ion channels mediate passive diffusion of ions across the impermeable lipid bilayer down the gradient and pumps utilize energy derived from ATP breakdown or other means to push these ions actively against the gradient (6). Ion channels are mostly selective for a particular ion which has led to the classification of channels into Na^+ , K^+ , Cl^- , and Ca^{2+} channels, but some can also be non-specific like the TRP ion channels (7). Ion channels can be considered as gateway inside cells or organelles. Each of them shuttles between a closed and open conformation to block or allow ion influx through them respectively. This conformational transition between closed and open states is referred to as 'Gating'(8). Channel opening can be triggered by various stimuli and depending upon their mechanisms of activation ion channels can be broadly classified into three categories. Majority of ion channels fall into the first category i.e. Ligand-Gated Ion Channels. Activation or opening of this class of ion channel depends upon binding of a specific ligand to conserved recognition domains present in these channels e.g. P2X, CNG, ORAI+STIM, Kir, etc. The second category of ion channels belongs to the Proton-Gated Ion Channels. Unlike the ligand gated ion channels, members of this category do

not harbour a specific recognition site for ligand binding. Rather, their gating is regulated by changes in protonation states of titratable groups distributed throughout the protein or localized in distinct functional domains e.g. ASICs, TRASK, TALK, GLIC etc. The third category encompasses channels that are gated by physical stimuli such as voltage, mechanical force, temperature, osmotic shock, pressure, membrane deformations etc. Examples of such ion channels are members of TRP channel family, K_v , Na_v , VRAC, Piezo, TREK etc. (9).

1.1.2. Discovery of TRP channels

Cells must signal in order to adapt with changing environment and for that they require messengers whose concentration varies with time. Ca^{2+} and PO_4^- ions emerged to rule the process of cell signalling by altering protein conformations and local electrostatic fields (10). Ca^{2+} permeable channels are particularly important because apart from being a charge carrier, calcium is one of the most essential second messengers. Prior to the discovery of TRP channels, Ca^{2+} channels were categorised into two classes: ligand gated and voltage gated. Regulation and activation of TRP channels share some similarities with members of both these classes of ion channels but they emerged as a completely new group of ion channels. It shows structural similarity with other voltage-gated ion channels in having six trans-membrane helices (S1-S6), a pore region between S5 and S6 helices but unlike others the positively charged S4 region is replaced with uncharged amino acids in TRP channels. Unlike other ligand gated ion channels, individual members of TRP family get activated by a plethora of different ligands (11). *Drosophila* or fruit flies utilise their ability to sense light for a wide array of functions like, circadian governed activities, perception of visual cues that initiate courtship, visualization for navigating in the surrounding environment, etc. (12). Light activation of photoreceptors present in retina

results in membrane hyperpolarization. Upon exposure to darkness the membrane becomes depolarized. Neurotransmitter release from photoreceptor synaptic terminals in retinal cells is dependent upon light intensity and subsequently the voltage gated calcium ion channels residing in these terminals. Photoreceptors remain depolarized in dark and consequently there are higher numbers of calcium channels in open conformation and augmented neurotransmitter release. However, light induced membrane hyperpolarization renders channel closure and subsequent drop in transmitter release (13). Cosens and Manning in 1969 discovered a spontaneously formed behavioural mutant of *Drosophila melanogaster* that behaved as though it is blind when exposed to bright illumination. This mutation was identified to lie on the 3rd chromosome of *Drosophila melanogaster*. Electrical responses of the entire eye in response to light or Electroretinogram (ERG) of WT versus mutant *Drosophila* eye showed that upon exposure to continuous bright light the receptor potential of mutant flies quickly returns to baseline whereas in case of WT it gradually reaches baseline. WT flies always respond to light stimuli regardless of the time interval between individual pulses. However, this mutant does not respond to a second pulse of light, apparently behaves as blind and rather needs a short period of darkness to recover its light responsiveness (14). As these visually compromised mutant flies exhibited a transient response to persistent illumination as compared to sustained responses by WT flies, these mutants were referred to as Transient Receptor Potential (trp phenotype) (15). In 1989, Montell and Rubin characterised the *Drosophila trp* gene and identified the product of this gene to be a new component in the photo-transduction system. According to their analysis none of the mutant alleles expressed the trp protein and this protein apparently plays an important role in phototransduction at a stage post production of IP₃. It is an integral membrane protein expressed in rhabdomeres. Thus the trp phenotype is an outcome of lack of trp protein

rather than expression of a defective gene product (16). In 1992 Philips et al. discovered a structural homolog of the *trp* gene in *Drosophila* eye and named it *trpl* (TRP like). Both *trp* and *trpl* exhibited structural similarities with vertebrate brain voltage-gated Ca^{2+} channels (17). Further experiments showed that *trp* gene encodes for a channel protein that has high Ca^{2+} -permeability and is a key participant in the phototransduction machinery of *Drosophila* (18).

1.1.3. Classification of TRP channel superfamily

After its discovery in *Drosophila*, TRP channel homologues have been cloned from organisms belonging to different phyla ranging from *Caenorhabditis elegans* to mammals (19). Contrary to other ion channels, TRP channels are distinguished on the basis of their homology rather than their ion selectivity or ligand preference, as their functions are diverse and many are unexplored (20). The TRP superfamily has been broadly categorised into two groups and members of both these groups have been subdivided into seven subfamilies (Figure 1). The eighth subfamily comprises of TRPY which includes yeast TRP and it is distantly related to the other seven. Members of these two groups have been distinguished on the basis of topological and sequence differences. The first group comprises of 5 sub-families which have the strongest sequence homology with the *Drosophila* TRP.

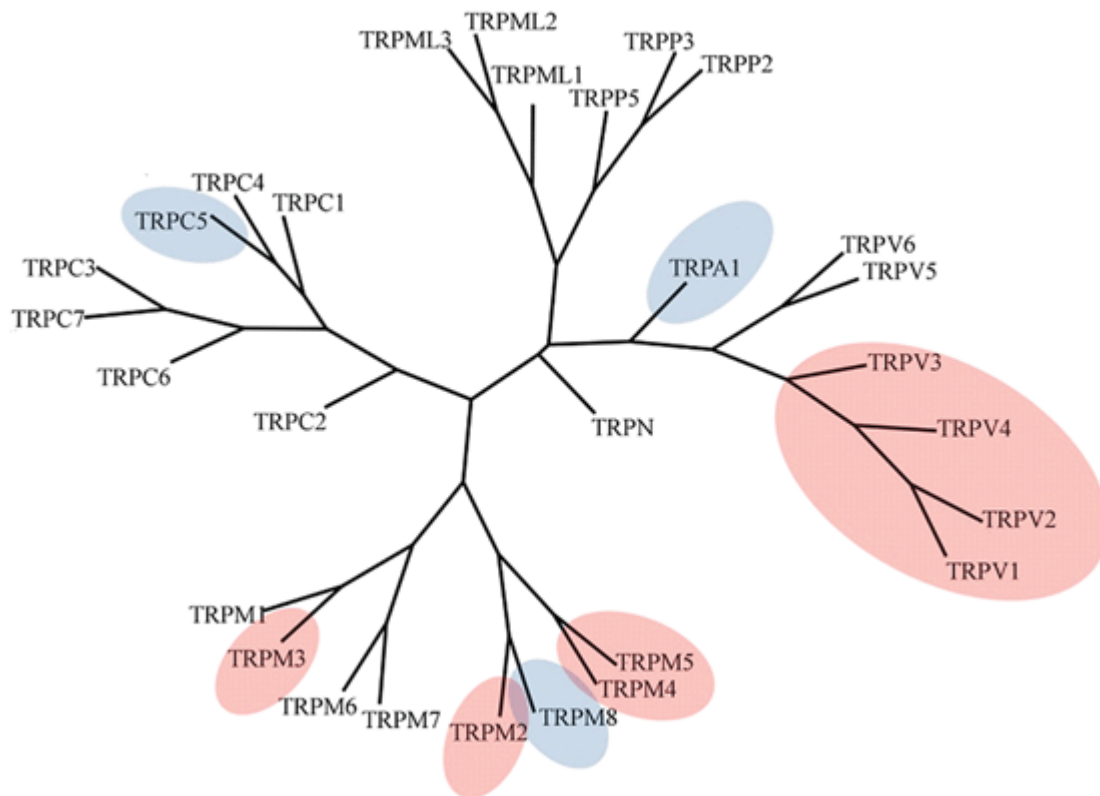


Figure 1. Classification of TRP channels. Figure taken from *Ferreira et al.2015* (21).

Members having the closest sequence similarity with *Drosophila* TRP have been grouped under the TRPC or canonical sub-family. The other sub-families of the 1st group are TRPA, TRPN, TRPV and TRPM. Nomenclature of these sub-families is according to their foremost identified member and depending upon the organism these sub-families have different members. For example, mammals do not have members belonging to TRPN subfamily whereas Zebrafish expresses some members of it. Group two is distantly related to group one and comprises of TRPP and TRPML subfamilies. These two classes of proteins share homology over trans-membrane regions and have a large extracellular loop separating S1 and S2. The founding members of TRPP and TRPML constitute gene products that were mutated in autosomal dominant Polycystic Kidney Disease and Mucopolysaccharidosis type IV diseases respectively (22).

1.1.4. Tissue specified distribution and function of different vertebrate TRP channels

Name	Distribution	Function	References
TRPV1	Keratinocytes, lung, urinary bladder, Trigeminal Ganglia(TG), Dorsal Root Ganglia (DRG), testes, tongue, spinal cord	Thermoregulation, osmosensation, chemosensation, taste perception, release of insulin and gastric hormones secretion of intestinal fluids, and saliva, release of proinflammatory cytokines, pain perception	(22)(23)
TRPV2	DRG, spinal cord, spleen, intestine, brain	Thermoregulation, osmosensation, exocytosis, release of insulin and glucose homeostasis	(22)(23)
TRPV3	Brain, spinal cord, keratinocytes, DRG, TG, tongue	Thermosensation, taste perception,	(22)(23)
TRPV4	Inner ear, spleen, kidney, brain, sensory neurons, spinal cord, heart, lungs, liver, testes, keratinocytes, endothelia	Thermosensation, osmosensation, mechanosensation, plays an important role in digestive, skeletal, respiratory, urinary system. Maintains endothelial cell function and vascular tone	(24)(22)(23)
TRPV5	Pancreas, kidney, placenta, intestine	Regulates urinary calcium excretion, calcium reabsorption in kidney,	(25)(22)
TRPV6	Placenta, pancreas, small intestine	Regulates calcium transport in kidney, facilitates Vitamin D regulates absorption of calcium in intestine, involved in maternal-fetal calcium transport, sperm motility	(25)(22)
TRPC1	Brain, heart, salivary glands, testes, smooth muscles, ovary, liver	Salivary fluid secretion, regulation of cell volume, vascular contraction, regulates cardiac hypertrophy, regulator of normal renal function and glomerular filtration rate, skeletal muscle regulation, neural function control and development, keratinocyte differentiation,	(26)(22)

		mechanosensitivity, maintenance of cell polarity, motility, asymmetry of phospholipids	
TRPC2	Vomer nasal organ (VNO) and testes	Pheromone signalling in rodents and lower vertebrates, regulator of acrosomal reaction	(26)(22)
TRPC3	Brain, heart, kidney	Controls neuronal development and functions, redox sensor, regulator of myometrical functions, skeletal and airway smooth muscle contraction, cardiac physiology	(26)(22)
TRPC4	Retina, brain, testes, adrenal gland, endothelia	Regulates endothelial cell function, neuronal regeneration, Vascular Smooth Muscle cell proliferation,	(26)(22)
TRPC5	Central Nervous System (CNS), Vascular Smooth Muscle (VSM) cell, aortic endothelial cells	Controls neurite outgrowth, migration of VSM cells, regulates cardiovascular functions, involved in IgE mediated degranulation of mast cells	(26)(22)
TRPC6	Heart, brain, VSM cells, lung, ovary, placenta	Regulates myogenic tone in VSM, cardiac fibroblast function, permeability of endothelial cells, neuronal cell function, calcium induced erythrocyte cell death	(26)(22)
TRPC7	Heart, eye, lung	Apoptosis induction	(26)(22)
TRPM1	Brain, skin, eye, heart	Proliferation and differentiation of melanocytes	(27)(28)(22)
TRPM2	Pancreas, heart, brain, liver,	Involved in host defence, insulin secretion	(28)(27)(23)(22)
TRPM3	Brain, kidney, pituitary	Maintains renal osmolarity, involved in shingolipid mediated signal transduction	(28)(27)(22)
TRPM4	Colon, bladder, pancreas, heart, intestine, prostate gland	Release of insulin, bladder function, forms a calcium activated sodium channel that mediates depolarization of plasma membrane	(23)(28)(27)(22)
TRPM5	Pituitary, prostate, kidney, pancreas, intestine, stomach, bone marrow, tongue	Taste perception, release of gastric hormones and insulin, forms a calcium activated sodium channel that mediates	(23)(28)(27)(22)

		depolarization of plasma membrane	
TRPM6	Intestine, brain, adipose, pituitary, prostate, bone marrow, kidney	Involved in intestinal uptake and renal reabsorption of magnesium	(28)(27)(22)
TRPM7	Heart, bone, pituitary, kidney, adipose	Regulates cellular magnesium homeostasis	(28)(27)(22)
TRPM8	Prostate, liver, stomach, bladder, sensory neurons	Thermoregulation, taste perception	(28)(23)(27)(22)
TRPA1	DRG, ovary, spleen, testes, hair cells,	Thermoregulation, involved in sensation of environmental irritants, taste perception,	(22)(23)
TRPP2	VSM, kidney, ovary, cardiac myocytes, epithelial cells, adrenal glands	Regulates development and functioning of several organs in humans, arrangement of visceral organs in correct right-left axis	(29)(30)(22)
TRPP3	Heart, kidney, brain, neurons surrounding central canal of spinal cord, tongue	Retinal development, kidney development, sour taste perception	(31)(32)(22)
TRPP5	Heart, testes	Limited information	(22)
TRPML1	Heart, brain, skeletal muscles, kidney, spleen	Regulates lysosomal pH	(33)(22)
TRPML2	Pancreas, Central Nervous System (CNS)	Immune cell development and function, mucopolipidosis	(34)(22)(23)
TRPML3	Strial and hair cells of inner ear, vomeronasal and olfactory sensory neurons, neonatal intestinal enterocytes, melanocytes, kidney, lung, thymus	Critical component of the endocytic pathway. Its dysfunction is associated with premature deafness, pigmentation problems and perinatal lethality in mice models	(34)(35)(22)

Table 1. Tissue specific distribution and function of different vertebrate TRP channel members.

1.1.5. General architecture of TRP channels

The common architecture shared by all TRP channel member monomer constitutes six transmembrane (S1-S6) helices interconnected by loops, a pore region between S5 - S6 and cytoplasmic N-terminus and C-terminus. These channels assemble

as homo-tetramers or hetero-tetramers (in specific cases) to form non-selective cation permeable pores (Figure 2). All TRP members are non-selective with a $P_{Ca}/P_{Na} \leq 10$ (Ratio of permeability for Ca^{2+} versus Na^{+}) with the exception of Ca^{2+} -selective channels TRPV5 and TRPV6 and Na^{+} -selective channels TRPM4 and TRPM5 and (20)(36). The trans-membrane region can be categorised into two regions: the “sensor region” formed by S1-S4 and the “pore region” comprising of S5 - S6. The pore harbours a selectivity filter that decides what kind of ions should be allowed via the channel pore through its electrostatic and stereochemical properties. Another critical aspect of the channel is the gate region that regulates opening or closing of the pore on receiving information from the sensor region that senses signal(s) (37). The TRP-domain is a stretch of around 25 amino acids immediately after the S6 region occupying the proximal C-terminal region that is sparsely conserved in almost all mammalian TRP members except TRPP and TRPA (36). Within this domain lies a short stretch of amino acids referred to as TRP-box that is highly conserved among members of TRPC, TRPV and TRPM subfamilies.

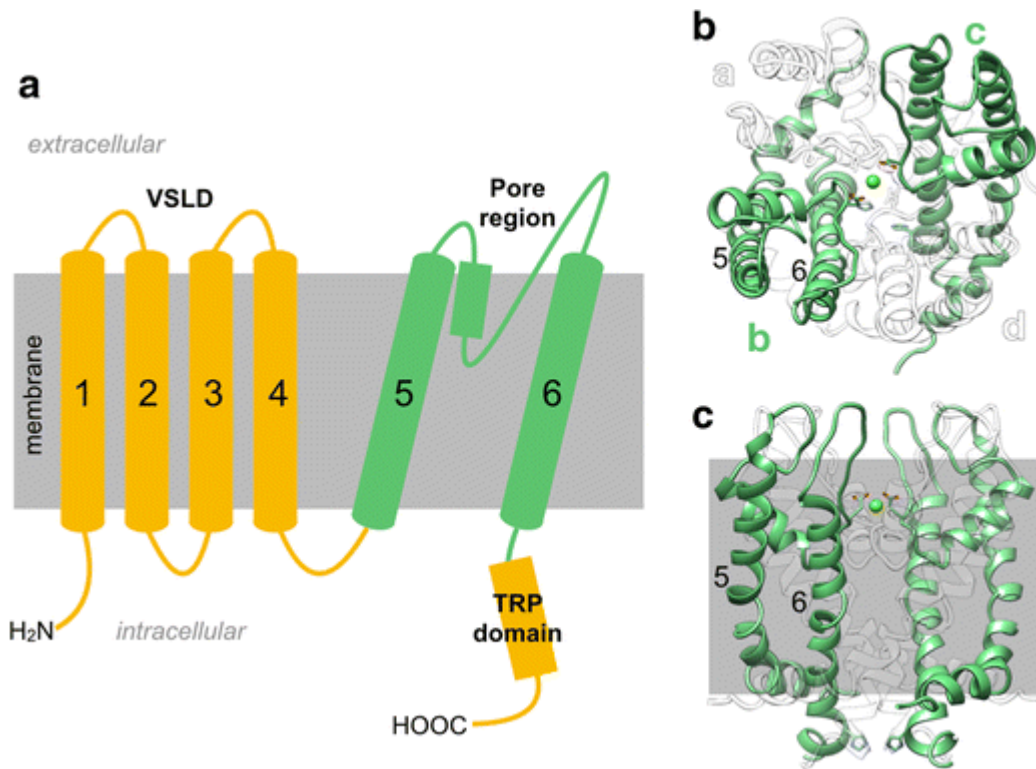


Figure 2. General structure of all TRP channel members. **a.** A single TRP channel monomer comprising of a cytoplasmic N and C terminus. The C-terminus harbours a TRP domain that is highly conserved across almost all TRP channel family members. Out of the 6 transmembrane helices (S1-S6) embedded in the lipid bilayer, S1-S4 forms the voltage-sensor like domain. The pore region lies between S5 and S6. **b-c.** Top and side view of tertiary structure of TRPV5's pore region complexed with Ca²⁺ ion. Out of the 4 monomers, 2 have been shown as green ribbons and 2 as transparent ribbons. TRP channels form homo-tetramers. Histidine and Aspartic acid residues lining the channel at the entrance and outlet as well as a trapped Ca²⁺ ion (indicated by green ball) have been indicated. Figure taken from *Madej et al, 2018*. (38)

Although the exact function of TRP box is unknown, however in some members like TRPM8, TRPM5 and TRPV5 it plays an important role in PIP₂ interaction (37). The N-terminal cytoplasmic domains of some TRP subfamilies namely TRPC, TRPN, TRPV and TRPA contain ankyrin repeats. These ankyrin repeat domains mediate protein-protein interaction, transcriptional regulation, various cytoskeletal assembling functions and other regulatory functions. Members of TRPM subfamily harbour four regions of high homology (TRPM Homology Regions or MHR) in their N-terminus. MHR's might have a plausible role in regulating membrane transport and oligomerization. The C-terminal region of some TRPM members (TRPM6, TRPM7 and TRPM2) contains domain that

mediate enzymatic reactions (kinase functions) and hence are referred to as chanzymes (37). Determination of TRP channel structure is crucial for identification of its different functionalities. Although its different members share a common transmembrane topology, they vary greatly in their N and C-terminal cytosolic domains. This variation in intracellular domains imparts TRP channels with the ability to sense diverse extracellular and intracellular stimuli. Cryo-EM has enabled resolution of the following TRP channel members: TRPV1, TRPV2, TRPA1, TRRP2, TRPML1, TRPML3, TRPM8, TRPM4, TRPN, TRPV5 and TRPV6.

1.2. Regulators of TRP Channels

TRP channels bestow a close sensory interface between cell's interior and the external environment. In order to accomplish this function, TRP channels exhibit polymodality i.e. their capability to get activated by variety of stimuli ranging from natural products, voltage, osmolarity, mechanical pressure, protons, temperature, synthetic compounds, endogenous ligands, mechanical pressure, ions, various membranous and sub-membranous components, etc. In order to understand the diverse physiological functions controlled by TRP channels, it is important to have knowledge about their modulation and regulation.

1.2.1. Phosphoinositides

One common aspect of TRP channel regulation is their modulation by plasma membrane phosphatidylinositol phosphates (PIPs), particularly phosphatidylinositol 4,5 bisphosphate [PI(4,5)P₂ or PIP₂]. PIP₂ constitutes about 1% of the lipid on the cytoplasmic leaflet of the plasma membrane (39) and acts as a precursor of significantly important signalling molecules like PIP₃, IP₃ and DAG. PIPs are negatively charged at

physiological pH and thereby mediate electrostatic interaction with cationic molecules or positively charged residues of membrane proteins (39). Phosphoinositide effect on various TRP channels have been tabulated below (40):

Name	Regulation/function	Phosphoinositide effects
TRPM1	Mutation causes night blindness in humans	No phosphoinositide effect reported yet
TRPM2	Activated by ADP ribose	Poly-lysine inhibits, and PI(4,5)P ₂ re-activates in excised patches (41)
TRPM3	Heat, pregnenolon sulfate	No phosphoinositide effect reported yet
TRPM4	Intracellular Ca ²⁺ activates, nonselective Ca ²⁺ impermeable cation channel	PI(4,5)P ₂ activates in excised patches (42)(43)
TRPM5	Intracellular Ca ²⁺ activates nonselective Ca ²⁺ impermeable cation channel	PI(4,5)P ₂ activate in excised patches (44)
TRPM6	Mg ²⁺ transporter, mutation causes human disease	PI(4,5)P ₂ activates in excised patches, rapamycin-inducible 5 phosphatase, and ciVSP inhibits (45)
TRPM7	cAMP, shear stress, plays important roles in development	PI(4,5)P ₂ activates in excised patches, activation of PLC inhibits (46) PI(4,5)P ₂ is needed for the activity of the cardiac magnesium-inhibited TRPM7-like channels (47) Role of PLC mediated inhibition is challenged (48) (49)
TRPM8	Cold, Menthol	PI(4,5)P ₂ activates in excised patches (50) (51) (52) PI(4,5)P ₂ depletion inhibits (rapamycin, ciVSP), plays a role in desensitization(51) (53) (52) PI(4,5)P ₂ but not PI(4)P activates in planar lipid bilayers (54)(55) PI(4,5)P ₂ regulates temperature threshold (56)
TRPV1	Heat, Capsaicin, low pH, involved in nociception	PI(4,5)P ₂ activates in excised patches (57)(58)(59)(60)(61)(62) Channel activity runs down in excised patches, MgATP restores activity in a PI4K dependent manner (62) In addition to phosphoinositides, many other negatively charged lipids

		<p>including phosphatidylglycerol and oleoyl-CoA also activate TRPV1 in excised patches (62)</p> <p>PI(4,5)P₂ inhibits desensitization in intact cells (50)(63)(58)(64)</p> <p>Channel activity is inhibited by combined depletion of PI(4,5)P₂ and PI(4)P using a rapamycin-inducible dual-phosphatase pseudojanin (65)(64)</p> <p>TRPV1 is inhibited by PI(4,5)P₂ depletion with a rapamycin-inducible 5 phosphatase (60)(66)</p> <p>PI(4,5)P₂ enhances thermosensation and thermal hyperalgesia. Depletion of PI(4,5)P₂ by prostatic acid phosphatase-induced PLC activation inhibits thermal sensitivity (67)</p> <p>PI(4,5)P₂ sensitivity was proposed to be mediated via a PI(4,5)P₂-binding protein Pirt (68), was challenged (61)</p> <p>PI(4,5)P₂ may partially inhibit in intact cells (69) (70)(58)(64)(71)</p> <p>PI(4,5)P₂ inhibits in lipid vesicles (72)</p> <p>PI(4,5)P₂ inhibits via competing for AKAP (73)</p>
TRPV2	Growth factors activate, noxious heat activates,	PI(4,5)P ₂ activates in excised patches (74)
TRPV3	Heat activates in keratinocytes	PI(4,5)P ₂ inhibits in excised patches (75)
TRPV4	Heat, hyposmosis activates	PI(4,5)P ₂ is required for osmotic and heat activation (76)
TRPV5	Constitutively active epithelial Ca ²⁺ channel	PI(4,5)P ₂ activates in excised patches (77)(51)
TRPV6	Constitutively active epithelial Ca ²⁺ channel	<p>PI(4,5)P₂ activates in excised patches and planar lipid bilayers (78)(79)(80)</p> <p>Rapamycin-inducible 5 phosphatase inhibits, PI(4,5)P₂depletion plays a role in Ca²⁺-induced inactivation (78)</p>
TRPC1	Activated downstream of PLC	PI(4,5)P ₂ activates in excised patches, native cells (81)(82)(83)
TRPC3	Activated downstream of PLC, DAG activates	PI(4,5)P ₂ activates in excised patches, expression system (84)

		VSP inhibits (85)(86)
TRPC4	Activated downstream of PLC	TRPC4 α but not TRPC4 β is inhibited by PI(4,5)P ₂ , whole-cell patch clamp (87) TRPC4 β is inhibited by PI(4,5)P ₂ depletion (rapamycin-inducible phosphatase) (88)
TRPC5	Activated downstream of PLC	PI(4,5)P ₂ activates in excised patches, but inhibits in whole cell, PI(4,5)P ₂ depletion may inhibit or activate it (89) PI(4,5)P ₂ inhibits desensitization in whole-cell patch clamp (90) PI(4,5)P ₂ activates in excised inside-out patches in complex with TRPC1 in native cells, but inhibits in the absence of TRPC1 (83)
TRPC6	Activated downstream of PLC, DAG activates	PI(4,5)P ₂ activates in excised patches (expression system) (84) VSP inhibits (85)(86) PI(4,5)P ₂ inhibits in excised patches (native smooth muscle cells)(91)(92) Extracellular PI(4,5)P ₂ enhances its activity in platelets (93) Calmodulin inhibits by displacing PI(3,4,5)P ₃ (94)
TRPC7	Activated downstream of PLC, DAG activates	PI(4,5)P ₂ activates in excised patches, expression system (84) VSP inhibits (85)(86) PI(4,5)P ₂ inhibits in excised patches, native channels (92)
TRPA1	Mustard oil and other noxious chemicals	PI(4,5)P ₂ inhibits heterologous desensitization by Capsaicin (95) PI(4,5)P ₂ activates in excised patches, inhibits desensitization in whole cell (96) PI(4,5)P ₂ inhibits sensitization by PAR in whole cell (97) PI(4,5)P ₂ inhibits in excised patches in the presence of PPPi, no effect w/o PPPi (98)(59)

		Depletion of PI(4,5)P ₂ with rapamycin-inducible phosphatase has no effect (99)
TRPML1	Intracellular channel, mutation causes mucopolipidosis	Specifically activated by PI(3,5)P ₂ (100)(101)
TRPP2	Mutated in polycystic kidney disease, mechanosensor?	PI(4,5)P ₂ inhibits, depletion of PI(4,5)P ₂ by EGF activates (102)

Table 2. Regulation of various TRP channel members by phosphoinositides

1.2.2. Post-translational modifications

The processes that a protein undergoes during or after its biosynthesis is collectively defined as post-translational modification (PTM). These events comprise attachment of co-enzymes, regulated proteolysis of the polypeptide chain and covalent modification of amino acids and their side chain residues. These modifications allow a limited pool of genes to generate a large variety of different proteins. They also influence protein localization and turnover, enzyme activity, regulation of several ion channels and their signalling cascades, protein-protein interactions, cell division and DNA repair (103). TRPs undergo various PTM's that regulate their structural and functional aspects. Some of these modifications include:

i. N-linked Glycosylation

Covalent addition of sugars to proteins or lipids via series of enzymatically catalysed reactions is referred to as glycosylation. Proteins can be glycosylated at two positions: hydroxyl group of Ser and Thr (O-linked glycosylation) or at the amino group of Asn residues (N-linked glycosylation) where the Asn lies within a consensus sequence of Asn-X-Ser/Thr. Here, X can be any amino acid except Pro. *Klotho*, a β -glucuronidase hydrolyses some sugar residues on N-glycosylated TRPV5 and thereby traps the ion channel at the apical membrane of kidney epithelial cells consequently enhancing its abundance in this compartment. This mechanism enables regulation of calcium

reabsorption in the nephron and thereby maintains normal blood calcium levels (104). Differences in glycosylation pattern of TRPC3 and TRPC6 regulated basal channel activity. TRPC3 exhibits constitutive activity whereas TRPC6 is a properly regulated one. The latter gets glycosylated at 2 positions whereas the former has a single glycosylation site. Disruption of the second glycosylation site in TRPC6 (absent in TRPC3) converts the highly regulated channel into a constitutively active one, a characteristic of the TRPC3 channel (105). TRPV1 undergoes N-glycosylation at Asn604 located in the 3rd extracellular loop. Loss of this PTM doesn't hamper the ion channels trafficking to the plasma membrane but it significantly alters some of its biophysical properties. Electrophysiological studies correlate N-glycosylation with the TRPV1s reduced sensitivity to its agonists like protons and Capsaicin, and antagonists like Capsazepine. Capsaicin induced pore dilation of TRPV1 is also partly dependent on its N-glycosylation status. The desensitization of TRPV1 is also regulated to some extent by its glycosylation pattern (106). Asn934 localized in the extracellular loop connecting transmembrane five and six undergoes N-glycosylation in TRPM8. TRPM8-Asn934Gln mutant lacking glycosylation exhibits a reduced response to menthol and cold. Lipid raft association of TRPM8 is also dependent upon its glycosylation status as the un-glycosylated forms show a significant reduction in lipid raft localization of the channel (106). In TRPV4, N-glycosylation occurs at Asn651 located in the pore loop region. A non-glycosylated mutant, Asn651Gln renders the channel more responsive to hypo tonicity and increases its plasma membrane trafficking compared to the wild type channel (107).

ii. Phosphorylation

Protein phosphorylation is a reversible post-translational modification that regulates several cellular processes. It involves catalytic addition of phosphoryl group to

hydroxyl group of serine, tyrosine or threonine residue on proteins by kinases (108). Within the TRPC family, TRPC3, 4, 5, 6 and 7 are negatively regulated by PKC phosphorylation. However, Fyn, a Src family protein kinase is known to activate TRPC6. Phosphorylation of TRPC6 by Calmodulin-dependent kinase II (CaMKII) is a prerequisite for channel activation. In contrast TRPC1 gets activated directly by PKC phosphorylation (109). TRPV1 gets regulated by multiple kinases. Phosphorylation tends to sensitize TRPV1 towards activation by its specific agonists, whereas dephosphorylation tends to make it less susceptible for activation (108). PKC phosphorylation of Rat TRPV1 at Ser502 and Ser800 potentiates the channels' responsiveness towards anandamide, Capsaicin and heat. Phosphorylation of Ser800 in TRPV1 by PKC ϵ abolishes its interaction with tubulin (110). CaMKII-mediated phosphorylation of Rat TRPV1 at Ser502 and Thr704 is required for activation by Capsaicin. PKA on the other hand phosphorylates Ser116 and Thr370 on Rat TRPV1 which reduces desensitization. De-phosphorylation of Thr370 by Calcineurin facilitates desensitization (109). Direct phosphorylation of TRPV4 by PKA and PKC augments the channels' response towards hypotonic stimuli. Phosphorylation of TRPV2 by PKA enhances Ca²⁺-influx through the channel in response to heat. SGK1 (Serum and Glucocorticoid Inducible Kinase) activates TRPV5. Ca²⁺-influx through TRPV6 is regulated by Calmodulin-PKC signalling. Calmodulin binds to TRPV6 and inactivates it, an effect that is countered by PKC phosphorylation. Similarly, phosphorylation of TRPV6 by Src tyrosine kinase causes channel activation and this effect is counterbalanced by de-phosphorylation mediated by tyrosine phosphatases. PKC directly activates TRPM4 by phosphorylating Ser1142 and Ser1145. TRPM7 is also activated by PKA and Src tyrosine kinase. TRPP1 is phosphorylated by PKA and tyrosine kinase. Although this tyrosine phosphorylation enhances its interaction with E-Cadherin but impedes its interaction with

focal adhesion kinase. Autosomal dominant polycystic kidney disease (ADPKD) occurs due to mutation in either of the two genes encoding TRPP1 or TRPP2. ADPKD patients harbour an over phosphorylated form of TRPP1 and this elevated phosphorylation status might interfere with the interaction of TRPP1 with TRPP2/E-cadherin/ β -Catenin resulting in depletion of β -Catenin and TRPP1 from the plasma membrane. Phosphorylation of Ser812 in TRPP2 by CK2 induces a marked increase in Ca^{2+} -sensitivity of the channel. Phosphorylation de-phosphorylation of TRPP2 regulates its trafficking to sub-cellular compartments (109).

iii. Covalent modification of TRP channels

A mechanism that regulates the activation of many TRP channel members is their covalent modification by ligands. Generation of reactive electrophiles like reactive nitrogen species (RNS), reactive oxygen species (ROS) and reactive carbonyl species (RCS) is a measure of the “redox state” of a cell. The redox signalling involves covalent modifications like S-nitrosylation whereby NO is covalently attached to cysteine residues (thiol group) on target proteins. NO activates mouse TRPC5 via S-nitrosylation of Cys553 and Cys558. Nitrosylation-induced Ca^{2+} -influx through activated TRPV1 is responsible for heat and pain sensation. Allicin, the pungent compound present in onion and garlic is also known to activate TRPV1 by covalent modification of specific cysteine residue located at its N-terminal region. TRPA1 undergoes covalent modification of cysteine by agonists like H_2O_2 , AITC, NO, Hypochlorite, Cinnamaldehyde, Nitrooleic acid, 4HNE, etc. (111).

1.2.3. Cytoskeletal components

The cytoskeletal network comprises of a large number of motor, structural and signalling proteins that coordinate together to regulate various cellular functions like cell division, migration, adhesion etc. (112). The localization and clustering of TRP channels in distinct domains of the plasma membrane have been reported to be crucial for their channel function and this is mostly brought about by the association of these channel proteins with the underlying cytoskeletal and scaffolding proteins. Crosstalk between cytoskeleton and TRPs is also important for the cytoskeletal framework. Ion influxes through these TRPs enable various cytoskeletal rearrangements and also functioning of proteins associated with them (113).

i. Regulation by actin

Members of the TRPC family are mostly regulated by cytoskeletal components such as actin. Mammalian TRPC channels have been seen to form Store Operated Calcium (SOC) channels which get activated upon calcium depletion from internal stores. There are many studies that attribute the redistribution of actin network as a requisite for activation of these channels in different cell types like human platelets, vascular endothelial cells, pancreatic acinar cells, etc. (113). TRPC1 interaction with actin regulates SOCE, cytoskeletal rearrangements, surface expression and shape changes (113). Some specific conditions arouse the requirement of association of some TRP channels localized in the plasma membrane with proteins expressing on the ER and this interaction is facilitated by an intact actin cytoskeletal network. Several members of the TRPC family undergo internalization upon actin depolymerisation (112). Ca^{2+} -Calmodulin complex activated Myosin Light Chain Kinase is very important for plasma membrane localization of TRPC5 (114). Other TRP channels like TRPM7 and TRPV4

establish contact with the actomyosin network by directly interacting with non-muscle myosin II and actin respectively (112). The C-terminal domain of TRPV4 also interacts with soluble and polymerized actin filaments (115). α -Actinin, an extensively distributed actin-bundling protein, is a very important component of the actin cytoskeleton. Activity of both TRPP2 and TRPP3 gets enhanced upon interaction with α -Actinin (116)(117). Capacitative Calcium Entry (CCE) involves regulation of Ca^{2+} channels present in the plasma membrane by the levels of Ca^{2+} in intracellular stores (118). In skeletal muscles, regulation of normal CCE depends upon the association of α 1-syntrophin and TRPC1 and loss in this interaction might be the plausible explanation for alterations in Ca^{2+} levels as seen in dystrophic muscle cells (119). Phosphorylation of Ser 824 in TRPV4 is a prerequisite for its interaction with F-actin and this association is important for its sub-cellular localization, Ca^{2+} -influx, single channel activity, stability and expansion of cell surface area (120). The surface localization of several TRPC members like TRPC1, TRPC3 and TRPC4 are regulated by the actomyosin network (113).

ii. Regulation by Microtubules

Microtubules play an important role in the functioning of several members of the TRP channel family. Function and redistribution of TRPP2 is regulated by microtubules. Microtubules facilitate SOCE in human platelets by mediating interaction between TRPC1 and type II IP_3R . TRPV1 interacts with both tubulin dimers and polymerised microtubules via its C-terminal end (121). Within the C-terminus of TRPV1, the exact binding regions were mapped to two stretches designated as Tubulin Binding Sequence-1 (TBS1, 710-730) and Tubulin Binding Sequence-2 (TBS2, 770-797). The interaction with β -tubulin is preferably more as compared to α -tubulin (122). TRPV1-tubulin interaction is enhanced with increasing Ca^{2+} concentration. This interaction aids in

microtubule stabilization under depolymerising conditions such as Nocodazole or cold (123). TRPV1 activation results in rapid disassembly of microtubules without affecting the integrity of actin and neurofilament network (124). TRPV1 activation in neurons results in rapid change in important structures such as retraction of growth cones and varicosity formation which happens mainly due to disassembly of microtubules (125). TRPV1 expression promotes neuritogenesis and induces formation of filopodial structures that are mostly enriched with microtubules and less of actin (126). Microtubule-TRPV1 interaction is required for central osmosensation and microtubules provide pushing force that mediates the mechanical activation of TRPV1 (127). TRPV4-microtubule interaction involves regulation of cell volume and cell motility (115).

1.2.4. Lipids

TRP ion channels are regulated by various lipids in their membrane environment. In case of TRPV1, S1-S4 provides a platform for binding of a large number of lipophilic compounds like Capsaicin, resiniferatoxin (RTX), anandamide or lipid mediators. Oleic acid, another lipophilic ligand, binds to the same region as that of Capsaicin but instead of activation it leads to TRPV1 inhibition. A lipid that profoundly regulates TRPV1 activity is membrane cholesterol. It modulates channel activity by either directly binding to a region within TRPV1 or indirectly by altering membrane properties. The major lipid component of plasma membrane is cholesterol. It remains unevenly distributed in the plasma membrane as lipid rafts- represent membrane micro domains that are enriched in sphingolipids and cholesterol (128). TRPV1 has been found to be localized in these lipid rafts and depletion of cholesterol impairs its function as well as membrane expression (129). Disruption of lipid rafts also results in reduced Ca^{2+} -influx upon TRPV1 activation (130). Rat TRPV1 has been seen to co-localize with lipid raft markers like Caveolin-1

and Flotillin-1 in DRG neuron derived cell line F-11. Cholesterol forms H-bond with Arg residues at positions 557 and 575 in TRPV1 and substitution of this Arg residue impairs the localization of TRPV1 in these rafts. This Arg-cholesterol interaction plausibly keeps the channel in a “closed- conformation” and the loss-of -interaction tends to keep the channel in an open conformation (131). N-methyl-D-glucamine (NMDG) is an amino sugar that becomes cationic at neutral pH. Depletion of membrane cholesterol decreased the permeability of NMDG through a persistently activated TRPV1 channel by Capsaicin under hypocalcaemic conditions. This indicates that alteration in membrane cholesterol levels affects ion permeability of TRPV1. The uptake of a large cationic dye YO-PRO1 was also reduced upon cholesterol depletion under hypocalcaemic conditions through TRPV1 that was sustainably activated with Capsaicin and protons. Thus, under hypocalcaemic conditions, the membrane cholesterol content regulates the pore dilation properties of TRPV1 (132).

TRPC1 and caveolin-1 interaction is necessary for localization of TRPC1 in plasma membrane and also for proper regulation of SOCE (133). TRPC3 is also considered to be a “lipid sensing” molecule as it gets activated by DAG and various other lipids like cholesterol. TRPC3 also requires cholesterol for its accurate cellular localization (133). In vascular smooth muscle cells, depletion of cholesterol by M β CD results in spontaneous TRPM3 activation even in absence of its activators. Whereas, cholesterol enrichment suppresses TRPM3 activation even in presence of its activator Pregnenolone Sulphate. Thus TRPM3 activity remains partly curbed by endogenous cholesterol levels but during atherosclerosis conditions when there is an overload of cholesterol, TRPM3 gets totally inhibited resulting in inadequate cell contractility in the cardiovascular system and release of pro-inflammatory cytokines (134). Cholesterol activates TRPM7 channels which results in entry of Ca²⁺-ions. This not only enhances

TRPM7 expression but also facilitates cell proliferation and migration of prostate cancer cells. Ca^{2+} entry, proliferation and migration of these prostate cancer cells could be decreased when either TRPM7 was silenced or cholesterol synthesis was inhibited using statins (135). TRPM8 has been seen to be localized in lipid rafts as observed in transiently transfected HEK293 cells or endogenously in DRG neurons. Lipid raft disruption by cholesterol depletion enhances TRPM8 activation by menthol and shifts the activation threshold of TRPM8 towards warmer temperatures (136). Cholesterol enrichment reduces the number of TRPM8 channels in the membrane whereas a decrease in the level of cholesterol increases the number of channel in the cell surface without altering its unitary conductance or open probability (137). Another TRPV member that gets positively regulated by cholesterol is TRPV3. Cholesterol enrichment not only sensitizes the channel at lower concentrations of its chemical agonists but it also results in channel activation at lower temperature thresholds (138). Activity of TRPV4 is also modulated by various lipophilic compounds like Arachidonic Acid (AA) metabolism products. It also localizes in lipid rafts and co-localizes with lipid raft markers like Filipin and Caveolin-1. Only the S4-Loop4-S5 region or the Loop4 of TRPV4 is capable of mediating direct interaction with not only cholesterol but also its precursor mevalonate as well as derivatives like aldosterone and stigmasterol. Membrane cholesterol content also influences the mobility of the channel (139). TRPV4 mutant Arg616Gln (shows gain-of-function) causes a pathophysiological condition known as "*Brachyolmia*", which is mostly due to its loss of interaction with cholesterol (140).

Membrane lipids like Lysophosphatidylcholine (LPC) is seen to increase the open probability of TRPM8 at 37°C, a temperature where it exhibits poor activity. LPC induces monocyte migration where Ca^{2+} -influx through non-selective cation channels has been observed. TRPV1 activation has been partly held responsible for this process. However,

the exact mechanism is still unknown. LPC does not affect TRPV1 temperature threshold for activation. TRPV2 gets activated by LPC whereby this lipid ensures its translocation to the plasma membrane and Ca²⁺-influx through this channel causes migration of cells (in the prostate cancer cell line PC3). PLC mediated TRPV2 activation results in fast and transient Ca²⁺-influx that causes cytotoxicity in osteoblast-forming like cells and is the plausible explanation for osteoporosis in patients suffering from atherosclerosis (141). Lysophosphatidic Acid (LPA) regulates neuronal development through its actions on TRPM2 channel. In a bone cancer model having elevated levels of LPA, it was observed that LPA potentiated Capsaicin-evoked currents through TRPV1 via a PKC-epsilon dependent pathway thereby inducing bone cancer pain. Mutagenesis and biochemical assays together suggested that the negatively charged phosphate group of LPA could directly bind with a positively charged residue Lys710 in the C-terminus of TRPV1 thereby leading to channel opening and perception of pain. Ethanol causes TRPV1 activation. Concerted administration of Palmitoleic acid (a non-oxidative metabolite of ethanol) and ethanol in mice resulted in acute pancreatitis. This phenomenon was not observed in TRPV1 null mice (*Trpv1*^{-/-}) nor in wild type mice injected separately with ethanol and palmitoleic acid. Relatively high concentrations of oleic acid imparts slight antagonising effects on Capsaicin activation of TRPV1. Inflammation induced oxidative stress generates an oxidized lipid named nitrooleic acid. It activates TRPV1 and TRPA1 plausibly by covalent modification of cysteine residues (141).

1.2.5. Plant and natural products

Plants are rich sources of bioactive compounds that are involved in the treatment of various diseases that helps in alleviating pain. Transient Receptor Potential (TRP) channels that are involved in the regulation of a large number of sensory and physiological

processes are the targets for most of these naturally derived bioactive compounds (Figure 3). Some of these components have been described below (142):

* **Capsaicinoids:** This group of biologically active compounds are present in chilli peppers or in plants categorised under *Capsicum* genus. Capsaicin is the most well studied Capsinoid. It was already known that application of Capsaicin ($EC_{50}=711.9$ nM) to peripheral neuron causes Ca^{2+} -influx and induces pain but the molecular mechanism was unknown (143). In 1997, Caterina et al demonstrated that binding of Capsaicin to TRPV1 activates this channel and results in influx of both Na^+ and Ca^{2+} ions. This causes depolarization of nociceptive neurons, firing of action potential and perception of spiciness (144). Capsaicin binds to a pocket formed by S3, S4 and S4-S5 linker of TRPV1 where it occupies a “tail-up head-down” configuration. This binding is mediated by both van der Waal’s interactions and hydrogen bonding and stabilizes the open conformation of the channel (145). Due to its bioactive relevance in different cells and tissues, Capsaicin is used to treat many pathophysiological conditions. For example, Capsaicin is an active component of a drug named Adlea that is used to treat osteoarthritis and post-surgical pain (142). Capsaicin exhibits analgesic, anti-cancer, anti-obesity, anti-inflammatory and anti-oxidative properties. Though most of the capsinoids are TRPV1 agonists but some like capsazepine imparts inhibitory role on TRPV1 channel opening. Other capsinoids like Dihydrocapsaicin, Nordihydrocapsaicin, Homodihydrocapsaicin, Homocapsaicin, Capsiate, Dihydrocapsiate, Nordihydrocapsiate exhibits similar properties like Capsaicin and functions by activating TRPV1 ion channel (142).

* **Resiniferatoxin:** RTX or Resiniferatoxin is an ultra-potent activator of TRPV1 ($EC_{50}=39.1$ nM) (146). It is an analog of Capsaicin naturally occurring in dried latex of cactus (*Euphorbia resinifera*). In terms of inflammation and thermoregulation, RTX is



Figure 3. Different plant products that modulate TRP channel activity. Figure taken from Yadav *et al.* 2019. (142)

much more potent than Capsaicin. RTX binds to a methionine (Met) residue at position 547 in TM3 region of TRPV1.

* **Piperine:** The alkaloid piperine attributes pungency to black pepper and long pepper. It is present in plants belonging to the Piperaceae family. It imparts pungency by activating TRPV1. Various studies indicate that piperine has a higher degree of cooperativity and efficacy as compared to Capsaicin.

* **Eugenol:** It is a naturally occurring component that can be extracted from cloves, cinnamon and other aromatic spices. It can activate TRPV1, TRPM8, TRPV3 and TRPA1. It has antiseptic and analgesic properties that is mainly used to alleviate toothache.

* **Gingerol:** The primary bioactive component of ginger is Gingerol and its dehydrated analogue 6-shogaol. Gingerol and its derivatives increase the intracellular Ca^{2+} concentration by TRPV1 activation.

* **Zingerone:** A component isolated from Ginger plant (*Zingiber officinale*) that activates TRPV1. It acts as an anti-oxidant that weakly inhibits peroxidation of phospholipid liposomes.

* **Evodiamine:** Plants belonging to the genus Tetradium synthesize an alkaloid Evodiamine. It is known to activate TRPV1 and Ca^{2+} - imaging experiments show that evodiamine evoked responses are similar to Capsaicin evoked responses. It functions as a stimulant that is capable of elevating core body temperature and body heat. Apart from this it also reduces fat uptake and inhibits metastasis and growth of cancerous cells.

* **Cannabinoids:** Extracts from *Cannabis sativa* has been used from time immemorial to treat several ailments including chronic pain. According to pharmacological studies cannabinoids and endocannabinoids target some TRP channels (TRPV1-TRPV4, TRPA1, and TRPM8) and thereby prove to be important in neuropathic pain management. These six TRP channels are collectively referred to as “Ionotropic Cannabinoid Receptors” (147). Cannabidiol or CBD is a phytocannabinoid that is extracted from *Cannabis sativa*. These compounds play an important role in alleviating inflammation, anxiety, convulsions and nausea. Some of these are even capable of inhibiting the growth of cancerous cells, exhibits anti-psychotic, anti-inflammatory and analgesic properties. CBD and its enantiomers activate TRPV1 resulting in Ca^{2+} -influx through the channel.

* **Polygodial:** A sesquiterpene dialdehyde derived from Dorrigo pepper that activates TRPV1 and TRPA1.

* **Isovelleral:** It is extracted from the fungi *Lactarius vellereus*. It plays an important role in inflammatory pain signalling by activating TRPA1 and TRPV1. It also exhibits anti-parasitic activity.

* **Camphor:** This waxy white terpenoid acts as an analgesic, antipruritic, local anaesthetic, anti-itch, anti-microbial agent by activating various TRP channels like TRPV1, TRPV3 and TRPA1.

* **Citronellal:** It acts as an insect repellent particularly for mosquitoes. It also possesses anti-fungal properties. Amongst the various pathways by which it exerts its biological activity, one is TRPA1 dependent.

* **Thapsigargin:** An extract from the plant *Thapsia garganica* that is used to treat rheumatic pain. It is capable of blocking TRPV1 mediated Ca^{2+} -influx.

* **Yohimbine:** It is reported to inhibit sodium channels and TRPV1 in a dose dependent manner.

* **α -Spinasterol:** Leaves of the medicinal plant *Vernonia tweedieana* produces this steroid that exhibits antagonist activity on TRPV1. Capsaicin induced edema and nociception can be relieved by application of α -Spinasterol.

* **Δ^9 -tetrahydrocannabinol (THC):** It is derived from cannabis plant. The principal molecular target of THC is CB1 but apart from that it also activates TRPV2.

* **Bisandrographolide A (BAA):** This plant extract from *Andrographis paniculata* potentially activates TRPV4. BAA exhibits cytotoxic and anti-HIV properties.

* **Cinnamaldehyde:** It is the primary bioactive compound of cinnamon oil extracted from the bark of cinnamon. It is known to have anti-inflammatory, anti-tumorigenic, anti-bacterial and hypoglycaemic activity. It is one of the principle agonists of TRPA1. Its

anti-obesity and anti-hyperglycaemic properties have recently been tested in mouse model.

1.2.6. Animal toxins

TRP ion channels also act as molecular targets of various venomous toxins. Venom from tarantula spider *Psalmopoeus cambridgei* specifically and robustly activated TRPV1. Reverse phase chromatography and Edman sequencing of this venom yielded three peptide toxins that could individually activate TRPV1 with different efficacies. These 3 closely related peptide toxins were collectively name as Vanillotoxins (VaTx 1-3) (148). However, Kunitz-Type Peptide HCRG21, a toxin from venom of Sea Anemone *Heteractis crispa* inhibits TRPV1 rather than activating it (149). DkTx, another Vanillotoxin derived from the venom of Chinese bird spider (*Ornithoctonus huwena*) binds to the outer pore region of TRPV1 and stabilizes the channel in a constitutively open conformation (150). Another TRPV1 specific activator is the RhTx peptide toxin purified from the venom of *Scolopendra subspinipes mutilans*, the Chinese red headed centipede. Its potential to activate TRPV1 is comparable to that of Capsaicin (151). A Scorpion toxin (from the venom of *Mesobuthus martensii*) BmP01, peptides from the venom of viper snake *Echis coloratus* are also known to activate TRPV1 (152). A non-peptide toxin from the spider *Agelenopsis aperta* inhibits TRPV1 (153). Soricidin, a toxin isolated from the salivary glands of the shrew (*Blarina brevicauda*) inhibits calcium uptake via TRPV6 ion channel (154). Bee stings produces sufficient pain and swelling. This is caused by the toxic component Melittin which possibly targets the TRPC channels expressed in the primary nociceptive neurons (155). A peptidergic Scorpion toxin WaTx specifically binds TRPA1 at intracellular sites that are potentially bound by electrophiles

that activate TRPA1. Its binding tends to keep the channel in a prolonged open state and alters its preference for monovalent cations instead of divalent cations (156).

1.2.7. Synthetic modulators

TRP channels are also regulated by various synthetic compounds. Some of these have a broad spectrum properties and regulate most of the TRP channel members whereas some are specific for some members only. The broad spectrum synthetic modulators are as follows:

* **SKF-96365:** It is an inhibitor of store operated as well as receptor mediated calcium entry. TRPC channels get blocked by SKF-96365 up to concentrations as low as 10 μM but TRPV and TRPM members get blocked by it at higher concentrations (an IC_{50} value ranging from 20-75 μM).

* **2-APB:** 2-aminoethoxydiphenyl borate (2-APB) is a non-selective modulator of TRP channels. TRPC family members are blocked by 2-APB. This compound exerts a stimulatory or inhibitory effect on all TRP family members except TRPM2. However, Togashi *et al.* reported that it is capable of blocking TRPM2 (157). 2-APB is capable of blocking sphingosine induced Ca^{2+} -influx through TRPM3 and Mg^{2+} -influx through TRPM7. TRPM6 gets potentiated at micromolar concentrations of 2-APB whereas TRPM7 gets inhibited at such concentrations. On the other hand, millimolar concentrations of 2-APB activate TRPM7 as well as TRPM6/M7 heteromultimers. This borate compound 2-APB manages to activate and sensitize TRPV1, TRPV2, TRPV3 and TRPV6. In case of TRPV2, activation by 2-APB is species specific i.e. rat and mouse TRPV2 get activated by it whereas human TRPV2 remains indifferent to it.

* **ACA:** N-(p-aminocinnamoyl) anthranilic acid or ACA partly blocks TRPV1 in a voltage dependent manner. Apart from this, it is also capable of blocking TRPC6, TRPC3,

TRPM2 and TRPM8 mediated currents.

* **Clotrimazole:** It is an azole derivative that is clinically used as an anti-fungal agent. It is a TRPM2 channel blocker whereas it activates TRPV1 and TRPA1. 30 μM Clotrimazole was capable of blocking TRPM3, TRPC6 and TRPV4.

Some of the TRP channel selective blockers are:

Pyr3 selectively blocks TRPC3 by directly binding to it. Hyp9 selectively activates TRPC6 but neither TRPC3 nor TRPC7. The synthetic cooling compound Icillin is known to activate TRPM8. AMTB is a TRPM8 specific blocker and has no effect on TRPV1 and TRPV4. Nifedepine specifically activates TRPM3. TRPV1 gets inhibited by capsazepine. SB-366791 is also a TRPV1 specific blocker. GSK1016790A is a TRPV4-selective agonist that is capable of inducing hyperactivity and bladder contractility. RN-1734 and RN-1747 are also some of the newly discovered TRPV4 antagonists (158). The synthetic phorbol ester, 4 α -phorbol 12, 13-didecanoate (4 α -PDD) specifically activates TRPV4. Ethanol inhibits TRPM8 but activates TRPV1 (159).

Although the channel pores allow conduction of divalent ions, trivalent cations like lanthanum (La^{3+}) and gadolinium (Gd^{3+}) have been seen to block most of the TRP channels. Gd^{3+} and La^{3+} blocks most members of the TRPC family but activates TRPC4 and TRPC5 in a concentration dependent manner. These two trivalent cations also differentially modulate the activity of TRPV members. TRPV2, TRPV4, TRPV5 and TRPV6 get blocked by them whereas TRPV1 get activated by Gd^{3+} ions. TRPM2 remains insensitive to around 100 μM La^{3+} ions whereas TRPM3 and TRPM8 get blocked by 100 μM gadolinium chloride (158).

1.2.8. pH

One of the basic principles of cellular homeostasis is to regulate the acid-base balance and maintenance of a pH of around 7.4. This balance gets disturbed under various circumstances like intake of excess acid, augmented secretion of gastric acid, defective acid containment in the urogenital and gastrointestinal tract, acidosis due to inflammation or hypoxia and metabolic acidosis (160). This proton imbalance is capable of damaging macromolecular structures and hence the ability to sense acid is conserved across most species. Nociceptors are furnished with an assorted collection of different acid sensors in order to detect changes in cellular pH. Subtle pH changes are detected by proton sensing GPCRSs, acid sensing ion channels (ASIC) and various two pore potassium channels. Greater pH fluctuations can be detected by TRPV1 ion channel (161). Some of the pH-sensitive TRP channels are:

* **TRPV1:** The ability of TRPs to sense protons was first characterized in TRPV1. TRPV1 gets activated only when the extracellular pH falls below 6 whereby it allows proton influx and causes intracellular acidification. Mild acidosis in the range of pH 7-6 is also capable of sensitizing TRPV1 to other stimuli like Capsaicin and heat. As a result, TRPV1 gets activated at normal body temperatures under conditions of acidosis. Synergistically various other factors like release of inflammatory molecules such as bradykinin, prostaglandins, NGF, 5-hydroxytryptamine, ATP facilitate TRPV1 channel opening by Capsaicin, heat and protons (161), (160).

* **TRPV4:** Just like TRPV1, TRPV4 is also potentiated by drop in extracellular pH below 6 and channel currents become maximum at pH 4. It is activated by citrate but not lactate and is seen to play a role in osmosensation and mechanosensation (161), (160).

* **TRPC4 and TRPC5:** Only subtle changes in extracellular pH causes activation of TRPC4 and TRPC5. If the pH falls beyond 6.5 then these channels are inhibited (160).

* **TRPP2:** Perception of sour taste that involves acidic stimuli is possible because of taste cells that co-express the TRP channel PKD2L1(TRPP2) and its partner PKD1L3 (162).

TRPP2 acts as a molecular sour sensor and its deletion leads to loss of this sensation.

* **TRPM7:** At physiological pH of around 7.4, TRPM7 binds to Mg^{2+} and Ca^{2+} and this prevents monovalent cationic currents. Whereas under acidic conditions when the extracellular pH is as low as 4 or 6, presence of higher concentrations of H^+ prevents the divalent cations from binding with TRPM7 and allows the influx of monovalent cations through it (163).

* **TRPA1:** It is involved in sensation of acid induced pain in humans. Only the human variant of TRPA1 was sensitive to low extracellular pH at a range of 7-5.4 but this extracellular acidosis failed to potentiate rhesus monkey and rodent TRPA1. In fact, protons exhibited an inhibitory role on rodent TRPA1. Thus TRPA1 acts as an acid sensor in human sensory neurons (164).

1.2.9. Mechanical stress

Mechanotransduction is the process whereby physical forces are converted into biochemical signals by specialized proteins resulting in physiological changes. TRP channels play an important role in mechanotransduction following changes in cell volume, augmented membrane tension, changes in osmolarity or fluid shear stress (165).

Most of the TRP channels are localized in the plasma membrane. Hence a direct force applied to the membrane or channel is capable of opening the channel without requirement of initiating a signalling cascade. Alternatively, a mechanical force that induces curvature of the lipid bilayer which culminates a tension that provokes channel opening. The TRPN channel of *C. elegans*, TRP-4, is directly gated by force and hence gets activated very quickly in less than a millisecond. It is required in the ciliated

mechanosensory cephalic neuron for force-induced conductance. *Drosophila* TRPN channel NOMPC is used by fruit flies to perceive the sense of touch. This channel is also directly gated by mechanical force (166).

In vivo, TRPV4 aids in the transduction of mechanical and osmotic stimuli. This property of TRPV4 is evolutionarily conserved as expression of mammalian TRPV4 in *osm-9* mutants of *C. elegans* was capable of rescuing its response to osmotic and mechanical stimuli (167). Mammals do not possess a TRPN ortholog. Nevertheless, TRPV4 endogenously expressed in urothelial cells as well as TRPV4 expressed in *Xenopus* oocyte can be activated by membrane stretch. Cell swelling due to osmotic force and fluid shear stress are also known to activate TRPV4 (168). TRPV1 present in osmosensory neurons is the primary osmosensor in brain. In vascular smooth muscle cells TRPV2 functions as a mechanosensor and plausibly gets activated by osmotic cell swelling. TRPC6 also gets activated by osmotic or mechanical stimuli. Hypotonic cell swelling activates human TRPM3. TRPM4 controls myogenic vasoconstriction in isolated vascular smooth muscle cells and cerebral arteries. It also regulates pressure-induced depolarization of smooth muscle cell. Cell stretch directly activates TRPM7. It is also potentiated by hypotonic cell swelling. The large number of ankyrin repeats of TRPA1 were proposed to act as a gating spring that generated mechanical forces leading to channel opening. Mammalian TRPA1 expression is observed in hair cell epithelia, however its deletion fails to reveal any auditory defects. However, experiments on cell lines, isolated neurons and mechanosensitive sensory afferent fibres prove TRPA1 to be mechanosensitive (165). Osmosensory transduction is the process whereby cell volume shrinkage due to certain conditions like dehydration results in TRPV1 activation. This causes membrane depolarization and spiking activity in osmosensory neurons. This TRPV1 activation is plausibly mediated by microtubules that physically interact with

TRPV1 (C-terminus) at the cell surface. Cell shrinkage causes the microtubules to exert a pushing force that results in channel opening (169).

1.2.10. Temperature

Four members of the TRPV family are known to be activated by warm to hot temperatures. TRPV3 (33°C) and TRPV4 (25°C-34°C) gets activated at warm temperatures whereas TRPV1 (>42°C) and TRPV2 (52°C) gets activated at noxiously hot temperatures (170). TRPV1 is gated by both voltage and temperature.

Expression of TRPV1 has been observed in small diameter sensory neurons of the TG, DRG and NG, hypothalamus where it might play an important role in thermoreception. TRPV1 knockout mice showed a decreased response towards noxious heat. Inflammatory mediators like ATP and bradykinin strongly reduces the temperature activation threshold of TRPV1 to around 30°C and as a result even warm temperatures become painful.

TRPV2 gets activated at extremely high temperatures of around 52°C. This channel is strongly expressed in the myelinated medium to large diameter DRG neurons, NG as well as in the hypothalamus. TRPV2 knockout mice exhibit lack of mechanical nociception but exhibits normal behaviour towards noxious heat stimuli (171)(172).

TRPV3 is activated at warm temperatures of around 34°C-39°C and they are thought to play an important role in thermosensation and thermal nociception. TRPV3 null mice demonstrate defects in perception of innocuous and noxious heat whereas their perception for other sensory stimuli remain intact (173). Experiments suggest that TRPV3 channels are much more involved in allowing mouse models to choose a comfortable temperature over value of the temperature itself. In the same line, TRPV4 gets activated at physiological range temperature. TRPV3 channels convey thermal stimuli via skin

keratinocytes and this information is finally transmitted to the sensory endings. These channels are also expressed in the sensory DRG and NG neurons as well as in the hypothalamus. TRPV1 and TRPV3 are found to co-localize in the DRG neurons.

TRPV4 channel responds dynamically to temperature changes within the physiological range. It plays an important role in thermoregulation as well as thermosensation (174).

Decreases in temperature are detected by 2 ion channels: TRPM8 (temperatures less than 25°C) and TRPA1 (temperature less than 18°C) (174). Experiments on mouse models suggest that activation of TRPM8 results in shivering-like muscle activity, hyperthermia, oxygen consumption, vasoconstriction of tail skin and heat seeking behaviour. Application of TRPM8 selective antagonists results in hypothermia, an effect that is absent from TRPM8 null systems (175). Cold temperature receptors are present on the corneal surface that detect minor fluctuations in temperature occurring on the ocular surface either due to exposure to dry environments or due to evaporation of the tear film during inter blinking period. One such cold thermoreceptor is TRPM8, which maintains the basal tear secretion that is required for ocular surface wetness (176).

The temperature threshold for TRPA1 activation is controversial as well as species specific. Many groups had initially claimed it be a sensor for noxiously cold temperatures in case of mammals (177), (178) but recently it has been declared to be a sensor for warm temperatures (179), (180). Apart from mammals, it is a warm sensor in insects, amphibians and reptiles (181).

1.2.11. Ca²⁺

Most of the TRP channels, if not all, are regulated by Ca²⁺. This ion may generate a positive or negative feedback loop on the channel but conducting Ca²⁺ ions through

them is one of their common physiological roles. In case of TRP channels, Ca^{2+} ions mediate desensitization via phosphatases, kinases, Calmodulin, phospholipases, etc. (182).

TRPV1: It is a Ca^{2+} permeable channel that is expressed in sensory nerves specialized for detection of painful stimuli. Persistent activation of TRPV1 leading to Ca^{2+} -influx results in channel desensitization and tachyphylaxis. This mechanism is thought to form the basis of pain management by Capsaicin application (183). Calcineurin, a Ca^{2+} -Calmodulin activated serine-threonine specific phosphatase, dephosphorylates TRPV1 resulting in channel desensitization (184). Whereas Ca^{2+} dependent activation of PKA and PKC tends to slow down the desensitization of TRPV1 (182). The N-terminal domain of TRPV1 contains a Calmodulin-binding site that overlaps with the ATP binding site. TRPV1 activation results in Ca^{2+} -influx, binding of Ca^{2+} to Calmodulin, activation of the Ca^{2+} -Calmodulin complex, binding of this complex to TRPV1 by substituting ATP, desensitization of TRPV1 (183). Ca^{2+} binding protein Calmodulin (CaM) binds to a 35 amino acid long segment in the C-terminus of TRPV1. Disruption of this segment inhibits TRPV1 desensitization (185). Similarly, Ca^{2+} -influx during TRPV1 activation results in activation of PLC that degrades PIP_2 . This disrupts the interaction of TRPV1 with its positive regulator PIP_2 and results in subsequent desensitization (182).

TRPV2: Ca^{2+} -influx due to TRPV2 activation results in channel desensitization due to PIP_2 hydrolysis.

TRPV3: Unlike other TRPV channels like TRPV1 or TRPV4, TRPV3 is unique as it gets sensitized upon repeated stimulations by its agonists. An Asp residue at position 641 in its pore region is involved in high affinity binding of extracellular Ca^{2+} that strongly blocks the channel. On the other hand, intracellular Ca^{2+} binds to Calmodulin (CaM) and this Ca^{2+} -Calmodulin complex binds to a stretch at the N-terminal region of TRPV3 and

inhibits sensitization. Repetitive stimulation of TRPV3 reduces the binding affinity of the channel for Ca^{2+} -CaM and thereby sensitizes the channel. Thus TRPV3 is inhibited by both extracellular as well as intracellular Ca^{2+} (186).

TRPV4: Activation of this channel results in Ca^{2+} -influx which then binds to CaM and this Ca^{2+} -CaM complex goes and binds to a region in C-terminal region of TRPV4. This generates a positive feedback loop for the channel thereby increasing the amplitude and speed of the response. This increased intracellular Ca^{2+} then generates as a negative feedback loop that inhibits further potentiation of TRPV4 even in presence of the stimulus. However, the exact mechanism behind this inhibition is still unclear (187).

TRPV5 and TRPV6: In contrast to other TRP channels, TRPV5 and TRPV6 are highly permeable to Ca^{2+} . Once activated, both these channels allow Ca^{2+} -influx which then generates a negative feedback to prevent further Ca^{2+} -influx by inactivating the channels. TRPV6 undergoes faster inactivation as compared to TRPV5. Like most other TRP channels, TRPV5 and TRPV6 are also inhibited by the binding of Ca^{2+} -CaM complex. PIP_2 acts a positive regulator of TRPV6. Ca^{2+} -dependent activation of PLC results in depletion of PIP_2 and thereby results in TRPV6 inactivation (183).

TRPA1: Ca^{2+} directly binds to TRPA1 and activates it at lower concentrations (<1 mM) but at higher concentrations (>1mM) it inhibits the channel.

TRPM2: Ca^{2+} -influx upon TRPM2 activation due to oxidative stress triggers several Ca^{2+} dependent signalling pathways that are necessary for a large number of pathological processes like release of cytokines, cell death, inflammatory responses, etc. Ca^{2+} ions are also involved in direct activation of this channel.

TRPM3: It is permeable to Ca^{2+} entry as well as positively regulated by Ca^{2+} ions.

TRPM4 and TRPM5: Unlike other TRP channels these two ion channels conduct monovalent ions and hence are Ca^{2+} impermeable. However, intracellular Ca^{2+} is both

necessary and sufficient for their activation. TRPM5 gets activated at intracellular Ca^{2+} concentration ranging from 0.3 μM to 1 μM but gets inhibited at concentrations exceeding 1 μM . TRPM4 on the other hand gets activated within the same intracellular Ca^{2+} concentration range as that of TRPM5 but higher concentrations have no inhibitory role on it.

TRPM8: It is Ca^{2+} -permeable but once active, Ca^{2+} entry rapidly triggers desensitization of the channel. *In vivo* experiments suggest that PLC mediated hydrolysis of PIP_2 forms the basis of TRPM8 desensitization.

TRPP2: It gets activated at lower Ca^{2+} concentrations whereas higher concentrations inhibit it. This ion directly binds to the EF-hand domain to activate it. Phosphorylation of TRPP channels by CKII increases the Ca^{2+} sensitivity of these channels (183).

1.3. TRP channels and disease

Diseases that occur due to defects in ion channels by either genetic or acquired factors are collectively referred to as Channelopathies (188). An autosomal dominant disorder known as *Gorlin syndrome* is thought to occur due to mutations in the TRPC1 gene. Type 2 Diabetes mellitus is associated with single nucleotide polymorphisms in TRPC1 gene. Focal and Segmental Glomerulosclerosis (FSGS) Type 2 has been linked with 6 mutations in TRPC6 gene. TRPV2 has been linked to diseases like cancer, *Duchenne muscular myopathy* and diabetes. Three mutations in TRPV3, namely G573S, G573C and W692G has been associated with *Olmsted Syndrome*, a skin disorder. TRPV3-G573A mutation has also been linked to *Olmsted syndrome*. TRPV4 gene defects have been linked to many bone-related disorders like autosomal dominant *Brachyolmia type 3*, *metatropic dysplasia*, *pseudo-Morquio type 2 syndrome*, *Spondylometaphyseal dysplasia (SMD) Kozłowski type (SMDK)*. TRPV4 gene mutations also lead to several neuropathic

disorders like Charcot-Marie-Tooth neuropathy type 2, congenital spinal muscular dystrophy. TRPM1 defects have been linked to retinal disorders like autosomal recessive congenital stationary night blindness type 1C. Mutations in TRPM2 and TRPM7 genes have been thought to cause two neurodegenerative disorders Guamanian amyotrophic lateral sclerosis (ALS-G) and parkinsonism-dementia complex of Guam (PD-G). TRPM4 mutations cause progressive familial heart block type I. Around 35 mutations have been reported in TRPM6 that results in faulty Mg^{2+} homeostasis and a disease named hypomagnesaemia with secondary hypocalcaemia (HSH)-1. A point mutation in TM4 region of TRPA1 has been linked to an autosomal dominant pain causing channelopathy named as familial episodic pain syndrome. Occurrence of a SNP in TRPA1 N-terminus has been associated with patients' suffering from acute pain and paradoxical heat sensation (188)(189). An autosomal recessive disorder named ML-IV is caused by mutations in the TRPML1 gene. This mutation results in lysosomal storage defects that's imparts neurodegenerative attributes to patients suffering from it. Mutations in TRPP1 causes Autosomal dominant polycystic kidney disease (ADPKD). Mutations in this channel has been also associated with structural defects in the heart e.g. defective formation of septum (189) (190). Elevated expression of TRPM7 mRNA has been observed in different types of cancer tumours (nasopharyngeal, breast, pancreatic). TRPM7 knockdown or silencing has substantially reduced metastasis in all these tumour types (191). TRPV4 knockdown in breast cancer cells did not improve their viability, but led to significant reduction in metastasis, migration and trans-endothelial migration (192). Elevated levels of TRPV2 mRNA has been also found in metastatic prostate cancer cells (193). Increased levels of TRPC5 has been associated with colon cancer progression (194). Several TRP channels namely TRPV1, TRPC5, TRPC1, TRPA1, TRPM8, TRPV4 have been linked with the progression of rheumatoid arthritis (195).

1.4. Specific Introduction to TRPV1

1.4.1. TRPV1 structure

Till 2008, no 3D structure of full-length TRPV1 was available. The first structure of TRPV1 was resolved at 19Å resolution by single particle cryo electron microscopy (cryo EM). According to this study, TRPV1 assumes a basket like structure when embedded in the plasma membrane with nearly 70 % of the structure lying in the cytoplasmic region that comprises the N-and C-terminal regions of the channel. The more compact region (~30%) remains tethered to the membrane that comprises the transmembrane portions of the channel (196). In 2013, using single particle cryo EM with some advancements the structure of TRPV1 was resolved at 3.4Å resolution without crystallization (Figure 4). In this structure, the first two ARD were not resolved and in the C-terminal region, the side chain densities were also not resolvable. The atomic model of TRPV1 was constituted from L360 to A719, which indicates that part of TBS1 and entire TBS2 structure remained unresolved. According to this structure the N-terminus consists of 6 Ankyrin Repeat Domains (ARDs) that is followed by a linker domain that connects it to a pre-S1 helix region. This linker region is a tightly packed domain comprising of β -sheets and α -helices that gets sandwiched between the 6th ARD one end and the pre-S1 helix and TRP domain on the other end. Each TRPV1 subunit comprises of a voltage sensing S1-S4 transmembrane region and an ion conducting S5-P-S6 pore region. A helical S4-S5 linker connects the S1-S4 region with the S5-P-S6 region in each TRPV1 subunit. The S6 helix is followed by the TRP-domain, a region that is conserved in almost all TRP channels. The pore region has a wider outer mouth and a short selectivity filter (197). TRPV1 undergoes different conformational changes upon being bound by different ligands. The model below (Figure 5) explains that in its closed state, the pathway for ion influx gets blocked by the “upper selectivity filter” (1) and the “lower gate” (2). Upper

right panel shows that some TRPV1 ligands like spider toxins and protons bind to the outer pore region that induces a conformational change mostly by the allosteric coupling between the S5 helix and the pore helix.

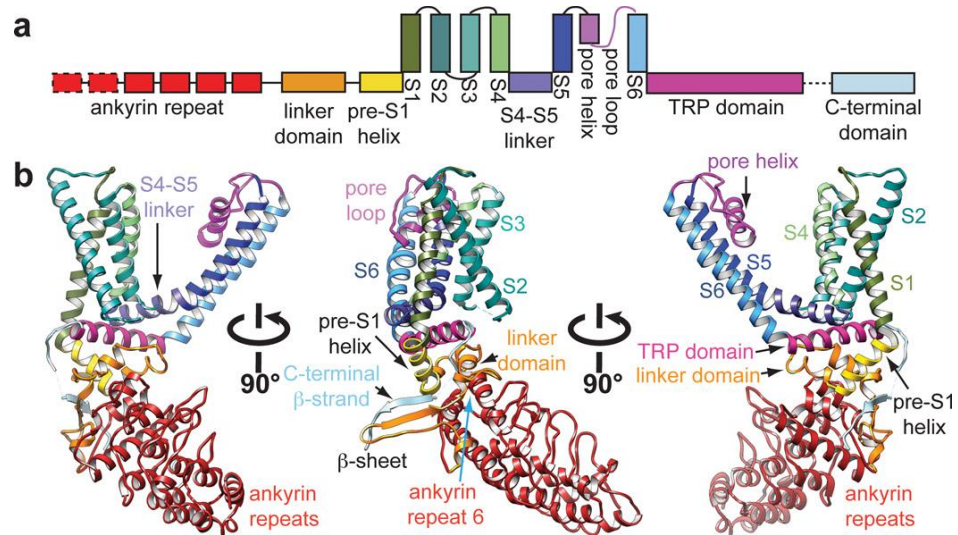


Figure 4. Structural details of Rat TRPV1 as revealed by Cryo EM at 3.4 Å resolution. a) Linear diagrammatic representation of a single TRPV1 subunit highlighting the major structural domains as revealed by Cryo EM. Dashed regions denote areas where sufficient densities were lacking or where exact residues could not be assigned. b) Ribbon diagrams depicting three different views of a TRPV1 monomer demarcating specific domains. Figure taken from *Liao et al, 2013* (197).

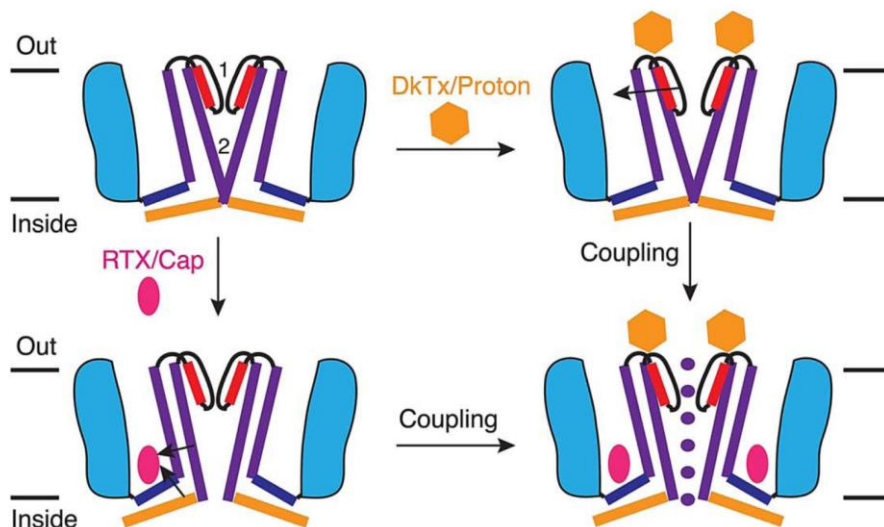


Figure 5. Dual gate mechanism of TRPV1 activation by its specific agonists. Figure taken from *Cao et al. 2013* (198).

This relieves the restriction by selectivity filter. Again, some Vanilloids like RTX and Capsaicin that bind to a hydrophobic pocket formed by the S3-S4 helix, S4-S5 linker and the pore, elicit conformational changes that dilate the lower gate (lower left panel). Expansion of the lower gate is plausibly brought about by the allosteric coupling of TRP domain, S6, S5 and S4 helices. The lower right panel shows that total expansion of the ion permeation pathway occurs upon opening of both upper and lower gates. This leads to maximal ion influx (198). Binding of DkTx (a tarantula spider toxin) to TRPV1 is stabilized by the formation of a toxin-membrane lipid-TRPV1 tripartite complex. Closed conformation of TRPV1 is stabilized by binding of phosphoinositides in its the Vanilloid-binding pocket. Vanilloid agonists displace these lipids in order to induce channel activation (199).

1.4.2. TRPV1 expression

Mammalian TRPV1 expression is most profound in the unmyelinated C-type sensory nerve fibres and partly in the sparsely myelinated A δ -type sensory nerve fibres. In the peripheral nervous system, this channel is principally expressed in trigeminal ganglia (TG), dorsal root ganglia (DRG), vagal ganglia and in some other small neurons. Within the central nervous system its expression can be traced in the amygdala, thalamus, striatum and some other areas. Various other organs within the human body like heart, lungs, kidney, stomach, pancreas, eyes, liver, small intestine, uterus express TRPV1 (200)(201)(202). In the gastrointestinal tract, TRPV1 is mainly distributed in the myenteric nerve plexus, submucosal nerve plexus, gastrointestinal muscle mucosa, gastric antral G cells, gastric mucosal cells and gastric parietal cells. In the cardiovascular system, TRPV1 expression can be seen in the vascular endothelial cells, perivascular nerve cells and smooth muscle cells. TRPV1 expression in the respiratory system is mostly seen in

the C-like sensory nerve fibres (200). TRPV1 distribution has also been observed in human odontoblasts of wisdom teeth (203). T-cells, mast cells, epidermal keratinocytes, sebocytes, cells of the hair follicles, sweat glands also express TRPV1 (204).

TRPV1 mostly localizes to the plasma membrane to execute its functions, but there are various intracellular organelles where its localization and functionality has been observed. TRPV1 expression has been observed in intracellular vesicles where it physically interacts with vesicular proteins like Synaptotagmin IX and Snapin. Upon activation these TRPV1 containing vesicles undergo PKC-dependent exocytosis (205). Amongst other subcellular organelles, TRPV1 expression has been also found in ER and Golgi apparatus (206)(207). It is also found in mitochondria. Mitochondrial TRPV1 induce the migration of microglial cells. Its activation increases intra-mitochondrial Ca^{2+} -levels that trigger depolarization and generation of mitochondrial ROS, MAPK activation and stimulates chemotactic movement of microglia (208). In microglia, TRPV1 is also seen to co-localize with lysosomal marker Lamp1 (208).

1.4.3. Cellular functions of TRPV1

Since its discovery in 1997 by Caterina et al., a lot of studies have focussed the importance of TRPV1 in nociception. It acts as an integrator of external physical stimuli and chemical stimuli and intracellular signalling pathways. However, presence of TRPV1 in intracellular organelle membranes in different cell types have paved the way for extensive studies on its role in regulating calcium homeostasis and various signalling pathways in these organelles. Activation of TRPV1 present in membranes of neuronal cells allow influx of Ca^{2+} ions. This generates action potentials and subsequent transmission of signals to the brain. Thus, sensory neurons isolated from TRPV1 knockout mice were responsive towards noxious mechanical stimuli, but were insensitive

to painfully warm temperatures, noxious Vanilloid compounds and exhibited minor thermal hypersensitivity under inflammatory conditions. Thus TRPV1 is essential for perception of pain, noxious stimuli and tissue injury induced thermal hyperalgesia (209). Apart from activation, TRPV1 gets sensitized by various components that are released during tissue injury or inflammation, such as neurotrophins, cytokines, neurotransmitters, lipids. These components of the inflammatory soup decrease the temperature threshold and proton concentrations required for TRPV1 activation. This forms the basis of hypersensitivity in damaged tissues to noxious stimuli (210). TRPV1 positive sensory neurons are capable of releasing neuropeptides like CGRP (Calcitonin Gene Related Peptide) and Substance P upon channel activation. These neuropeptides are involved in various signalling events that have various physiological implications. TRPV1, CGRP and substance P mediates nociception during acute pancreatitis (211). TRPV1 activation and the subsequent release of CGRP regulates osteoclastogenesis that prevents loss of alveolar bone in models of acute periodontitis (212). Glucose induced insulin secretion is also mediated by TRPV1 activation induced release of CGRP and substance P (213). Activation of TRPV1 in vascular smooth muscle cells induces vasoconstriction (214). Cardiac differentiation of mouse embryonic stem cells is positively regulated by TRPV1. Capsaicin-induced activation of TRPV1 in endothelial cells produced NO that causes vasorelaxation (210).

1.4.4. Physiological functions of TRPV1

TRPV1 is responsible for perception of noxiously warm temperatures exceeding 42°C that triggers pain *in vivo*. TRPV1 knockout animals showed a reduced response towards painful heat, Capsaicin and protons. Various studies have shown that TRPV1 plays an important role in controlling obesity, diabetes and insulin resistance. Infection

induces inflammation and upregulates the expression of various aminoglycoside permeant ion channels, including TRPV1. Aminoglycoside containing antibiotics help in treating bacterial infections but cause cochlear toxicity and thereby hearing loss as a side effect. Infection triggered upregulation of TRPV1 induces cochlear toxicity by increased permeation of aminoglycosides, a phenomena absent in *TRPV1*^{-/-} mice. Thus blocking the channel can aid in preventing auditory impairments (215). This channel is also responsible for normal functioning of urinary bladder. Cystitis, a condition of inflamed urinary bladder that causes visceral pain can be treated by application of TRPV1 specific antagonists in mouse models. In fact, this condition is not observed in TRPV1 null mice. Various polymorphisms in TRPV1 gene expressed in neurons innervating the lungs play an important role in the pathophysiology of asthma (216). Extensive studies on the role of TRPV1 in brain has revealed that apart from its role in pain transduction, it plays an important role in synaptic transmission, neuronal plasticity, communication between neurons and microglia and in overall brain development. Its activities also have implications in neurodegenerative disorders like Epilepsy, Alzheimer's disease, psychiatric disorders like depression, anxiety and Schizophrenia (217). The role of TRPV1 has also been studied in drug addiction related behaviours (218). It plays an important role in thermoregulation however the exact mechanisms governing such functions require further unravelling (218). The cardiovascular pathology is largely regulated by TRPV1. The motor functions of gastrointestinal tract are also controlled by this channel (217).

1.4.5. Regulation of TRPV1 by microtubules

The C-terminus of TRPV1 is capable of binding to both tubulin dimers and polymerised microtubules in a Ca²⁺-sensitive manner. This interaction is mostly mediated

by β -tubulin. Under depolymerisation conditions as those induced by cold temperature and Nocodazole, this TRPV1-microtubule interaction tends to stabilize the latter (121). TRPV1 activation induces rapid disassembly of dynamic microtubules whereas the stable populations of microtubules, actin and neurofilaments remain unaffected (124). TRPV1 activation induced disassembly of microtubules causes' growth cone retraction and collapse as well as varicosity formation due to imbalance in the anterograde and retrograde force operating within the neurites (125). The C-terminus of TRPV1 contains two tubulin binding sequences (TBS), namely TBS1 and TBS2 that mediate its interaction with the tubulin dimers and polymerised microtubules. These two stretches were found to be highly conserved across vertebrate evolution (122). TRPV1 expression in neurons initiates filopodia formation and neuritogenesis by stabilizing microtubules in these structures (126). Phosphorylation of Ser800 in C-terminus of TRPV1 by PKC causes disassembly of microtubules in an ion-channel independent manner (110). Integrity of microtubules is important for maintenance of TRPV1 function and its responsiveness towards activation stimuli (219). Microtubule-TRPV1 interaction in osmosensory neurons forms the basis of osmosensation (169) and this interaction simply pushes open these channels (127). A *Drosophila* TRPV channel homologue, *Inactive*, regulates neurotransmission and synaptic development. Loss of this channel resulted in destabilization of pre-synaptic microtubules and subsequent reduction in synaptic growth. However, expression of human TRPV1 in these *Inactive* deficient neurons restored back the normal functions. Thus, *Inactive* regulates synaptic structure and function by maintaining resting levels of calcium in pre-synaptic neurons (220).

1.4.6. Regulation of TRPV1 by cholesterol

TRPV1 activity as well molecular presence of functional channels on the plasma membrane is determined by the levels of membrane cholesterol (129). Gating behaviour of TRPV1 by different Vanilloid and non-Vanilloid compounds were altered upon depletion of different components of the lipid rafts, namely, by depletion of cholesterol, sphingomyelin and gangliosides (130). Rat TRPV1 exhibited significant reduction in membrane currents in presence of Capsaicin upon saturation of cholesterol. Even in absence of Capsaicin, cholesterol enrichment inhibited TRPV1 mediated currents upon activation with voltage and elevated temperature. The S5 helix of TRPV1 contains a cholesterol binding site which when bound by cholesterol prevents channel opening even in presence of its agonists (221). Cholesterol enrichment also shifted the activation temperature of TRPV1 to higher values whereas cholesterol depletion had no effect on the activation temperature threshold (222). Dietary Monoacylglycerols act as TRPV1 agonists that increases the expression of UCP1 (Uncoupling Protein 1) in brown adipose tissues and thereby prevent accumulation of visceral fat (223). Development of atherosclerosis occurs largely due to accumulation of lipids in Vascular Smooth Muscle Cells (VSMC). High fat diet induced atherosclerosis can be alleviated by TRPV1 activation (224). Membrane cholesterol levels alter the pore dilation properties of TRPV1 (132). Moxibustion is a Chinese traditional medical practice for treating various diseases by applying heat to specific regions on the body surface with an ignited moxa wool. Temperature dependent activation of TRPV1 forms the basis of moxibustion in reducing blood cholesterol levels in mice with acute hyperlipidaemia (225). Eugenol exerts its hypolipidemic and anti-fatty liver effects by interacting with TRPV1 (226).

1.5. Specific introduction to TRPA1

1.5.1. TRPA1 structure

Single particle cryo-electron microscopy has helped in determining the three dimensional structure of full-length Human TRPA1 at $\sim 4\text{\AA}$ resolution when bound to its specific agonist AITC as well as its antagonists HC-030031 and A967079 (Figure 6). Each monomer comprises of six transmembrane helices (S1-S6) with a re-entrant “pore-loop” between S5 and S6. The cytoplasmic N and C-termini comprise around 80% of its total mass. A homo-tetrameric assembly of such monomers is brought about by domain swapping that renders a functional channel. A tetrameric coiled coil domain exists just near the C-terminal region below the ion permeation pore. It provides a locus for interaction of all 4 subunits, mediates cytosolic interactions with other proteins and helps the channel to associate with polyphosphates. TRPA1, unlike other TRP channels, lack the conserved TRP domain as it does not harbour the canonical TRP box motif. However, an alpha helix just after TM6 structurally and topologically resembles this TRP domain and is therefore described as TRP-like domain. The N-terminus of TRPA1 contains about 14-18 Ankyrin Repeat Domains. The channel assembly is stabilized by the interaction between AR12 and coiled coil region as well as AR16 and the first helix-turn-helix. The Ankyrin Repeat Domains (ARD) are connected to the TM regions by a pre-S1 region. This region comprises of 2 elements: a linker domain followed by pre-S1 helix. This region is of particular interest as this is the site of action of most electrophilic compounds. The central cavity in the ion permeation pathway of agonist bound TRPA1 grossly resembled TRPV1 in having two constrictions. However, it differed with TRPV1 in having two pore helices in its outer pore domain. One of these helices is negatively charged and thereby attracts cations and repels anions from the pore mouth. Whereas TRPV1 has only a single pore helix. TRPA1 and TRPV1 also differed in the gate regions

of the ion selectivity filter. Gly643 and Met644 formed the upper gate in TRPV1 whereas only a single residue Asp915 forms the upper gate in TRPA1. This upper pore gate has a diameter of 7Å and allows the entry of partially dehydrated Ca²⁺ ions. Previous reports have shown the importance of Asp915 in mouse TRPA1 in regulating its permeability to calcium ions. TRPV1 and TRPA1 also differ in their lower gate structure. The lower gate of Rat TRPV1 contains a single constriction at residue Ile679. Human TRPA1 lower gate contains two constrictions formed by Ile and Val at positions 957 and 961 respectively. However, it differed with TRPV1 in having two pore helices in its outer pore domain. One of these helices is negatively charged and thereby attracts cations and repels anions from the pore mouth. Whereas TRPV1 has only a single pore helix. TRPA1 and TRPV1 also differed in the gate regions of the ion selectivity filter. Gly643 and Met644 formed the upper gate in TRPV1 whereas only a single residue Asp915 forms the upper gate in TRPA1. This upper pore gate has a diameter of 7Å and allows the entry of partially dehydrated Ca²⁺ ions. Previous reports have shown the importance of Asp915 in mouse TRPA1 in regulating its permeability to Ca²⁺ ions. TRPV1 and TRPA1 also differ in their lower gate structure. The lower gate of Rat TRPV1 contains a single constriction at residue Ile679. Human TRPA1 lower gate contains two constrictions formed by Ile and Val at positions 957 and 961 respectively. This creates a highly constricted ion permeation funnel that prevents entry of rehydrated cations (227). Deletion of ARD in TRPA1 renders a non-functional channel that exhibits erratic trafficking to the plasma membrane (228). The pre-S1 helix region contains highly conserved cysteine residues namely Cys-622, Cys-642, Cys-666 that are crucial for interaction with electrophilic compounds (229). TRPA1 activation might depend upon disulphide bonding between these critical cysteine residue pairs: Cys-666-Cys-622, Cys-666-Cys-463, Cys-622-Cys-609, and Cys-666-Cys-193 (230).

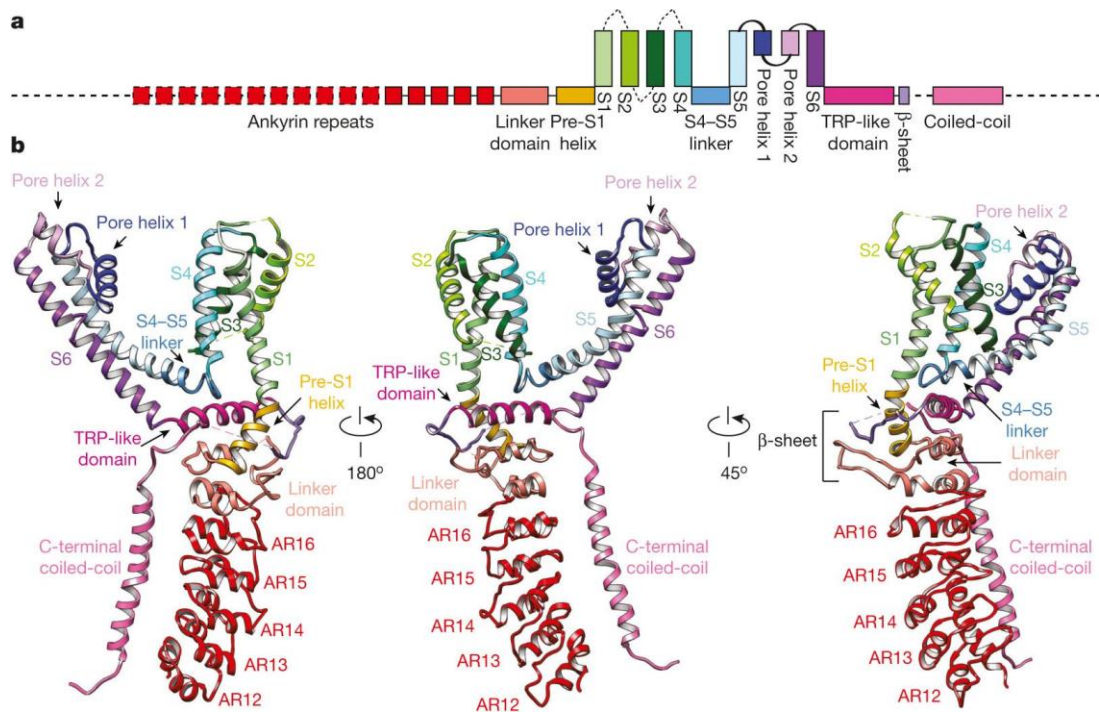


Figure 6. Structural details of Human TRPA1 as revealed by Cryo EM at $\sim 4 \text{ \AA}$ resolution. a) Linear diagram demonstrating major structural domains of Human TRPA1. The colour coded match with the ribbon diagrams below. Boxes and dashed lines designate regions of insufficient density that were unresolvable. The unresolvable regions are : loop containing Cys 665, sequence before ARD12, S1–S2, S2–S3 and S3–S4 linkers, the connection between third β -strand and coiled-coil, C terminus subsequent to coiled-coil), or where specific residues could not be definitively assigned (portion of the linker before and after the coiled-coil). b) Ribbon diagrams depicting three views of the TRPA1 subunit. Figure taken from Paulsen *et al*, 2015 (227).

The Cys residue at 622 position is very critical, as its mutation to serine renders the channel insensitive to electrophilic compounds like cinammaldehyde and AITC, whereas its response towards non-electrophilic agonists like menthol and polygodial remains intact. In fact covalent modification of Cys622 in only two TRPA1 monomers, out of four, was sufficient to open the channel (231). Human TRPA1 gets activated by increase in intracellular Ca^{2+} ion concentrations. These Ca^{2+} ions bind the EF-hand motif (466-477 AA) present in N-terminus of TRPA1. Deletion of this segment or substitution of Asp466 and Asp477 with Alanine, rendered the channel completely insensitive to intracellular Ca^{2+} (232).

1.5.2. TRPA1 expression

TRPA1 was originally discovered in cultured human fibroblasts. Its expression has been found in a subset of somatic (DRG, TG) and visceral primary sensory neurons. TRPV1 expressing neurons also express TRPA1 (177). TRPA1 expression has been detected in basal cells of corneal epithelium. Loss of TRPA1 or blocking it with its specific antagonist's suppressed fibrogenic and inflammatory reactions in a chemically injured cornea (233). Noxious cold sensations in teeth are perceived by TRPA1 expressed in odontoblasts (203). Within the Human urethra, TRPA1 channels have been seen to express in urothelial cells, detrusor muscle and C-fibre afferents in lamina propria. Activation of TRPA1 in these regions enhanced frequency of micturition and contraction of detrusor muscles (234). In colonic epithelial cells, activation of TRPA1 results in rapid anion secretion which is a part of the host defence mechanism (235). Human airway cells comprising of smooth muscle cells, fibroblasts, epithelial cells express functional TRPA1 channels. Acrolein and cigarette smoke activated TRPA1 in these cells that caused release of IL-8, a phenomenon that was blocked by application of TRPA1 specific antagonists (236). TRPA1 expression has been also observed in pancreatic β cells, where its activation by various endogenous and exogenous ligands causes depolarization of membrane followed by Ca^{2+} -influx and a subsequent release of insulin (237). A population of brain astrocytes express TRPA1 where they mediate significant Ca^{2+} signalling events (238). Apart from these, TRPA1 expression has been detected in keratinocytes, vascular endothelial cells, lung, gut, synoviocytes, epithelial melanocytes, etc. (239). Recently, its expression has also been observed in T-cells isolated from mouse and human spleen. Its activation regulates various T-cell functions including release of interleukins and leads to increase in intracellular Ca^{2+} -levels (240).

1.5.3. Cellular functions of TRPA1

TRPA1 acts as a redox sensor which gets activated by electrophiles, Nitric Oxide (NO) and hydrogen peroxide. Its activity is modulated by noxious compounds that covalently modify reactive cysteine residues present in its cytosolic domains. This causes activation of the channel and subsequent signalling of tissue damage via the pain pathway (241). TRPA1 acts as an oxygen sensor under both hypoxic and hyperoxic conditions in mammals (242). In cancer cells, TRPA1 promotes ROS tolerance by activation of Ca^{2+} -dependent anti-apoptotic signalling pathways (243). Tissue damage results in accumulation of reactive oxygen species (ROS), a condition termed as oxidative stress that greatly affects cellular functions. TRPA1 serves as an integrator of cellular stress and is capable of sensing ROS and noxious stimuli. Tissue injury and inflammation generates various lipid peroxidation products as well as oxidised lipids that are capable of activating TRPA1 (239). Apart from ROS, reactive nitrogen species are also capable of activating TRPA1. High concentrations of hydrogen sulphide elicit pain by activation of TRPA1 (244). In *Drosophila*, light induced production of hydrogen peroxide activates TRPA1 isoforms that enable them to detect strong UV light (245). In mouse brochopulmonary C-fibres, acute mitochondrial dysfunction generates ROS that activates TRPA1 (246). Carbon dioxide (CO_2) diffuses inside cells and causes intracellular acidification which activates TRPA1. Thus, TRPA1 forms an integral part of the CO_2 sensing machinery (247). TRPA1 stimulation is associated with release of pro-inflammatory neuropeptides like substance P and CGRP which henceforth induces leakage of plasma proteins, vasodilation and stimulatory effects on adjacent immune cells. The role of TRPA1 in inflammatory hypersensitivity was first evidenced when it was seen to get activated by an inflammatory peptide Bradykinin via a PLC/ Ca^{2+} dependent pathway (248). PIP_2 acts a positive modulator of TRP channel activity. Though its effects are less as compared to

other TRP channels but PIP₂-depletion results in desensitization of TRPA1 (96).

1.5.4. Physiological functions of TRPA1

TRPA1 is a non-selective cation channel that is permeable to Ca²⁺ ions, gated by voltage, temperature, mechanical stimuli as well as various exogenous and endogenous molecules. TRPA1 was initially considered to be a sensor for noxiously cold temperature (177) (249). It mediates the burning cold pain sensation evoked by noxious cold temperature. TRPA1 deficient mice showed reduced sensitivity to cold temperatures as low as 0°C and acetone evaporation that produces a cooling sensation (178). However, several others reported that TRPA1 was not required for cold sensation both at the cellular and behavioural level (250) (251). This ambiguity regarding TRPA1's role as a thermosensor holds true only in case of mammals. In other species like Western Clawed frog and lizard, it gets activated at warm temperatures at about 40°C and 34°C (252). *Drosophila* TRPA1 also gets activated within a warm temperature range of 24°C-29°C (253). Trigeminal neurons innervating the pit organs of snakes have an extensive enrichment of mammalian TRPA1 orthologue. These pit organs are heated up by the infrared rays emanating from the bodies of preys or predators. Thus TRPA1 in snakes not only enable in infrared sensation but also plays an important role in thermoregulation and also act as an critical molecule involved in pray-predator relationships (254). However, TRPA1 does not act as a temperature sensor in Zebrafishes. Both the TRPA1 orthologues in Zebrafishes respond to chemical stimuli that activate mammalian TRPA1 but they play no role in thermosensation or mechanosensation (255). In mammals, TRPA1 also acts a sensor for Poly Unsaturated Fatty Acids (PUFA) (256). The TRPA1 orthologue in *Caenorhabditis elegans* is gated by mechanical stimuli (257). TRPA1 activation directly evokes pain and induces vasodilation and neurogenic inflammation (258). TRPA1 has

been seen to be responsive towards bacterial and viral products. For example, Lipopolysaccharide (LPS) the toxic components of gram negative bacterial cell wall, activates TRPA1 that causes immediate stimulation of nociceptors (259). In vagal and somatic nociceptors, LPS induced activation of TRPA1 causes release of neuropeptides like CGRP that results in pain, inflammation and vasodilation (259). Monosodium iodoacetate (MIA) induced osteoarthritis in mice cause acute joint pain, inflammation and cartilage degradation. All these responses are mediated by TRPA1 as TRPA1 deficient mice failed to elicit such responses in presence of the stimuli. Thus TRPA1 acts a potential mediator as well as drug target in osteoarthritis (260). TRPA1 acts as potential drug target for treating headache and migraine pain because it gets activated by their causative agents like acrolein, formaldehyde, cigarette smoke, chlorine, various prostaglandins, reactive oxygen and nitrogen species (261). Itch, a protective response against cutaneous irritants and parasites, is also mediated by TRPA1 (248).

1.5.5. Regulation of TRPA1 by cholesterol

Integrity of lipid rafts plays an important role in channel gating. Disruption of lipid rafts by depleting cholesterol with methyl- β -cyclodextrin, sphingomyelin with sphingomyelinase and ganglioside with myriocin significantly and in a concentration dependent manner decreased the opening probability of TRPA1 when stimulated with its specific agonists AITC or formaldehyde (262). The most important factor for development of atherosclerosis is deregulation of cholesterol metabolism. ABC transporters play an important role in cholesterol homeostasis by regulating cholesterol efflux and reverse cholesterol transport. This aids in protecting arteries from atherosclerosis. TRPA1 inhibition or its genetic ablation results in augmented lipid accumulation in macrophage foam cells by decreasing ABC transporter mediated efflux

of cholesterol, thereby intensifying systemic inflammation and atherosclerosis progression in Apolipoprotein E deficient mice. Contrarily, TRPA1 activation by AITC resulted in upregulation of ABC transporters. Thus TRPA1 plays an important role in cholesterol metabolism and atherosclerosis progression (263). Mouse TRPA1 preferentially localizes in cholesterol enriched micro domains of the lipid bilayer termed as lipid rafts. Depletion of membrane cholesterol decreased the sensitivity of the channel towards its agonists. Two motifs in TM2 and TM4 of mouse TRPA1 mediates its interaction with cholesterol, a cross-talk that is important for the channels' membrane localization and function (264).

1.6. Specific objectives of this study

TRPV1 and TRPA1 are capable of perceiving diverse chemical and temperature stimuli and mediate stimulation to sensory neurons and also mediate neurogenic inflammation and pain in certain conditions. Thus, these two channels provide an example where different genes with similar structure and biological functions influence each others and such aspects are fine-tuned during the course of evolution. Notably, there are several reports that suggests that both TRPV1 and TRPA1 often co-express in same cells, located in the same membranous environments. Results from different studies suggest that these two ion channels can have very similar aspects resulting in “biological synergism” or have opposite effects resulting in “biological antagonism”. Therefore, studying these two channels in similar biological context is useful to understand how minute changes can lead to gross functional changes.

Approximately 30% of TRPV1 expressing sensory neurons express TRPA1, whereas 97% of TRPA1 expressing neurons express TRPV1 (214). In sensory neurons as well as in heterologous expression systems, mustard oil induced desensitization of

TRPA1 is regulated by TRPV1 (95). Apart from neuronal functions, these two channels are also expressed in diverse non-neuronal cells. Various non-neuronal cells like smooth muscle cells and endothelial cells also co-express these ion channels (265). Even in CD4⁺ T-cells, TRPA1 and TRPV1 co-express together and TRPA1 exhibits anti-inflammatory response by inhibiting TRPV1 in T-cell mediated colitis (266). Apart from mammals, ancestral vertebrates like Western Clawed frog and Green Anole lizard also co-express TRPA1 and TRPV1 (252). It has been observed that TRPA1 channel properties are regulated by TRPV1 mostly by a direct interaction between the two channels that form a complex at the plasma membrane and this interaction affects single channel characteristics of TRPA1, including its open probability and voltage-current relationships at negative membrane potentials (267). In fact, co-expression of TRPV1 and TRPA1 is necessary for agonist induced voltage gating of TRPA1, a feature that gets disrupted in neurons expressing only TRPA1. The specific agonists of each of these channels are also capable of cross desensitisation of each other and this can play an integrative role in regulating nociceptor function (268). Hence it will be intriguing to study the crosstalk between membranous and sub-membranous components with TRPA1 and TRPV1, the channels which functionally regulate each other. In view of this, the following four objectives were aimed to be studied in this thesis:

- * Importance of TRPV1-tubulin complex in channel localization and cellular functions
- * Importance of TRPV1-cholesterol complex in channel localization and cellular functions
- * Expression of TRPA1 in vertebrate sperm cells, its function and interaction with microtubule cytoskeleton.
- * Molecular evolution of TRPA1 during vertebrate evolution and importance of TRPA1-cholesterol complex in channel localization.

Chapter 2

Results

2.1. Importance of TRPV1-tubulin complex in channel localization and cellular functions

The C-terminus of TRPV1 is capable of binding both tubulin dimers as well as intact polymerised microtubules. This interaction gets enhanced with increasing Ca^{2+} concentrations and is important for stabilization of microtubules when subjected to depolymerizing conditions such as Nocodazole or cold. TRPV1-Ct preferably interacts with β -tubulin as compared to α -tubulin. When the exact regions within TRPV1-Ct that mediate interaction with tubulin/microtubules were mapped down, it was seen that there are 2 stretches: Tubulin Binding Sequence 1 (TBS1) spanning a region of 710-730 amino acid and Tubulin Binding Sequence 2 (TBS2) spanning a region of 770-797, that are responsible for this interaction. It is postulated that these two stretches are enriched with highly basic residues that enable the negatively charged tubulin dimers to mediate this interaction. It has been already seen that out of the two TBS's, TBS-1 is evolutionarily more conserved than TBS2 across different vertebrates.

Taking this into consideration, the highly conserved positively charged residues in TBS1 (Lys710, Lys714, Arg717, Lys718, Arg721, Lys724) were mutated to Alanine residues and a mutant was generated that had all these six positions substituted by Alanine (henceforth referred to as TRPV1-TBS1-Hexamutant) in order to test the hypothesis whether these positively charged residues mediate the interaction with the negatively charged Tubulin tails and if this interaction gets perturbed due to differential charge substitution then what is the implication in channel behaviour. The importance of TRPV1-TBS1 interaction with tubulin/microtubule in the context of channel function was also investigated by pharmacological manipulation of microtubule integrity.

2.1.1. TRPV1-TBS1-Ct mutants retain interaction with tubulin dimers in presence as well as absence of Ca²⁺

TRPV1-WT-Ct is known to interact with tubulin/MT in presence or absence of Ca²⁺. When the positively charged residues present in TBS1 region were mutated to alanine to generate 6 point mutants and a Hexamutant. Subsequently, ability of mutants for tubulin interaction was tested. For this purpose, the C-terminal fragment of TRPV1-WT, TRPV1-Lys710Ala, TRPV1-Lys714Ala, TRPV1-Arg717Ala, TRPV1-Lys718Ala, TRPV1-Arg721Ala, TRPV1-Lys724Ala and TRPV1-TBS1-Hexamutant fused to MBP were expressed, purified and then pull-down experiments with tubulin dimers (purified from Goat brain) were performed. Only MBP-LacZ protein was also over expressed and used as a negative control. All these proteins were allowed to interact in absence as well as in presence of CaCl₂ (1mM). The samples were analysed by Western Blotting after being probed with various tubulin antibodies detecting α and/or β -tubulin (components of tubulin dimer), β -III tubulin (neuron-specific marker), Acetylated tubulin (marker for stable microtubules) and Tyrosinated tubulin (marker for dynamic microtubules) (Figures 7-13). Amongst all the point mutants, TRPV1-Lys710Ala when probed with β -tubulin Antibody, showed significant reduction in interaction with tubulin dimers as compared to TRPV1-WT in presence as well as absence of Ca²⁺. TRPV1-TBS1-Hexamutant showed a significant reduction in interaction in presence of Ca²⁺ when probed for β -III tubulin and Tyrosinated tubulin. TRPV1-TBS1-Hexamutant also exhibited reduced interaction as compared to TRPV1-WT both in presence as well as absence of Ca²⁺ when probed for Acetylated tubulin. However, in all cases TRPV1-TBS1-Hexamutant retained some basal level of interactions with tubulin. These also suggest that in no conditions (as tested), in spite of changing these positively charged residues, tubulin interaction was abolished completely.

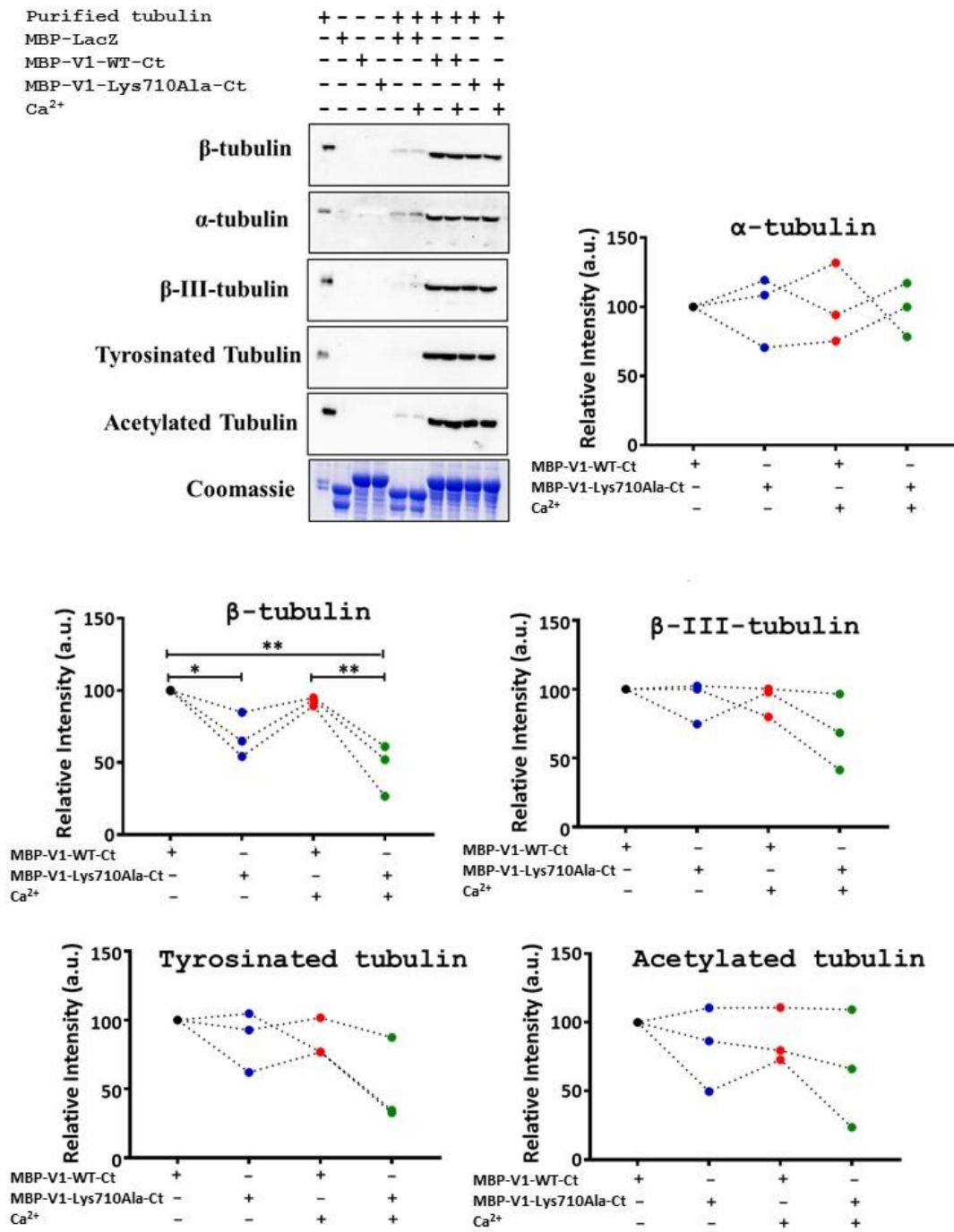


Figure 7. Tubulin pull down by TRPV1-Lys710Ala with tubulin dimers in presence and absence of Ca²⁺. Western blot analysis of TRPV1-Lys710Ala pull down with tubulin dimers in presence and absence of 1mM CaCl₂ (n=3) and the corresponding densitometry plots suggest that this mutation doesn't cause a significant reduction in interaction as compared to TRPV1-WT when probed with different tubulin antibodies: α , β , β -III, Tyrosinated and Acetylated. However, when probed for β -tubulin, there was a significant reduction in interaction as compared to TRPV1-WT both in presence and absence of Ca²⁺. The amount of tubulin observed to be interacting in case of MBP-TRPV1-WT-Ct in control conditions (in absence of Ca²⁺) is considered as 100%. Each dot on the graph thus represents the normalised band intensity derived from n=3 experiments. The WB images are representation of the individual experiments demonstrating specific type of tubulin interaction observed.

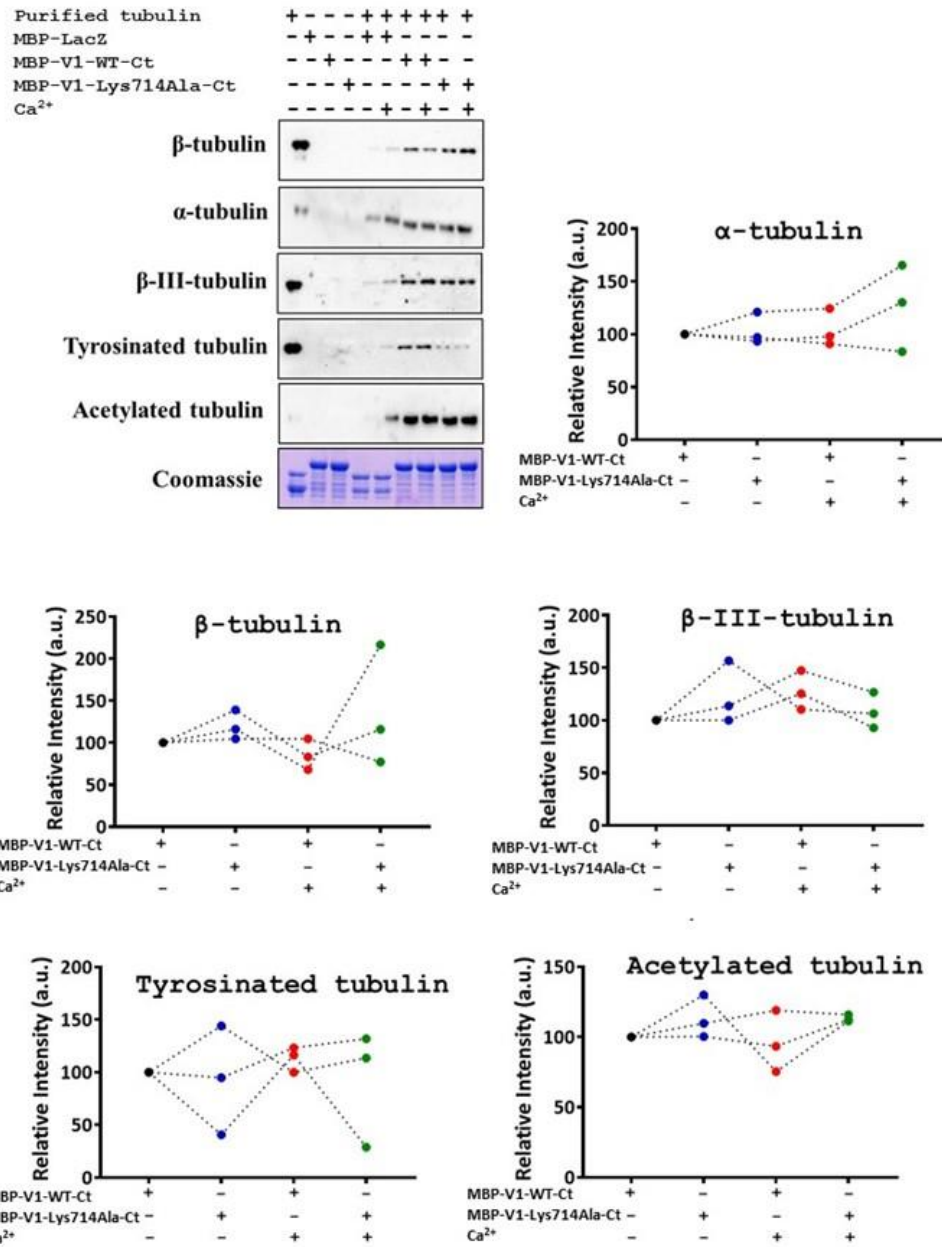


Figure 8. Tubulin pull down by TRPV1-Lys714Ala with Tubulin dimers in presence and absence of Ca²⁺. Western blot analysis of TRPV1-Lys714Ala pull down with tubulin dimers in presence and absence of 1mM CaCl₂ (n=3) and the corresponding densitometry plot suggest that this mutation doesn't cause a significant reduction in interaction as compared to TRPV1-WT when probed with different tubulin antibodies: α, β, β-III, Tyrosinated and Acetylated. The amount of tubulin observed to be interacting in case of MBP-TRPV1-Ct in control conditions (in absence of Ca²⁺) is considered as 100%. Each dot on the graph thus represents the normalised band intensity derived from n=3 experiments. The WB images are representation of the individual experiments demonstrating specific type of tubulin interaction observed.

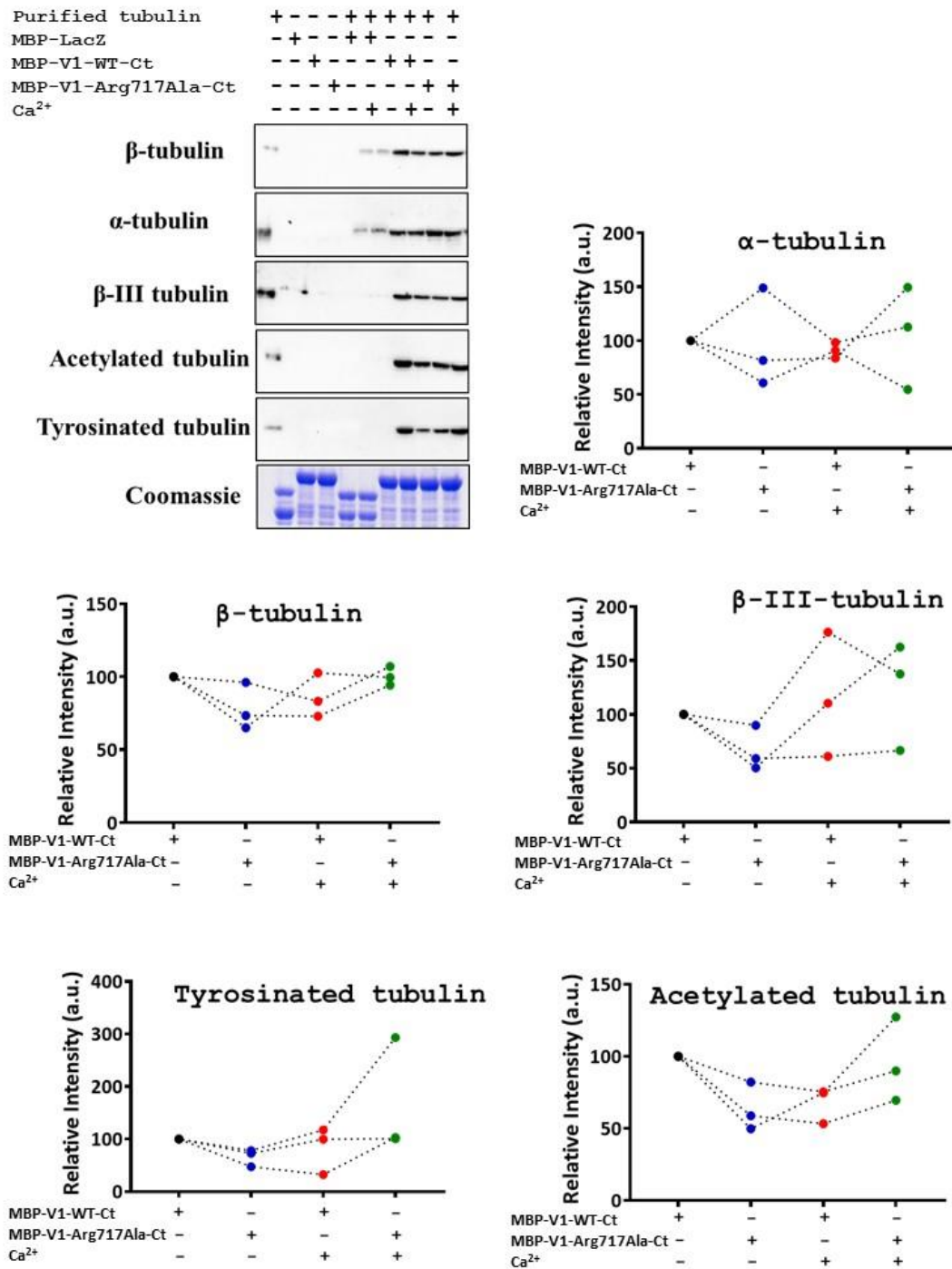


Figure 9. Tubulin pull down by TRPV1-Arg717Ala with Tubulin dimers in presence and absence of Ca²⁺. Western blot analysis of TRPV1-Arg717Ala pull down with tubulin dimers in presence and absence of 1mM CaCl₂ (n=3) and the corresponding densitometry plot suggest that this mutation doesn't cause a significant reduction in interaction as compared to TRPV1-WT when probed with different tubulin antibodies: α, β, β-III, Tyrosinated and Acetylated. The amount of tubulin observed to be interacting in case of MBP-TRPV1-Ct in control conditions (in absence of Ca²⁺) is considered as 100%. Each dot on the graph thus represents the normalised band intensity derived from n=3 experiments. The WB images are representation of the individual experiments demonstrating specific type of tubulin interaction observed.

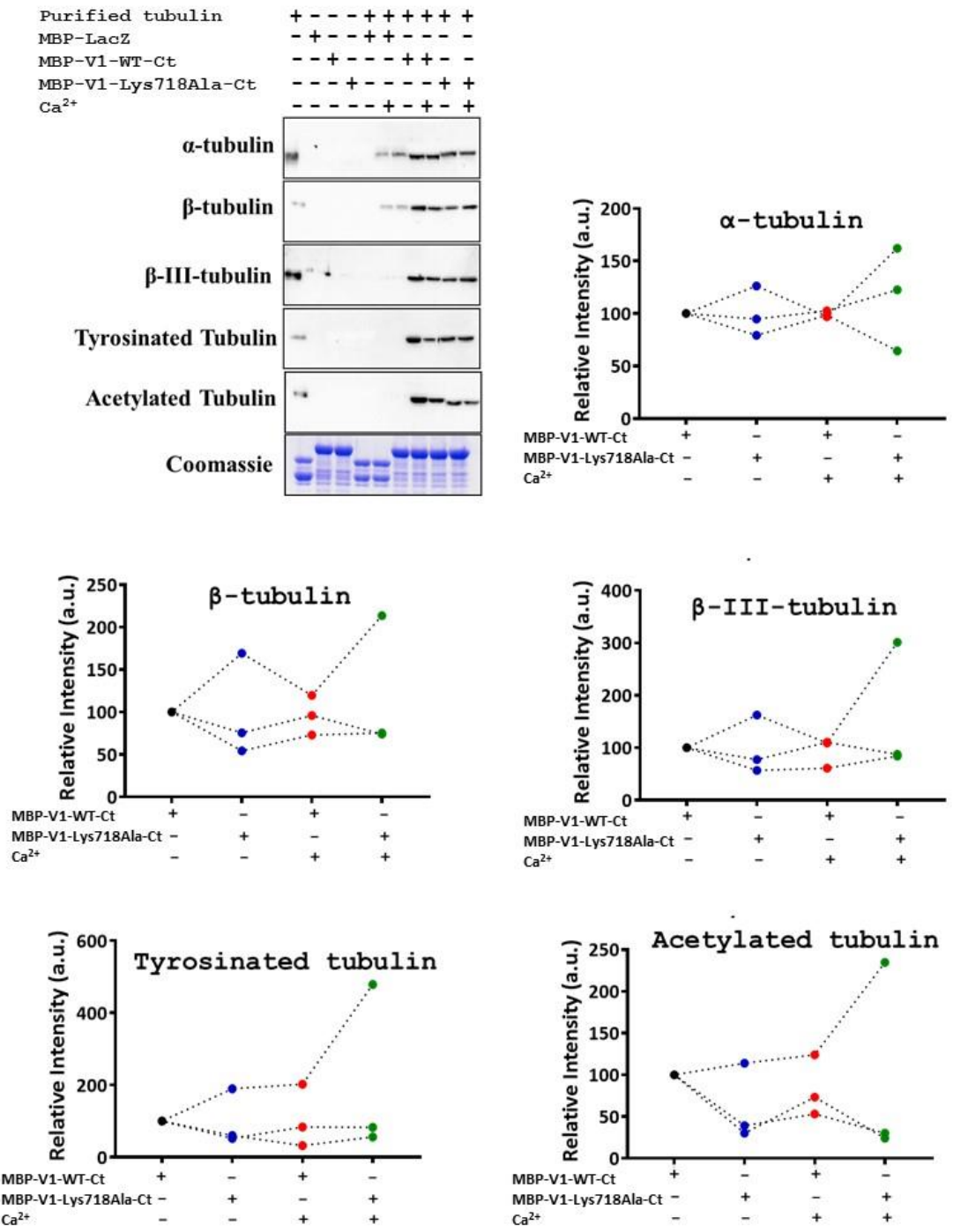


Figure 10. Tubulin pull down by TRPV1-Lys718Ala with Tubulin dimers in presence and absence of Ca²⁺. Western blot analysis of TRPV1-Lys718Ala pull down with tubulin dimers in presence and absence of 1mM CaCl₂ (n=3) and the corresponding densitometry plot suggest that this mutation doesn't cause a significant reduction in interaction as compared to TRPV1-WT when probed with different tubulin antibodies: α, β, β-III, Tyrosinated and Acetylated. The amount of tubulin observed to be interacting in case of MBP-TRPV1-Ct in control conditions (in absence of Ca²⁺) is considered as 100%. Each dot on the graph thus represents the normalised band intensity derived from n=3 experiments. The WB images are representation of the individual experiments demonstrating specific type of tubulin interaction observed.

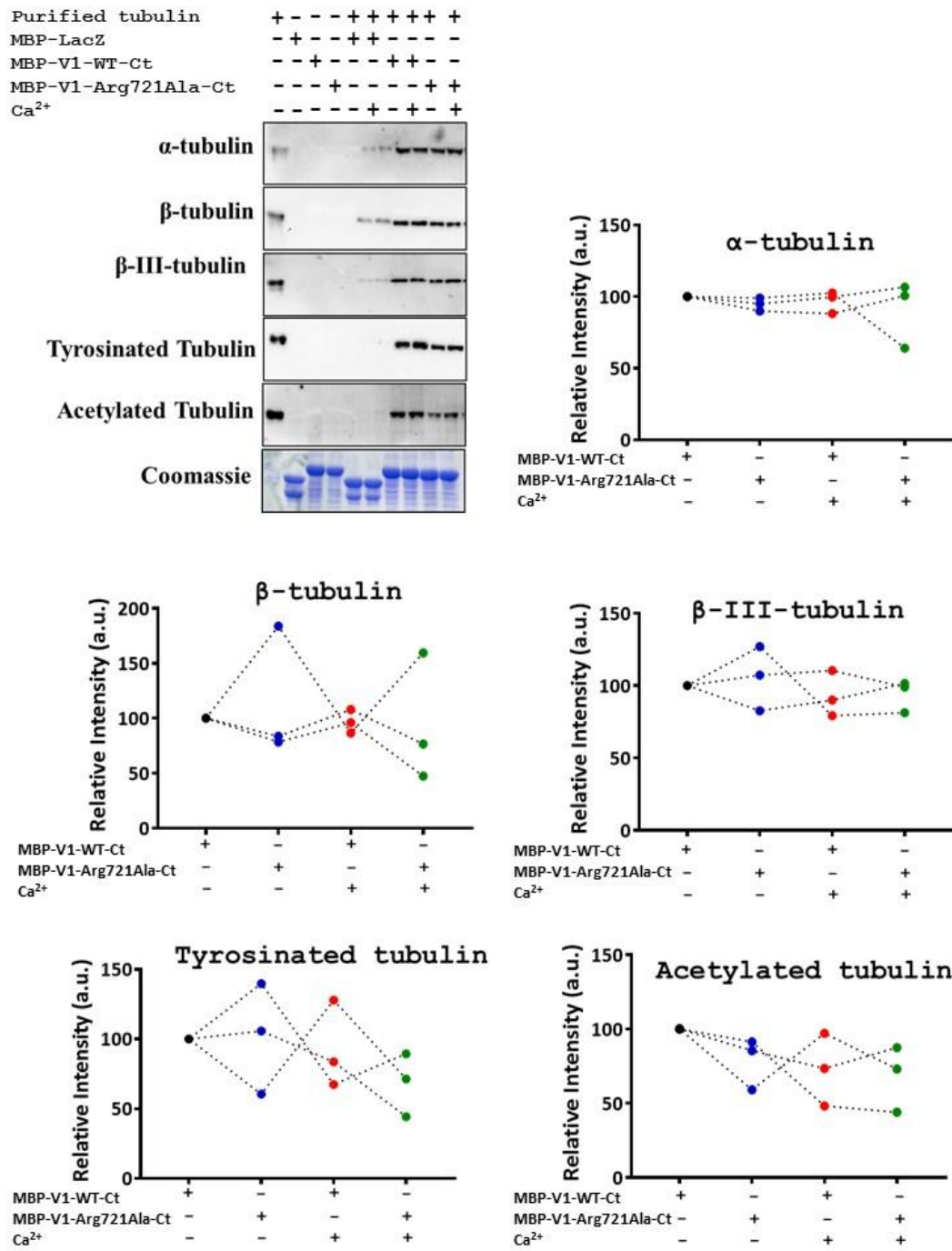


Figure 11. Tubulin pull down by TRPV1-Arg721Ala with Tubulin dimers in presence and absence of Ca²⁺. Western blot analysis of TRPV1-Arg721Ala pull down with tubulin dimers in presence and absence of 1mM CaCl₂ (n=3) and the corresponding densitometry plot suggest that this mutation doesn't cause a significant reduction in interaction as compared to TRPV1-WT when probed with different tubulin antibodies: α , β , β -III, Tyrosinated and Acetylated. The amount of tubulin observed to be interacting in case of MBP-TRPV1-Ct in control conditions (in absence of Ca²⁺) is considered as 100%. Each dot on the graph thus represents the normalised band intensity derived from n=3 experiments. The WB images are representation of the individual experiments demonstrating specific type of tubulin interaction observed.

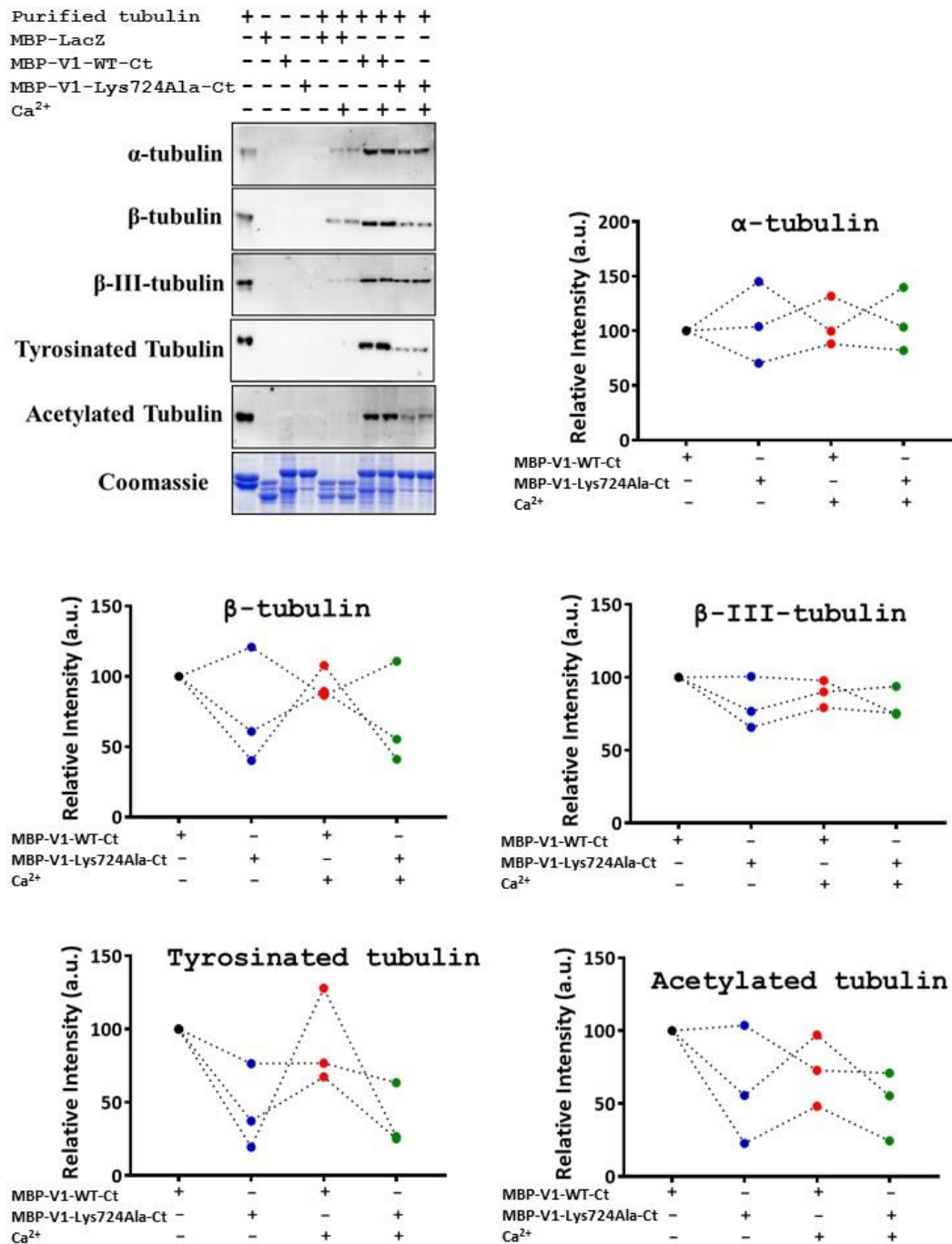


Figure 12. Tubulin pull down by TRPV1-Lys724Ala with Tubulin dimers in presence and absence of Ca²⁺. Western blot analysis of TRPV1-Lys724Ala pull down with tubulin dimers in presence and absence of 1mM CaCl₂ (n=3) and the corresponding densitometry plot suggest that this mutation doesn't cause a significant reduction in interaction as compared to TRPV1-WT when probed with different tubulin antibodies: α , β , β -III, Tyrosinated and Acetylated. The amount of tubulin observed to be interacting in case of MBP-TRPV1-Ct in control conditions (in absence of Ca²⁺) is considered as 100%. Each dot on the graph thus represents the normalised band intensity derived from n=3 experiments. The WB images are representation of the individual experiments demonstrating specific type of tubulin interaction observed.

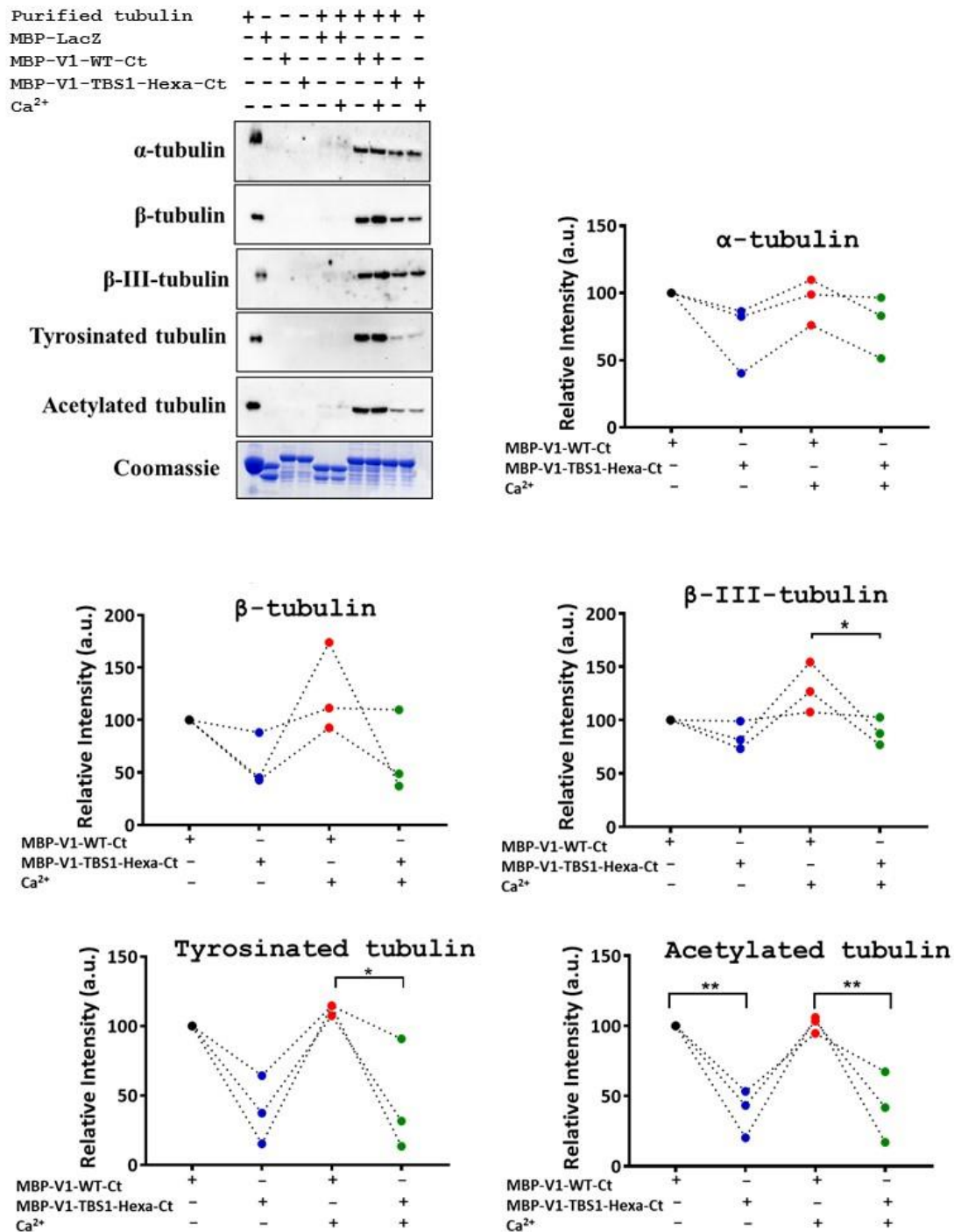


Figure 13. Tubulin pull down by TRPV1-TBS1-Hexamutant with Tubulin dimers in presence and absence of Ca²⁺. Western blot analysis of TRPV1-TBS1-Hexamutant pull down with tubulin dimers in presence and absence of 1mM CaCl₂ (n=3) and the corresponding densitometry plot suggest that this hexa-mutation causes a significant reduction in interaction as compared to TRPV1-WT when probed with β-III and Tyrosinated tubulin antibodies in presence of 1 mM CaCl₂. In case of Acetylated tubulin, the reduction is significantly reduced both in presence as well as absence of Ca²⁺. The amount of tubulin observed to be interacting in case of MBP-TRPV1-Ct in control conditions (in absence of Ca²⁺) is considered as 100%. Each dot on the graph thus represents the normalised band intensity derived from n=3 experiments. The WB images are representation of the individual experiments demonstrating specific type of tubulin interaction observed.

2.1.2. TRPV1-TBS1-Hexamutant retain interaction with polymerised microtubules in presence as well as absence of Ca²⁺

As TRPV1-WT-Ct has been seen to elicit interaction with both tubulin dimers as well as polymerised microtubules (MT), it was tested if the same was applicable for TRPV1-TBS1-Hexamutant-Ct. In order to test this hypothesis, TRPV1-WT, TRPV1-TBS1-Hexamutant and MBP-LacZ were allowed to interact with polymerised microtubules in presence and absence of 1 mM CaCl₂ (Figure 14).

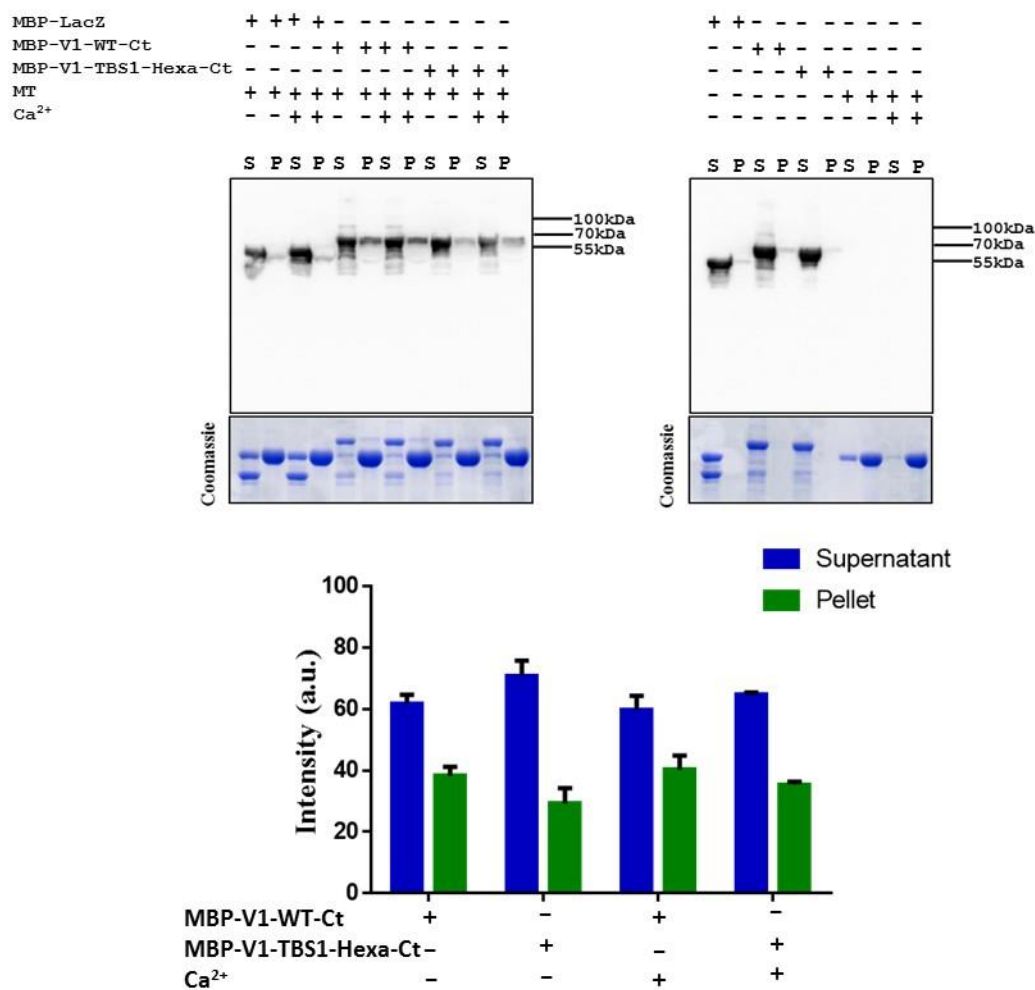


Figure 14. Co-sedimentation of TRPV1-WT and V1-TBS1-Hexamutant with polymerised microtubules in presence and absence of Ca²⁺. TRPV1-WT-Ct, MBP-LacZ and TRPV1-TBS1-Hexamutant-Ct were allowed to interact with polymerised MT's in presence and absence of 1mM CaCl₂. When probed with MBP antibody, MBP-LacZ was only found in the S fraction as it does not interact with MT. Both TRPV1-WT and TRPV1-TBS1-Hexamutant appears in the pellet fraction and both did not exhibit significant differences in their abundances in the S and P fraction. The corresponding densitometry plot is given below. Band intensities of 3 biological replicates for each conditions were summed up. The S and P fraction of each condition were summed up and their percentage distribution out of 100 were calculated and plotted.

These were further subjected to high speed centrifugation at 40,000 RPM for 30 minutes which resulted in a supernatant (S) and pellet (P) fraction. Abundance of overexpressed protein in the supernatant fraction indicated that majority of the protein had failed to interact with polymerized MT. In contrast, presence of TRPV1 fragment in the pellet fraction indicates that the protein interacts with the polymerized MT's and thus appears in the pellet fraction. The distribution of all these proteins in different fractions (supernatant and pellet) were probed by anti-MBP antibody (Figure 14). Notably, TRPV1-TBS1-Hexamutant-Ct does not exhibit any statistically significant difference in comparison to TRPV1-WT-Ct in absence as well as presence of Ca^{2+} . MBP-LacZ, used as a control protein only appeared in the (S) fraction in all cases as it does not interact with MT under any conditions tested here.

2.1.3. TRPV1-TBS1-Hexamutant takes subtly longer time to form high molecular weight complexes with tubulin dimer in presence of chemical cross-linker

Chemical cross-linking experiment provides sufficient information about biochemical complexes, its formation and stability. Therefore, TRPV1-WT-Ct as well as TRPV1-TBS1-Hexamutant-Ct were allowed to form high molecular weight complexes with purified tubulin dimers in presence of a chemical cross-linker, namely DMS (20 μ g). The cross-linking reaction for each construct was stopped after 1', 3', 6', 10', 20', 40' and 60' incubation with DMS. Both non-cross-linked product and cross-linked samples were further separated by SDS-PAGE in order to get the properties of the respective complexes. TRPV1-WT-Ct was capable of forming high molecular weight complexes with tubulin dimers in presence of 20 μ g DMS. The molecular weight of the complexes formed was directly proportional to the incubation time of the two interacting proteins with the same concentration of DMS. However, similar phenomenon was observed for

TRPV1-TBS1-Hexamutant but the rate of high molecular weight complex formation was slightly

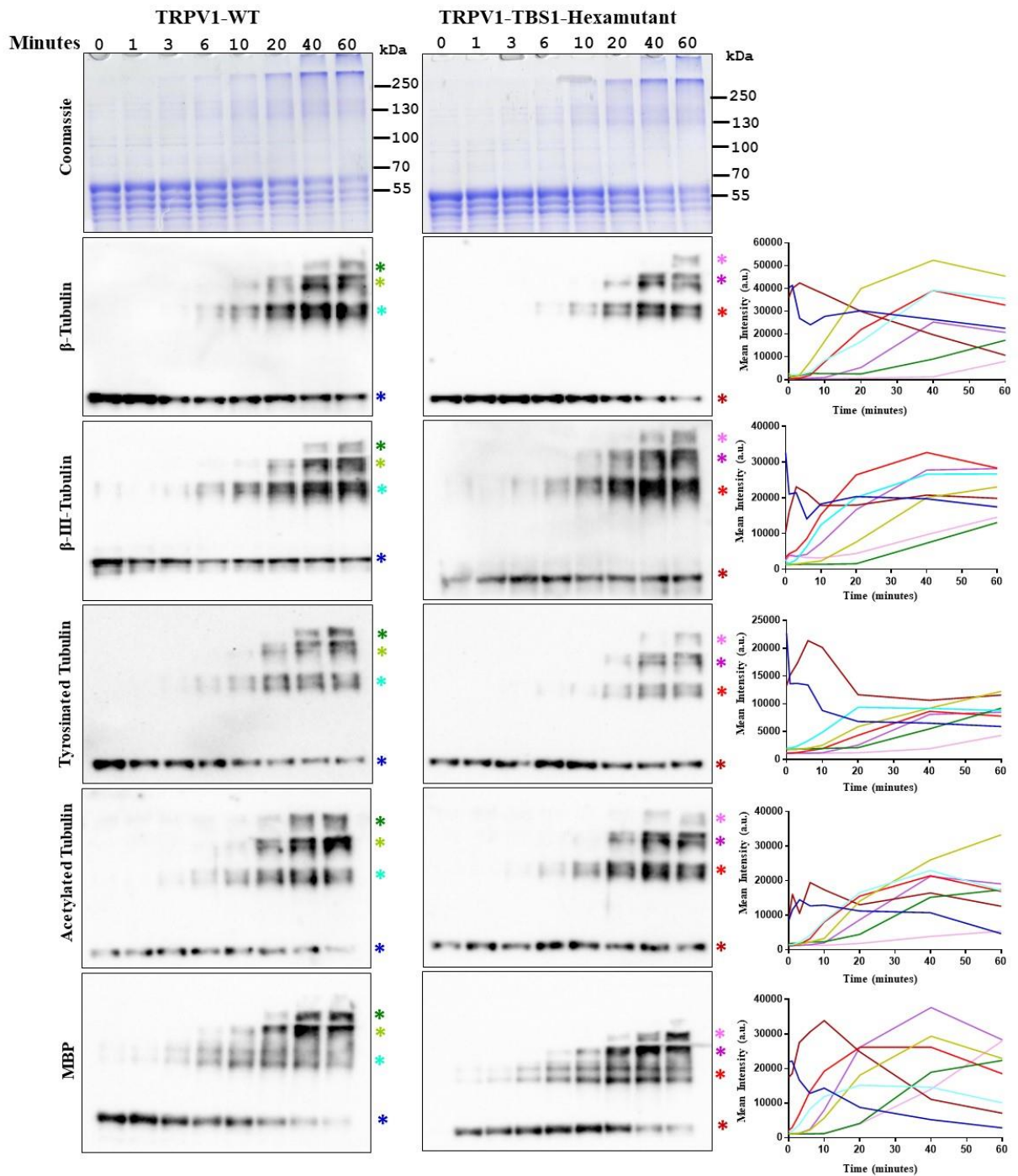
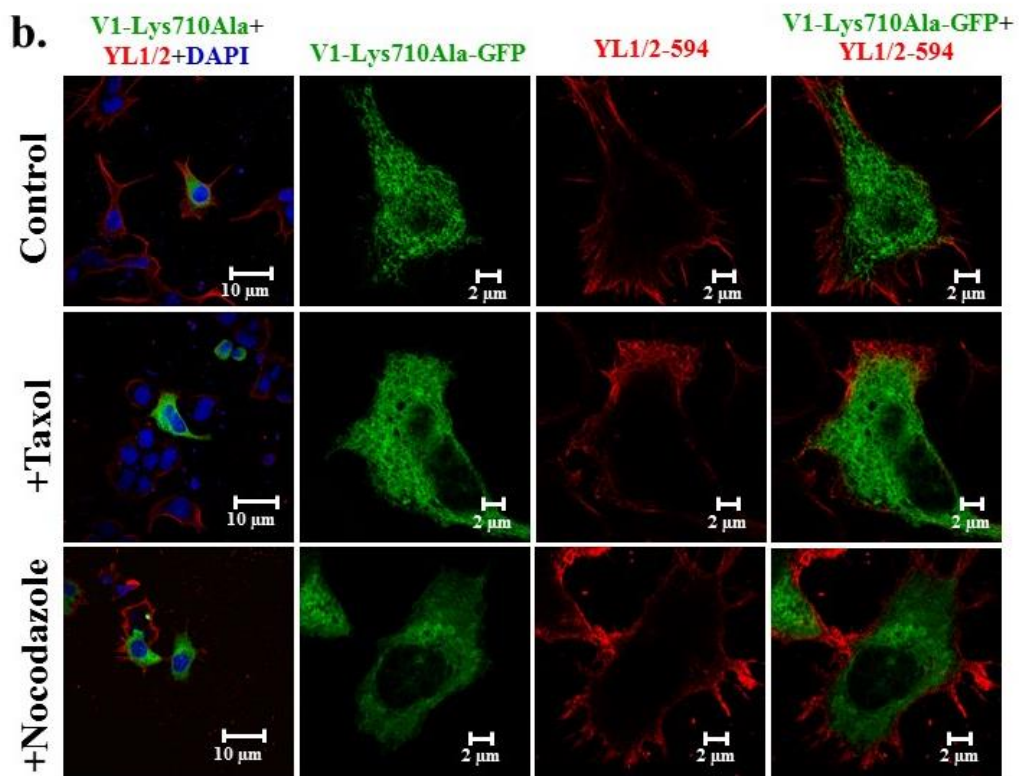
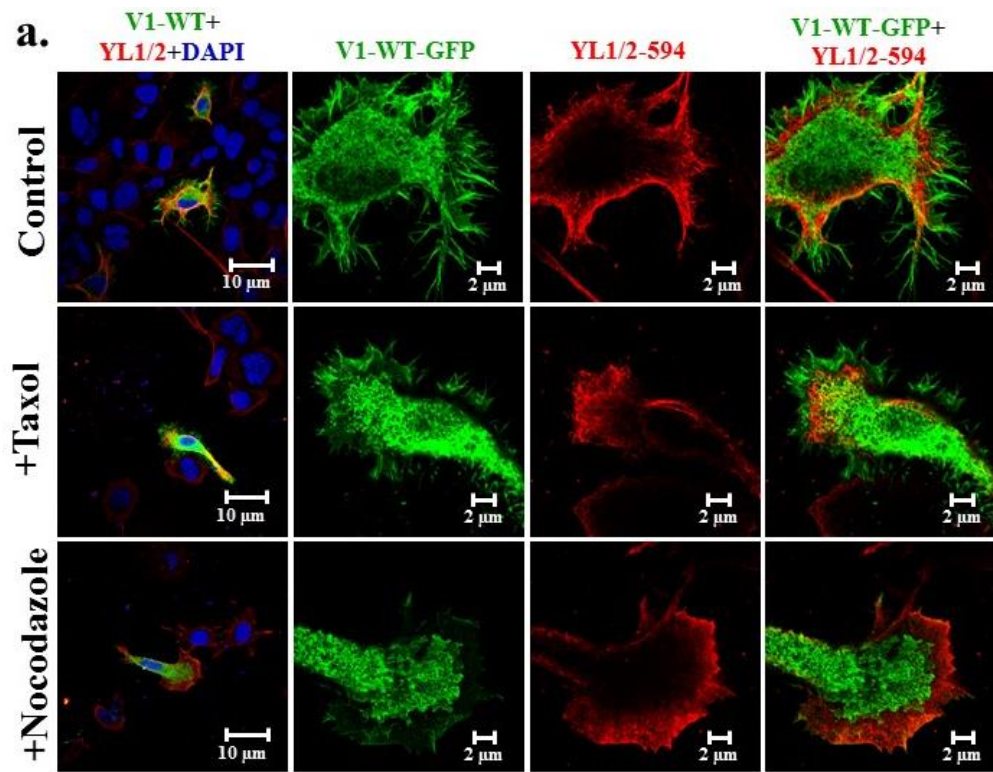


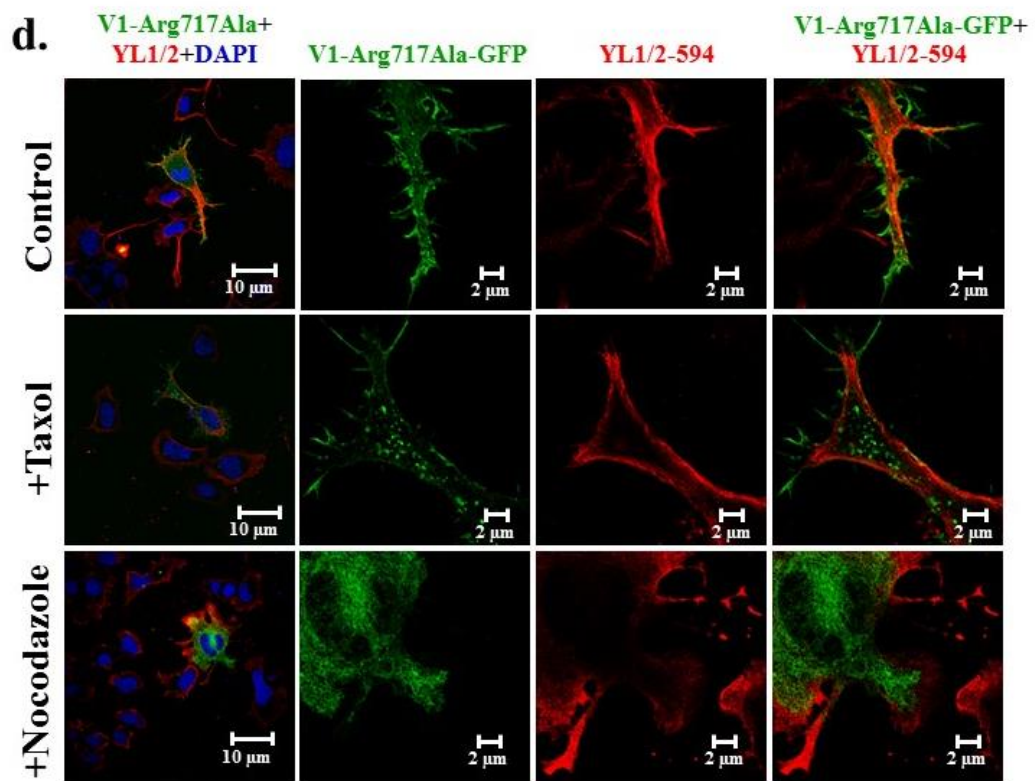
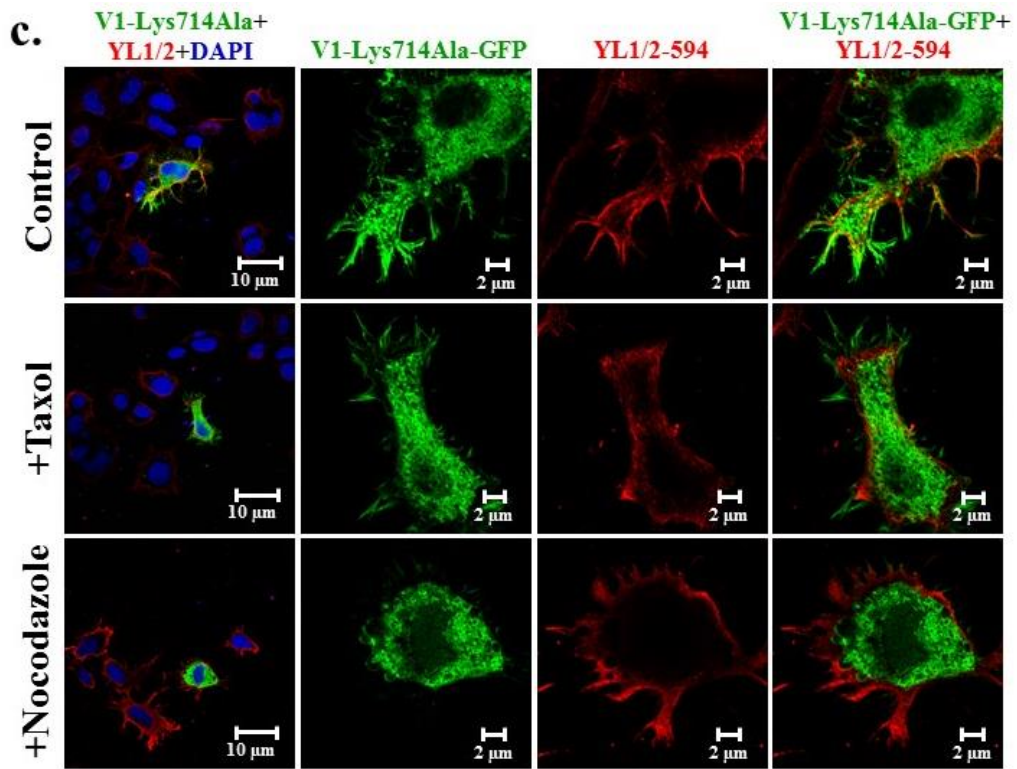
Figure 15. Cross-linking of TRPV1-WT and TRPV1-TBS1-Hexamutant with tubulin dimers in presence of chemical cross-linker DMS. Both TRPV1-WT-Ct and TRPV1-TBS1-Hexamutant-Ct forms high-molecular weight complexes with tubulin dimers with progression in incubation time in presence of DMS. In absence of any cross-linker (0' sample), the band appears at 55 kDa corresponding to tubulin. With increasing time of cross-linker incubation, high molecular weight complexes start forming that is slightly slower for the mutant. Colored asterisks indicate the specific bands and corresponding intensities of the bands with respect to time have been plotted in the adjacent graphs.

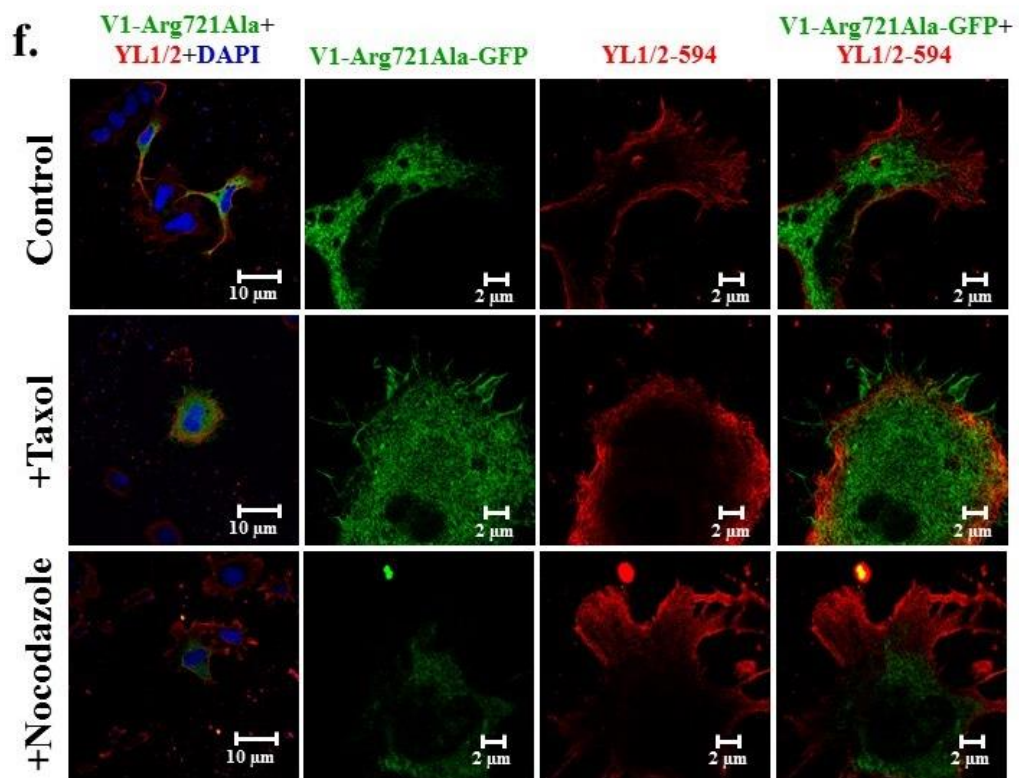
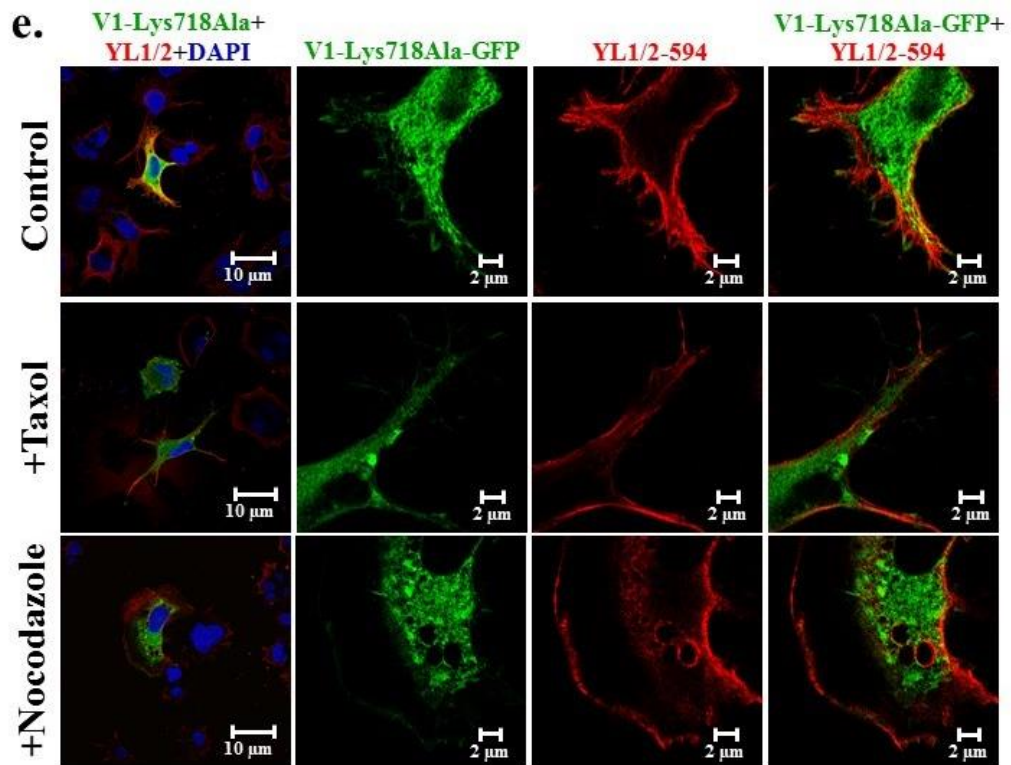
slower as compared to TRPV1-WT as probed by different tubulin and modified tubulin antibodies: β , β -III, Tyrosinated and Acetylated. The band at 0' demarcates the status before addition of cross-linker (Figure 15). This experiment also suggests that TRPV1-TBS1-hexamutant is able to retain the tubulin interaction, yet there are differences as compared with TRPV1-WT-Ct.

2.1.4. TRPV1-TBS1 point mutants as well as TRPV1-TBS1-Hexamutant exhibit defects in membrane localization

Full-length Rat TRPV1-WT and other TRPV1-TBS1 mutants (all in pSGFP2C1 vector) were transiently transfected in F11 cells, a DRG neuron derived cell line. Approximately, 36 hours after transfection, the cells were treated with Taxol (1 μ M) or Nocodazole (1 μ M) for 30 minutes and then fixed with 4% PFA. Control and treated cells were subsequently stained for tyrosinated alpha tubulin with YL1/2-594 antibody (Figure 16). Unlike TRPV1-WT which localizes to the cell membrane, some of the TRPV1-TBS1 point mutants, such as TRPV1-Lys710Ala and TRPV1-Arg721Ala as well as TRPV1-TBS1-Hexamutant failed to localize to the cell membrane. However, some of them such as TRPV1-Lys714Ala, TRPV1-Arg717Ala, TRPV1-Lys718Ala and TRPV1-Lys724Ala were capable of localizing to the membrane. Microtubule stabilization by Taxol did not impact channel localization but destabilization of microtubules by Nocodazole not only altered the membrane localization of TRPV1-WT but also the other mutants that exhibited membrane localization. Thus, only two of the TBS1 point mutants (TRPV1-Lys710Ala and TRPV1-Arg721Ala) and TRPV1-TBS1-Hexamutant failed to manifest surface expression, a phenomenon that remain unaltered even upon microtubule stabilization or destabilization by adding Taxol or Nocodazole respectively.







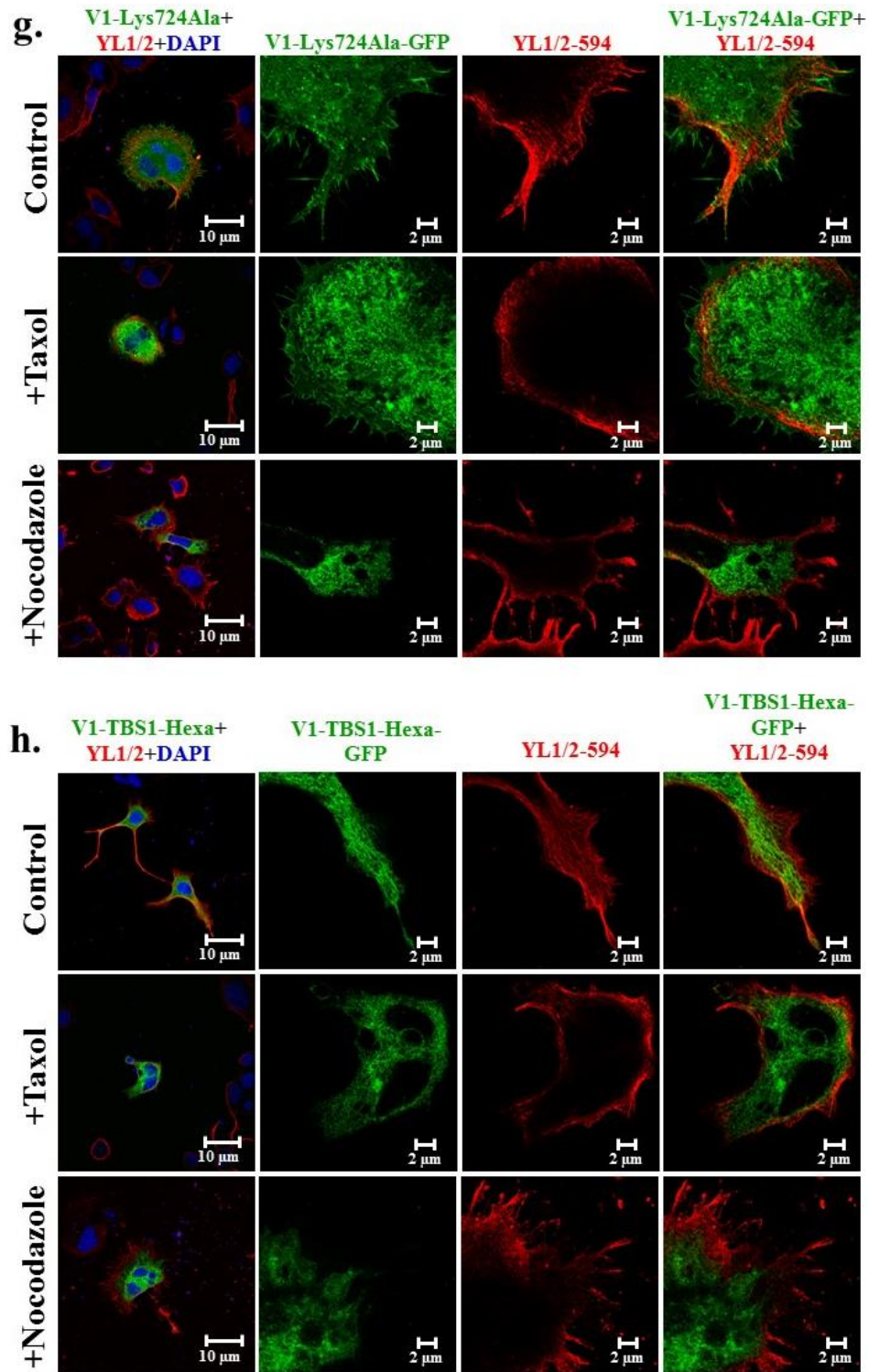


Figure 16. Lack of membrane localization by TRPV1-TBS1 mutants. (a-h) Confocal images of F-11 cells transiently transfected with full-length Rat TRPV1-WT, TRPV1-Lys710Ala, TRPV1-Lys714Ala, TRPV1-Arg717Ala, TRPV1-Lys718Ala, TRPV1-Arg721Ala, TRPV1-Lys724Ala and TRPV1-TBS1-Hexamutant in pSGFP2C1. Control and Taxol-treated cells do not show any significant differences in membrane localization. However, Nocodazole-induced microtubule destabilization causes alteration in channel localization for not only TRPV1-WT but also some mutants like TRPV1-Lys714Ala, TRPV1-Arg717Ala, TRPV1-Lys718Ala and TRPV1-Lys724Ala. Tyrosinated alpha tubulin has been stained with YL1/2 Antibody (Red).

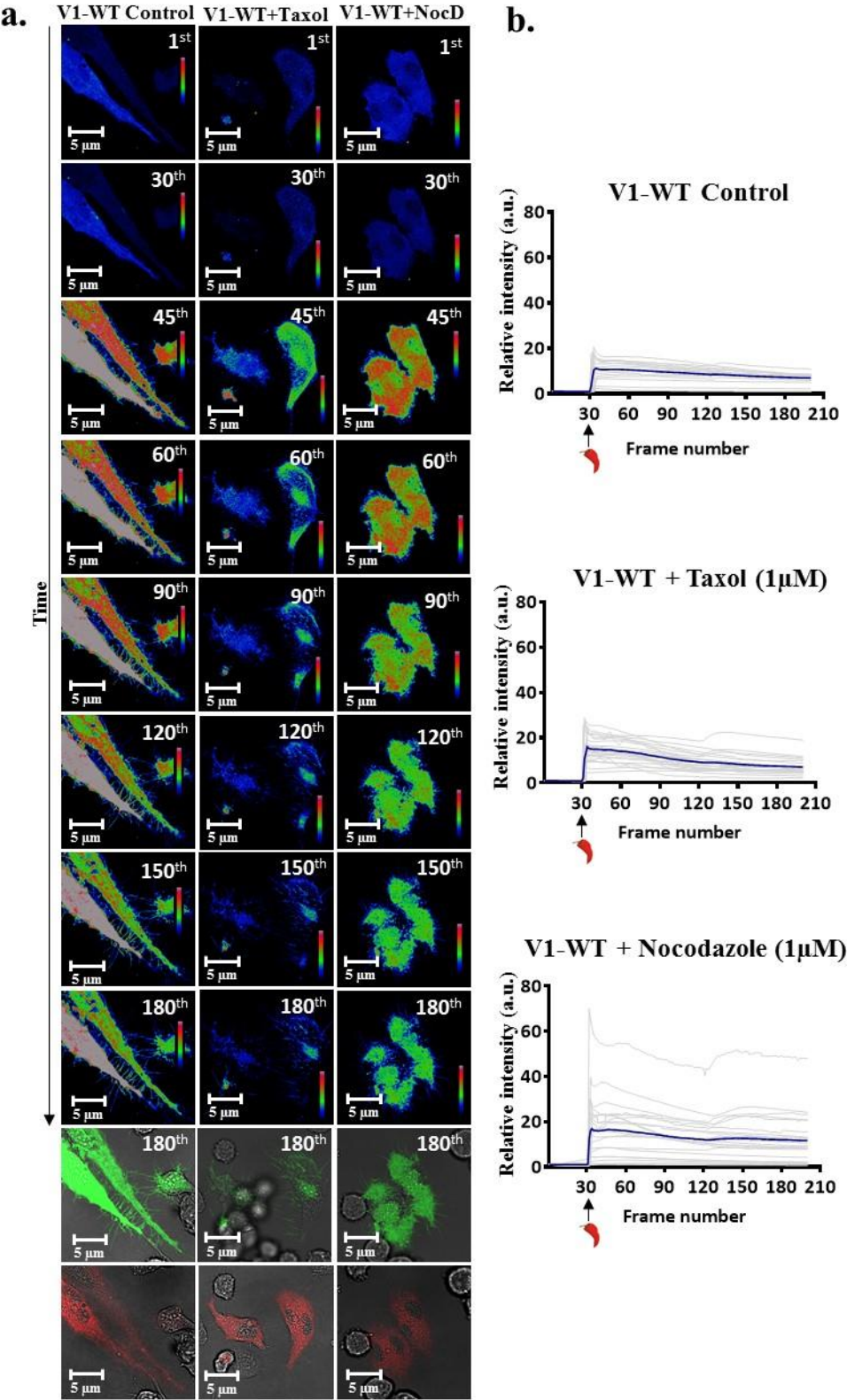
2.1.5. TRPV1-TBS1-Hexamutant forms a defective channel that is insensitive to Capsaicin-induced Ca²⁺ influx

DRG neuron derived F-11 cells were transiently co-transfected with full-length Rat TRPV1-WT (present in pmCherryC1 vector) and a Ca²⁺-sensor pGP-CMV-GCaMP6f. The same was repeated for TRPV1-TBS1-Hexamutant (present in pmCherryC1 vector). This Ca²⁺-sensor works on a principle where binding of calcium enhances the fluorescence emission of the GFP-tagged to this sensor (269). Approximately, 24 hours post transfection, some dishes were subjected to incubation with Taxol (1µM) and some with Nocodazole (1µM) for 30 minutes. Live cell imaging of only doubly transfected cells in absence as well as in presence of Taxol (1µM) or Nocodazole (1µM) were executed using a microscope for 200 frames (1.085 seconds per frame). Capsaicin (10 µM) was added at the 30th frame for each condition. However, all the experiments were done in a bath system where the added Capsaicin remained in the live cell dish and was not flushed out after addition.

For TRPV1-WT, addition of Capsaicin at the 30th frame triggered a rapid influx of Ca²⁺ ions as observed by the increase in green fluorescence intensity ([Figure 17a](#)). However, Capsaicin addition to TRPV1-TBS1-Hexamutant transfected cells triggered no visible increase in Ca²⁺-influx. In order to confirm that the experiments were conducted on live and functional cells, 2 µM Ionomycin was added at the 120th frame only for the mutant transfected cells which subsequently resulted in increased fluorescence from the sensor ([Figure 17c](#)). Thus, substitution of positively charged residues in TBS1 region of TRPV1 makes the channel insensitive to Capsaicin.

Pharmacological manipulation of microtubules by Taxol and Nocodazole were also capable of altering TRPV1 function in both WT and mutant transfected cells. Stabilization of microtubules by Taxol and disassembly of microtubules into soluble

tubulin dimers by Nocodazole increased the average fluorescence intensity of the Ca²⁺-sensor as compared to



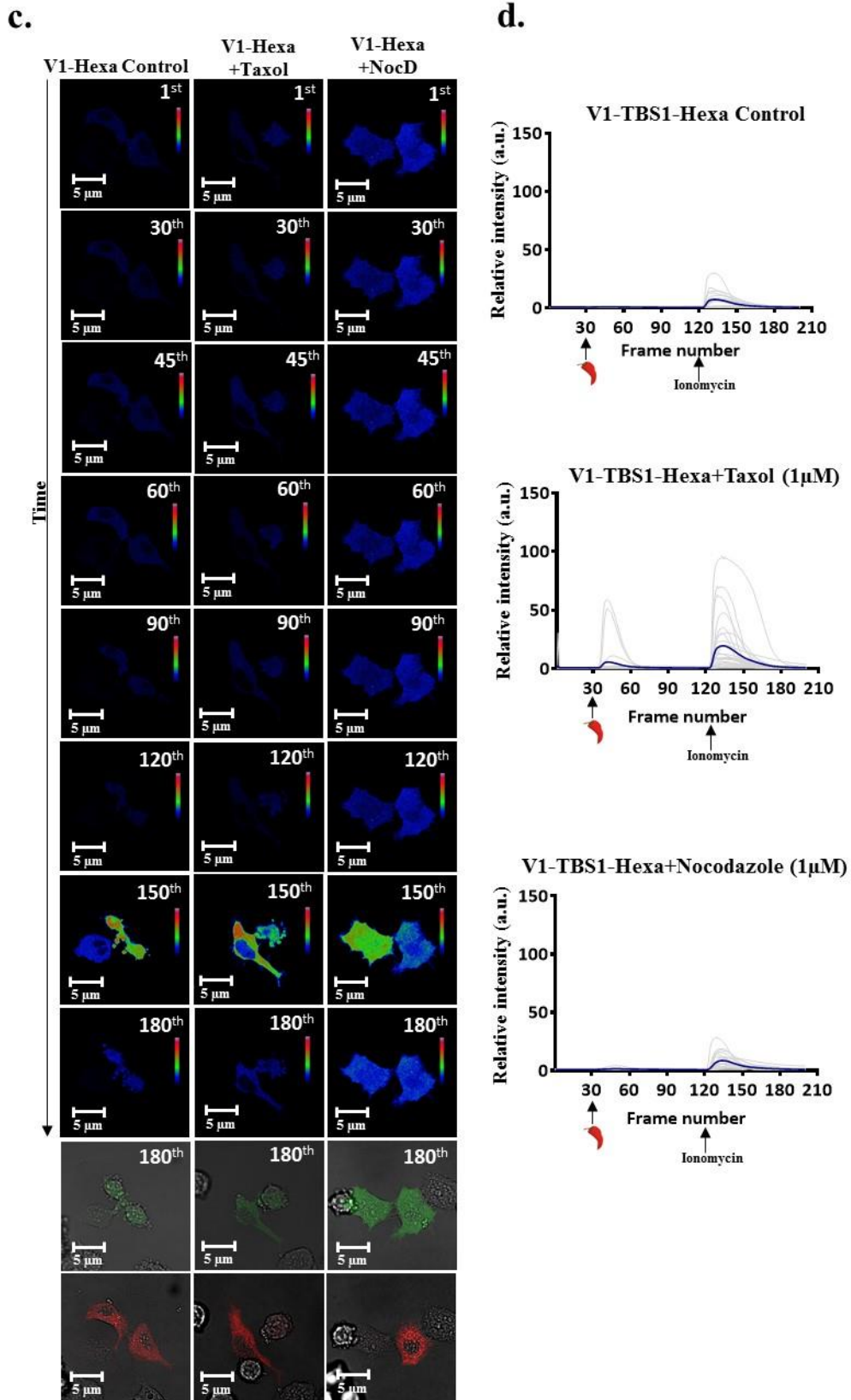


Figure 17. Substitution of positive charges to neutral in TBS1 region results in Capsaicin-insensitive TRPV1. a) Time series of F-11 cells transiently co-transfected with full-length Rat TRPV1-WT-pmCherryC1 (red) and pGP-CMV-GCaMP6f (green). 10 μ M Capsaicin was added at the 30th frame in all cases (control, Taxol and Nocodazole-treated) and a total of 200 frames for each condition was acquired (but only the 1st, 30th, 45th, 60th, 90th, 120th, 150th and 180th frame has been displayed). Last

panel depicts that only cells co-transfected with both constructs had been considered for imaging. **b)** Quantification of pGP-CMV-GCaMP6f (green) intensity with respect to time for control (n = 15 cells), Taxol (n = 22 cells) and Nocodazole (n = 22 cells) treated cells that have been co-transfected with TRPV1-WT-pmCherry (red) and pGP-CMV-GCaMP6f (green). **c)** Time series of F-11 cells transiently co-transfected with full-length Rat TRPV1-TBS1-Hexamutant-pmCherry (red) and pGP-CMV-GCaMP6f (green). **d)** Quantification of pGP-CMV-GCaMP6f (green) intensity with time for control (n=17), Taxol- (n=26) and Nocodazole-treated (n=21) cells that have been co-transfected with TRPV1-TBS1-Hexamutant-pmCherryC1 (red) and pGP-CMV-GCaMP6f (green). The quantification for both TRPV1-WT and TRPV1-TBS1-Hexamutant were done considering the initial value recorded at the 1st frame as 1. The intensities for the remaining frames were subsequently calculated relative to the 1st frame.

control conditions in case of TRPV1-WT (Figure 17b). In case of TRPV1-TBS1-Hexamutant transfected cells, some of them were capable of eliciting response towards Capsaicin addition upon treatment with Taxol, but with Nocodazole-treatment no such peaks were visible (Figure 17d). The mutant transfected cells showed a prominent peak only after Ionomycin-treatment after 120th frame under all conditions. Thus, microtubule stabilization but not destabilization resulted in partial restoration of “Capsaicin-sensitivity” in TRPV1-TBS1-Hexamutant transfected cells.

2.1.6. TRPV1-TBS1-Hexamutant exhibits lack of surface expression:

In order to check the surface expression of Rat TRPV1-TBS1-Hexamutant with respect to TRPV1-WT, F-11 cells were transiently transfected with both the constructs in pmCherryC1

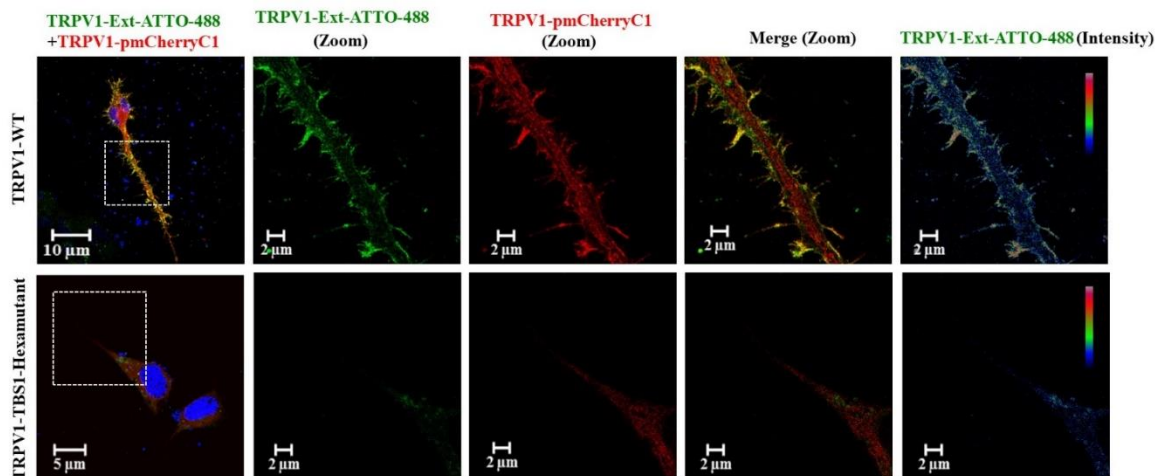


Figure 18. TRPV1-TBS1-Hexamutant exhibits lack of surface expression. Confocal images of F-11 cells transiently transfected with full-length Rat TRPV1-WT and TRPV1-TBS1-Hexamutant (both in pmCherryC1 vector) and stained with TRPV1-extracellular-ATTO-488 antibody (green) and DAPI (blue). TRPV1-WT shows distinct surface expression, a phenomenon absent in case of TRPV1-TBS1-Hexamutant.

vector and subsequently stained with TRPV1-ATTO-488 antibody that was directed against the 3rd extracellular loop of TRPV1 (residues 605-619 whereby the cysteine at position 616 has been substituted by serine, NSLPMESTPHK*SRGS). TRPV1-TBS1-Hexamutant exhibited no surface expression whereas TRPV1-WT exhibited distinct surface localization ([Figure 18](#)).



2.2. Importance of TRPV1-cholesterol complex in channel localization and cellular functions

TRPV1 is a thermo-sensitive ion channel involved in neurosensory and other physiological functions. The trans-membrane helices of TRPV1 undergo quick and complex conformational changes governed by thermodynamic parameters and membrane components leading to channel opening. However, the molecular mechanisms underlying such events are poorly understood. The molecular evolution of TRPV1 at the lipid-water-interface region (LWI) was analysed. LWI is typically defined as a layer of 6 Å thickness on each side of the membrane with less availability of free water.

In this work, the conservation analysis of amino acids demarcating the end of the trans-membrane helices (at the LWI regions) were performed. Importance of cholesterol in the stabilization of closed and open conformation of TRPV1 was analysed. Also the possible residues present in LWI region and involved in cholesterol interaction was identified. This analysis sheds light on the molecular interaction of cholesterol with TRPV1, critical amino acids involved in such as interaction and possible influence of such interaction on the channel gating (typically in a time scale of milliseconds). This analysis also sheds light on the molecular selection of certain amino acids in LWI region of TRPV1 happened in a time scale of 400 million years.

On the basis of molecular conservation and *in silico* interaction studies, TRPV1 mutants were generated at positions that interfered with TRPV1-cholesterol interaction. Membrane localization and co-localization of these mutants with lipid raft markers were assessed. Lethality of a particular LWI mutant, i.e. TRPV1-Arg575Asp was rescued by introducing another mutation that was generated on the principle of “maintenance of ratio of positive to negative charged amino acids at inner the LWI region”. The lethality was also partially recovered by blocking a constitutively open channel. The channel

functionality of TRPV1-WT, its lethal phenotype and the rescue mutant in response to Capsaicin was also evaluated.

2.2.1. Determination of the lipid-water interface amino acids of TRPV1

The lipid-water interface (LWI) region represents a unique physico-chemical microenvironment in a membrane-bound system where the concentration of free water is less [$<0.5 \text{ pg/cm}^3$] and the residues present in this region are mainly unstructured and offer possibilities of various non-covalent interactions through their side chains with specific components present in the lipid bilayer (270)(271). The LWI-residues have been defined as the 5 amino acids stretch sequence ($\sim 6 \text{ \AA}$ to 10 \AA in linear length) on both sides of the N-terminal and C-terminal ends of each TM helices. This analysis was done using two different membranes, made of POPC and PEA (Figures 19a and 19b). This consideration is according to the conventional way of determining interactions at the interface proven experimentally as well as by computational studies (272)(273). The particular behaviour of snorkeling residues (amino acids with flexible side chains which fluctuates inside and outside of the lipid bilayer depending on the microenvironment) located within this LWI-region and the dynamic interactions between lipids and peptides is relevant for biological functions of proteins and thus for molecular evolution too (270)(271)(274)(275).

2.2.2. Amino Acids present in the lipid-water interface are highly conserved

To analyse the conservation of amino acids present at the LWI, the 5 residue stretches flanking the TM regions were considered and upon analyses it was found that they were quite conserved. This analysis was conducted in both POPC and PEA membrane independently. In total, these 12 stretches were more conserved than full-

length TRPV1 suggesting that the residues present at the LWI are under positive selection (Figures 19c and 19d). Among all, the N-terminal portion of TM1 (termed as TM1N), C-terminal portion of TM2 (i.e. TM2C) and C-terminal portion of TM4 (i.e. TM4C) were highly conserved (Figures 19c and 19d). The N-terminal portion of TM2 (i.e. TM2N), the C-terminal portion of TM3 (i.e. TM3C) and the N-terminal portion of TM4 (i.e. TM4N) were divergent to some extent (Figures 19c and 19d). Analysis at the single residues revealed that mainly some charged amino acids (Arg, Glu, and Asp) and aromatic amino acids (Tyr, Phe and Trp) were distinctly conserved in these specific positions, suggesting that these residues have been positively selected during vertebrate evolution. However, only few regions (such as loop region between 1st and 2nd TM region) show differences in their relative position in POPC or in PEA membrane, suggesting that indeed TRPV1 conformation can be different in different lipids. This also suggests that these residues may play critical role in the LWI operations.

2.2.3. Amino Acids present at the inner leaflet evolved under more stringent selection pressure

The lipid composition of the inner and outer membrane layers are not same (271)(274)(275)(276). In order to explore if the lipid composition of outer and inner lipid bilayer has any effect on the molecular evolution of TRPV1, the 5 amino acid stretch sequences present in inner and outer sides were analysed. The analysis revealed that residues present in the inner leaflet (marked as “All Inside”) were highly conserved as compared to the residues present at the outer leaflet (marked as “All Outside”) (Figures 19c and 19d). This trend remained same in different micro environments such as lipid bilayer made of POPC and PEA. This confirms that the amino acid residues present at the

inner leaflet have more importance in the determination of structure-function relationship of TRPV1 (discussed later).

2.2.4. The LWI-residues have undergone different selection pressure throughout vertebrate evolution due to N- and C-terminal peptide directionality

Next the importance of N- and C-terminal directionality (with respect to the lipid bilayer) of the transmembrane helices on the molecular evolution of TRPV1 was explored. If such directionality has no importance, then it is expected that unbiased selection pressure will prevail and similar level of conservation in both N- and C-terminal amino acid stretches at the LWI is expected. It was noted that in case of PEA membrane, the residues located at the C-terminal of the TM regions (marked as all C) were more conserved than the residues that were located at the N-terminal regions (marked as all N) of the TM helices (Figure 19d). In contrast, in case of POPC membrane, the residues located at the C-terminal of the TM regions (marked as all C) were less conserved than the residues that are located at the N-terminal regions (marked as all N) of the TM helices. In case of PEA membrane, among 6 N-terminal and 6 C-terminal stretches, TM1N, TM2C, TM4C were highly conserved and remained unaltered during the course of vertebrate evolution. Similarly, in case of POPC membrane, TM1N, TM2N, TM4C, TM5N, TM6N and TM6C were highly conserved. Taken together, the non-random, biased and contrasting levels of conservation of C-terminal vs. N-terminal residues in different lipid microenvironments are intriguing. Similarly, differential conservation of inner residues vs. outer residues present in LWI regions is suggestive. Such information provides a “topological identity” of TRPV1 in different lipid bilayers which has been optimized in last 450–400 million years of evolution. This biased selection of amino acids seems to reflect the nature of microenvironments that prevail in these positions too.

2.2.5. Arg and Tyr residues are preferred in the LWI of TRPV1

The diversity and random-ness of the distribution of the LWI amino acids as a 5 amino acid long sequence in all vertebrates where TRPV1 is present in different lipid bilayers

Amino acid	TRPV1			Natural frequency observed in nature
	Lipid water interface	TM region	Full-length	
Arg	9.3	3.6	5.4	4.2
Tyr	8.5	9.3	4.1	3.3
Asp	8.5	1.1	5.3	5.9
Gln	7.9	1.2	3	3.7
Lys	7	2.4	6.2	7.2
Val	6.8	10.6	6	6.8
Glu	6.3	3.2	6.2	5.8
Phe	5.4	13.9	5.8	4.0
Ile	5.3	7.4	5	3.8
Ser	5	4.7	7.2	8.1
Asn	4.1	1.9	4.5	4.4
Gly	4.1	5.1	5.8	7.4
Pro	3.6	0.1	4.2	5.0
Leu	3.3	15.8	11.6	7.6
Thr	3.3	6.2	6	6.2
Ala	3.2	5.5	6.1	7.4
His	3.1	0.4	1.8	2.9
Met	2.1	5.5	2.6	1.8
Trp	1.7	0.6	1.2	1.3
Cys	1.4	1.4	2	3.3

Table 3: Enrichment of snorkeling amino acids in the lipid water interface of TRPV1. Percentage of amino acids present in lipid-water interface region, only in TM region and in full-length TRPV1 are shown. In a completely unbiased condition, frequency of each amino acid is assumed to be 5%. Amino acids that are selected neither positively nor negatively (frequency remain as just 5%) are marked in black. Positively (frequency is >5%) and negatively (frequency is <5%) selected amino acids are written in green and red respectively. Amino acids that are selected neither positively nor negatively are marked in black. The natural frequency of each amino acids is given in the right-most column.

and across were explored. For that purpose, conservation analysis of the LWI-regions at single residue level (Figures 19e and 19f) was performed. Analysis suggested that in both

POPC and PEA membrane, snorkeling amino acids such as Arg and Tyr were highly conserved at the LWI of TRPV1. In several cases, Arginine replaced other positively charged amino acids, such as Histidine in these regions in evolutionary time course suggesting that local pH and protonation-deprotonation events play an important role in this position (Figures 19e and 19f). As LWI impose specific micro-environment suitable for certain amino acids only, the frequency distribution of all 20 amino acids in the LWI-regions of TRPV1 across vertebrates were explored. Frequency calculation of all 20 amino acids also reveals that Arg and Tyr are preferred in the LWI-regions only during vertebrate evolution (Table 3). In PEA membrane, full-length TRPV1 (considering all vertebrate sequences) contains lower level of Arg (5.4%) and Tyr (4.1%) while the LWI-region contains higher level of Arg (9.3%) and Tyr (8.5%) residues. Similar enrichment is also observed when TRPV1 is inserted in POPC membrane (data not shown). This “enrichment” of Arg and Tyr residues suggests specific involvement of these amino acids in the LWI of TRPV1 which form specific micro-environment there. The above mentioned “enrichment” at the LWI is also supported by the observation that full-length human TRPV1 contains 5.2% Arg and 3.9% Tyr residues in entire sequence whereas only the LWI region of TRPV1 contains 9.09% Arg and 15.15% Tyr respectively.

Marking of Arg and Tyr residues on the rat TRPV1 structure also reveals that these amino acids are predominantly clustered in the LWI regions (Figure 20). This in general indicates the importance of snorkeling amino acids such as Arg, Tyr and few others like Asp (8.5%), Gln (7.9%) and Lys (7%) and their preferential selection during vertebrate evolution, probably for the suitability of a microenvironment in LWI. In this context, non-covalent interaction with different membrane components, such as cholesterol is relevant and this might have acted as a selection pressure during molecular evolution of TRPV1.

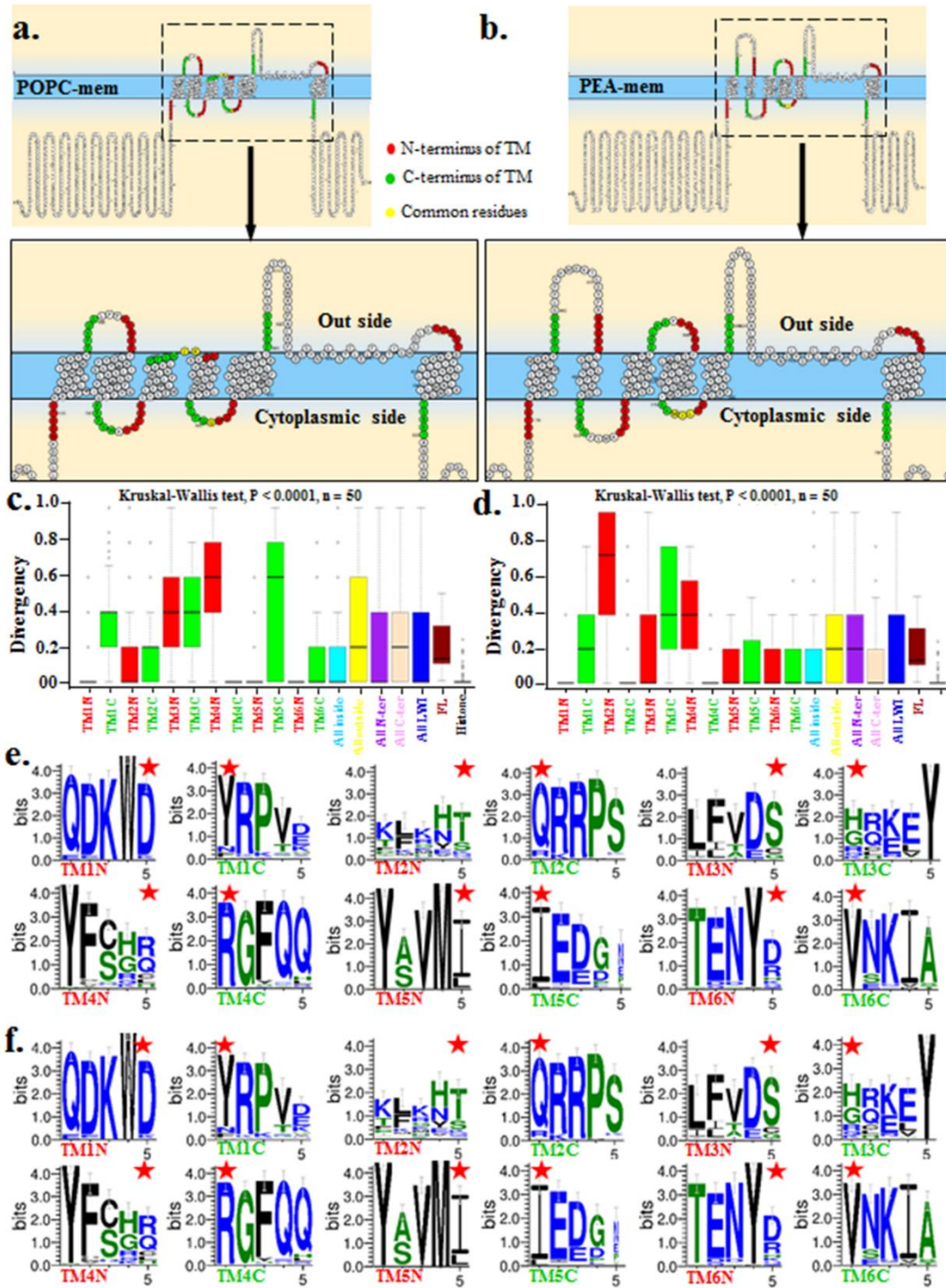


Figure 19. Preferential selection of snorkeling amino acids located at the lipid-water interface of TRPV1 during vertebrate evolution. (a, b) Schematic representation of hTRPV1 sequence in lipid bilayer made of POPC (left) and PEA (right) is shown. Residues located at the lipid-water interface are highlighted (red and green indicate the residues at the N-terminal and C-terminal of each TM helices respectively. Yellow indicates few residues that are common for both N-terminal and C-terminal of each TM helices, between TM3 & TM4 as well as TM4 & TM5). (c, d) Box plot showing conservation of 5 amino acid stretch sequences (marking the amino acids present in LWI) in each side of the TM made of POPC (left) and PEA(right) membrane. The LWI residues present in the inner leaflet of the membrane are highly conserved in vertebrates. (e, f) Conservation analysis of each residue present in the LWI. Snorkeling amino acids such as Arg and Tyr are highly conserved in the LWI of TRPV1. The residues which demarcate the exact boundary-point of individual TM in lipid bilayer are indicated by red colour asterisks (*).

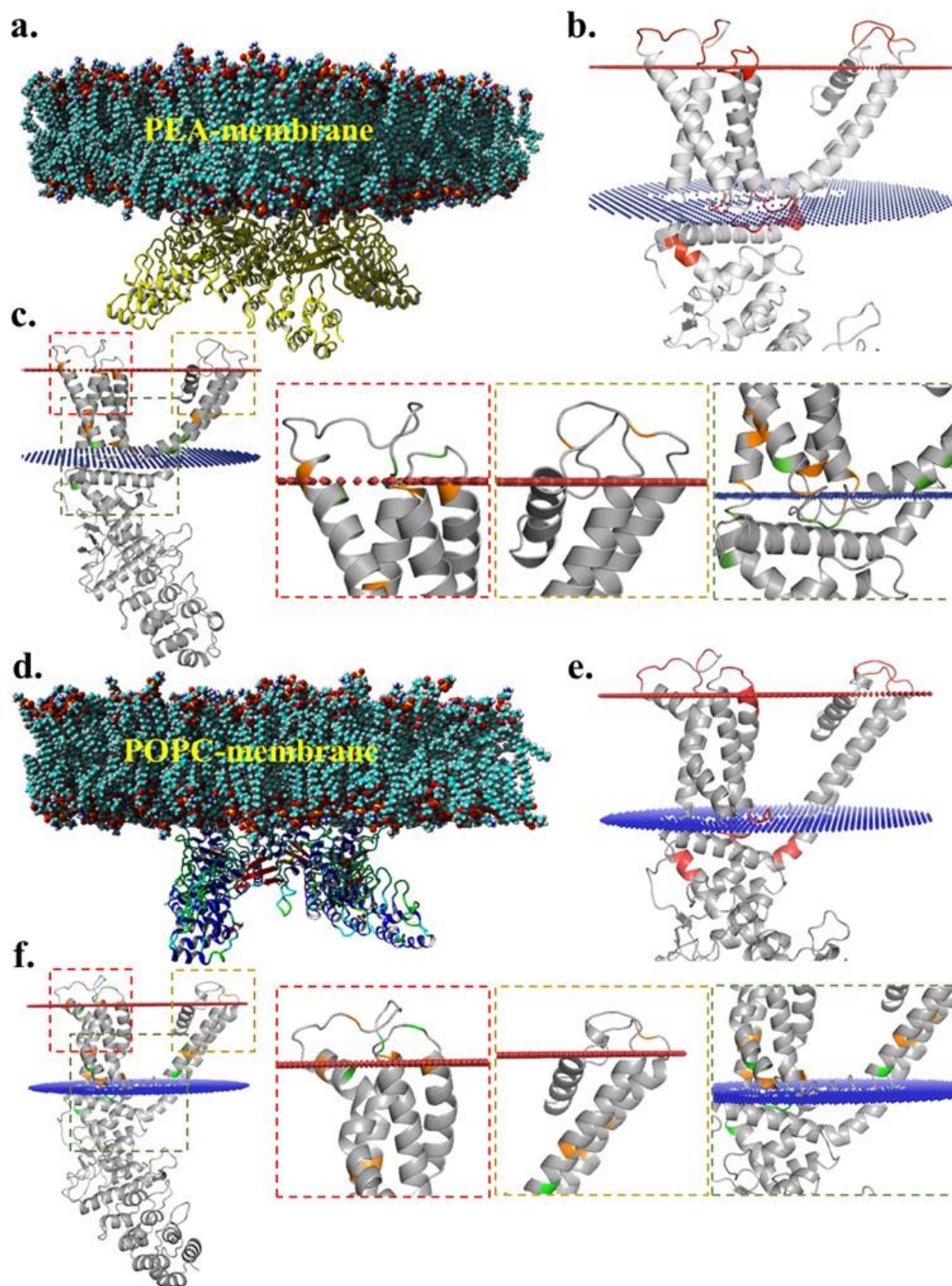


Figure 20. Arg and Tyr residues are enriched in the lipid-water interface of rTRPV1 and are preferentially selected in the lipid-water interface region. Side view of a 3D structure of Rat TRPV1 tetramer (197) embedded in a lipid bilayer made of PEA-membrane (a) or in POPC membrane (d) are shown. The rTRPV1 closed conformation (3J5P) was used and the entire system is stabilized in the lipid bilayer after a short equilibration of 250 ps simulation. (b and e) Residues marking the lipid-water interface of rTRPV1 embedded in PEA-membrane (a) or in POPC membrane are coloured in red. (c and f) The Arg (Green) and Tyr (Orange) residues constitute a large fraction of the lipid-water interface residues and the magnified images of specific lipid-water interface regions are shown in right side.

2.2.6. Identification of possible cholesterol-recognition motifs within TRPV1

Cholesterol is a membrane component and functions of several transmembrane proteins are regulated by cholesterol.

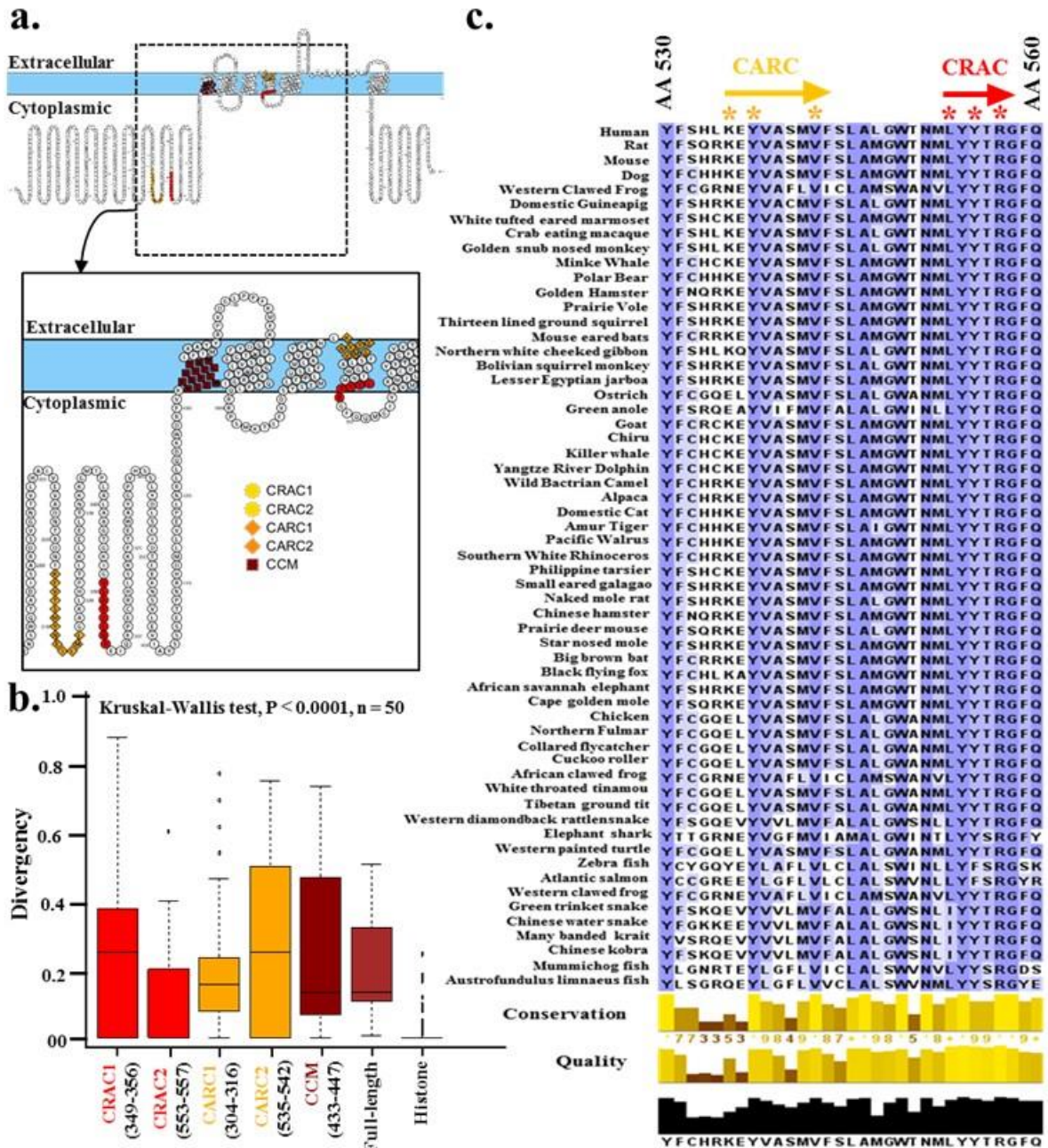


Figure 21. TRPV1 has conserved cholesterol-binding sequences at the lipid-water interface region. (a) Five possible cholesterol-binding sites, namely CRAC (Red) or CARC (Orange) or CCM (maroon) motifs are identified in hTRPV1. (b) Box plot depicting the conservation of individual CRAC, CARC and CCM motifs are shown. The amino acid numbers are indicated below and the CRAC motif (aa 553–557) is the most conserved among all these cholesterol-binding motifs. (c) Sequence alignment of the S4-loop segment (aa 530–560) containing conserved CRAC- and CARC-motifs of TRPV1 of vertebrates are shown. Critical amino acids defining this motif [L/V-X(1-5)-Y-X(1-5)-R/K] are indicated by asterisk (*).

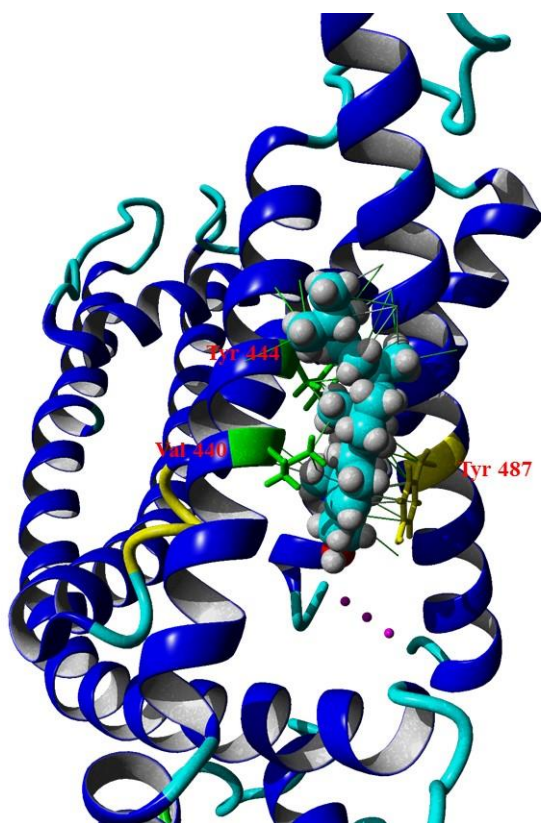


Figure 22. Cholesterol intercalates between CCM motif formed by TM1 and TM2 of TRPV1. Cholesterol forms hydrophobic bonds with Valine at 440 (down) and Tyrosine at 444 (up) on TM1 (green) and 487 at Tyrosine on TM2 (yellow) with a binding energy of 8.54 kcal/mol.

Full-length TRPV1 was searched for the presence of cholesterol Recognition Amino acid Consensus (CRAC) motif (L/V-X(1-5)-Y-X(1-5)-R/K) and conservation analysis of such motifs across vertebrate evolution was assessed. 2 CRAC, 2 CARC (Inverted CRAC) and 1 CCM-motif (amino acid 433–447) in hTRPV1 was identified (Figure 21a). Conservation analysis revealed that among these 5 motifs, the CRAC-motif present in the S4-Loop4 region (aa 553–557) and the CCM motif were most conserved throughout vertebrate evolution (Figure 21b and 21c). This result is in agreement with the recent reports suggesting that the TRPV1 channel function is regulated by cholesterol and amino acids present in the S4-Loop4-S5 region (553–571) are critical for the cholesterol-mediated regulation of TRPV1 (129)(221). The interaction of cholesterol with TRPV1 via CCM motif has been illustrated in Figure 22.

2.2.7. Cholesterol interacts with TRPV1 in closed conformation through highly conserved Arg 557 and Arg 575 residues

In order to explore if cholesterol can bind to TRPV1 through the conserved CRAC-motif with high-binding affinities, global and local docking of cholesterol were performed onto the conserved CRAC-motif (aa 553–571). It was seen that cholesterol had a high binding energy (<-6 kcal/mole) in this region of TRPV1 and involved Arg557 and Arg575 residues respectively by forming H-bonds (binding energy: -7.73 kcal/mole and -8.4 kcal/mole in two different possible binding modes) (Figure 23). Such interactions were visible in different membrane composition and are mainly independent of the level of cholesterol present in the membrane (data not shown). Apart from Arg557 and Arg575, Cholesterol interactions in such positions were favoured by few other hydrophobic and weak interactions. Such interactions with cholesterol were not observed with the open conformation of Rat TRPV1 (Figure 24). Notably, the interaction with cholesterol is possible when the side chains of these Arg residues are charged. These results suggest that changes in Arg-cholesterol interaction correlate well with the opening and closing of TRPV1. This also suggests that Arg557 and Arg575 interaction with cholesterol are important structural determinants of TRPV1 channel functions.

2.2.8. Arg557 and Arg575 of TRPV1 are essential for interaction with cholesterol in closed conformation

The closed conformation of rTRPV1 docked with cholesterol (in the best binding modes) was superimposed to the open conformation of rTRPV1. No interaction of cholesterol with Arg557 or Arg575 of the open rTRPV1 conformation was observed (Figure 24). To analyse if Arg residues at 557 and 575 positions are essential for the interaction of TRPV1 with cholesterol, point mutations were induced in these two

positions and similar docking experiments were performed keeping other parameters unchanged.

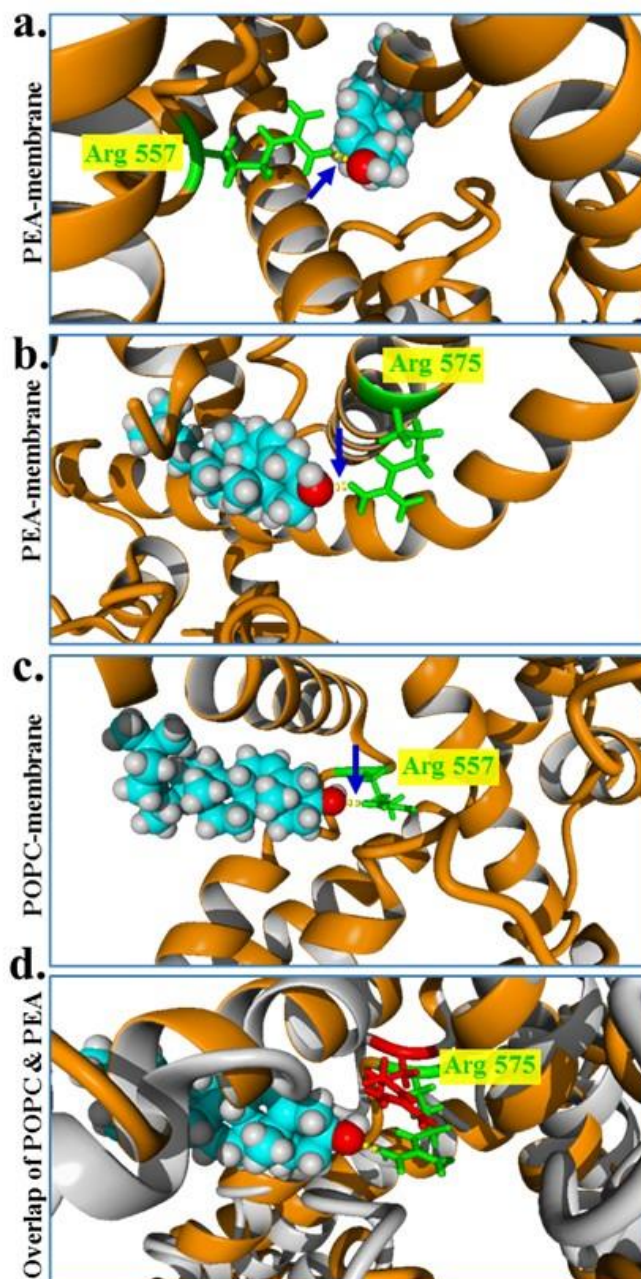


Figure 23. The conserved cholesterol-binding motifs present in TRPV1 interacts with cholesterol through Arg557 and/or Arg575 residues in closed conformation. (a,b) Cholesterol docked on the TRPV1 (closed conformation monomer, 3J5P) in PEA membrane reveals presence of hydrogen bond (denoted by a blue arrow) between the NH1 of Arg557 and NH1 of Arg575 (Green) and OH- of cholesterol. (c) Cholesterol docked on the TRPV1 in POPC membrane reveals presence of hydrogen bond (denoted by a blue arrow) between the NH1 of Arg575 (Green) and OH- of cholesterol with a binding energy of -8.4 kcal/mol. (d) Overlap of Arg575 in PEA and POPC membrane. Arg 575 of TRPV1 in closed conformation interacts with cholesterol when present in PEA membrane (green) but not when present in POPC membrane (red).

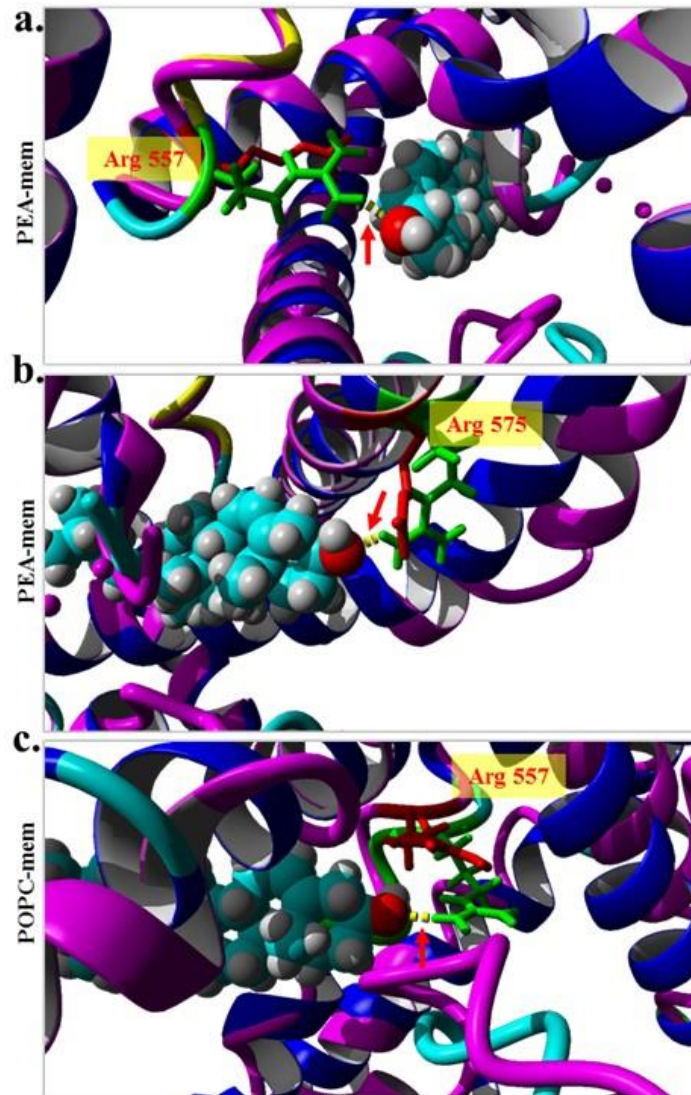


Figure 24. Closed- but not the open-conformation of TRPV1 interacts with cholesterol. (a, b) TRPV1 in closed conformation (3J5P, monomer, indicated in blue ribbon) present in PEA membrane superimposed with open conformation (3J5R, monomer, indicated in magenta ribbon) and further docked with cholesterol. Arg557 (in fig a) and Arg575 (in fig b) are indicated in green (for closed conformation) and in red (for open conformation). H-bond is formed with the closed conformation only. (c) TRPV1 closed conformation (3J5P, monomer, and indicated in blue ribbon) in POPC membrane superimposed with open conformation (3J5R, monomer, indicated in magenta ribbon) further docked with cholesterol is shown. Arg575 is indicated in green (for closed conformation) and in red (for open conformation). H-bond is formed with the closed conformation only. These results suggest that changes in Arg-cholesterol interaction correlates well with the opening and closing of TRPV1.

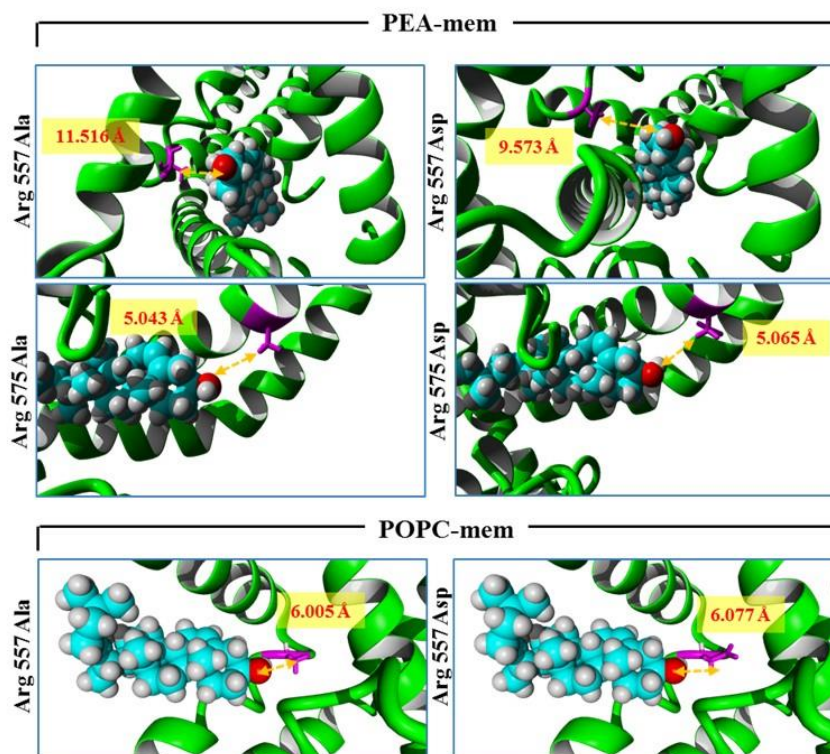


Figure 25. Arg residues at 557th and 575th position of TRPV1 are essential for interaction with cholesterol. Replacing Arg by negatively charged (Asp) or neutral (Ala) residues results in increased distance between the OH- group of cholesterol and these mutated residues causing disruption of the cholesterol interaction within the lipid-water interface region when TRPV1 is present in either PEA or POPC membrane. This result suggests that cholesterol present in the inner leaflet of the lipid bilayer impose a strong positive selection pressure leading to the conservation of snorkeling amino acid Arg in this lipid water interface region.

Arg557 was substituted to Ala (neutral amino acid) or to Asp (negatively charged amino acid) and observed that the mutated residues did not interact with cholesterol as the distances between these amino acids and the OH- group of cholesterol went beyond permissible limits ($>4.5 \text{ \AA}$) of non-covalent interactions (Figure 25). The same was observed when Arg575 was mutated to Ala or Asp respectively (Figure 25). Notably substituting these two positions with other positively charged residues namely by Lys and His also resulted in loss of interaction with cholesterol. These results suggested that the Arg residues at 557 and 575 positions of rTRPV1 are best suited for possible interaction with cholesterol in LWI-regions. These results also suggest that availability and exact

level of cholesterol in the membrane may act as a “regulatory factor” relevant for TRPV1 response.

2.2.9. Substitution of Arg557 and Arg575 by any other amino acid alters localization of TRPV1 and presence in lipid raft

So far, only few reports have confirmed that TRPV1 is present in lipid raft, which is a cholesterol-enriched microdomain fraction of biological membrane. In order to understand the importance of Arg557 and Arg575 of TRPV1 in the context of cholesterol interaction, we generated 8 substitution mutants for each position, namely Arg557 and Arg575. All these mutations (henceforth referred as LWI mutants) were made using full-length Rat TRPV1-pBF1 as the template. Subsequently both full-length TRPV1-WT and TRPV1-LWI mutants were cloned into pSGFP2C1 vector. TRPV1-WT, TRPV1-Arg557Lys, TRPV1-Arg557His, TRPV1-Arg557Asp, TRPV1-Arg557Ala, TRPV1-Arg575Lys, TRPV1-Arg575His, TRPV1-Arg575Asp and TRPV1-Arg575Ala in GFP were subsequently transfected in DRG neuron derived F-11 cell line to analyse the localization of these mutants with respect to TRPV1-WT (Figure 26). Unlike TRPV1-WT, none of these 8 LWI mutants were capable of localizing to the plasma membrane or to the ends of the neurites and/or filopodia. To check the lipid raft localization of full-length Rat TRPV1-WT and these eight LWI mutants in GFP vector, the transfected cells were stained with Cholera Toxin Subunit- B-594 (abbreviated as CTXB-594 henceforth), an endogenous lipid raft marker, under normal as well as in cholesterol depleted conditions (treated with 5mM M β CD for 30 minutes). Compared to TRPV1-WT which co-localized with the lipid raft marker, the mutants failed to show co-localization under control as well as cholesterol-depleted conditions (M β CD treated conditions). WT-TRPV1 failed to exhibit co-localization with CTXB in M β CD treated conditions (Figure 27). In an over-expression system, when these GFP-tagged

constructs were co-transfected along with two other lipid raft markers Flotillin-1-RFP and Caveolin-1-RFP (Figure 28 and Figure 29), similar results were obtained.

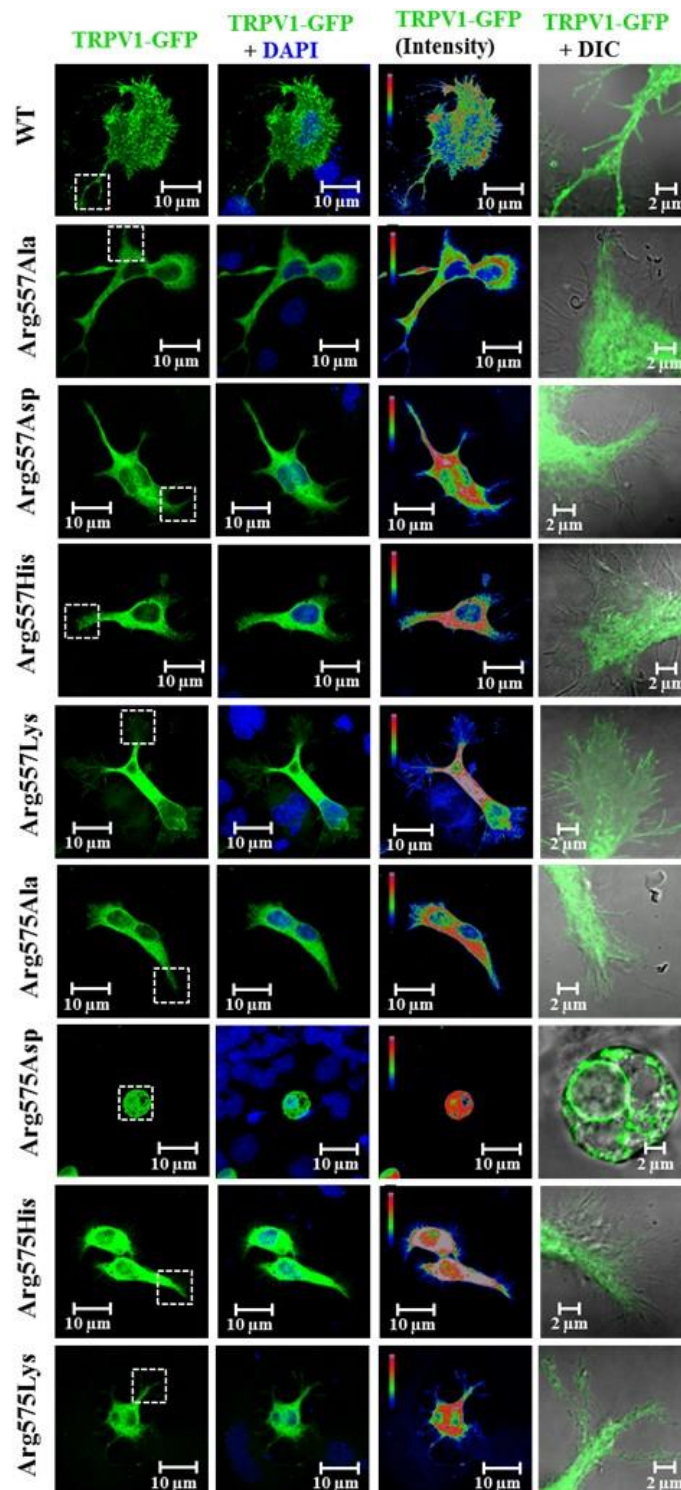


Figure 26. Arg residues at the Lipid-Water-Interface (LWI) are required for proper surface expression and membrane localization. Confocal images depicting the localization pattern of GFP-rTRPV1-WT or different LWI mutants. These GFP-tagged proteins (green) were transiently expressed in F-11 cells for 36 hours, fixed and imaged using confocal microscope. WT-rTRPV1 shows distinct membrane localization, whereas the LWI mutants fail to localize at the membrane. Often the LWI mutants

are retained in the ER and/or cause fragmentation of ER. The intensity of GFP-tagged proteins are shown in the rainbow scale. Nucleus is stained with DAPI (blue). Enlarged view of surface areas (indicated by dotted square) for GFP fluorescence at the membrane merged with DIC image are shown in the right side.

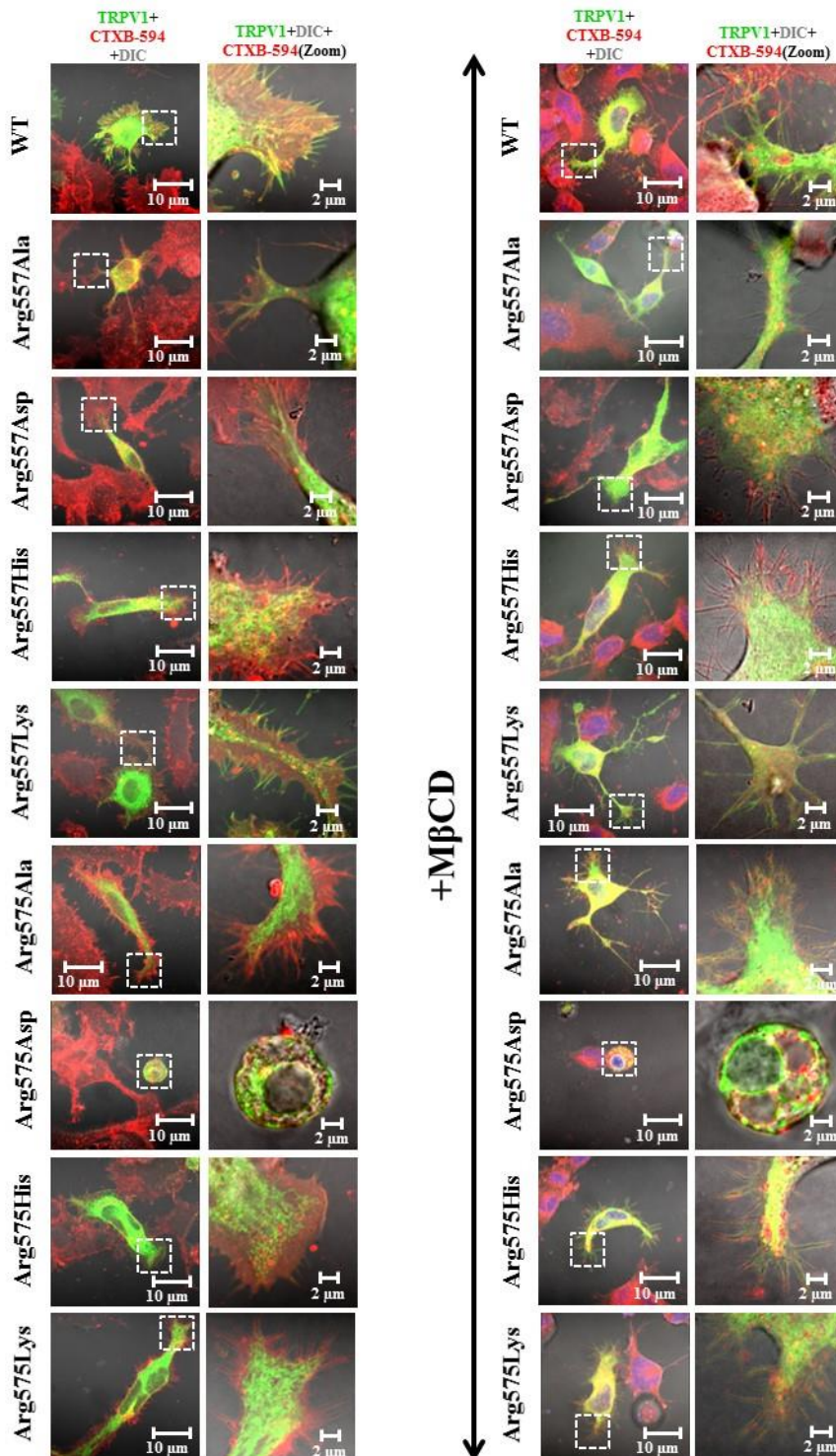


Figure 27. TRPV1-WT but not the LWI mutants co-localize with endogenous lipid raft marker. GFP-TRPV1-WT (green) and different LWI mutants (green) were expressed in F11 cells. Cells were fixed 36 hours post transfection and stained for lipid raft with Cholera Toxin B-594 (red). All images were acquired by confocal microscope. Same experiment was performed with cells that were treated with 5mM

M β CD for 30 min to deplete cholesterol before cell fixation. GFP-TRPV1-WT shows distinct co-localization with Cholera Toxin B in the membranous region while LWI mutants are distinctly excluded from Cholera Toxin B-enriched membranous regions. However, cholesterol depletion only affected co-localization of TRPV1-WT with CTXB.

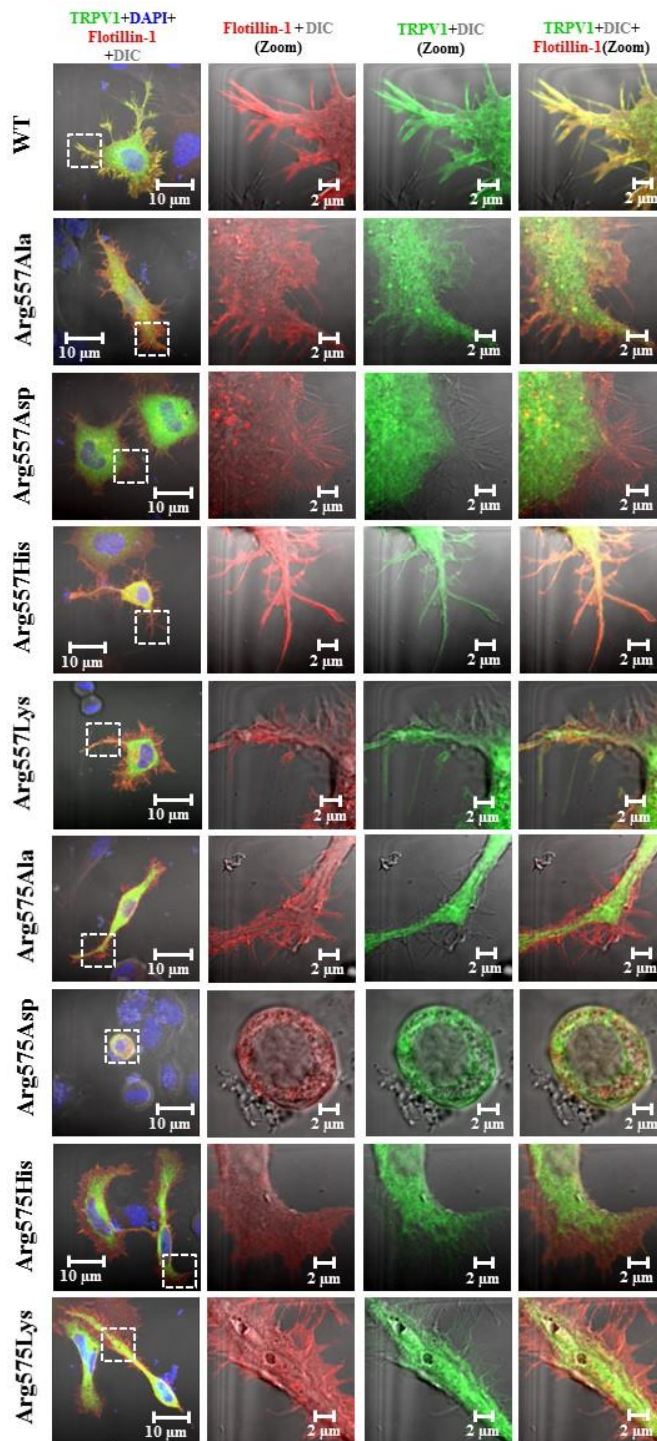


Figure 28. TRPV1-WT but not the Lipid Water Interface (LWI) mutants co-localize with overexpressed lipid raft marker Flotillin1. GFP-tagged (green) TRPV1 wild type (WT) and different LWI mutants were co-expressed with lipid raft marker Flotillin-1-RFP (red) in F11 cells. Cells were fixed 36 hours post transfection and images were acquired by confocal microscope. TRPV1-WT shows distinct co-localization with Flotillin-1-RFP in the membranous region. The LWI mutants are distinctly excluded from Flotillin-1-RFP enriched membranous regions even after over expressing both.

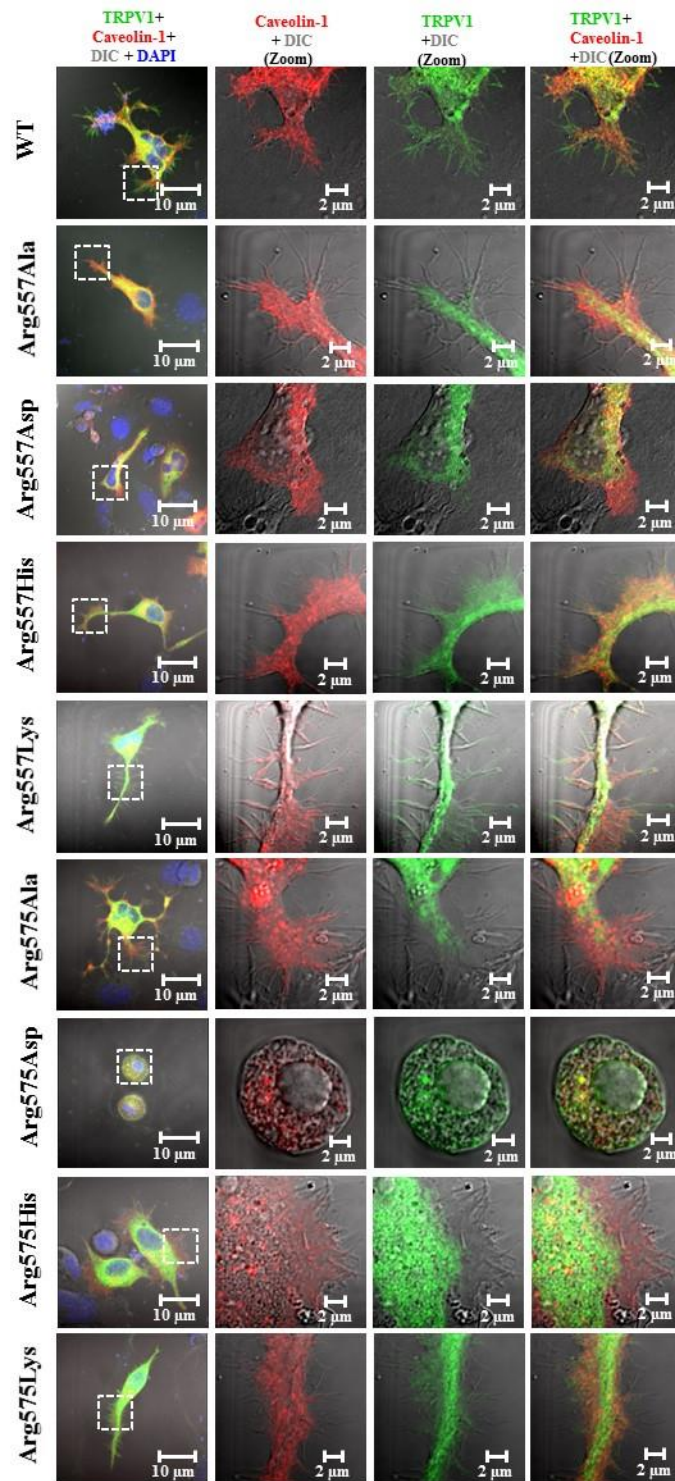


Figure 29. TRPV1-WT but not the Lipid Water Interface (LWI) mutants co-localize with overexpressed lipid raft marker Caveolin1. GFP-tagged (green) TRPV1 wild type (WT) and different LWI mutants were co-expressed with lipid raft marker Caveolin-1-RFP (red) in F11 cells. Cells were fixed 36 hours post transfection and images were acquired by confocal microscope. TRPV1-WT shows distinct co-localization with Caveolin-1-RFP in the membranous region. The LWI mutants are distinctly excluded from Caveolin-1-RFP enriched membranous regions even after over expressing both.

Caveolin-1 and Flottilin-1 co-localized with TRPV1-WT-GFP but not with the LWI mutants which show little or no co-localization. Thus, Arg at positions 557 and 575 is important for proper localization of TRPV1-WT to the lipid rafts. All the eight TRPV1-LWI mutants exhibit membrane trafficking problems, yet none of these imparted an alteration in cellular morphology upon expression, except for TRPV1-Arg575Asp mutant. Most of the F-11 cells expressing TRPV1-Arg575Asp started shrinking soon after transfection, exhibited no neurites or filopodial structures and often tended to detach from the surface. Thus, it can be concluded that although all TRPV1 LWI mutants elicit defects in membrane and lipid raft localization, only TRPV1-Arg575Asp imparts a peculiar phenotype to transfected cells.

2.2.10. Analysis of molecular selection and exclusion of amino acids in the lipid-water interface regions of TRPV1 throughout vertebrate evolution

A total of 14 mammals, 4 birds, 14 reptilians, 2 amphibians and 4 piscine TRPV1 sequences were considered. The frequency-of-occurrence of all 20 different amino acids at the lipid-water-interface (LWI) region was calculated. The same calculation was also performed for the outer as well as inner LWI region separately (Figure 30). Analysis revealed that the frequency-of-occurrence of positively-charged amino acids in inner LWI remain mostly constant during vertebrate evolution, however with different values. Amongst all the positively-charged amino acids, Arg (having the highest pI of 13.5 for the side group) occurs most frequently (10%) in the inner LWI region of TRPV1 and this percentage remain conserved from amphibians to mammals. The other positively-charged amino acids, Lys (pI = 10.4 for the side group) also show a conserved frequency-of-occurrence (6.67 %) across evolution on the inner leaflet, especially from amphibians to mammals. However, frequency-of-occurrence of

another positively-charged amino acid, namely His (pI = 6.8 for the side group) remain conserved, yet at a very low value or at zero value suggesting that His residue is never selected in the inner LWI region while other positively-charged residues were selected there. Notably, the frequency of Arg, Lys and His in the inner LWI region also suggests that positively-charged residues with high pI values (for side group) only are selected and retained in the inner LWI region. This is in concert with the “positive-inside rule” that states the preferential occurrence of positively charged amino acids on the cytoplasmic face of transmembrane helices (277).

For the negatively-charged residues at the inner LWI region, higher the pI, lower was the frequency-of-occurrence. Asp residue (pI of 4 for the side group) occurred more frequently on the inner leaflet as compared to Glu residue (pI of 4.4, for the side group). Moreover, the % frequency of Asp residue on the inner LWI has increased from fishes to amphibians (indicative of positive selection) and subsequently remained conserved throughout the evolution (indicative of stabilization). On the other hand, frequency of Glu had decreased from nearly 10% in fishes to almost 0% in amphibians (indicative of negative selection), and remain at 0% value to mammals suggesting gradual exclusion of this amino acid in this LWI region. However, in the outer LWI region, frequency-of-occurrence of Glu and Asp residues are random and remain at a relatively high frequency.

Aromatic amino acids, namely Trp, Tyr and Phe have relatively low frequency-of-occurrence across evolution in the inner LWI. Both Trp and Tyr remain at less than 5% frequency, yet remain conserved at the inner LWI region throughout the vertebrate evolution (indicative of critical function played by these amino acids). Frequency-of-occurrence of Phe remain random in the inner as well as outer LWI region. Out of these

three aromatic amino acids, only Tyr (pI of 9.6 for the side group) retains a higher frequency-of-occurrence (13%) at the outer LWI.

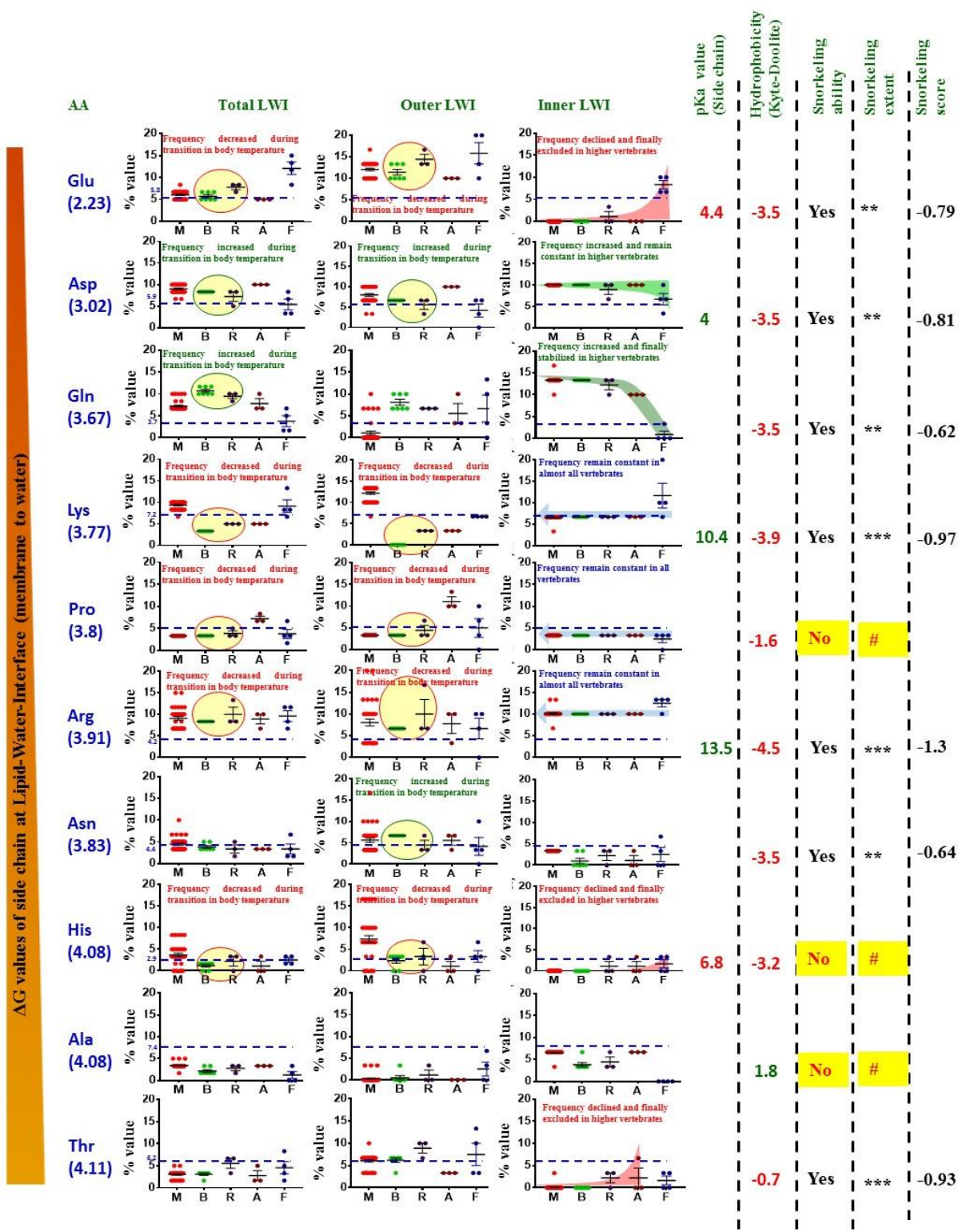


Figure 30. “Frequency-of-occurrence” analysis for different amino acids at the lipid-water-interface (LWI) of TRPV1 in different phylogenetic groups. The “frequency-of-occurrence” of all 20 different amino acids at inner LWI (right-most row), at outer LWI (middle row), and total (combining inner and outer LWI, left-most row) have been shown separately. Frequency-of-occurrence of different amino acids

of TRPV1 LWI region across different vertebrate species ranging from fishes (F), amphibians (A), reptiles (R), birds (B) and mammals (M) are shown. (P.T.O)

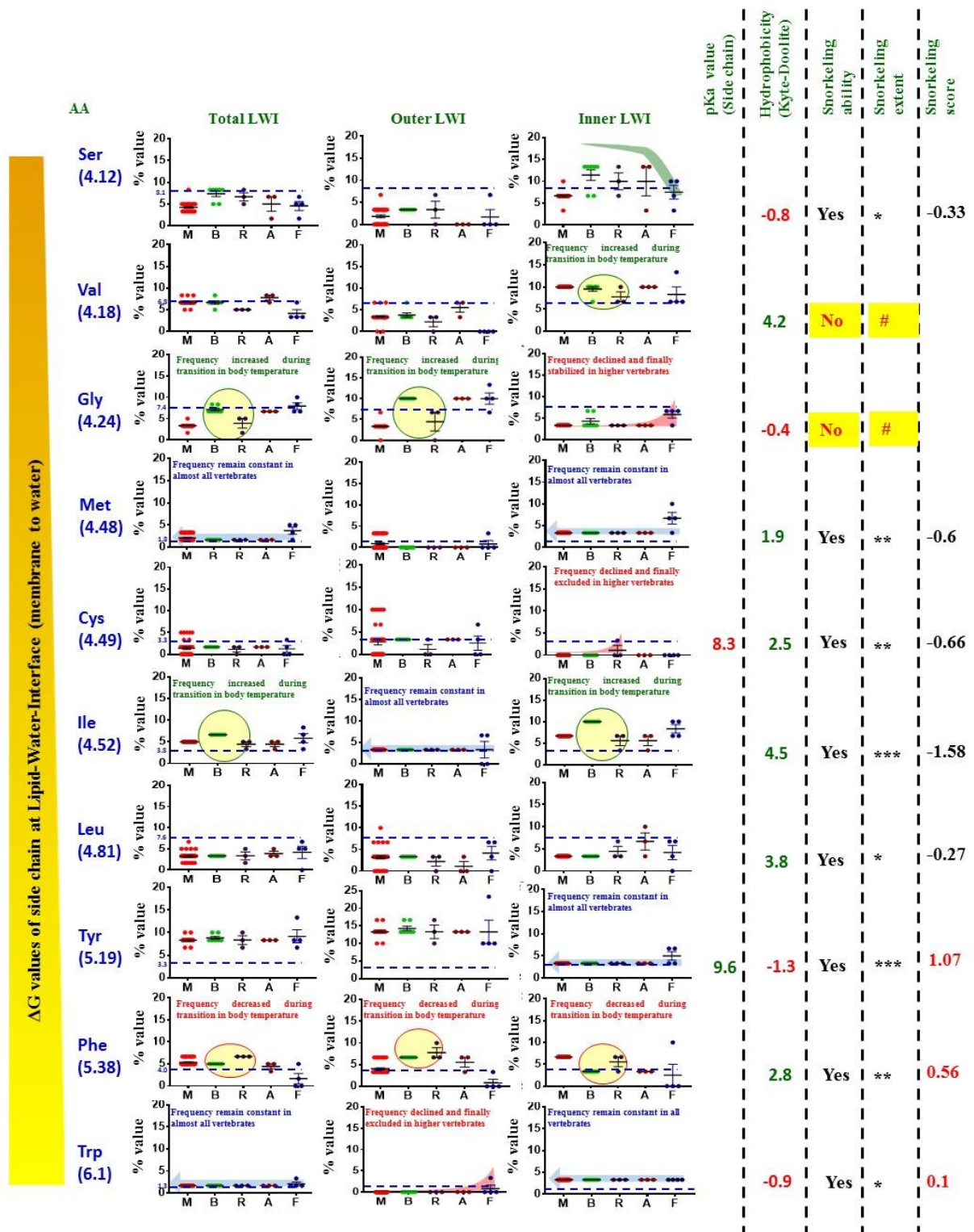


Fig.30 (Contd.) The amino acids were arranged according to the low to high ΔG values of the side-chain values (278). In cases where percentage of amino acids remain constant are indicated by blue arrow as back ground. Similarly, positively selected and negatively selected (or excluded) are marked with green or red background. The circles with green (for positive selection) or red (for negative selection) lines indicate

the changes in frequency-of-occurrence during transition from reptiles to birds as a result of change in body temperature.

The dotted blue line indicates the observed frequency of amino acids in vertebrates (source: <http://www.tiem.utk.edu/~gross/bioed/webmodules/aminoacid.htm>)

Helix-breaking amino acid Pro has more or less equal distribution throughout evolution both in outer 3.33%) and inner LWI (3.33%) region, especially in the higher vertebrates. Another helix-breaking amino acid, namely Gly has been retained at less than 5% frequency at the inner LWI region, but mostly remain conserved throughout the vertebrate evolution.

Individual hydrophobic amino acids, namely Ile, Leu, Val and Ala retained different percentages of frequency-of-occurrence and conservation. Notably, Isoleucine remained conserved in outer LWI. Among other amino acids Met remained conserved in the inner LWI region. At inner LWI region, the frequency-of-occurrence for Cys was low in all vertebrates and eventually excluded in the higher vertebrates. Taken together, the analysis suggest enrichment or reduced occurrence of specific amino acids at the inner LWI region and therefore provides important clue of TRPV1 function in different species.

2.2.11. Changes in the Arg and/or Tyr content in the LWI of TRPV1 during Piscean to mammal evolution correlates with increasing cholesterol content and increased body temperature

In spite of variations due to species, tissue, age, sex and other factors, the average level of cholesterol is generally low in lower vertebrates (such as in fish) and generally high in higher vertebrates (such as in mammals). This is mainly due to the fact that cholesterol biosynthesis is an exclusive feature of eukaryotes. Specific sterols have evolved in different evolutionary time points, and the entire sterol pathway shares close relationship with vertebrate evolution (279). Specifically, different levels of cholesterol

are known to alter several properties of biological lipid membranes, such as fluidity, rigidity, lipid-packing, phase-shift, freezing behaviour, mechanical stiffness, etc. (280)(281). Notably, most of these properties are also temperature-dependent and slight changes in temperature can induce major changes in these properties. TRPV1 has a significant role in the maintenance of core body temperature, at least in mammals and during infection and inflammation (282)(283). It is hypothesized that if interactions of snorkeling amino acids with cholesterol (and also with other sterols) are relevant for the function of TRPV1 within the lipid bilayers, then core-body temperature and/or average level of cholesterol should play important roles and such importance should also be reflected in the conservation and frequency distribution of snorkeling amino acids present in the LWI of TRPV1. In other words, physico-chemical factors disturbing the interaction of snorkeling amino acids with cholesterol should have specific signature in the evolutionary history of TRPV1. To address this, the frequency distribution of snorkeling amino acids present in the total 60 amino acids representing 12 LWI regions of TRPV1 was calculated. For that purpose; species ranging from all vertebrate phyla were considered. A total of 14 mammals, 4 birds, 14 reptilians, 2 amphibians and 4 piscean TRPV1 sequences were considered and the percentage distribution of Arg and Tyr residues in them were compared. It was noted that the total frequency of snorkeling amino acids (Arg and Tyr) is high in fishes and low in mammals (Figure 31a). Total content of snorkeling amino acids (Arg and Tyr) in the LWI of TRPV1 is also more in cold-blooded (fishes, amphibians and reptilians grouped together) animals than in warm-blooded (birds and mammals grouped together) animals, suggesting that core body temperature may have effects on the selection of these residues and/or these residues may play critical role in thermo-gating (Figure 31a). The same analysis was performed for Tyr residue only, and it was seen that the percentage of Tyr content (mean value) in the LWI does not vary

much between cold- and warm-blooded animals, or across the different phyla when compared among all vertebrates. Though these differences remain statistically non-significant (mainly due to insufficient gene sequences representing each phyla), comparison within cold-blooded animals indicate that the percentage (mean value) of Tyr decreased steadily from Piscean to reptilian evolution.

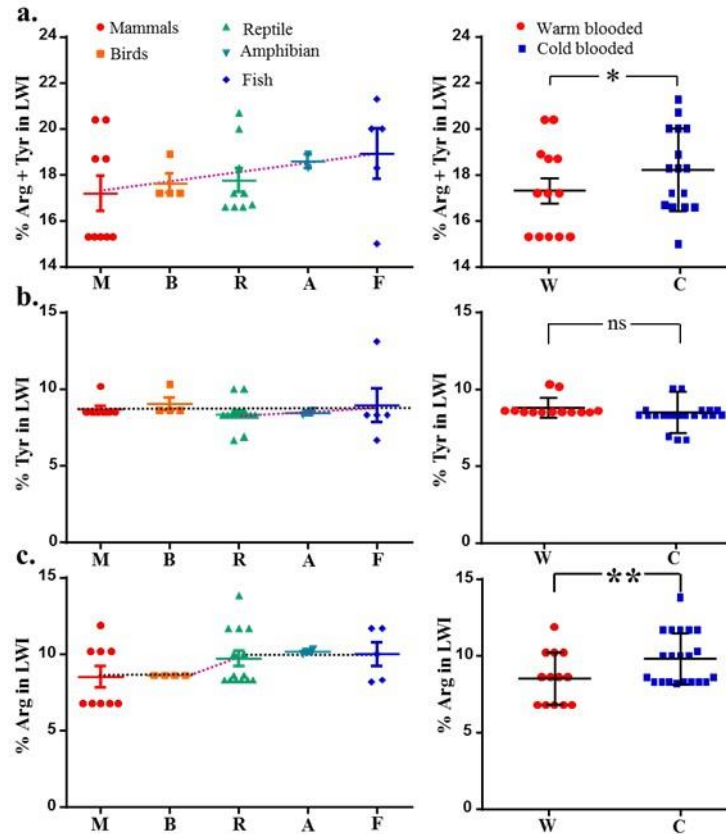


Figure 31. Frequency of snorkeling residues present in the lipid water interface of TRPV1 share inverse relationship with body temperature and average cholesterol level throughout the vertebrate evolution. Total 60 aa representing all 12 LWI regions of TRPV1 sequences from 34 were considered and percentage of only Arg and Tyr was analysed in individual phyla or in cold-blooded (C) and warm-blooded (W) animals. **(a)** The total percent of snorkeling residues (Arg and Tyr) present at the LWI of TRPV1 from different phyla are shown. These aa (mean value) decreased steadily (indicated by dotted line, violate) during the Piscean (avg. cholesterol level is low) to mammalian (avg. cholesterol level is high) evolution in each phyla, indicating that these snorkeling residues are selected under very specific and stringent conditions, such as level of membrane cholesterol. Total content of snorkeling aa in the LWI of TRPV1 is also more in cold-blooded than in warm-blooded animals, suggesting that core body temperature may have effects on the selection of these residues and/or these residues may play critical role in thermo-gating. **(b)** The percent Tyr content (mean value) in the LWI does not vary much between C and W animals, or across the different phyla. This difference remains statistically non-significant (ns). However, among cold-blooded animals, the percent Tyr content decreased steadily (indicated by dotted line, violate) during the Piscean to reptilian (Avg. cholesterol level is moderate) evolution in each phyla, indicating that in case of low body temperature, the level of membrane cholesterol has influence on the selection of Tyr residues in the LWI. **(c)** The total percentage (mean value) of Arg at the LWI of TRPV1 remain same in all cold-blooded animals, decreased rapidly during the transition of C to W animals and then remain same within all W animals (with a lower value). This suggests that core-body temperature has a strong influence on the selection of Arg residues. Total Arg content in LWI of TRPV1 is more in cold-blooded than in warm-blooded animals,

strongly suggesting that these residues play critical role in thermo-gating too. This difference is statistically significant (* $p < 0.05$, ** $p < 0.01$).

These results may also suggest that in case of constant low body temperature, the level of membrane cholesterol may have influence on the selection of Tyr residues in the LWI (Figure 31b). Notably, the total percentage (mean value) of Arg at the LWI of TRPV1 remained same in all cold-blooded animals, decreased rapidly during the transition of cold-blooded to warm-blooded animals and then remained same within all warm-blooded animals (though with a lower value) (Figure 31c). This result suggests that core-body temperature influences the selection of essential Arg residues in the LWI and other Arg residues have been eliminated during the transition of cold-blooded to warm blooded animals. Total Arg content in LWI of TRPV1 is more in cold-blooded than in warm-blooded animals, suggesting that the Arg residues retained in higher mammals may play critical role in thermo-gating functions of TRPV1. Together, these results suggest that the frequency of snorkeling residues, namely Arg and Tyr present in the lipid water interface of TRPV1 share close relationship with body temperature and/or average cholesterol level throughout the vertebrate evolution.

2.2.12. Ratio of positive-negative amino acids in the inner LWI region remain constant in TRPV1 through-out the vertebrate evolution

All positively-charged amino acids (Arg, Lys, and His) have a higher frequency-of-occurrence at the outer LWI region in mammals but its pattern of occurrence is not conserved throughout evolution. Though the frequency-of-occurrence of positively-charged amino acids is less on the inner LWI but its frequency-of-occurrence has remained conserved throughout vertebrate evolution from amphibians to mammals (Figure 32). Similarly, negatively-charged amino acids have a higher frequency-of-occurrences on the outer LWI, but is more conserved on the inner LWI. While frequency-

of-occurrence for individual amino acids are variable, the ratio of the total number of positively-charged amino acids and total number of negatively-charged amino acids at the inner LWI show a ratio of 1.67:1 and this ratio remain conserved in the entire vertebrate evolution. This ratio is not conserved in case of outer LWI. These findings strongly suggest that during vertebrate evolution, this conserved ratio at the inner LWI has played a strong selection pressure in case TRPV1 function.

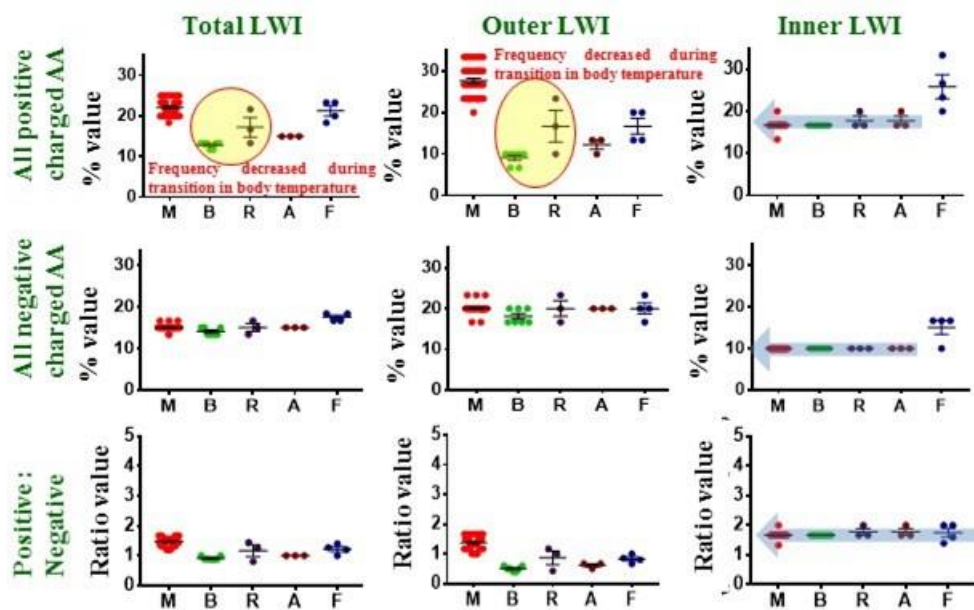


Figure 32. Ratio of positive/negative amino acids remain constant at the inner lipid-water-interface of TRPV1. Frequency-of-occurrence of positively- and negatively-charged residues at the lipid water interface of TRPV1 during vertebrate evolution are shown. Positively-charged amino acids (Arg, Lys, His) and negatively-charged amino acids (Asp and Glu) at the lipid water interface region of TRPV1 across different vertebrate species ranging from fishes, amphibians, reptiles, birds and mammals has been calculated. Negatively-charged amino acids on the inner leaflet appear to be more conserved across evolution. The ratio of positively-charged to negatively-charged amino acids on the inner leaflet at a value of 1.6:1 remain conserved throughout vertebrate evolution.

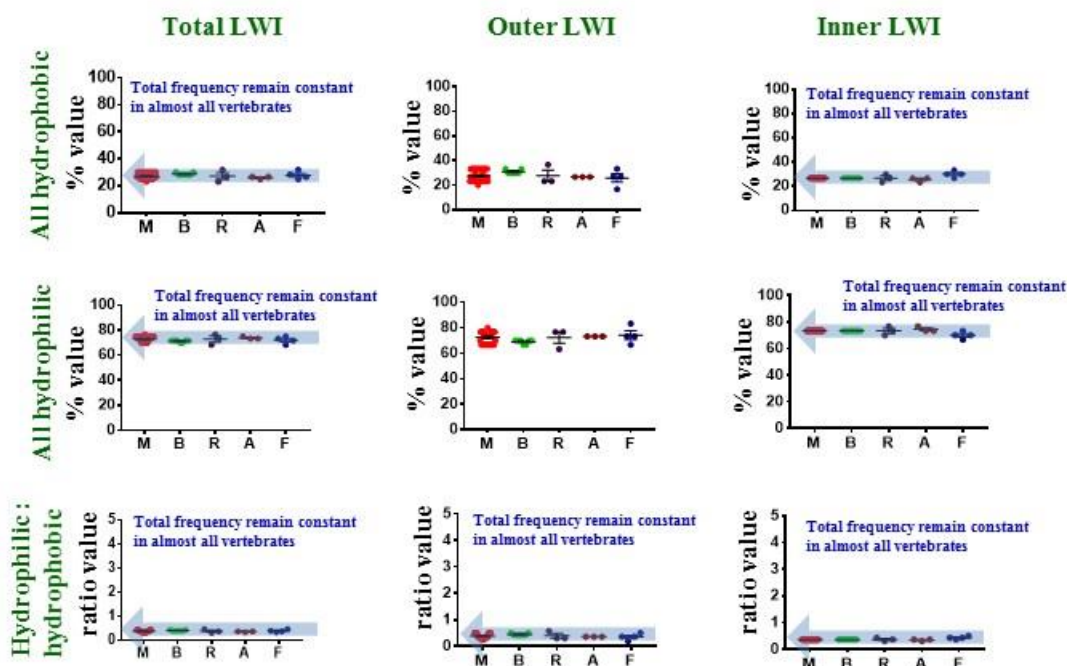


Figure 33. Ratio of hydrophobic/hydrophilic amino acids remain constant at the inner lipid-water-interface of TRPV1. The frequency-of-occurrence of hydrophobic amino acids (Cys, Phe, Ile, Leu, Met, Trp, Tyr), hydrophilic amino acids (Ala, Asp, Glu, Gly, His, Lys, Asn, Pro, Gln, Arg, Ser, Thr, Val) and their ratio are shown. The ratio of hydrophilic/hydrophobic amino acids at the inner leaflet remain conserved at a value of 0.36 throughout the vertebrate evolution.

2.2.13. TRPV1 retains unique combination of hydrophobic and hydrophilic amino acids in its inner lipid-water interface

Hydrophilic amino acids (Ala, Asp, Glu, Gly, His, Lys, Asn, Pro, Gln, Arg, Ser, Thr, Val) have a higher incidence of occurrence (~73.14% in total) on the inner LWI region as compared to the hydrophobic residues (Cys, Phe, Ile, Leu, Met, Trp, Tyr, Total ~26.85%). This difference in distribution of hydrophobic and hydrophilic amino acids at the inner LWI region has been more or less conserved across evolution from fishes to mammals. However, when the ratio of occurrence of the all hydrophobic and all hydrophilic amino acids is considered, the ratio remain conserved in the inner, outer and total LWI (Figure 33). These findings strongly suggest that during vertebrate evolution, the conserved ratio at LWI region of TRPV1 has played a strong selection pressure in case TRPV1 function. Therefore; the data clearly suggest that ratio of hydrophilic-

hydrophobic amino acids as well as ratio of positive-negative charge plays important selection pressure, at least in the inner LWI region.

2.2.14. Arg575Asp induced cellular morphology impairment can be rescued by maintaining overall positive-negative charge ratio

As this Arg575Asp mutation disrupts the positive-negative charge ratio at the inner LWI (especially in the TM5 region which regulates pore opening), this perturbation could be one of the plausible cause leading to constitutive channel opening and thus lethality observed in cells transfected with this construct. In order to explore this possibility, the adjacent residue having a conserved Aspartic Acid at 576 position was mutated to Arginine in the TRPV1-Arg575Asp mutant. Notably, the ratio of positive- and negatively-charged residue in this double mutant is same as in wild-type TRPV1. F11 cells expressing the double mutant, i.e. GFP-TRPV1-Arg575Asp Asp575Arg retain their normal morphology. Therefore, the lethality observed in case of TRPV1-Arg577Asp can be rescued by introducing positive charge at 576th position (Figure 35a). When the length, breadth, area and perimeter of F-11 cells transfected with GFP-TRPV1-WT, GFP-TRPV1-Arg575Asp and GFP-TRPV1-Arg575Asp-Asp576Arg- (100 cells each) were calculated, a significant increase in the length, perimeter and area of cells transfected with GFP-TRPV1-Arg575Asp-Asp576Arg was observed as compared to cells expressing GFP-TRPV1-Arg575Asp (Figure 35b). However, even though TRPV1-Arg575Asp-Asp576Arg was capable of retaining the viability of transfected cells, its migration to the plasma membrane and its capability to form neurites and filopodia remained slightly compromised in comparison to TRPV1-WT. GFP-TRPV1-Arg575Asp-Asp576Arg was neither able to co-localize with overexpressed lipid raft markers like Caveolin-1-RFP and Flotillin-1-RFP, nor with lipid rafts endogenously stained with CTXB-594 (Figure 36) in

presence as well as cholesterol depleted conditions. This suggests that TRPV1 is optimized for a positive charge at 575th position and negative charge at 576th position. This particular phenotype attributed by TRPV1-Arg575Asp was not specific to F-11 cells. SaOS (Figure 37a) and HaCaT (Figure 37b) cells when transfected with TRPV1-Arg575Asp also assumed a similar type of rounded morphology that could be rescued by TRPV1-Arg575Asp-Asp576Arg.

In order to demonstrate the effects imparted by TRPV1-Arg575Asp mutant, TRPV1-WT, TRPV1-Arg575Asp and TRPV1-Arg575Asp-Asp576Arg (all in pSGFP2C1 vector) were co-transfected with pDsRed2-Bid in F-11 cells. Bid is proapoptotic protein that normally resides in the cytosol in a healthy non-apoptotic cell as a soluble protein exhibiting a uniform distribution all over the cytosol. Upon induction of apoptosis, Bid undergoes proteolytic cleavage and translocates to mitochondria (284). The uniform cytosolic distribution of Bid-DsRed2 was observed in TRPV1-WT and TRPV1-Arg575Asp-Asp576Arg expressing cells. However, in case of TRPV1-Arg575Asp, the expression of Bid-DsRed2 became significantly reduced (Figure 34).

2.2.15. TRPV1-Arg575Asp exhibits impaired surface expression that is partly rescued by TRPV1-Arg575Asp-Asp576Arg

In order to check the surface expression of full-length Rat TRPV1-Arg575Asp and TRPV1-Arg575Asp-Asp576Arg with respect to TRPV1-WT, all three constructs in pmCherryC1 vector were transiently transfected in F-11 cells and subsequently stained with TRPV1-ATTO-488 antibody directed against the 3rd extracellular loop of TRPV1. Whereas, TRPV1-WT showed discrete surface expression, TRPV1-Arg575Asp showed a complete loss of surface expression. Though, TRPV1-Arg575Asp-Asp576Arg is

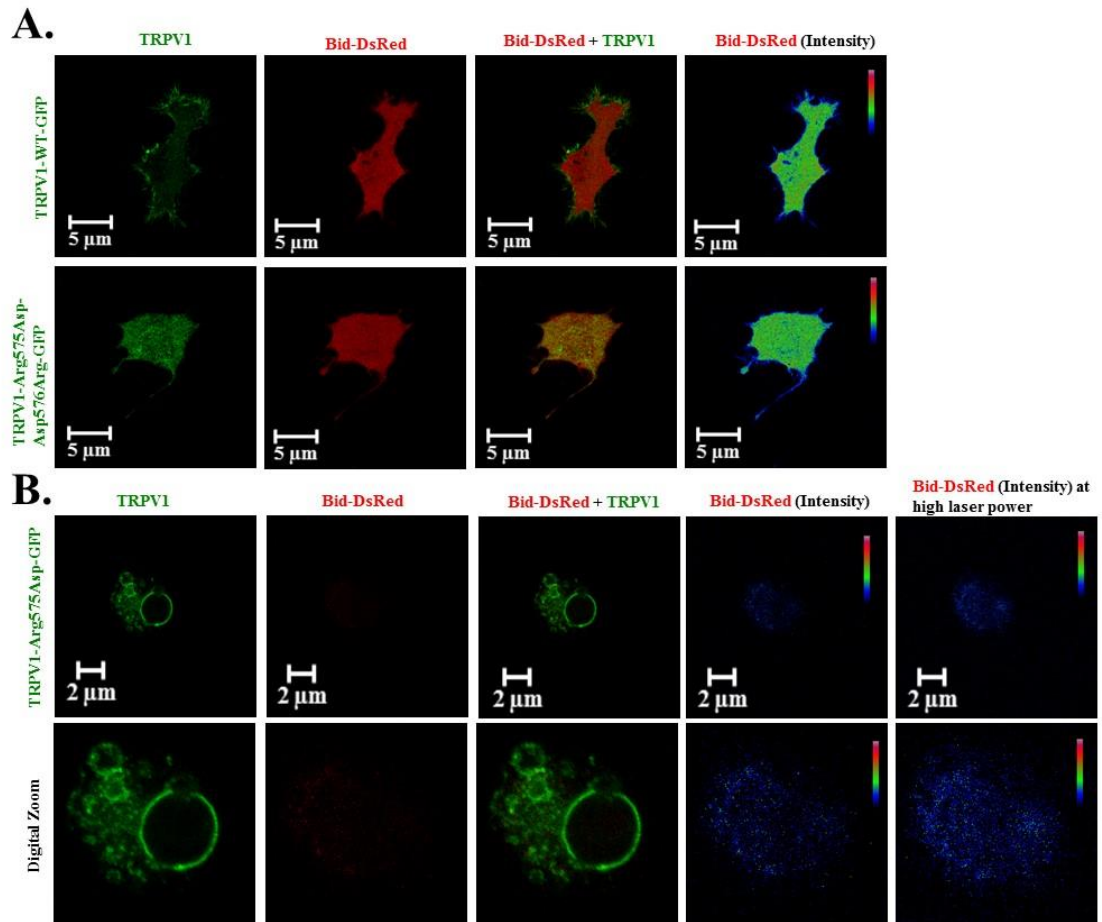


Figure 34. Localization of Bid- DsRed2 in TRPV1-WT and TRPV1 LWI mutants. (A) F-11 cells transiently transfected with TRPV1-WT-GFP and TRPV1-Arg575Asp-Asp576Arg-GFP. They were co-transfected with Bid- DsRed2. Live cell imaging showed uniform cytosolic distribution in both of them. (B) F-11 cells transiently transfected with TRPV1-Arg575Asp-GFP and Bid- DsRed2 exhibits extremely low levels of Bid even upon exposure with high laser power.

capable of rescuing several defects observed in case of TRPV1-Arg575Asp mutant, the double mutant is also not observed in surface except certain distinct dots located on the surface non-uniformly (Figure 38).

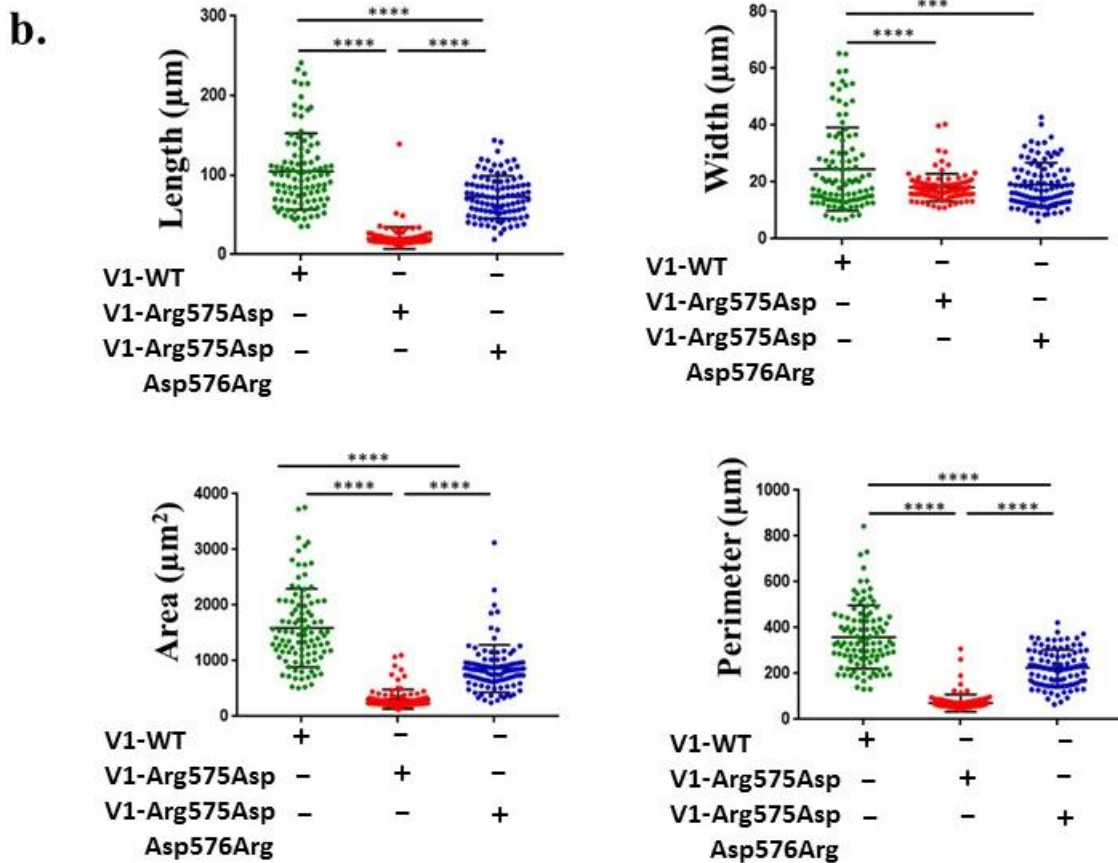
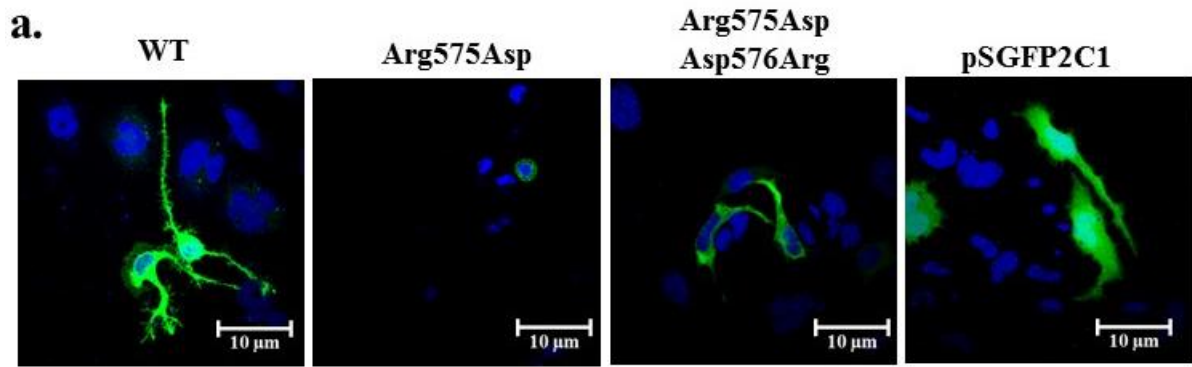


Figure 35. Change in cellular morphology due to Arg575Asp mutation can be rescued by introducing another mutation. **a.** Confocal images of TRPV1-WT, TRPV1-Arg575Asp and TRPV1-Arg575Asp-Asp576Arg in GFP vector expressed in F11 cells. Cells expressing Arg575Asp mutation tend to assume a circular morphology and decreased surface adhesion behaviour. **b.** Quantification of different morphology parameters such as length, width, area and perimeter suggest that Arg575Asp mutant induce reduction in cell size and introducing of Asp576Arg on Arg575Asp rescues all these parameters. In all cases, minimum 100 cells were quantified. The **** (P < 0.0001) and *** (P < 0.0003) indicate values that are significantly different.

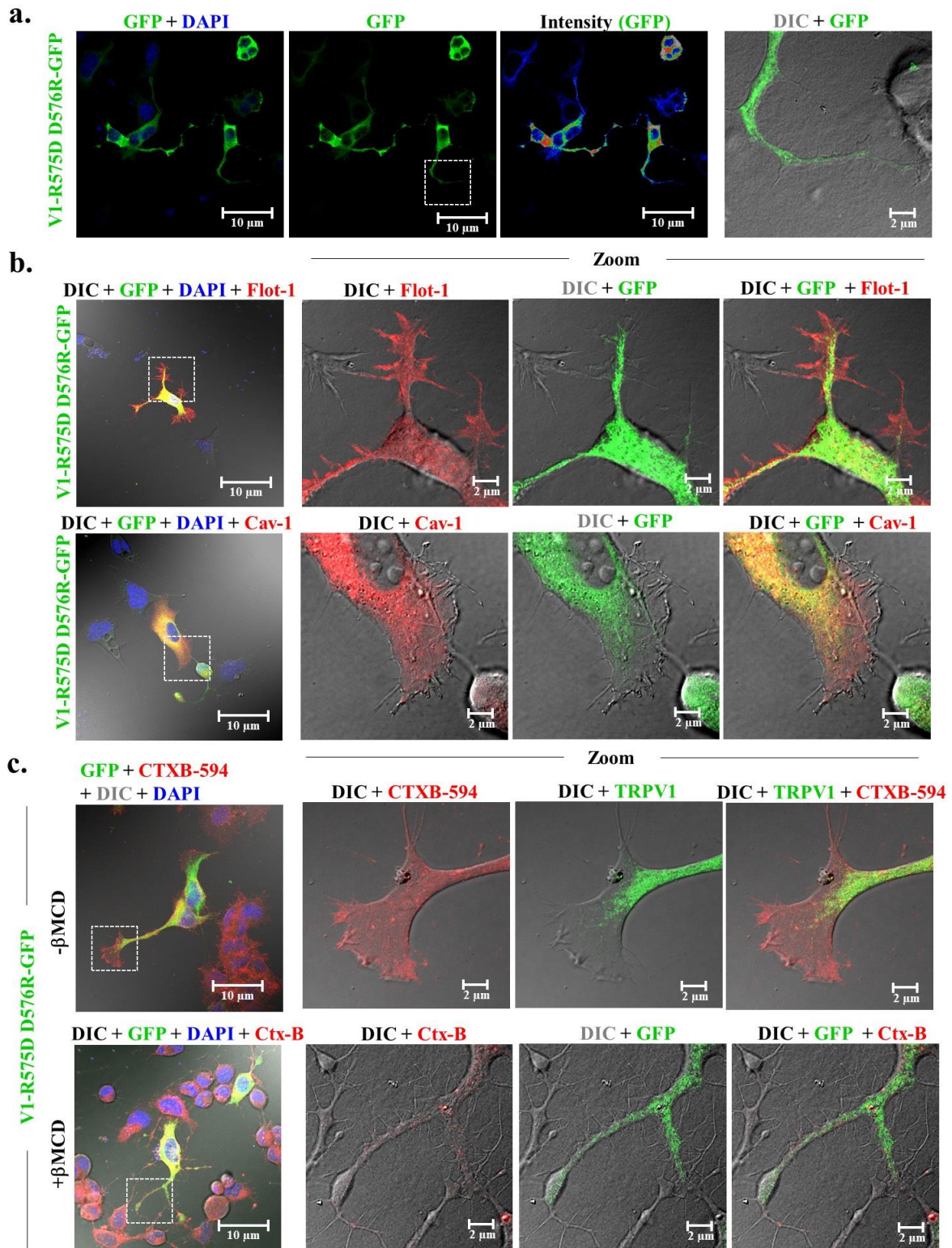


Figure 36. Localization of TRPV1-Arg575Asp Asp576Arg-GFP in F-11 cells and its co-localization with different lipid raft markers. TRPV1-Arg575Asp Asp576Arg in GFP vector was transiently transfected into F-11 cells. (a) Unlike TRPV1-WT it did not show distinct membrane localization. (b) Overexpression of GFP-TRPV1-Arg575Asp Asp576Arg with lipid raft markers Flotillin 1-RFP (Flot-1) and Caveolin 1-RFP (Cav-1) also demonstrated its lack of co-localization with these markers. (c) When stained with endogenous lipid raft marker CTXB-594, then also this mutant failed to localize in lipid raft in control as well as cholesterol depleted conditions with M β CD.

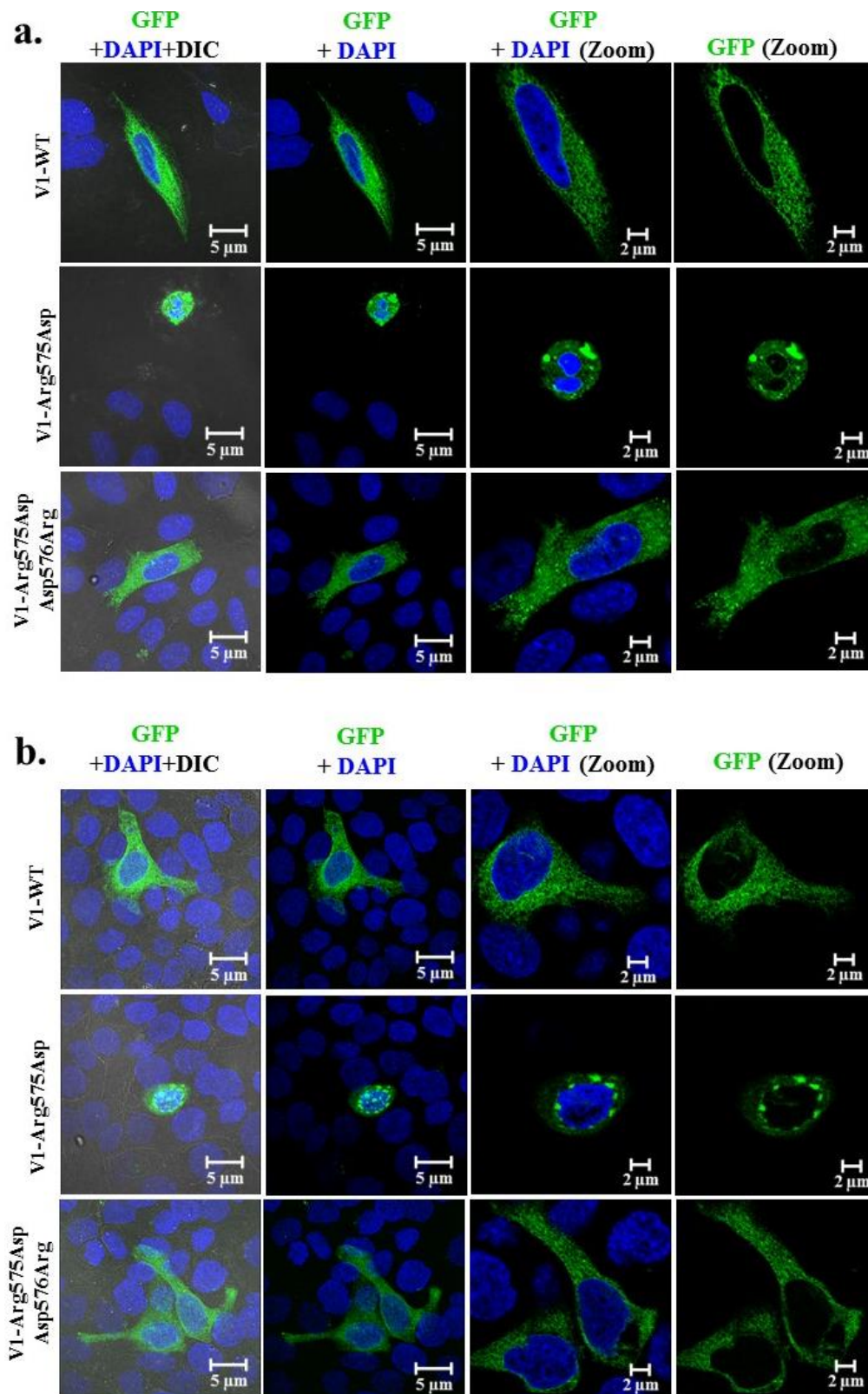


Figure 37: TRPV1-Arg575Asp induced changes in cellular morphology in SaOS and HaCaT cell lines can be restored by TRPV1-Arg575Asp-Asp576Arg. a) SaOS cells transiently transfected with TRPV1-WT, TRPV1-Arg575Asp and TRPV1-Arg575Asp-Asp576Arg (all in pSGFP2C1 vector). b) HaCaT cells transiently transfected with TRPV1-WT, TRPV1-Arg575Asp and TRPV1-Arg575Asp-Asp576Arg (all in pSGFP2C1 vector). In both cases changes induced by TRPV1-Arg575Asp is restored by TRPV1-Arg575Asp-Asp576Arg.

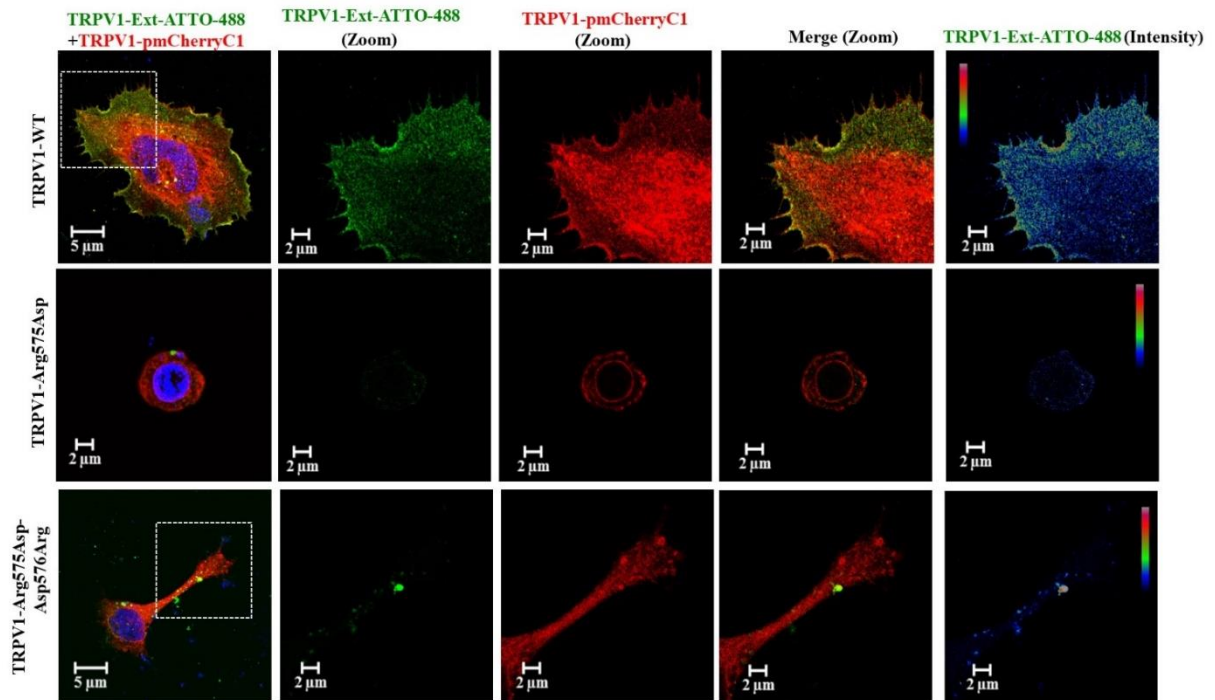


Figure 38: TRPV1-Arg575Asp shows lack of surface expression that is partly rescued by TRPV1-Arg575Asp-Asp576Arg. Confocal images of F-11 cells transiently transfected with TRPV1-WT, TRPV1-Arg575Asp and TRPV1-Arg575Asp-Asp576Arg (all in pmCherryC1 vector) and subsequently stained with TRPV1-extracellular-ATTO-488 antibody (green) and DAPI (blue). TRPV1-WT shows distinct surface expression, a phenomenon absent in case of TRPV1-Arg575Asp, which is partly restored by TRPV1-Arg575Asp-Asp576Arg.

2.2.16. Alteration in cellular phenotype due to TRPV1-Arg575Asp can be partly rescued by long-term channel inhibition

It was hypothesized that one of the reasons for changes induced by Arg575Asp might be the constitutive channel opening. In order to test this hypothesis F-11 cells were transiently transfected with GFP-TRPV1-WT and GFP-TRPV1-Arg575Asp, and cells were grown in presence of 5'-IRTX (1 μ M) for 36 hours and then fixed with 4% PFA. Images of treated as well as untreated transfected cells were acquired (Figure 39a) and the length, breadth, area, perimeter of cells for each condition was measured (Figure 39b). Application of TRPV1 specific channel blocker 5'-IRTX prevented rounding of cells expressing Arg575Asp suggesting that the probable cellular toxicity is mainly due to the excess channel function *per se*.

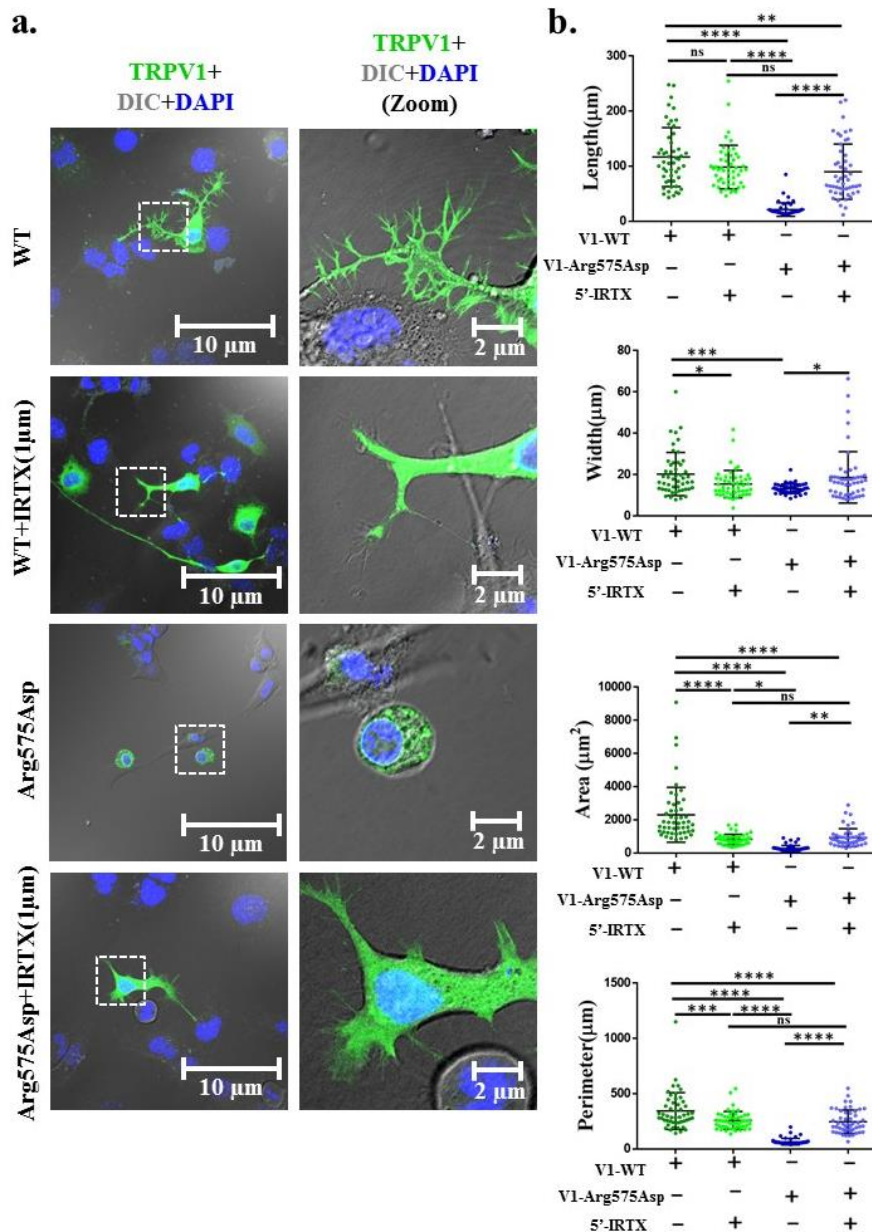


Figure 39. Cellular morphology parameters due to Arg575Asp mutation can be rescued by TRPV1 channel blocker. **a.** Confocal images of GFP-TRPV1-WT or GFP-TRPV1-Arg575Asp expressed in F11 cells and grown in absence and presence of 5'-IRTX, a specific inhibitor of TRPV1. F11 cells expressing GFP-TRPV1-Arg575Asp become much elongated and produce neurites and filopodia in presence but not in the absence of 5'-IRTX. **b.** Quantification of different morphology parameters such as length, width, area and perimeter of cells mentioned above. In all cases, minimum 50 cells for each condition were quantified. The ** (P = 0.0098), **** (P<0.0001) and *** (P=0.0006) indicate values that are significantly different while ns indicate values that are non-significantly different.

2.2.17. TRPV1-Arg575Asp forms a Capsaicin-insensitive channel that is rescued by Arg575Asp-Asp576Arg

F-11 cells were transiently co-transfected with full-length Rat TRPV1-WT (present in pmCherryC1 vector) and a Ca²⁺-sensor pGP-CMV-GCaMP6f. The same was

repeated for TRPV1-Arg575Asp (present in-pmCherryC1 vector), TRPV1-Arg575Asp-Asp576Arg (present in-pmCherryC1) and only mCherry (empty vector of pmCherryC1). Approximately 24 hours post transfection, live cell imaging of only doubly transfected cells were executed using a microscope for 200 frames (time gap between two frames is 1.085 seconds). Capsaicin (10 μ M) was added at the 30th frame for each condition. Unlike, TRPV1-WT which showed a rapid increase in Ca²⁺-influx upon Capsaicin addition, TRPV1-Arg575Asp showed no visible change in fluorescence intensity upon Capsaicin application. In order to rule out the fact that the imaged cells are live and functional at the time of experiments, Ionomycin (2 μ M) was added at the 120th frame for all constructs, which resulted in a Ca²⁺- spike. However, TRPV1-Arg575Asp-Asp576Arg exhibited similar Capsaicin-sensitivity like that of TRPV1-WT. Capsaicin, fails to show any Ca²⁺-influx in cells transfected with only pmCherryC1 (Figure 40a). Quantification of pGP-CMV-GCaMP6f fluorescence intensities from doubly transfected cells show that TRPV1-WT and TRPV1-Arg575Asp-Asp576Arg were “Capsaicin-responsive” and thus there was a peak immediately after the 30th frame and another one at the 120th frame upon addition of Ionomycin which opened all Ca²⁺-channels. TRPV1-Arg575Asp and pmCherryC1 remained unresponsive to Capsaicin and show a peak only after the 120th frame upon Ionomycin addition (Figure 40b).

2.2.18. TRPV1-Arg575Asp-Asp576Arg exhibits delayed response to Capsaicin activation upon depletion of Ca²⁺ from intracellular stores

F-11 cells were transiently co-transfected with full-length Rat TRPV1-WT (present in pmCherryC1 vector) and a Ca²⁺-sensor pGP-CMV-GCaMP6f. The same was repeated for TRPV1-Arg575Asp-Asp576Arg (present in-pmCherryC1).

Approximately 24 hours post transfection, the cells were treated with 1 μ M Thapsigargin for another 12 hours.

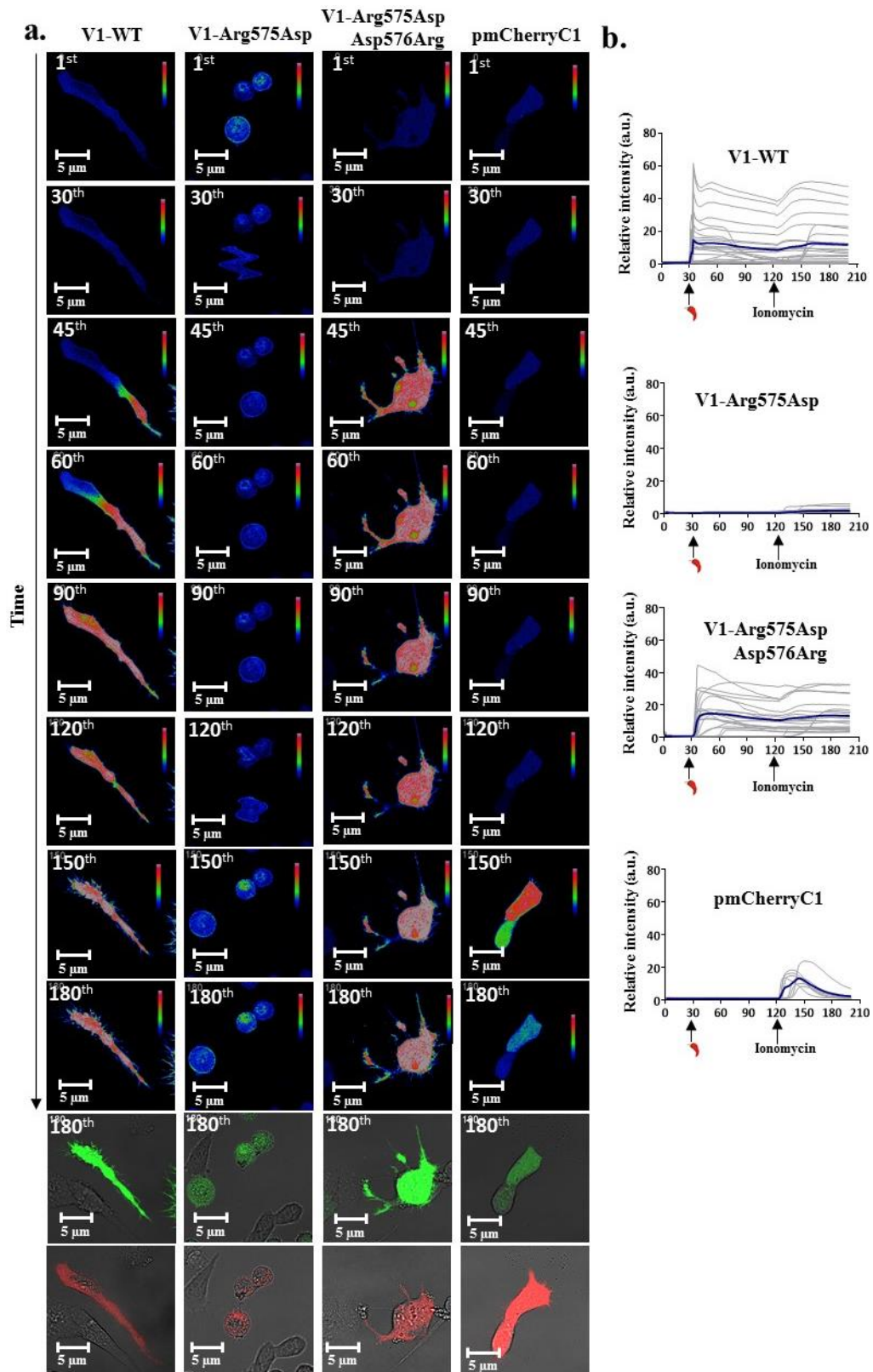


Figure 40. Ca²⁺-imaging of TRPV1-WT, Arg575Asp, Arg575Asp-Asp576Arg and pmCherryC1. F-11 cells doubly transfected with TRPV1-WT-pmCherryC1, TRPV1-Arg575Asp-pmCherryC1, TRPV1-

Arg575Asp/Asp576Arg-pmCherryC1 and pmCherryC1 and the calcium sensor pGP-CMV-GCaMP6f shows levels of Ca²⁺-influx upon addition of TRPV1 specific agonist Capsaicin (10 μM) at 30th frame and the ionophore Ionomycin (2 μM) at 120th frame. a) TRPV1-WT and TRPV1-Arg575Asp-Asp576Arg show a rapid influx of Ca²⁺ upon Capsaicin activation. The change in fluorescence intensity of pGP-CMV-GCaMP6f before and after agonist stimulation has been depicted in RGB mode. TRPV1-Arg575Asp remained insensitive to (P.T.O) Capsaicin addition. b) Quantification of pGP-CMV-GCaMP6f fluorescence intensity from cells transfected with TRPV1-WT (n = 26 cells), TRPV1-Arg575Asp (n=20 cells), TRPV1-Arg575Asp/Asp576Arg (n = 21 cells) and pmCherryC1 (n = 8 cells) shows a graphical representation of the change in intensities upon addition of Capsaicin at the 30th frame and Ionomycin at the 120th frame. The quantification for all the constructs were done considering the initial value recorded at the 1st frame as 1. The intensities for the remaining frames were subsequently calculated relative to the 1st frame.

Thapsigargin blocks SERCA pumps and depletes Ca²⁺ mainly from ER (285) Live cell imaging of only doubly transfected cells was executed using a microscope for 200 frames (time gap between two frames is approximately 1.085 seconds). Capsaicin (10 μM) was added at the 30th frame for each condition. Unlike, TRPV1-WT which shows a rapid increase in Ca²⁺-influx upon Capsaicin addition even after Thapsigargin pre-treatment, TRPV1-Arg575Asp-Asp576Arg shows a significantly delayed response after Capsaicin application post incubation with Thapsigargin ([Figure 41](#)).

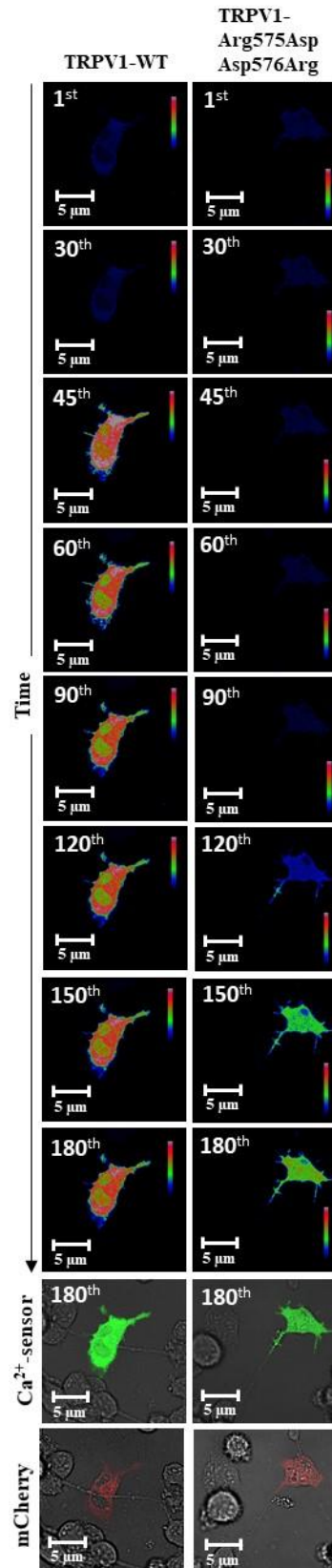


Figure 41. Depletion of intracellular Ca²⁺-stores causes significant delay in response of TRPV1-Arg575Asp-Asp576Arg towards Capsaicin activation. F-11 cells doubly transfected with TRPV1-WT-pmCherryC1 or TRPV1-Arg575Asp-Asp576Arg-pmCherryC1 and the Calcium sensor pGP-CMV-GCaMP6f shows levels of Ca²⁺-influx upon addition of TRPV1 specific agonist Capsaicin (10 μM) at 30th frame, pre-treated with 1 μM Thapsigargin for 12 hours. The change in fluorescence intensity of pGP-

CMV-GCaMP6f before and after agonist stimulation has been depicted in RGB mode. TRPV1-WT (n=6) show a rapid influx of Ca^{2+} upon Capsaicin activation whereas TRPV1-Arg575Asp-Asp576Arg shows a significant delay in Ca^{2+} influx (n=10).



2.3. Expression of TRPA1 in vertebrate sperm cells, its function and interaction with microtubule cytoskeleton

Sperm physiology appears to be very tightly regulated by specific pool of ion channels. Sperm are kept inactive by low pH, low HCO_3^- and high Zn^{2+} concentrations of the seminal fluid till ejaculation (286). Upon mixing with fluids of the female reproductive tract, the pH and concentrations of Na^+ , Cl^- , and HCO_3^- are increased while that of K^+ is decreased (287). As the sperm swim past the acidic female reproductive tract (pH ~5) and pass through the utero tubal junction (pH ~8), they undergo intracellular alkalization (288)(289). The alkalization events operate simultaneously with other events till sufficient levels of alkalinity is reached and such events have been recently shown to be initiated due to the depolarizing effect of a thermosensitive ion channel TRPV4 via Na^+ -influx which activates the voltage-gated channel Hv1 to extrude H^+ , influx of Na^+ via sperm-specific Na^+/H^+ exchanger or due to entry of HCO_3^- anions during capacitation (290)(291)(292)(293). Both CatSper and SLO3 channels get activated at alkaline pH, mediate Ca^{2+} -influx and K^+ efflux respectively and induce hyperactivation of sperm (294)(295)(296). Heat sensitive ion channels TRPV1 and TRPV4 have been shown to guide sperm thermotaxis in human and murine sperm respectively(297)(298). Therefore, it is important to understand different ion channel(s), their molecular evolution guided by stimulants as well as interacting partners, and determine the properties and functions of these ion channels involved in specific steps towards reproduction, namely their role in spermatogenesis, sperm motility and fertilization. Accordingly, TRPA1 can have multiple roles in sperm functions. However, so far there is no report available that has demonstrated the presence of TRPA1 in sperm cells.

In this work the molecular evolution of TRPA1 was examined at gene and amino acid levels. Such analysis suggested that TRPA1 is evolutionary selected yet maintained

as a highly diverged protein. Therefore, the presence of TRPA1 in the sperm cells of representative vertebrates and its role in sperm functions were evaluated. On the basis of its localization and function, its possible interaction with microtubule cytoskeleton has also been investigated.

2.3.1. TRPA1 remain as a semi conserved protein throughout vertebrate evolution

The molecular evolution of TRPA1 through the Bayesian phylogenetic history was explored, which depicted that there is at least a single copy of TRPA1 is retained in all vertebrates with high statistical support (299) (Figure 42a). Available sequences in ancient species indicate that TRPA1 has evolved during the Neoproterozoic Era (ca 900 MYA). The rate of changes in TRPA1 sequence was measured (300) (301) (Figure 42b). The evolutionary slope of TRPA1 indicates that it was selected with lower rate of changes in the initial period, especially before 600 MYA. The variations increased through the course of evolution. In comparison to the semi-conserved protein Cytochrome-C and the highly conserved protein Histone, TRPA1 seems to have incorporated more changes, and probably has not been stabilised yet even at present. From the Cambrian to Devonian era, TRPA1 has incorporated maximum changes indicating a molecular stabilization process which coincides with the vertebrate evolution.

2.3.2. TRPA1 syntenic locus is highly conserved in vertebrates

Chromosomal rearrangement events are intimately linked with the speciation events and the allocation pattern of genes on a chromosome is referred to as Synteny (Figure 43a). Synteny analysis indicate that in the human chromosome 8, TRPA1 gene is localized in a 2.75 Mb region flanked by a conserved tetrad of genes (TRAM1–LACTB2–MSC–EYA1) on the one side, while other side possesses another tetrad of genes

(KCNB2-TERF1-RPL7- RDH10a). This arrangement is conserved in several other mammals [mouse (chromosome 1),

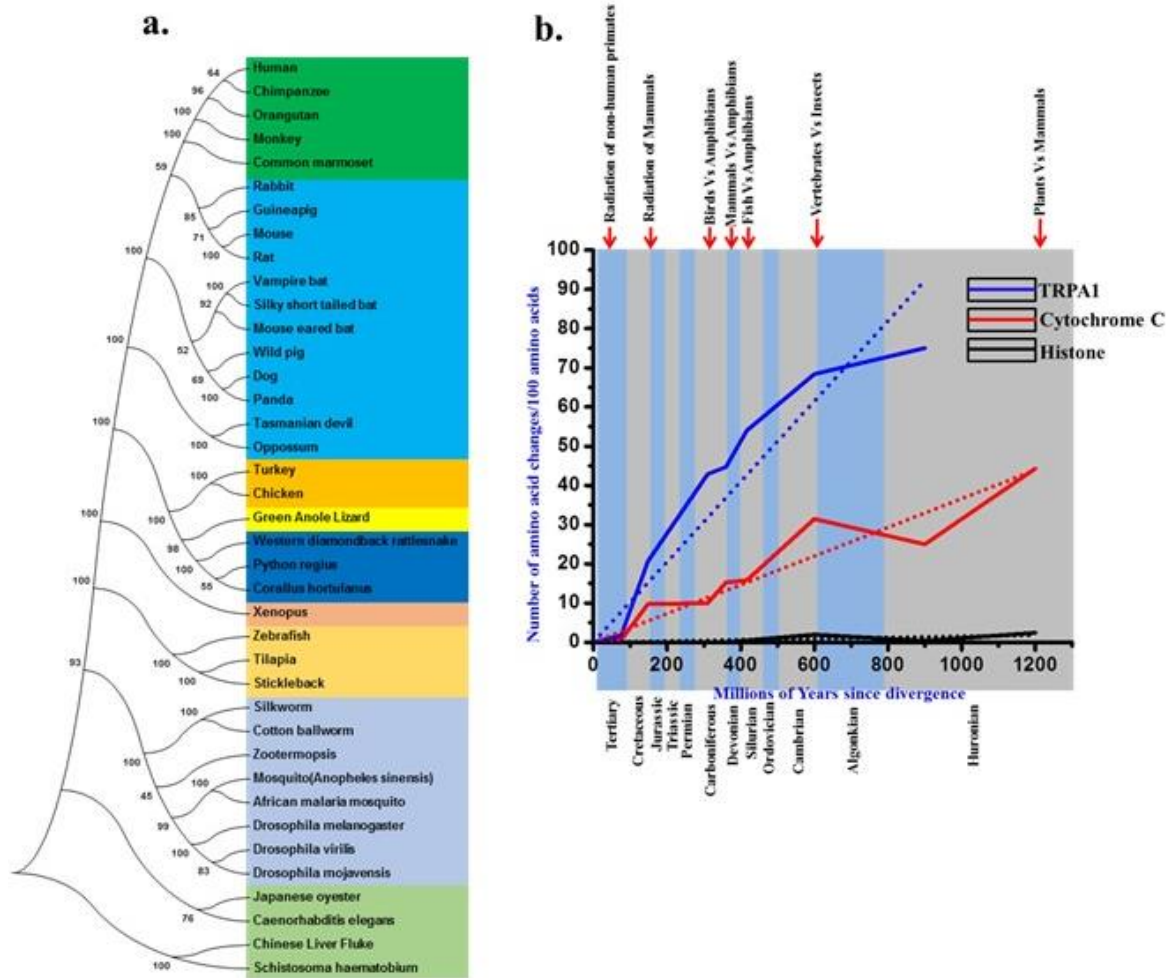


Figure 42. Phylogenetic tree and molecular evolution of TRPA1. a. Maximum likelihood tree illustrates evolution of TRPA1 from invertebrates to vertebrates. TRPA1 had evolved around 900 MYA and traces back to the evolution of invertebrates. b. Million year plot depicting changes in TRPA1 protein in evolutionary time-scale. Histone-H4 and Cytochrome-C were used as control.

rat (chromosome 5) and dog (chromosome 29)]. In tetrapods, this genomic fragment is retained in chicken (chromosome 2) and in zebrafish (chromosome 2) within about 1 Mb region with TRPA1 flanking with exactly same sets of genes. It is also found in other tetrapods like in turkey (chromosome 3), anole lizard (chromosome 4) Chinese softshell turtle (scaffold JH211036.1) and in *Xenopus* (scaffold GL172896.1).

Coelacanth possesses this syntenic architecture, surpassing into two different scaffold JH126702.1 and JH127618.1 with a total size of about 2.4 Mb. This genomic

fragment is maintained in several ray-finned fishes. A 322 kb segment in Medaka on the chromosome 20 harbours this fragment. It is also retained in genomes of ray-finned fishes as Atlantic cod

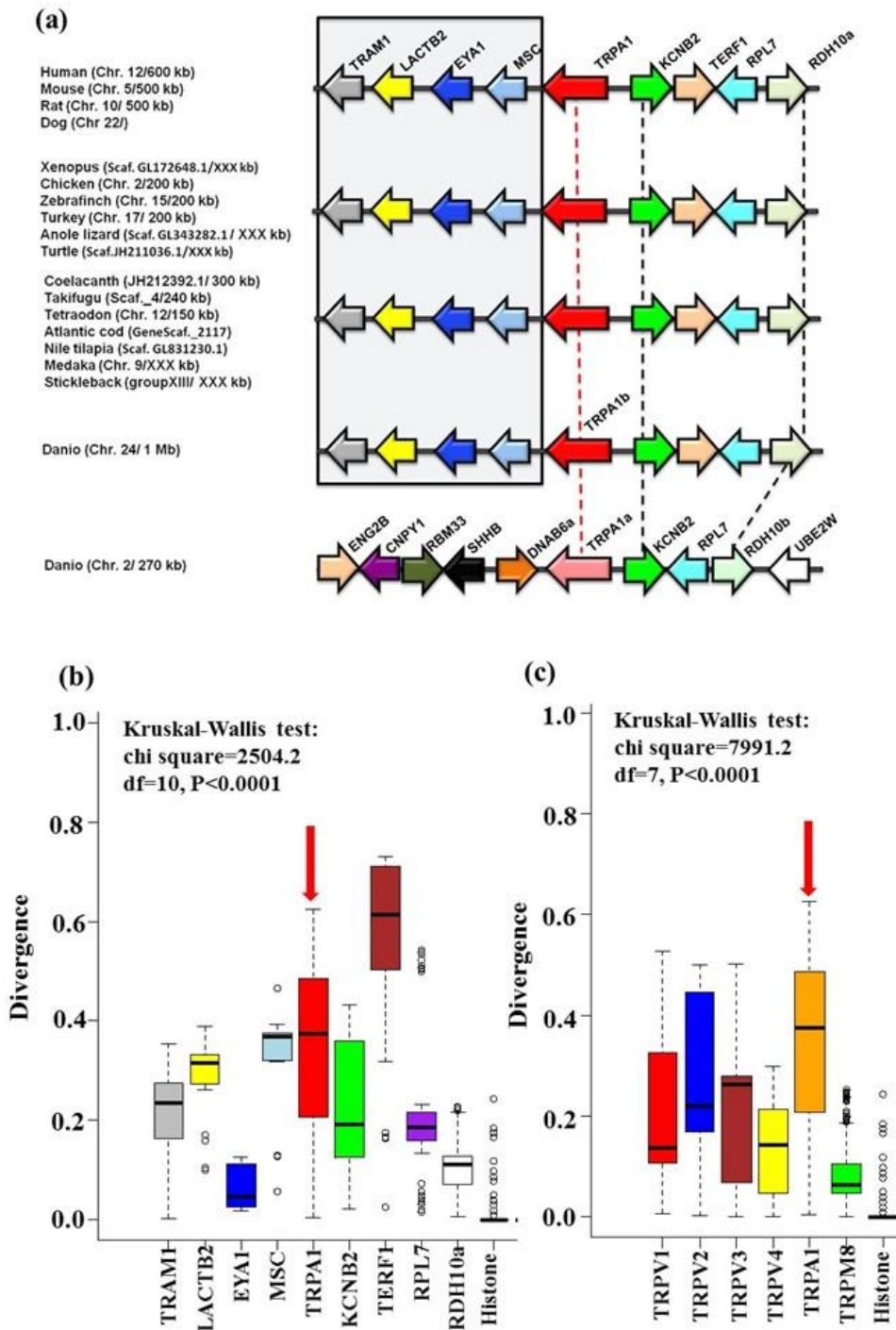


Figure 43. TRPA1 synteny and genes are well conserved while TRPA1 protein is highly diverged. a) Genomic architecture of TRPA1 locus in various vertebrates depicts conservation of this loci across vertebrates and duplication of TRPA1 in zebrafish genome (TRPA1a and TRPA1b). CNPY1 - canopy FGF signalling regulator 1; DNAB6a – DnaJ (Hsp40) homolog, subfamily B, member 6a; ENG2B - engrailed

homeobox 2b; EYA1 - eyes absent homolog 1 (Drosophila); RDH10 - retinol dehydrogenase 10; RPL7 – ribosomal protein L7; RBM33 - RNA binding motif protein 33b; SHHB - sonic hedgehog b; TERF1 - telomeric repeat binding factor (NIMA-interacting) 1; TRAM1 e translocation associated membrane protein 1; UBE2W - Ubiquitin conjugating enzyme E2. **b)** Among all the genes present in TRPA1 synteny, MSC, TRPA1 (indicated by red arrow) and TERF1 genes products remain highly diverged in vertebrates. **c)** TRPA1 (indicated by red arrow) is highly diverged at when compared with similar ion channels, i.e. with TRPV1, TRPV2, TRPV3, TRPV4 and TRPM8.

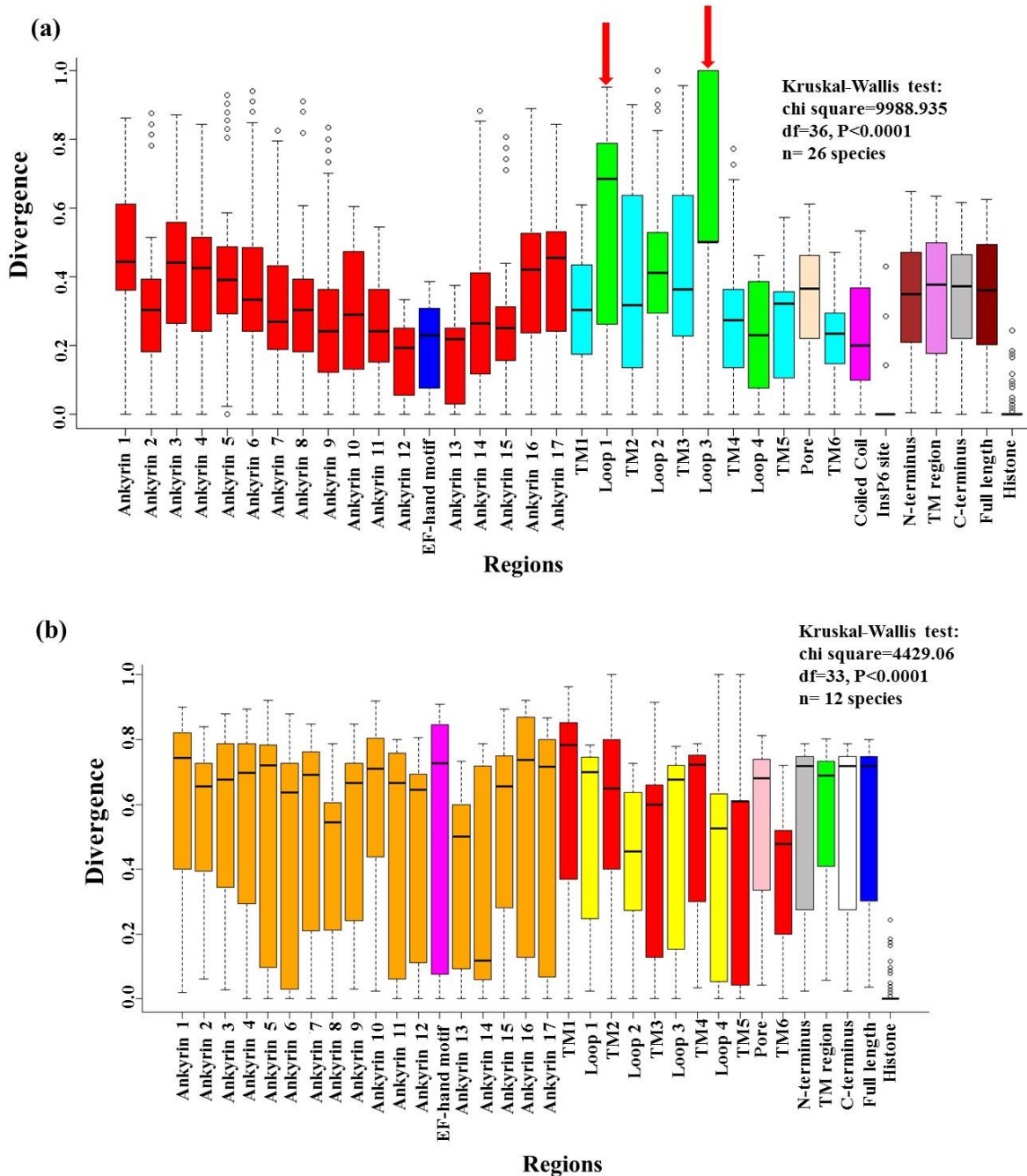


Figure 44. TRPA1 domains are highly diverged among both vertebrates and invertebrates. a) Conservation analysis of TRPA1 protein and its specific domains and motifs. Except InsP6-interacting site, none of the TRPA1 domains and motifs are conserved. Among all; extracellular loop 1 and loop 3 (indicated by red arrows) are most diverged. In all these analysis, higher values indicate more divergence. **b)** The domains of invertebrate TRPA1 are highly diverged across evolution.

(GeneScaf. 681), Nile tilapia (Scaf. GL831157.1), *Takifugu* (Scaf._95), *Tetraodon* (chromosome 6), spotted gar (Chromosome LG9) and stickleback (group XXI). Interestingly, zebrafish has 2 copies of TRPA1 genes namely TRPA1a and TRPA1b. Zebrafish (*Danio rerio*) harbours TRPA1b gene on the same syntenic structure spreading about 1 Mb region on the chromosome 24, while a duplicated fragment possesses TRPA1a. The duplicated genomic region span over 270 kb in chromosome 2 with a set of pentad of genes (ENG2B-CNPY1-RBM33-SHHB-DNAB6a) and other side has 3 out of tetrad of genes (KCNB2-RPL7-RDH10b) with second copy of RDH10b gene and loss of TERF1 gene and UBE2W is also found on this locus. UBE2W gene is tracked back to close to TRPA chromosome maps in the coelacanth. This indicates that zebrafish has second copy of TRPA1 gene, while most of vertebrates have single copy of TRPA1 gene. All in all, TRPA1 gene is conserved in various vertebrate genomes with few variations.

2.3.3. Genes retained in TRPA1-synteny are diverged in nature

The conservation of these gene products present in the same genomic locus were tested. The analysis strongly suggested that proteins coded by TRPA1 and other genes present in this Synteny are highly divergent since last 400 MY, i.e. throughout vertebrate evolution (Figure 43b). Overall conservation of TRPA1 is also much less than many other comparable ion channels (such as TRPV1-4) that have even originated at much later points (Figure 43c). In other word, the data suggested that at least one copy of TRPA1 gene remained selected in all vertebrates, yet has maintained high-variability among species.

2.3.4. TRPA1 domains and motifs are highly diverged

Conservation of different domains and motifs present in TRPA1 were analysed. All these domains and motifs (except InsP6-interacting site) remain highly divergent in nature (Figure 44a). Notably, both the extracellular loops of TRPA1 (namely loop 1 and loop 3) are most diverged among all other domains and motifs and such variation is maintained for more than 400 MY. This strongly suggests that variation in these extracellular loops is necessary for survival and such variation is maintained in order to accommodate TRPA1 functions in different environmental niches. Divergence in TRPA1's different domains have been also observed among invertebrates (Figure 44b).

2.3.5. TRPA1 expression in mature sperm is conserved throughout vertebrate evolution

In case of TRPA1 expression in certain single cells (such as in sperm cell), the extracellular loops are in the direct contact with the external environment (such as water bodies for species with external fertilization and female reproductive tract for species undergoing internal fertilization) that can be critical for the entire species survival. This allowed us to test the expression and function of TRPA1 in the context of reproductive functions and also at the mature sperm cells. Presence of TRPA1 in sperm of all representative species belonging to different vertebrate phylum signifies its functional importance in male gametes (Figure 45). However, the localization and expression of TRPA1 differs from species to species. TRPA1 is present at the head, neck and tail of sperm from rohu (fish), toad (amphibian), chicken (avian) and bull (mammalian). TRPA1 appears to be mainly localized at the head of lizard (reptile) sperm. The bull sperm has intense TRPA1 signal throughout the tail, mid-piece and at the centrosome region, faint expression at the post-acrosomal and acrosomal region.

2.3.6. TRPA1 modulation does not alter average values of motility parameters in bull sperm

Since motility of sperm is an important criterion for determining the fertilizing ability, motility of bull sperm samples was evaluated using 'Computer Assisted Sperm Analysis' (CASA) system. As TALP media is recommended as the best available media that mimics *in-vivo* fertilizing conditions (302), all the motility parameters were recorded after re-suspending the semen in TALP medium (pH = 6.8). In order to check the effect of TRPA1 activation on

bull sperm motility, fresh neat semen suspended in TALP media were treated with TRPA1-specific activator AITC at different doses (1 μ M, 10 μ M, 100 μ M) and TRPA1 specific inhibitor A-967079 (1 μ M, 10 μ M, 100 μ M). Motility parameters were evaluated at 60 min (data not shown) and 120 min post treatment (Figure 46a-46c). The percentage of motile sperm, percentage of progressively motile, and percentage of rapidly moving sperm were analysed. Data suggests that TRPA1 activation or inhibition does not change the average value of these parameters significantly in any of these doses.

2.3.7. TRPA1 activation induces hyperactivation in bull sperm

Interestingly, ALH (Amplitude of Lateral Head Displacement) and VCL (Curvilinear Velocity) increased with higher concentrations of AITC (Figure 46e and 46f). BCF on the other hand decreased with increasing concentrations of AITC (Figure 46d). A hyperactive spermatozoon is characterized by increased ALH as well as VCL and decreased BCF, WOB, STR and LIN. Bull sperm showing a VCL > 70 μ m/s and ALH > 7 μ m is considered to be hyperactive (302)(303). Thus, TRPA1 activation induces a characteristic hyperactive pattern (increased ALH as well as VCL and decreased BCF) to sperm motion with increasing concentrations of AITC. This effect was slightly reduced

after 2 hours of treatment. Although TRPA1 activation lead to significant changes in some of the motility parameters (average values), all parameters were not affected equally and TRPA1 inhibition with its specific inhibitor A-967079 did not exhibit much changes in the sperm movement patterns.

2.3.8. TRPA1 doesn't affect capacitation or acrosomal reaction in bull sperm

The mammalian sperm needs to undergo capacitation in the female reproductive tract followed by acrosomal reaction at the vicinity of the oocyte in order to fertilize. Commencement of capacitation in many mammalian species triggers an escalation in the level of phosphotyrosination of sperm cell proteins. Thus, phosphotyrosination is considered as a hallmark event for capacitation (304). Successful capacitation reaction requires three primary components: serum albumin, Ca^{2+} -ions and bicarbonate (304). Neat semen from individual bulls were suspended in capacitating TALP media (also in non-capacitating media as negative control) and changes in the level of phosphotyrosination upon TRPA1 activation and inhibition was measured. The cells present in capacitating media was treated with various drugs like TRPA1-specific activator AITC (100 μM), TRPA1-specific inhibitor A-967079 (100 μM), progesterone (10 μM), heparin (20 $\mu\text{g/ml}$), progesterone + A-967079, and heparin + A-967079. Western blot of these samples using anti phospho tyrosine antibody show that neither TRPA1 activation, nor inhibition affects global phosphotyrosination levels (Figure 47a). TRPA1 inhibitor is not able to block heparin or progesterone-mediated increase in global phosphotyrosination either, at least as evaluated by Western blot analysis (Figure 47a). FITC-PNA staining was employed to evaluate the acrosomal integrity of cells (305).

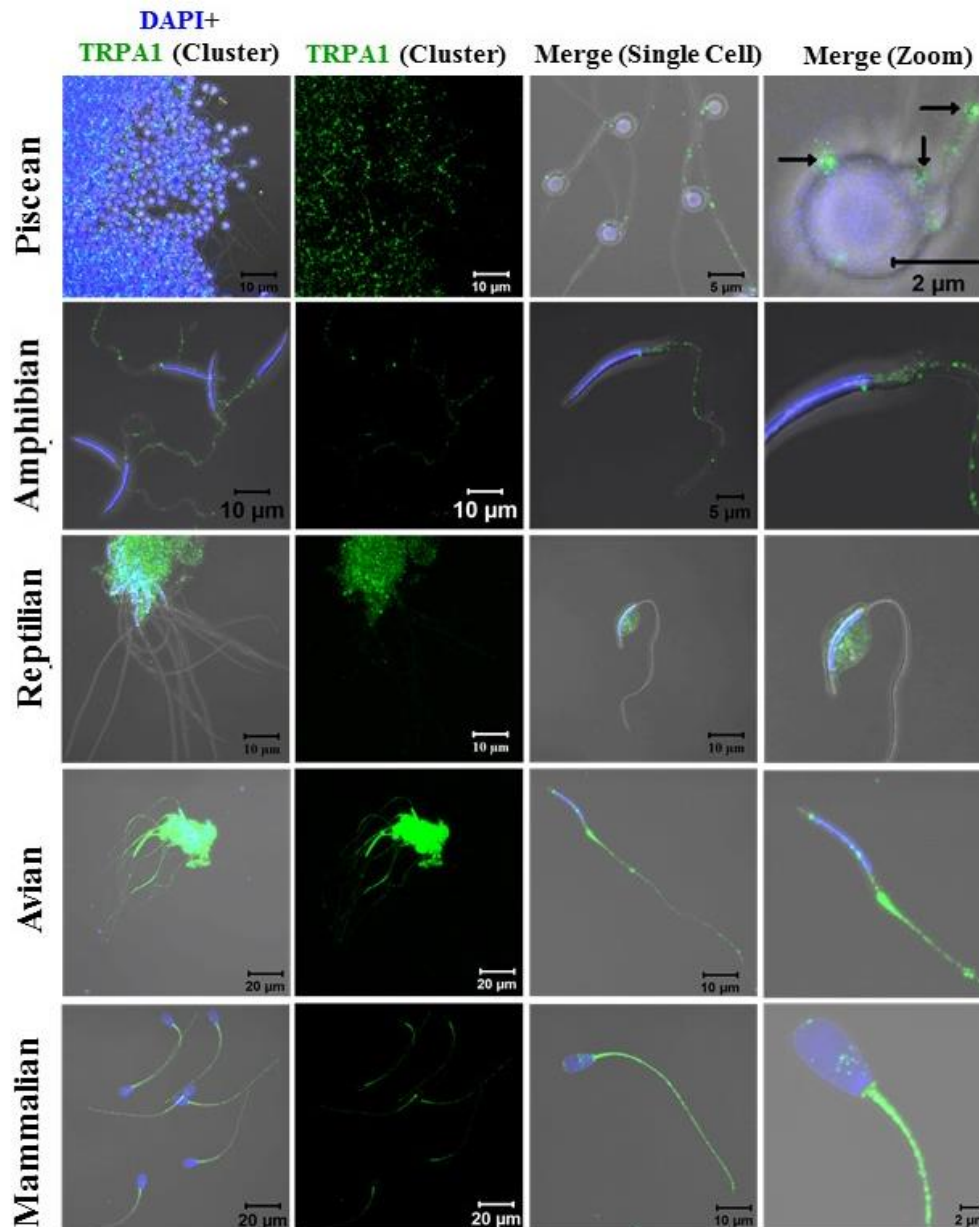


Figure 45. Endogenous expression of TRPA1 is conserved in all vertebrate sperm. Confocal images demonstrating the presence of endogenous TRPA1 in cluster and in single cells isolated from different vertebrates. Fluorescence images depict TRPA1 (green) and Nucleus (blue) merged with DIC images.

This staining classifies two populations: “A” type of cells that are “PNA positive” (represent cells with intact acrosome, i.e. cells that have not undergone acrosomal reaction). “B” type of cells are “PNA negative” (represents cells that have undergone acrosomal reaction) (Figure 47b). In non-capacitating media (media without BSA, NaHCO₃ and CaCl₂·2H₂O), pharmacological modulation of TRPA1 induce slight changes in % of cells (average value) undergoing acrosome reaction. Heparin and progesterone

induce acrosomal reaction and cause an elevated population of cells without PNA labelling (306)(307). However, when A-967079 was added with heparin there was not much effect on the loss of acrosomes (average value). A-967079 (100 μ M) added with heparin (20 μ g/ml) increases the average value of acrosome reacted cells marginally from only heparin-treated cells. However, the effect of A-967079 with progesterone is different. Progesterone alone is capable of inducing ~61.4% (average value) of the cells to undergo acrosome reaction but when A-967079 is given along with it then the acrosome reacted sperm population decreases to ~50.82% (average value). Thus, inhibition of TRPA1 partially inhibits progesterone-mediated acrosome reaction. When individual samples were analysed, TRPA1 activation or inhibition induces more variability in % of cells that are undergoing acrosomal reaction or failed to do that within certain time duration (Figure 47c).

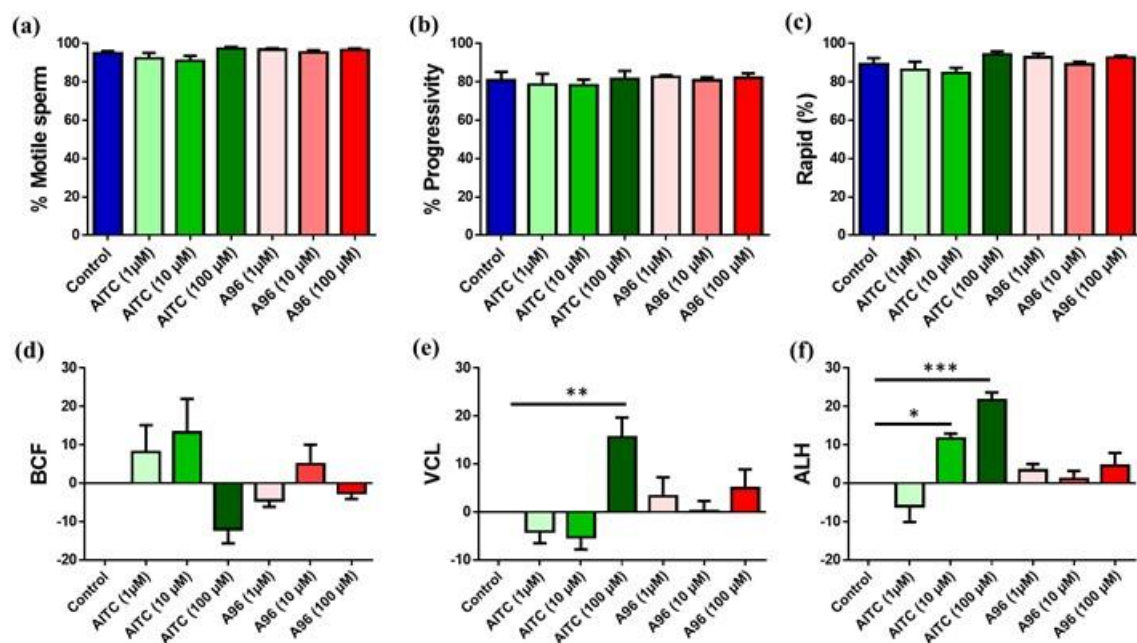


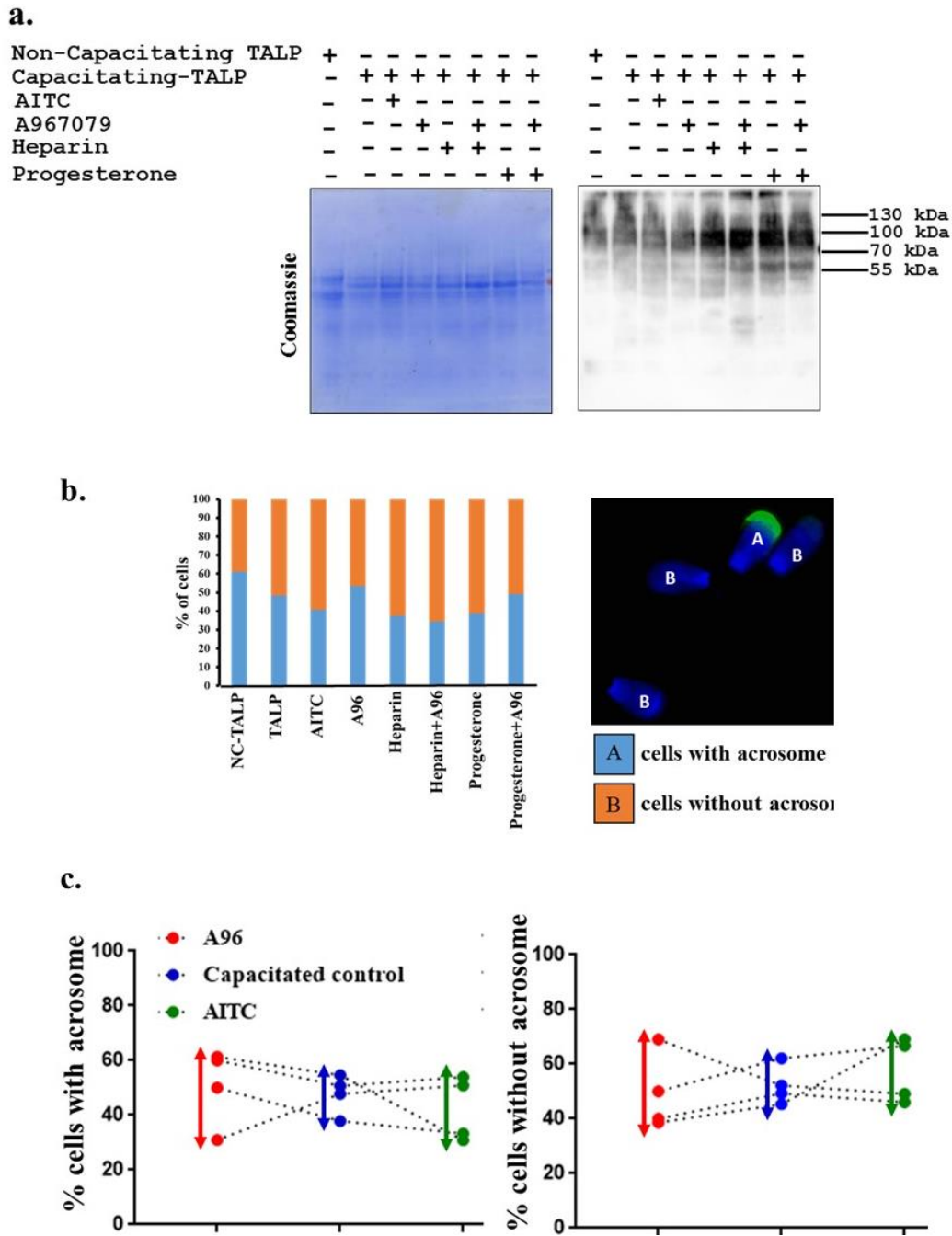
Figure 46. TRPA1 activation in bull sperm results in hyper-activated motility. a-c. TRPA1 activation or inhibition doesn't drastically affect the average percentage of motile cells, their progressivity as well as the percentage of cells that exhibit rapid movement. A dose-dependent increase in the activator or inhibitor doesn't have much impact on the "average values" of these motility parameters. d-f. Dose-dependent increase of TRPA1 activator, AITC, results in decreased BCF and augmented VCL and ALH which are characteristics of hyperactivated motility. Inhibition of TRPA1 by its specific inhibitor A967079 doesn't have much impact on average values representing hyper-activated motility. BCF = beat cross frequency; VCL = curvilinear velocity; ALH = amplitude of lateral head displacement. (This data is from n = 4 bull sperm samples in TALP media, 120 min).

2.3.9. TRPA1 activation or inhibition increases variability in different parameters

The “variability” induced in sperm cell parameters as a function of TRPA1 modulation was explored. For that purpose, a large data set representing motility parameters were analysed. It was seen that both activation as well as inhibition of TRPA1 induces “variability” in different parameters such as % of motile cells, % of cells with progressive movement, % of cells with linear movement, straightness, VCL, ALH, VSL, VAP, and BCF values respectively (Figure 48). From the results and evidences taken together, it is demonstrated that TRPA1 is an evolutionary ancient/primitive protein and have conserved expression in vertebrate spermatozoa. Expression of TRPA1 also correlates with its potential role in spermatogenesis and hyper-activation of mature sperm, at least in case of mammals. TRPA1 activation or inhibition induce variability in several sperm cell parameters and such variability may contribute to the reproductive fitness.

2.3.10. Localization of TRPA1 with different modified tubulin in Bull sperm cells

Considering the importance of TRPA1 activation in hyperactivated motility and its conserved pattern of endogenous expression mostly in the tail and neck region of sperm cells isolated from warm blooded organisms (mammals and birds), it was indispensable to study the localization of TRPA1 with flagellar microtubules. The sperm tail can be considered as a special form of cilium which contains a 9+2 microtubule structure. Concerted action of these microtubules and their associated motor proteins aid in the typical beating pattern of sperm tails which is responsible for their hyper-activated motility (308). Freshly isolated Bull sperm samples were treated with TRPA1 specific agonist AITC and antagonist A967079, Heparin and Progesterone. Heparin is known to induce capacitation (309) and Progesterone is known for its capability to induce hyperactivation and acrosomal reaction (310). The cells were fixed



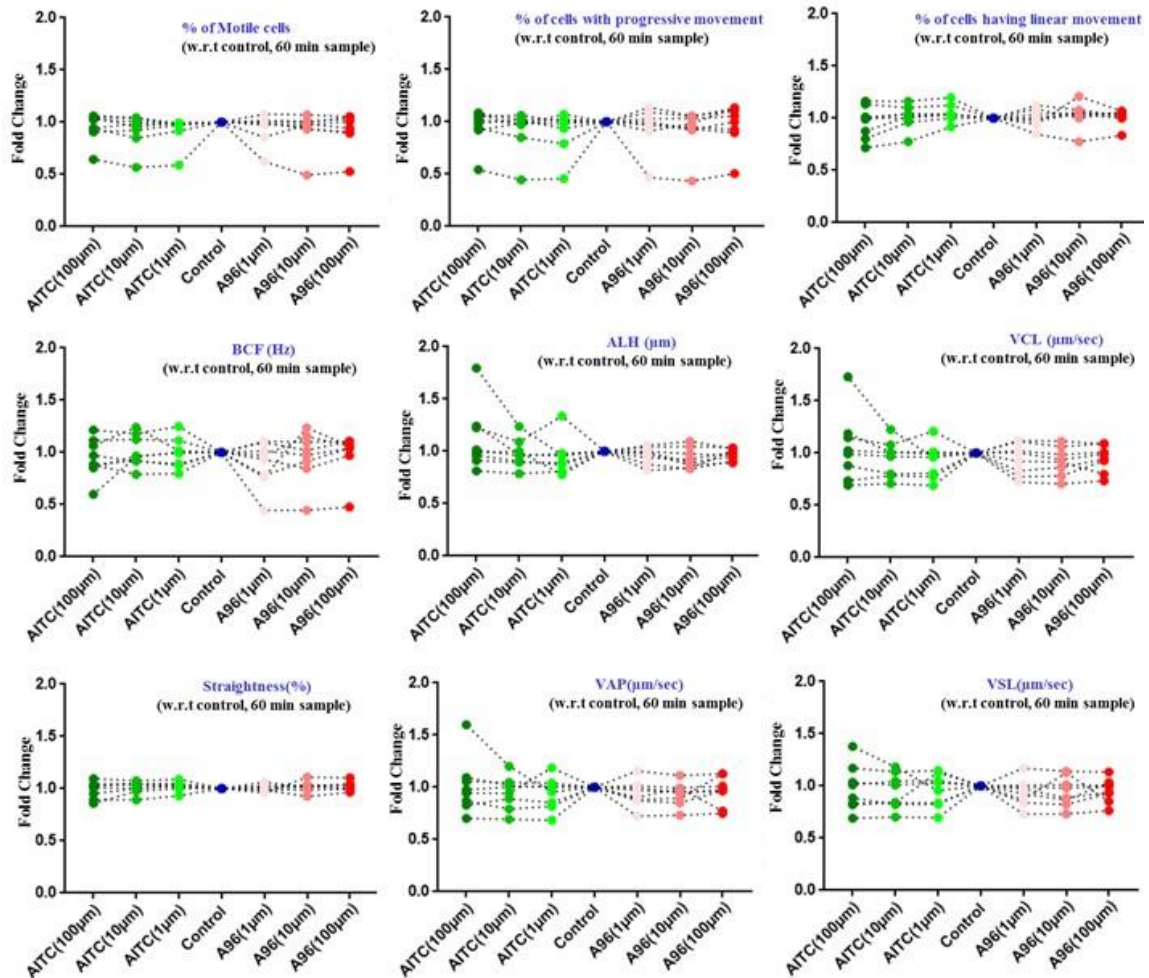
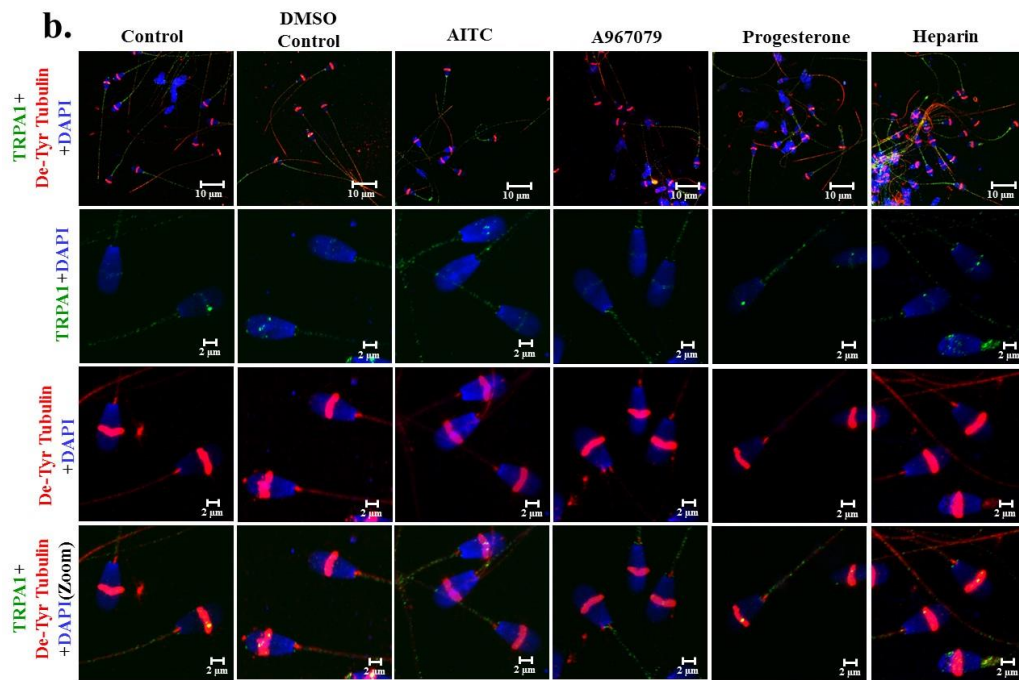
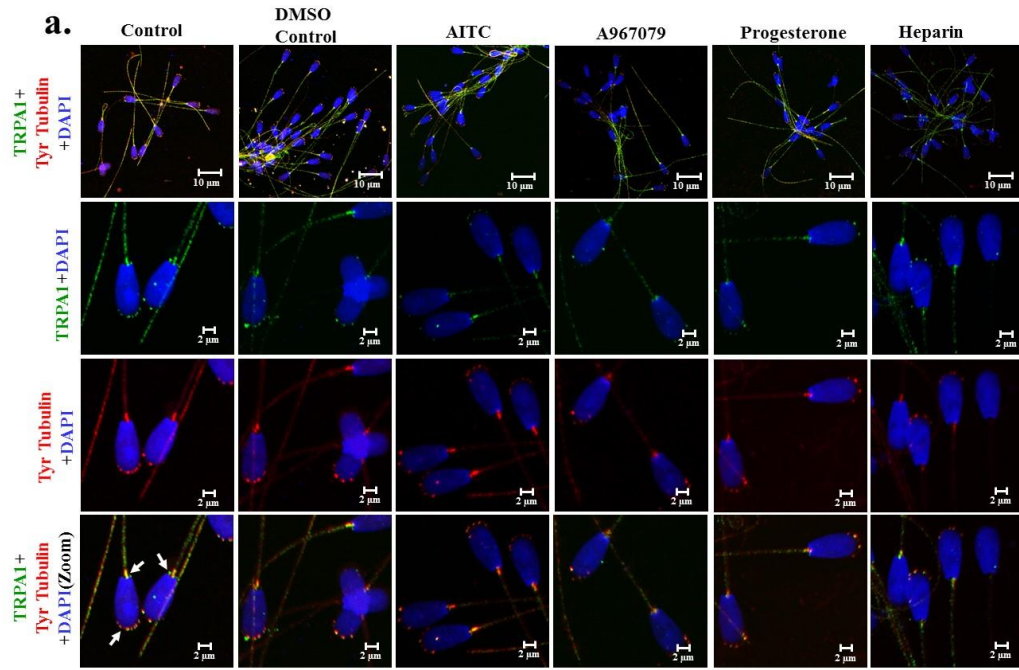
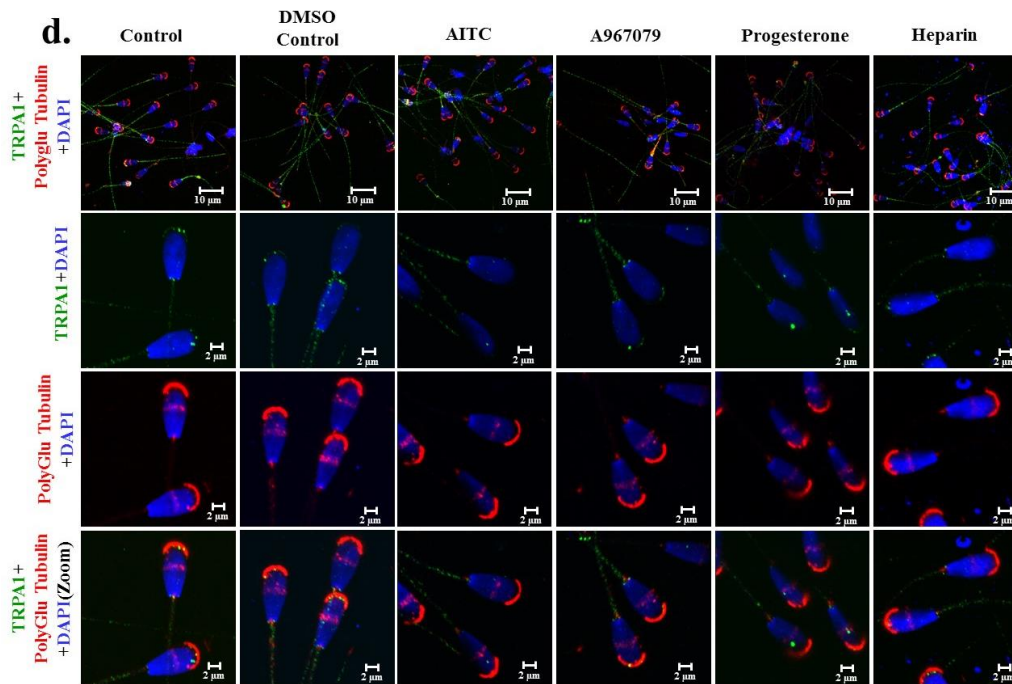
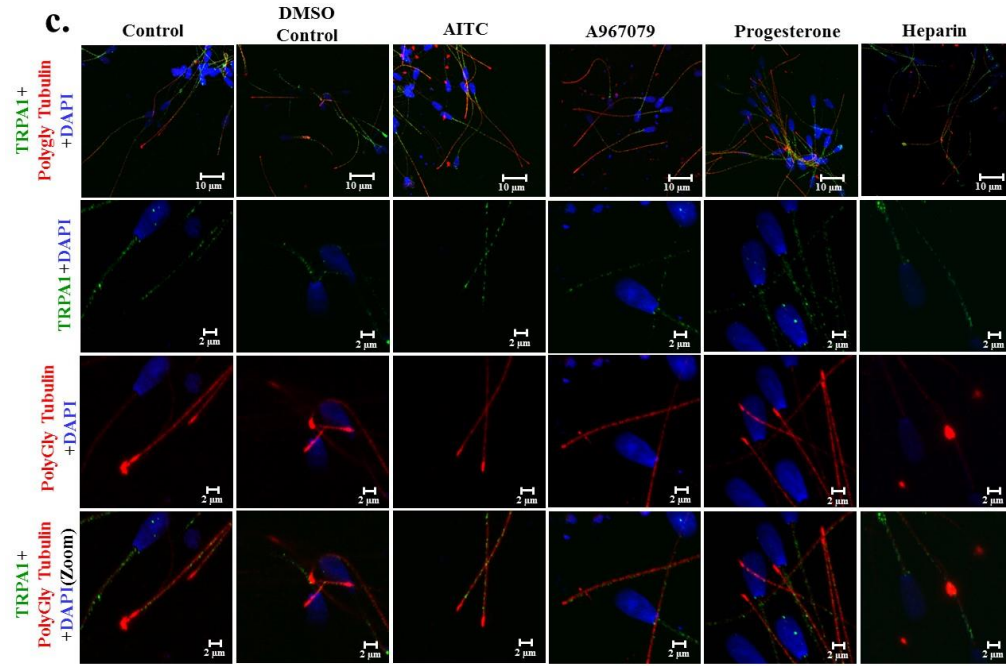


Figure 48. TRPA1 activation or inhibition induce variability in motility parameters. a-i. TRPA1 activation by AITC or TRPA1 inhibition by A96 in 3 different increasing concentrations induce “variability” in several motility parameters. Often such parameters show a trend of dose-response. All values are represented as “fold change” with respect to control sample (considered as value 1). (This data is from n = 8 bull sperm samples in TALP media, 60 min).

with 4% PFA post 60 minutes of drug incubation and were stained for TRPA1 (green) and various modified tubulin like Tyrosinated (Figure 49a), Detyrosinated (Figure 49b), Polyglycylated (Figure 49c), Polyglutamylated (Figure 49d) and Acetylated tubulin (Figure 49e). Out of all these tubulin types, only Tyrosinated, Polyglycylated and Acetylated tubulin exhibited a tail specific expression pattern. However, Tyrosinated tubulin signals were partly noticed in the peripheral head region also. In spite of enrichment of various modified tubulin





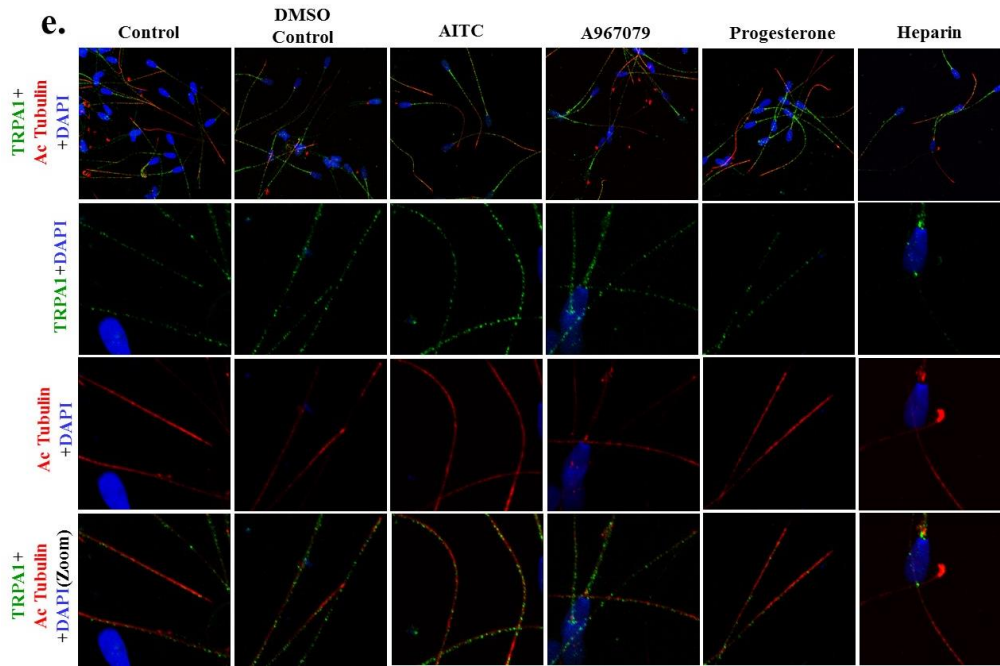


Figure 49. Localization of TRPA1 with different modified tubulin in bull sperm. Confocal images of untreated as well as drug treated Bull sperm cells stained for TRPA1 (green) and different modified tubulin like Tyrosinated (a), Detyrosinated (b), Polyglycylated (c), Polyglutamylated (d) and Acetylated (e) (red). TRPA1 co-localized with only Tyrosinated tubulin as highlighted by white arrows in the neck and parts of tail and head region.

in the tail region, TRPA1 co-localized with only Tyrosinated tubulin (demarcated by white arrows) suggesting a possible role of this specific interaction in hyperactivated motility.



2.4. Molecular evolution of TRPA1 during vertebrate evolution and importance of TRPA1-cholesterol complex in channel localization

Expression and functioning of TRP channels are greatly influenced by the local lipid environment in which they are embedded, particularly the ones that segregate into cholesterol enriched micro domains of the plasma membrane, the lipid rafts. These include TRPV1, TRPM8, TRPV4, several members of TRPC family (TRPC1, TRPC3, TRPC4, and TRPC5). There are increasing evidences about TRPA1 regulation by changes in lipid environment (165). Membrane deformations induced by charged amphipathic molecules may be regulating TRPA1 gating behaviour (311). Bacterial lipopolysaccharides (LPS) activate TRPA1 by inducing mechanical perturbations within the lipid bilayer (312). Phosphatidylinositol 4,5-bisphosphate (PIP₂), a membrane phospholipid negatively regulates TRPA1. Ca²⁺ induced depletion of PIP₂ upon TRPV1 activation by Capsaicin relieves TRPA1 inhibition by PIP₂. Another membrane lipid that negatively regulates TRPA1 is Lysophosphatidylcholine (141). Burn injury releases several lipid metabolites that activates both TRPA1 and TRPV1 resulting in chronic pain. However, injection of inhibitors targeting both these channels were capable of significantly subsiding post-burn thermal and mechanical allodynia (313). Experiments on Rat trigeminal neurons have shown that disruption of lipid rafts by Sphingomylinase, Methyl β-cyclodextrin and myriocin resulted in decreased Ca²⁺-influx upon TRPV1 activation with Capsaicin and TRPA1 activation with AITC (262).

In this work, the Lipid Water Interface (LWI) stretches in full-length Human TRPA1 were analysed, their conservation across vertebrate evolution were determined. Conservation of individual amino acids at the LWI regions of TRPA1 across vertebrate evolution was also assessed. Frequency of occurrence of different amino acids at TRPA1

LWI, determination of cholesterol binding motifs, docking of cholesterol onto TRPA1 and localization of TRPA1 in lipid rafts were also analysed.

2.4.1. Determination of LWI stretches in human TRPA1 and their conservation across vertebrate evolution

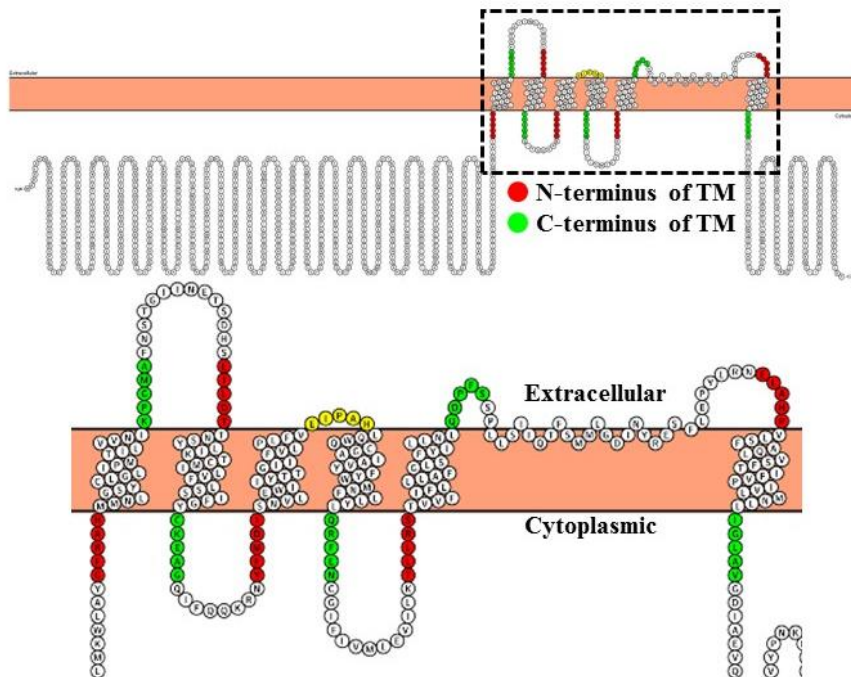
The loop regions interconnecting the transmembrane segments of TRPA1 are the sites of action of most ligands, electrophilic compounds and modulators of channel activity. Lipid Water Interface (LWI) is a 6-10 Å thick region on either side of the membrane where availability of water is less but not totally absent as it is in the hydrophobic core of the lipid bilayer spanned by the transmembrane segments. Thus the properties of amino acids lying in these LWI areas (loop regions) are likely to be different which is very crucial for their structure and function.

Thus, with an objective to determine the LWI stretches (5 amino acid long regions on either side of the transmembrane regions) in all vertebrate TRPA1 considered in this study, the human TRPA1 channel (derived from Uniprot) was embedded in a lipid bilayer in Protter.. Total 12 such stretches on the N and C-terminus of each transmembrane region was identified ([Figure 50a](#)) and a conservation analysis of the amino acids lying at the LWI regions of TRPA1 across 27 different vertebrates from five different phyla was conducted. A conservation analysis of the different LWI stretches throughout vertebrate evolution showed that these regions are not highly conserved with the exception of TM6C on the inner leaflet that is highly conserved across vertebrate evolution. Unlike the different domains of TRPA1 that have highly diverged across evolution in order to adapt itself with the different environments and function, these LWI stretches are relatively conserved indicating importance of these residues in channel function ([Figure 50b](#)).

2.4.2. Amino acids demarcating TRPA1 LWI are partially conserved

The sequence logos depict that only some of the amino acid residues demarcating the LWI stretches in Human TRPA1 are highly conserved across vertebrate evolution.

a.



b. Kruskal-Wallis test: $\chi^2=5145.2$, $df=236$, $P<0.0001$, $n=27$

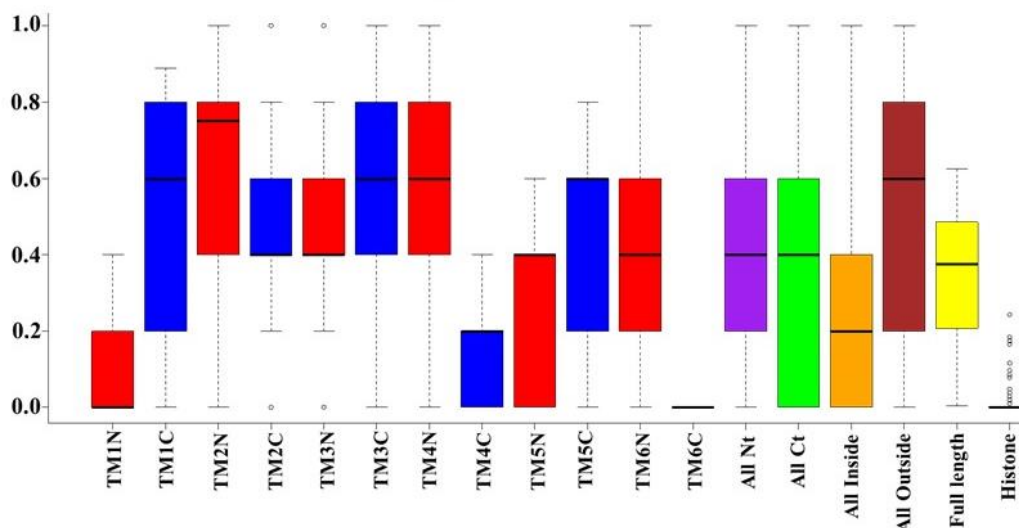


Figure 50: Distribution of amino acids at the lipid water interface region of Human TRPA1 and their conservation across vertebrate evolution. a) Schematic representation of Human TRPA1 embedded in lipid bilayer using Protter. 5 amino acid long regions on either side of the bilayer representing the LWI stretches have been highlighted in red (representing the N-terminus part of TM helices) with and green (representing the C-terminus part of TM helices). TM3C and TM4N overlap each other and hence have

been highlighted in yellow. **b)** Box plot analysis of different LWI regions in Human TRPA1 across vertebrate evolution shows that these LWI regions are not highly conserved except TM6C at the inner leaflet which is highly conserved.

These include the His residue of TM1N, Gln residue of TM4C, Gln residue of TM5C and Ile residue of TM6C. Some of the partly conserved residues include Pro at TM6N and Ser at TM5N. Apart from these the other residues lining the interfacial region of Human TRPA1 are highly variable indicating that these regions might be under constant selection pressure (Figure 51).

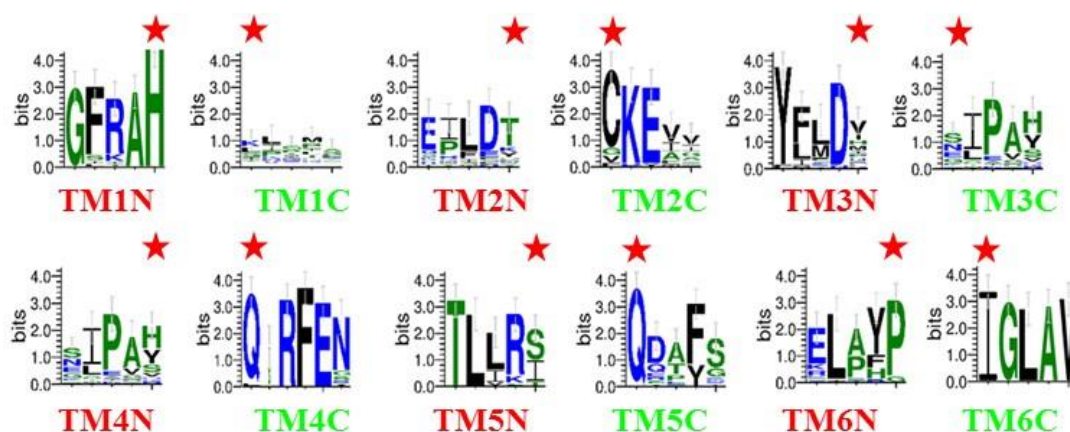


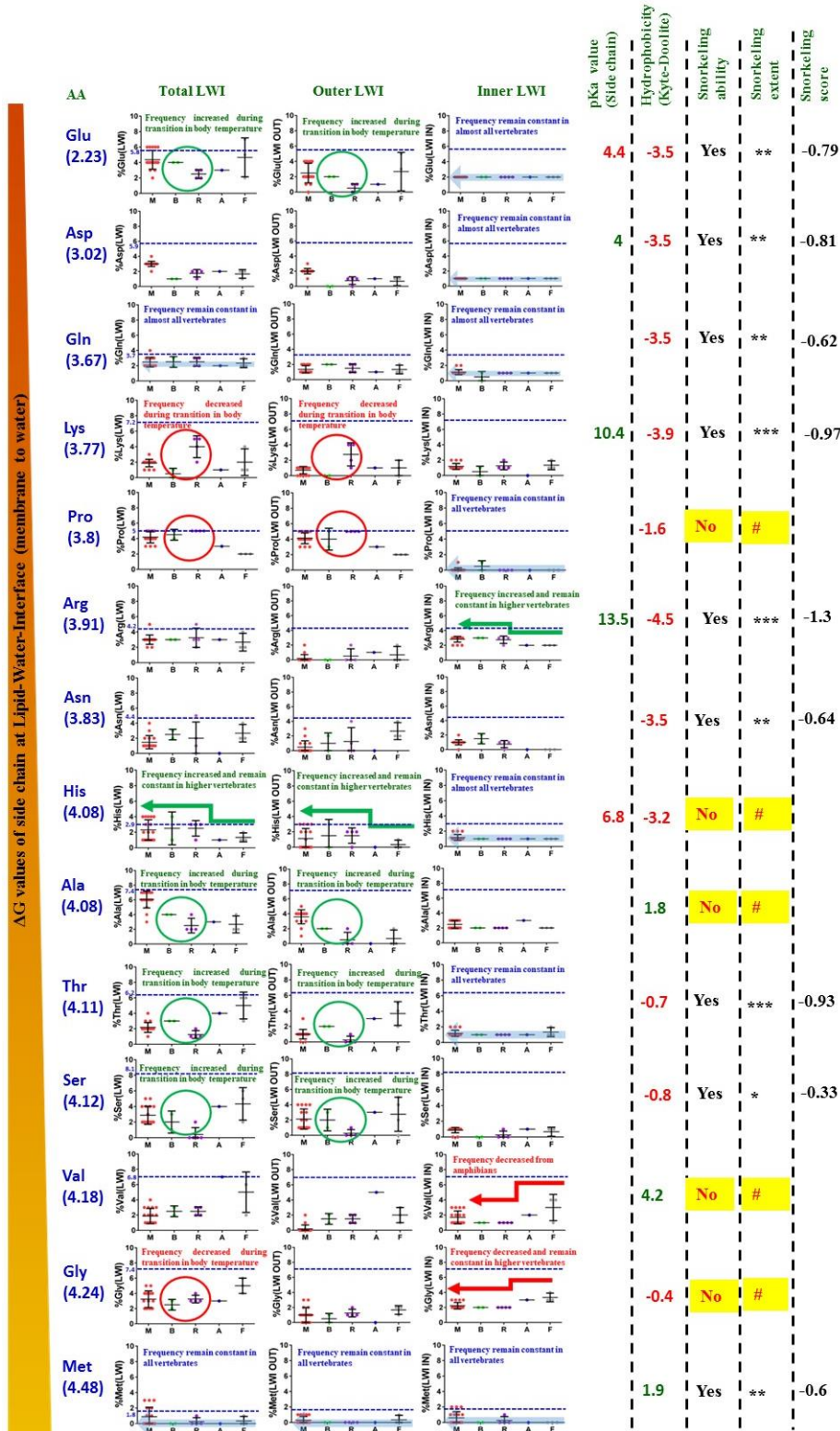
Figure 51. Conservation of amino acids lining the TRPA1 LWI regions. Conservation analysis of each amino acid residue at the LWI of Human TRPA1. The amino acids demarcating the interfacial regions have been highlighted by a star mark.

2.4.3. Frequency of occurrence of different amino acids at the LWI regions across different vertebrate phylum's in TRPA1

A total of 17 mammals, 2 birds, 4 reptilians, 1 amphibian and 3 piscean TRPA1 sequences were considered i.e. only vertebrate TRPA1 sequences were considered. The frequency-of-occurrence of all 20 different amino acids at the lipid-water-interface (LWI) region was calculated. The same calculation was also performed for the outer as well as inner LWI region separately (Figure 52). Analysis reveals that the frequency-of-occurrence of positively-charged amino acids at the different leaflets are quite

variable. % of Arg at the inner LWI has increased from amphibians to reptiles and then has remained fairly constant. On the other hand, its frequency of occurrence at the outer LWI is relatively less and close to zero in mammals and birds. % of His at the inner LWI is constant across all phylums but at the outer LWI there is an increased frequency of His from practically zero in case of fishes and amphibians to (~2%) in reptiles. Occurrence of Lys at the outer LWI shows a negative selection, whereby its % frequency has dropped from amphibians to birds and mammals during transition from cold blooded to warm blooded organisms. Negatively charged residues like Glu and Asp have remained conserved throughout all the considered vertebrates on the inner LWI. Glu has also undergone a positive selection during the transition from reptiles to birds. Aromatic amino acids like Trp, Tyr and Phe have variable frequencies ranging from zero in case of Trp to occurrence of both positive and negative selection for Tyr on the outer LWI and inner LWI respectively. Phe is positively selected on the inner LWI but is only pronounced on the mammalian outer LWI. Helix breaking amino acids Pro and Gly are also negatively selected in total. Apart from Ala, the other hydrophobic amino acids Ile, Leu and Val are mostly negatively selected at the LWI regions across vertebrate evolution. The frequency of occurrence of Met is only noticeable in the mammalian LWI regions (both outer and inner) but for the other phylum's it frequency equals zero. Cys, the residue that gets covalently modified by the electrophilic compounds that activate TRPA1, is nearly equal to zero on the outer LWI but is positively selected on the inner LWI with an increase in frequency from amphibians to reptiles and mammals. Amino acids undergoing phosphorylation like Ser and Thr are positively selected on the outer LWI region. Unlike Asn that is highly variable in occurrence on the both the leaflets, Gln is fairly conserved on the inner LWI.

Taken together, the analysis suggest selection, retention or exclusion of specific amino acids at the inner LWI region and therefore provides important clue of TRPA1 function in different species.



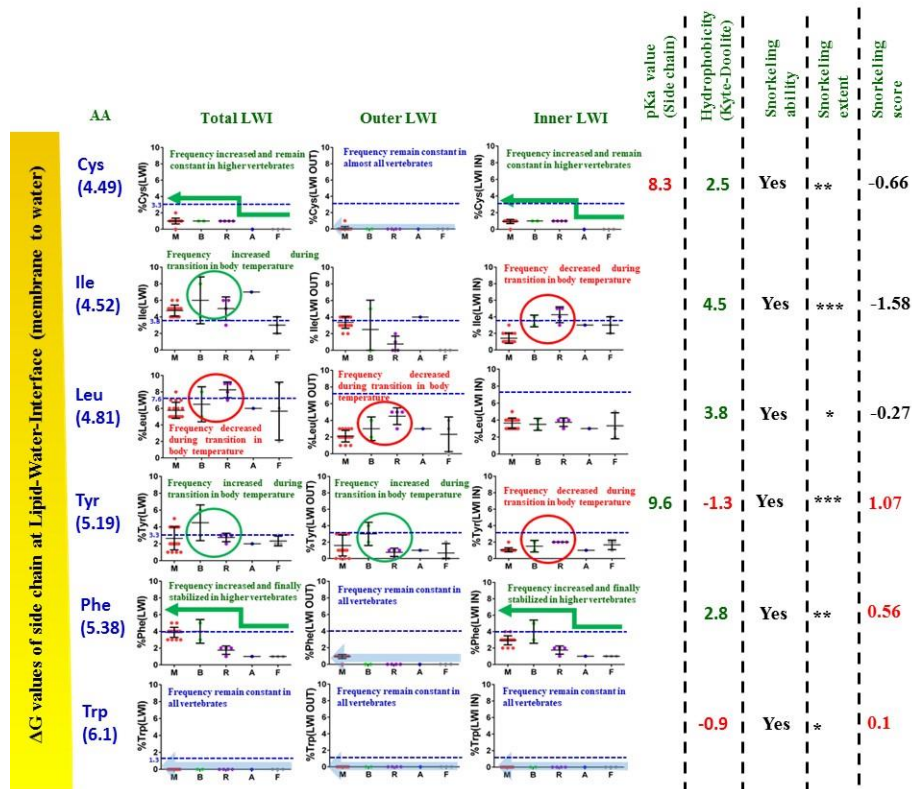


Figure 52. Frequency-of-occurrence of different amino acids at the lipid-water-interface (LWI) of TRPA1 in different phylogenetic groups. The “frequency-of-occurrence” of all 20 different amino acids at inner LWI (right-most row), at outer LWI (middle row), and total (combining inner and outer LWI, left-most row) have been shown separately. Frequency-of-occurrence of different amino acids of TRPA1 LWI region across different vertebrate species ranging from fishes (F), amphibians (A), reptiles (R), birds (B) and mammals (M) are shown. In cases where percentage of amino acids remain constant are indicated by blue arrow as back ground. Similarly, positively selected and negatively selected (or excluded) are marked with green or red arrows. The circles with green (for positive selection) or red (for negative selection) lines indicate the changes in frequency-of-occurrence during transition from reptiles to birds as a result of change in body temperature. The dotted blue line indicates the observed frequency of amino acids in vertebrates (source: <http://www.tiem.utk.edu/~gross/bioed/webmodules/aminoacid.htm>).

2.4.4. Analysis of hydrophilic, hydrophobic, positive and negatively charged residues at TRPA1 LWI across vertebrate evolution

Frequency of occurrence of hydrophobic (Cys, Phe, Ile, Leu, Met, Trp, Tyr) and hydrophilic amino acids (Ala, Asp, Glu, Gly, His, Lys, Asn, Pro, Gln, Arg, Ser, Thr, Val) at the LWI regions on the inner and outer leaflet do not show any conservation. Even their ratio is highly diverged across all vertebrate evolution (Figure 53a). Percentage of hydrophobic and hydrophilic amino acids has undergone positive selection on the outer and inner leaflet of TRPA1 LWI respectively. Analysis of the frequency of occurrence of

positively charged versus negatively charged amino acids at TRPA1 LWI shows that the frequency of occurrence of negatively charged amino acids (Asp and Glu) on the inner leaflet has remained almost constant across vertebrate evolution (Figure 53b). Whereas, the ratio of positive to negatively charged residues at both the leaflets seem to be variable. On the other hand, the positively charged residues (Lys, Arg, His) shows an appreciable increase in occurrence at the inner LWI of TRPA1 whereas the outer LWI there is a negative selection of these amino acids.

2.4.5. TRPA1 has fairly conserved CRAC and CARC motifs

As cholesterol is one of the principle component of lipid rafts and the expression and function of many TRP channels is regulated by this component, it was necessary to identify whether Human TRPA1 harbours any such motifs that could mediate its interaction with cholesterol. Based on the consensus sequences for CRAC (L/V-X (1-5)-Y-X (1-5)-R/K), CARC (inverted CRAC), 14 CRAC and 6 CARC motifs in Human TRPA1 were identified. Out of these CARC 5 was the most conserved in all vertebrates. Rest of the motifs were also fairly conserved as their divergence values range mostly less than 0.5. (Figure 54).

2.4.6. Human TRPA1 forms H-bond with cholesterol

Upon identifying the presence of probable cholesterol interacting motifs in TRPA1, it was necessary to perform a global and local docking with the available closed conformation of Human TRPA1 (PDB ID: 3J9P) and cholesterol. Two residues were identified, Arginine 852 and Asparagine 855 that are capable of forming H-bond with cholesterol (Figure 55). Upon global docking with cholesterol, it was capable of forming H-bonds with Arg852 of TRPA1 in 2 different conformations, one with a binding energy of 6.67

kcal/mole and a bond length of 2.121 Å, another with a binding energy of 6.4 kcal/mole and 2.163 Å. Upon local docking with cholesterol, it was capable of forming H-bond with Asn855 of TRPA1 with a binding energy of 5.96 kcal/mole and a bond length 3.127 Å.

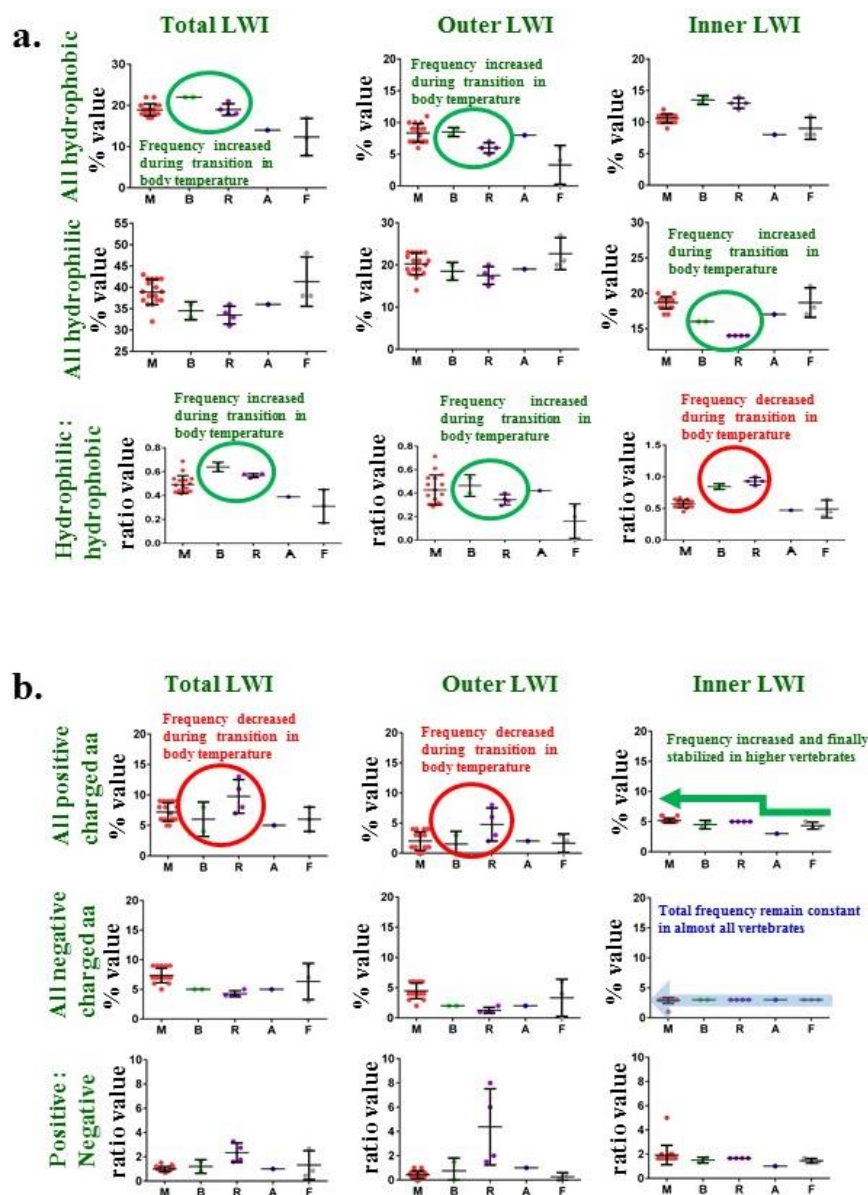


Figure 53. Frequency of occurrence of hydrophilic, hydrophobic, positive and negatively charged amino acids at TRPA1 LWI. a) The frequency-of-occurrence of hydrophobic (Ala, Cys, Ile, Leu, Phe, Met, Pro, Tyr, Val), hydrophilic amino acids (Arg, Asp, Asn, Glu, Gln, His, Lys, Ser, Thr) and their ratio are shown across different vertebrates, i.e. in fishes (F), amphibians (A), reptiles (R), birds (B) and mammals (M). **b)** The frequency-of-occurrence of positively-charged (Arg, Lys, His), negatively-charged amino acids (Glu and Asp) and their ratio are shown across different vertebrates, i.e. in fishes (F), amphibians (A), reptiles (R), birds (B) and mammals (M).

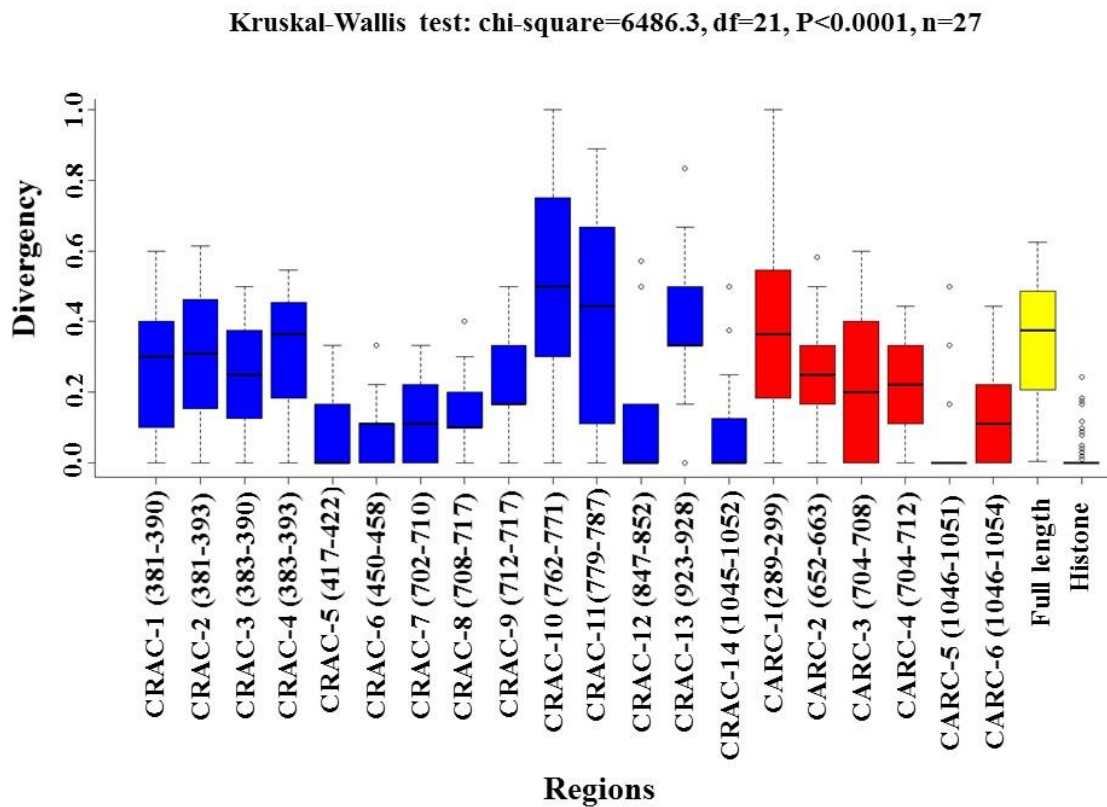


Figure 54. Conservation of different CRAC and CARC motifs in HumanTRPA1. Sequence analysis of different CRAC and CARC motifs shows that HumanTRPA1 has 14 CRAC and 6 CARC motifs for plausible interaction with Cholesterol. Out of these only CARC 5 is highly conserved across vertebrate evolution.

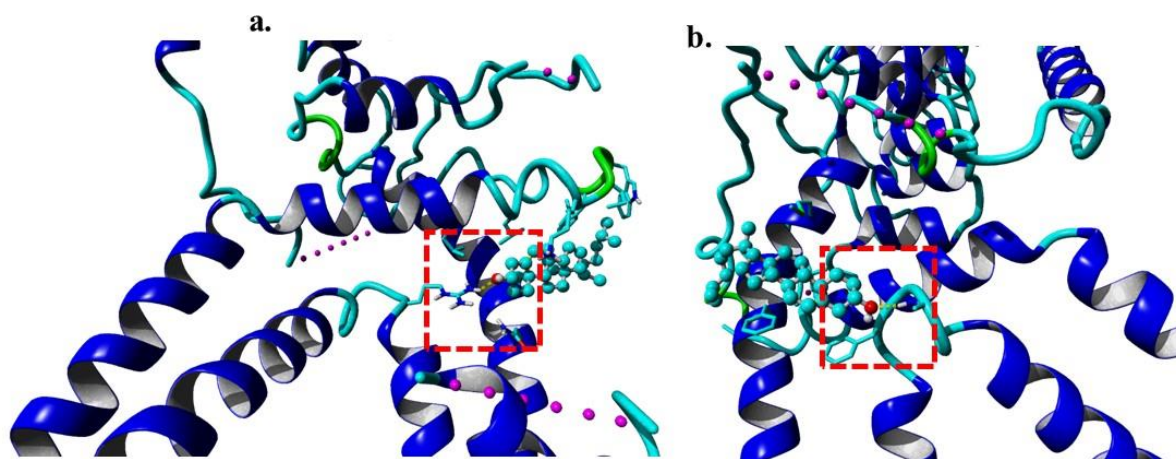


Figure 55. Docking of Cholesterol with Human TRPA1. Closed conformation of Human TRPA1 interacts with Cholesterol by forming H-bond with Arginine 852 (a) and Asparagine 855 (b).

2.4.7. Human TRPA1 localizes in lipid rafts

In order to validate the docking results that predicted the probable interaction of TRPA1 with cholesterol by formation of H-bonds with Asparagine 855 and Arginine 852, full-length Human TRPA1-pSGFP2C1 was transiently transfected in F-11 cells and stained with the *bonafide* lipid raft marker Cholera Toxin B-594. Apart from this endogenous marker, TRPA1-GFP was overexpressed with two other lipid raft markers Caveolin1-RFP and Flotillin-1-RFP. In all these cases, we found TRPA1 co-localizing with these lipid raft markers. Thus, hTRPA1 localizes in lipid raft domains enriched in cholesterol (Figure 56).

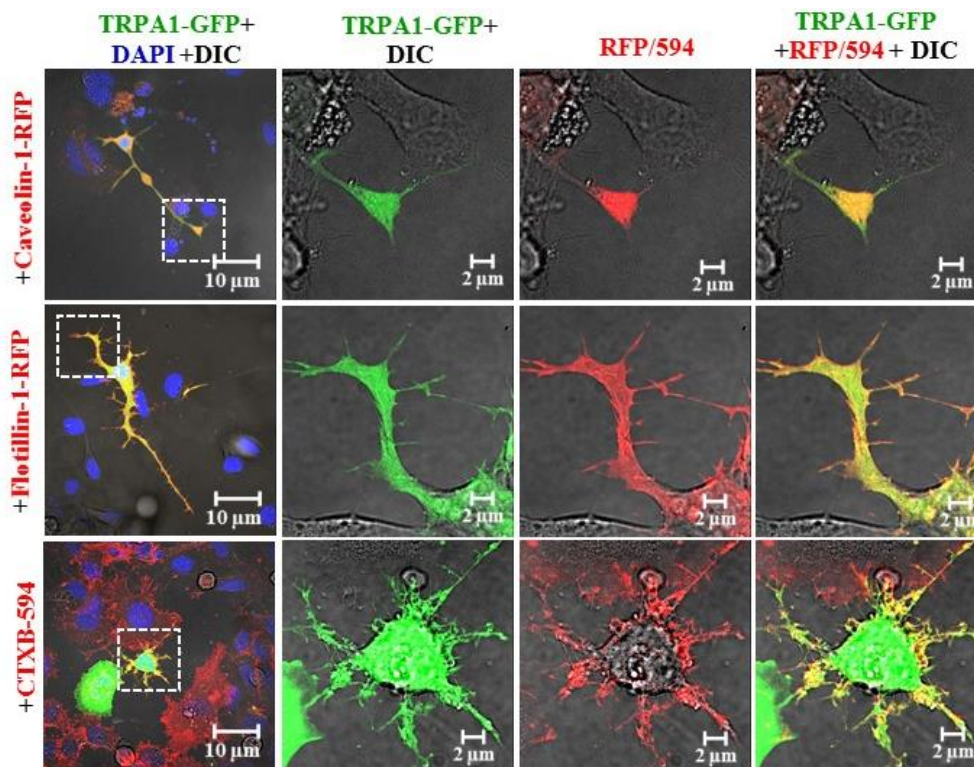


Figure 56. Localization of TRPA1 with lipid raft markers. F-11 cells transiently transfected with Human TRPA1-pSGFP2C1 and Caveolin1-RFP, Human TRPA1-pSGFP2C1 and Flotillin1-RFP and Human TRPA1-pSGFP2C1 subsequently stained with Cholera Toxin B-594 (CTXB-594) revealed that TRPA1 localizes in lipid rafts.

Chapter 3

Discussion

3.1. Molecular evolution of TRP channels

The ancestors of cells, referred to as protocells, just had a lipid envelope surrounding them which was devoid of any membrane proteins or intracellular organelles. This would have created extremely limited options for these cells to communicate with the external environment, particularly to access nutrients or to eliminate wastes. This aroused the need for membrane proteins that would selectively allow communication to and fro between the cell and its surrounding which led to the advent of ion channels. It is believed that the ancestor of all ion channels is a common Ca^{2+} ion channel which is mechanosensitive in nature (314). Bacteria and Archaea possess homologs of several eukaryotic ion channels (315). Presence of ion channels have been detected throughout the animal kingdom from protists till chordates (316). In primitive cells, they were only permeable for selective ions and stimuli, but with evolution their gating properties began to evolve ultimately leading to the evolution of polymodal ion channels like the TRP family of ion channels.

Ambient temperature sensation is a crucial factor that determines the execution of a large number of physiological processes in living organisms. Thermosensory systems of different species have undergone various changes in order to respond to the fluctuations in environmental temperature in course of evolution. The key players in this adaptive process are the thermal sensors expressed in the peripheral sensory cells/neurons that are capable of transforming temperature changes into chemical and/or electrical signals. Functional changes in these thermal receptors have led to diversification in the sensory perception amongst various species (317). Changes in temperature affect all neurons and ion channels but only some neurons can be designated as thermoreceptors and accordingly only few ion channels are considered as thermosensors. Ion channels having a temperature co-efficient (Q_{10}) value $\geq 2-5$ are considered to be thermally gated (174).

Most of these thermal sensors belong to the TRP superfamily (318). Till now, ten such thermos TRP's have been identified in mammals: i.e. TRPV1, TRPV2, TRPV3, TRPV4, TRPM2, TRPM3, TRPM4, TRPM5, TRPM8 and TRPA1. These temperature dependent ion channels have very high Q₁₀ values (>20) (20). Apart from TRPs, other thermosensitive ion channels belong to the TREK sub-family (174).

3.1.1. Molecular evolution of TRPV1

Out of all these, TRPV1 and TRPA1 are co-expressed in the nerve endings of DRG and TG where they play an important role in perception of noxious thermal as well as chemical stimuli which are crucial for animal survival (319) (320). Phylogenetic analysis demonstrates that most of the thermo-TRP's in mammals had already emerged in the ancestral vertebrates (in the common ancestors of terrestrial vertebrates and teleost fishes). Various "gene- duplication" and "gene-loss" events had occurred in the course of evolution that led to the diversification of these thermo-TRP's in different species (321) (322). Teleost fishes possessed genes similar to TRPV1 and TRPV2 and hence were described as TRPV1/2. TRPV1 and TRPV2 emanated as an outcome of gene duplication event and were found to exist separately in the ensuing terrestrial vertebrates. Phylogenetic studies have shown that a single copy of TRPV1 gene has been highly conserved throughout different vertebrate lineages. Its evolution can be traced back to around 400 MYA, a time when amphibians started evolving from fishes (300).

3.1.2. Critical residues involved in chemical and thermal sensitivity of TRPV1

Upon comparison of the channel properties of TRPV1 among different vertebrate species; it is evident that heat activation characteristic of TRPV1 is well conserved across most vertebrate species (i.e. it gets activated at temperature >42°C under normal

physiological conditions) but there is a diversity in its ligand sensitivity probably as different ligands are available in different extent. For example, different species have different sensitivity towards the classical TRPV1-specific agonist, i.e. Capsaicin. Human, rodent, dog and most mammalian TRPV1 are highly sensitive to Capsaicin whereas chicken, tropical clawed frog, rabbit and zebrafish TRPV1 are barely sensitive towards Capsaicin (317). Extensive studies on this species specific difference towards the same ligand by the same receptor has brought forward differences in critical amino acid residues. For example, S512 and T550 in Rat TRPV1 are important for Capsaicin sensitivity, but these residues are different in tropical clawed frog TRPV1 at the corresponding positions (Y523 and A561) (323). In case of Rat TRPV1, S512 and T550 are capable of forming H-bonds within and near the Vanilloid ring of Capsaicin respectively (199). Tyrosine having a larger side chain as compared to Serine and Alanine having a smaller side chain as compared to Threonine, are not capable of forming H-bonds with Capsaicin and that might be the reason for decreased sensitivity of TRPV1 in these species towards Capsaicin (317). Even within the same phylum, African clawed frog and Tropical clawed frog show a difference in “Capsaicin sensitivity” due to changes in the critical amino acid in the Capsaicin-binding site. The C521 residue in African Clawed Frog TRPV1 corresponding to S512 in Rat TRPV1 is capable of binding Capsaicin as the side chains of both these amino acids are more or less similar. Substituting C521 with Tyrosine (present in Tropical clawed frog) in African clawed frog TRPV1 makes it Capsaicin-insensitive (324). Binding of different ligands at the same site also alter the gating property of an ion channel. For example, Vanilloids and phosphatidylinositides occupy the same binding site on TRPV1. Substitution of phosphatidylinositides in the closed state by Vanilloids triggers opening of TRPV1 (199).

3.1.3. TRPV1 channel gating by various components

The Cryo-EM structure of TRPV1 shows that there are two constrictions in the ion permeation pathway that regulate the gating behaviour (opening and closing) of the ion channel. These include the “upper selectivity filter gate” (SF) and the “lower helix bundle crossing gate” (HBC). At the SF gate, the central pore region lined by carbonyl oxygen atoms of G643 and the side chains of M644 forms a constriction of 4.6 Å in diameter. At the HBC gate, on the intracellular end of S6 gate, a hydrophobic seal is formed by the side chains of I679 to generate a diameter of 5.3 Å. Capsaicin binding broadens the lower HBC gate to 7.6 Å keeping the upper SF gate diameter unchanged. Application of more potent agonists like the phytochemical RTX or the tarantula toxin DkTx, which preferentially interact with the outer pore domain, TRPV1 enters into a “fully open state” with considerable opening of both the gates. The upper and lower gates diameter increased up to 7.7 Å and 9.3 Å respectively (198) (Figure 57).

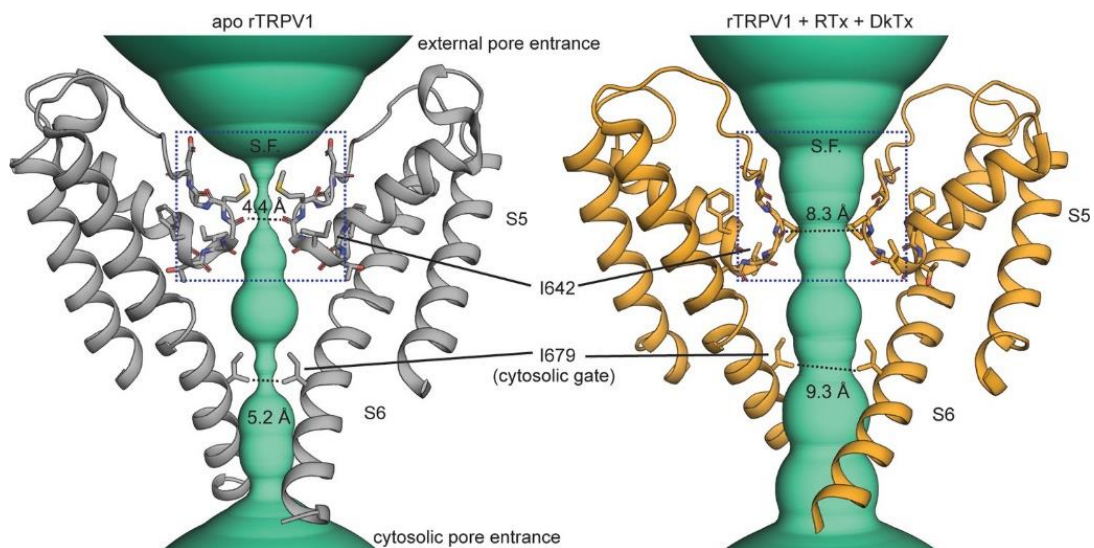


Figure 57. Pore region of TRPV1 in closed and agonist bound state. Figure taken from Oseguera *et al*, 2019 (325).

These ligand-channel interactions are also favoured by the surrounding lipid environment. For example, insertion of DkTx in the lipid bilayer results in upward and lateral displacement of a phospholipid adjacent to Finger 1 of DkTx, as well as downward and lateral displacement of another phospholipid proximal to Finger 2 of DkTx. This interaction between channel, displaced membrane lipids and the toxin determines the affinity and kinetics of toxin binding (199). The major residue is Ile679 that forms the hydrophobic seal of the lower gate. In RTX/DkTx bound state an H-bond is formed b/w Asp576 and Met682 but during Capsaicin binding, this H-bonding is lost and there is a larger shift in opening of the lower gate (198). However, a recent report suggests that the selectivity filter in the outer pore region doesn't serve as a gate. Even in absence of any stimulus, this selectivity filter allows the passage of ions through it. Thus the selectivity filter serves as an actuator instead of an activation gate that enables coupling of structural rearrangements in the outer pore region upon stimulation by an agonist, to those in the cytosolic S6 gate (325). Several regions within TRPV1, precisely, N-terminal ARD, C-terminal domains, Pore region, transmembrane domains have been implicated to play an important role in the channels' thermo-gating behaviour. Thus, heat might be absorbed by several regions within the channel, each of them contributing partially to channel opening, but repeated channel activation by thermal stimuli renders certain regions of the channel to undergo partial polypeptide denaturation. This makes the channels less efficient in absorbing more heat or converting the absorbed heat into channel opening. Finally, once it manages to open, the sufficiently distorted channel enters into an irreversibly inactive state (326). The cryo-EM structure of TRPV1 showed that in its conducting state, the S6 helix adopts a bent conformation due to the presence of a π -helical turn within S6. This flexible π -helix plays an important role in the gating behaviour of all TRPV channels (327).

3.1.4. Importance of membrane lipid, cytoskeleton and ion channel interaction

Membrane lipids in eukaryotic plasma membrane consists of sphingolipids, glycerophospholipids and sterols (particularly cholesterol). Incorporation of cholesterol occurred during evolution when there was an increase in environmental oxygen concentration around 2.5 billion years ago. Thus its introduction into eukaryotic lipid bilayer occurred much later as compared to other membrane lipids (328). Specific domains of the lipid bilayer enriched in glycosphingolipids and cholesterol are referred to as Lipid Rafts or Membrane Lipid Rafts (MLRs) (329). Interaction between these membranous MLRs and sub-membranous cytoskeletal elements regulate MLR assembly/clustering as well as cytoskeletal remodelling (330). Various factors contribute to the gating mechanism of an ion channel. For example, cytoskeletal rearrangements due to a mechanical stimulus can alter the associated membrane energy profile culminating in regulation of tethered ion channels in it (165). Several TRP channels require a proper cytoskeletal matrix interaction in addition to a lipid microenvironment for their proper functioning (331). For example in *C. elegans*, a mechanosensory channel MEC-4 required for gentle touch response in worm, when moves to establish connections with cytoskeletal/extracellular matrix proteins, loses its connections with lipid bilayer which triggers channel opening (332).

3.2. TRPV1-cholesterol interaction

3.2.1. The specific micro environment at the LWI and behaviour of transmembrane proteins

Lipid water interface is a very specialized thin zone formed around the lipid bilayers where availability of free water is less but is not totally absent (333). This low abundance of free water forms a distinct microenvironment at the LWI where protonation-

deprotonation of biomolecules are fundamentally different than other environments where amount of free water is much high, such as in cytosol. This imposes very different physico-chemical properties and local pH fluctuations at the LWI affecting the behaviour of amino acid side chains located there. Though the surface of the lipid bilayer is negatively charged due to the presence of the polar group of phospholipids, the extent of charge distribution at the surface is non-homogeneous throughout the membrane for several reasons (330) (334). This is mainly due to the fact that most membranes contain a large variety of lipids differing not only in their apolar parts, but also these lipids differ in their size, surface charge, and chemical reactivity of their polar head groups (335). In addition, the chemical environment of both layers, i.e. the inner- and outer leaflet, in most cases are significantly different and such asymmetries subsequently induce and/or maintain specific micro-domains of the various phospholipids in general. As the membrane components are diverse in nature, their relative presence are variable with respect to time and largely depends on the cellular metabolism *per se*. Constant changes in the microenvironments at both the LWI regions of lipid bilayer is routine, both in actual time scale (for example due to metabolic fluctuations) as well as in evolutionary time scale (due to change in species, body temperature and other factors). All these variable factors contribute to the generation of biological membranes which is actually dynamic, non-homogenous in chemical composition, asymmetric in nature and are regulated by thermodynamic parameters at the molecular level (271)(276)(335)(336)(337)(338)(339)(340)(341)(342)(343)(344)(345). In spite of this variability, several transmembrane proteins reside in lipid bilayers and exclusively need membranous environments to remain functional. In this context, the transmembrane proteins represent complex and dynamic structures that are optimised for their lipid-protein interactions in order to have proper regulation and functions. In biological

systems, such optimization is spontaneously achieved through different mechanisms and in different time scale ranging from quick lateral diffusion of membrane components in milliseconds/seconds to positive selection of different mutants which takes millions of years during evolution. Therefore, systemic analysis of the exact amino acid sequences of transmembrane proteins facing the lipid-water interface can indicate the actual nature of micro environment available and/or needed to that sequence. In this work, such analysis has been executed for TRPV1, a non-selective cation channel which is known to be activated by high temperature as well as by Capsaicin, an exogenous compound (144). It has been elucidated that evolutionary selection of specific amino acids present in the LWI of TRPV1 in different membranes (made of PEA as well as POPC) correlates well with the specific physico-chemical properties of that microenvironment there and *vice versa*. The interaction of Arg residues with OH- group of cholesterol at the inner leaflet seem to be a critical physico-chemical aspect for the channel structure-function relationship and thus act as an evolutionary selection pressure. In this context, it is important to note that PEA is present in several biological membranes, such as in sperm cell membrane, neurons, etc.(346). In many cases, TRP channels are present and functional in such membranes made of/enriched of PEA. The bond forming abilities of Arg residues with cholesterol is conserved in both PEA as well as in POPC membrane. Cholesterol interacts with TRPV1 present in different membranes and is independent of relative saturation level of cholesterol.

Membranes simulated in the experiments are simple membrane systems with lipids having two tails. The aim was to study the ion channel at the computational level after embedding it in a suitable membrane environment. PEA was chosen because it is the most stable membrane lipid and it is also the second-most abundant phospholipid in mammalian cells (347).. PEA comprises ~15-20% of the total lipid in mammalian cells

and is enriched in the inner leaflet of membranes (347). In contrast, POPC has a large headgroup which cannot form hydrogen bonds among themselves, and thus reduces membrane stability. A 250 ps restrained equilibration simulation was run while embedding TRPV1 in the membrane where the membrane is artificially stabilized so that it can repack and cover the solute, while solvent molecules are kept outside. Several reports suggest that TRP channels are regulated by different membrane lipids. Phosphatidylethanolamine (PEA) and phosphatidylcholine (POPC) are the most abundant glycerophospholipids in eukaryotes (348). Apart from being the principle structural component of all cellular membranes, they have various other functions. POPC acts as the major source for formation of lipid mediators and second messengers (349). Any perturbation in its production interferes with cell proliferation, differentiation, and membrane movement (350). On the other hand, PEA plays essential roles in autophagy, cell division and protein folding and represents a precursor for the synthesis of several protein modifications (351). In addition, both POPC and PEA are intermediates in the synthesis of other glycerophospholipids (352). The maintenance of molar ratio of PEA and POPC is important for normal physiological functions (348). The highest amount of PEA (up to 45% of all phospholipids) is found in the membranes of neuronal tissues, such as in the white matter of the brain, nerves, and spinal cord, which is of particular interest to us. Due to its “conical shape”, PEA modulates membrane curvature and lateral pressure and thus supports membrane fusion and function of several membrane proteins like the ones under investigation in this thesis. In fact, mammalian sperm membranes are also enriched in POPC and PEA (353). All these aspects allowed us to consider PEA and POPC membrane as a suitable membrane model at the computational level.

3.2.2. Selection of amino acids at the LWI of transmembrane proteins

In this work it has been demonstrated that the amino acids present in the LWI of TRPV1 are more conserved than the average conservation of full-length TRPV1 suggesting that these amino acids are under positive selection pressure. The N- to C-terminal directionality of the polypeptide also imparts biasness on the molecular selection of amino acids in the LWI. Amino acids present in the inner leaflet are more conserved than the amino acids present in the outer leaflet. This fact strongly suggests three aspects: First, the difference in the membrane components between inner and outer-leaflet has significant effect on the selection of amino acids in the LWI-regions. Second, interaction with membrane components, intracellular proteins, phosphorylation by kinases etc. are possible intracellular functions that may define the importance of LWI residues present in the inner leaflet than in the outer leaflet. Third, the residues present at the inner leaflet have a more definitive role in establishing the polarity gradient among the less polar or nonpolar amino acids present in the hydrophobic core and the more polar amino acids towards the LWI. These results are also in line with the fact that residues present in the LWI-region in turn regulates the interaction of membrane proteins with other lipids and may also determine their precise localization and orientation at the interface (270). In this work it has been demonstrated that snorkeling amino acids, mainly Arg and Tyr are predominant at the LWI of TRPV1. Notably, analysis of the sequence as well as the recently resolved 3D structure of TRPV1 suggests that a large fraction of the Arg and Tyr residues present in the entire sequence (full-length TRPV1) are actually clustered in the LWI regions only. These facts strongly suggest that Arg and Tyr residues are positively selected and therefore enriched at the LWI. Notably, Lysine is absent totally in these specific positions in any sequence (representing vertebrate TRPV1 sequences analysed in this work). A relevant and preliminary data has been added in the annexure ([Annexure 5](#))

of this thesis which suggest that TRPV1 has a specific pattern of arrangement of amino acids at its LWI regions. Other membrane proteins/TRP channels have different patterns and ratios. The evolutionary significance of “such pattern” could be linked with ion channel functions that are modulated by temperature (both internal as well as external), metabolism affecting compositions of lipid bilayers and reproduction success. Presence or absence of specific residues in the LWI region may also be helpful for detecting certain stimulus more effectively and can also form a strong molecular basis of receptor-ligand interaction that can be relevant for molecular evolution. However, more studies are needed to elucidate this. Interestingly, during the course of vertebrate evolution, His is replaced by Arg, suggesting that the positive charge as such is not the prime selection factor in these positions as such and/or the need for positive charge is independent of pH. This biasness in frequency distribution at the LWI (in both sides) of the transmembrane helices accords well with the “snorkeling abilities” of certain amino acids that are better suited in these microenvironments only (354). This is also in line with the differential ability of Arg (over Lys) to organize within lipids (355). It is important to mention that Arg attracts more water molecules and lipid head groups into the bilayers and such behaviour minimizes the large dehydration energy costs (356). Cholesterol and/or membrane deformations are known to stabilize Arg residues in its protonated form in the LWI and thereby can cause a shift in the pKa of Arg (357). Such stabilization of Arg residues at the LWI can significantly alter the biophysical properties of ion channels and other transmembrane proteins (358)(359)(360). The peptide sequences corresponding to the different transmembrane regions are certainly selected throughout the evolution. Such selection is critically determined by the availability of the suitable biological membrane. The relative level of certain lipids in different biological membranes largely depends on the anabolic and catabolic metabolism of such lipids and enzymes present in such

biological systems. In addition, the bio-physical behaviour of biological membranes is largely dependent on body temperature, lateral mobility of the membrane components and molecular vibration. As metabolism and body temperature increased during evolution, the critical amino acids located within this LWI-region with snorkeling behaviour are also subjected to selection through molecular evolution. In this context, ability of Arg557 and Arg575 to form H-bond with the OH- group of cholesterol is very important and it is proposed that the specific interaction of cholesterol with these Arg residues served as a selection pressure on these two positions. This argument is supported by the fact that both these residues are located at the LWI regions, located at the inner leaflet, and are part of the cholesterol interacting CRAC motifs (L/V-X(1-5)-Y-X(1-5)-R/K). Accordingly, these two residues are also highly conserved and/or are selected throughout vertebrate evolution. These results accord well with the fact that cholesterol represents a vertebrate-specific molecule (cholesterol biosynthesis pathway is established in vertebrates only). Cholesterol is also present in high amount in lipid rafts and in synapses (361)(362). It is also produced in high amount during early phases of neuronal development (363)(364). Never-the-less, it can be proposed that the absence of bulk free water in the LWI region is critical for the interaction between Arg and cholesterol. Indeed, *in silico* analysis suggest that Arg575 can also interact with PIP₂ and regulate the PIP₂-mediated TRPV1 activation (365). However, the *in silico* analyses indicates that Capsaicin preferably interacts between 2nd and 3rd TM region. Even local docking experiments also suggest that Capsaicin has limited binding affinity near Arg557 and Arg575 positions. In a reverse manner, cholesterol cannot occupy the Capsaicin-binding site. This may suggest that ligand-mediated activation of TRPV1 (such as by Capsaicin) may not be directly affected by cholesterol as such.

3.2.3. Importance of cholesterol at the LWI-regions

Cholesterol is an important molecule present in the lipid bilayer. In general cholesterol amount in upper leaflet and inner leaflet is mostly same (mainly due to less energy cost of cholesterol). However, its relative abundance is often more in the inner leaflet than the outer leaflet (366)(367). The exact amounts of cholesterol present in two different leaflets are variable and the degree of variability is also different in different biological membranes. Several reports suggests that in neuronal cells and especially in synaptic structures, the relative amount of cholesterol is high in the inner leaflet rather than in outer leaflet (361)(368)(369). Though the amount varies from biological system to system, analysis suggest that cholesterol distribution ranges from 65% in the outer leaflet to 75–80% in the inner leaflet (368). Also the fast flip-flop exchange is dependent on the availability of the corresponding enzymes. Availability of flippase in certain biological membrane appears as a chance factor and is dependent on many other factors also. Therefore, in case of no or less enzyme activity, the concentration of cholesterol is expected to be high in the inner membrane than outer membrane, especially when the cell is capable of synthesizing cholesterol *de novo*. Cholesterol also represents a vertebrate-specific biomolecule as cholesterol biosynthesis pathway is established in vertebrate only (279)(280) whereas invertebrates acquire cholesterol from dietary supplements. Invertebrates do not have a full-biochemical pathway that allow them to synthesize cholesterol (also relevant in the evolutionary context). Therefore, cholesterol represents a vertebrate-specific biomolecule as only vertebrates are capable of cholesterol biosynthesis *de novo*. So far there are several reports which strongly suggest that cholesterol content is critical for the function of many transmembrane proteins (370)(371). Several transmembrane proteins contain specific cholesterol interacting motif sequences that binds to cholesterol present in the lipid bilayers (372)(373). Often multiple

cholesterol molecules bind to different transmembrane helices and form “annular belt-like structures” which provides conformational stability – instability (372)(373). The strength of lipid-peptide interaction at the LWI-region and the conformational change in the peptide are often energetically coupled (341). Therefore, interaction (as well as loss of interaction) of cholesterol with the specific motif sequences are important for the structure-function relationship of transmembrane proteins and such interactions can provide important selection pressure relevant for molecular evolution. Ability of cholesterol through their OH-group to interact with specific residues such as Arg and Tyr at the LWI is established (275)(374). This specific ability enforces these two residues as critical factors for the proper functioning and regulation of these transmembrane proteins. Cholesterol interaction with TRPV1 can be relevant for different aspects. For example, “number of cholesterol binding sites” present in TRPV1 of a specific species, the actual “cholesterol-binding possibilities” a functional channel might have, and/or the “actual cholesterol occupancy rate” on a specific site or on the functional tetramer are important parameters that can be different in different species, isotypes, in case of mutants and also in different biological membrane. The calculation of binding energies suggests that cholesterol interacts with TRPV1 present in different membranes and is independent of relative saturation level of cholesterol. Also, changing Arg557 or Arg575 to other amino acids alter the number of modes in which cholesterol interacts with TRPV1 as well as the binding energies at which such interactions may happen. These results therefore suggest that “probability” of cholesterol binding to TRPV1, the “flexibility” (i.e. the number of modes in which interaction is possible) with which cholesterol interacts to TRPV1, and the “occupancy level” of cholesterol on single functional TRPV1 tetramer is high. These analyses suggest that during vertebrate evolution, the number of snorkeling amino acids, especially Arg and Tyr in the Lipid-Water Interface of TRPV1 got decreased and thus the

probability of bond formation with cholesterol in LWI region is decreased. However, this does not imply that bond formation is abolished completely. In fact, these data indicate that the few motifs and certain key residues become more relevant for critical interactions with cholesterol, and such residues got selected through evolution and this can be correlated with channel gating as well as certain other channel functions. Mammals have the highest amount of cholesterol and fishes have the lowest amount of cholesterol (375). During evolution, the body temperature increased and fish, amphibian and reptiles represented cold blooded animals whereas birds and mammals represent warm blooded animals. Accordingly, analysis of cold verses warm blooded animals also suggests that the frequency of specific snorkeling amino acids (for example Arg + Tyr) in the LWI region of TRPV1 decreased as evolution progressed from cold-blooded animals to warm blooded animals. However, analysis with other thermosensitive/ non-thermosensitive and/or other TRP/non-TRP channels (with TRPV2, TRPV5, TREK and Mu Opioid) suggest that such variations can be unique for TRPV1 and other channels ([Annexure 4](#)).

3.2.4. Possible importance of Arg-cholesterol interaction in channel activity of TRPV1

Based on this work, it is proposed that Arg-cholesterol interaction may act as an “evolutionary selection factor” which also signifies the importance of this interaction in TRPV1 channel functions. Previously it has been demonstrated that cholesterol act as an important regulator of TRPV1 localization as well as its channel activity. For example, proper membrane localization of TRPV1 needs cholesterol (129). Similarly, endogenous TRPV1 is preferably present in the cholesterol-enriched detergent resistant membrane microdomains of sperm cells and cholesterol levels regulate the exact localization depending on the functions and status of the sperm cells (376). In accordance to the need

for cholesterol for proper channels functions, depletion of membrane cholesterol affects TRPV1 activation in trigeminal sensory neurons and in transfected cell line (130). Cholesterol depletion also reduces the thermal threshold required for TRPV1 activation suggesting that interaction with cholesterol actually restricts spontaneous channel opening (129)(130). Indeed, it has been demonstrated that cholesterol depletion leads to the rise in intracellular Ca^{2+} concentration, which can be effectively blocked by capsaizepine, a specific inhibitor of TRPV1(377)(378). These reports therefore strongly suggest the importance of cholesterol in “channel-gating” events. This work suggests that cholesterol interaction with TRPV1 at the lipid-water interface is crucial and is also essential for proper functioning of TRPV1. Indeed, recently it has been shown that cholesterol depletion alters the pore dilation of TRPV1 (132). The possibility of cholesterol-mediated channel regulation is very realistic in other TRPV channels too, as single mutation in human TRPV4 results in “loss-of-interaction” with cholesterol with TRPV4 and thus can also explain the constitutive nature, i.e. the gain-of function” of this R616Q mutant of TRPV4 (140). Considering that other TRPV channels, such as TRPV3 and TRPV4 are also regulated by cholesterol, the actual mechanism seems to be similar for all these channels with minor variations (139)(379)(140). There are critical cellular functions that depends on the membrane cholesterol and Ca^{2+} signalling events such as development and maturation of synaptic structures. Therefore, regulation of TRPV1 by cholesterol can be relevant for such functions. Phosphorylation of 2nd and 4th loop regions located at the lipid-water interface (cytoplasmic side) of TRPV1 are considered as critical regulatory mechanisms relevant for channel opening (380). This is mainly due to the fact that phosphorylated population of TRPV1 only represent the “sensitized channel” which can respond to stimuli and undergo channel opening, a thermodynamically unfavourable event. Phosphorylation also induce more negative charge and therefore increase the

hydration of loop regions (due to phosphorylation) and such modifications seem to reduce the activation energy needed for channel opening. Such aspect suggests that detachment of the 2nd and/or 4th loop of TRPV1 from the inner LWI-region is a prerequisite for TRPV1 channel opening. In a reciprocal manner, interaction of these two intracellular loops to the membrane surface stabilizes the closed conformation. Indeed, recent report has validated that Capsaicin potentially stabilizes TRPV1's open state by 'pull-and-contact' interactions between the Vanillyl group and the S4-S5 linker (221). This also suggests that fine conformational changes at the lipid water interface are needed for channel opening. It seems that Arg557 and Arg575 of TRPV1 interact with cholesterol only when the channel is in close conformation and not in its open state, and such observations correlate well with channel opening and closing events. Previously few reports have confirmed that Arg557 and Arg575 are critical for several functions attributed to TRPV1 (381). For example, Arg557Ala and Arg557Lys mutants have a significantly lower rate of activation, and the estimated deactivation time is significantly longer in Arg557Lys mutant compared to the wild type TRPV1 (which is not the case for Arg557Ala or Arg557Leu mutants) (381). These results accords well with the previous findings demonstrating the importance of Arg557 residue (382). The other mutants such as Arg557Leu and Arg557Lys is reported to reduce the inward currents induced by 300 μ M 2-APB (380). Also the Arg557Ala and Arg557Leu mutants are weakly voltage-dependent under control conditions (380). Arg575Ala mutation cause a significantly higher threshold for heat activation and this residue (Arg 575) was shown to be involved in voltage sensing and in TRPV1-Lipid interactions(380). These unique side-chain property (rather than its positive charge only) of the Arg residue at 557 and 575 positions are important for the deactivation and gating process. Conformation specific interaction (with close state) with cholesterol can be relevant for these positions and most likely such

interactions stabilizes the “closed-state” and restrict “spontaneous opening” probability to a large extent. Ability of chloroform, isoflurane and ethanol to potentiate and/or activate TRPV1 also suggest the importance of LWI-regions in TRPV1 structure-function regulation (383). This is mainly due to the fact that ethanol and anaesthetics such as Chloroform and isoflurane are known to be enriched in LWI-regions and these compounds are known to alter diffusion of membrane components.

In this work it has been demonstrated that the average content of two snorkeling amino acids (Arg and Tyr) present in vertebrate TRPV1 gradually decreased during piscine to mammalian evolution. Considering that mammals contain higher level of cholesterol than fish, the average Arg content in the LWI-region of TRPV1 seem to share an inverse relationship to the average cholesterol content. It is proposed that such relationship between Arg (as a snorkeling but not as a positively charged amino acid) and cholesterol level and closed conformation-specific interaction of TRPV1 with cholesterol may provide important clue for thermo-gating behaviour of TRPV1. The observation that the average Arg content in the LWI-region of TRPV1 is significantly different in cold-blooded animals compared to warm-blooded animals, further justify the importance of Arg-cholesterol interaction in thermo-gating behaviour of TRPV1. Such relationship may be critical for understanding the channel gating mechanism of TRPV1.

3.2.5. What we learn from the frequency calculation: importance of certain amino acids in channel functions

Analysis of the frequency of occurrence of different amino acids at the LWI region of TRPV1 sheds light on the structure-function relationship of TRPV1. Considering the codon-bias of each aminoacids at different levels, the natural frequency of amino acids observed in nature and the actual frequency of different amino acids observed in case of

inner and outer LWI region of TRPV1 and TRPA1 are intriguing. Notably, in inner LWI region, amino acids with titrable side group has undergone two clear trajectories. Either such amino acids were retained at a conserved frequency or such amino acids were enriched in comparison to observed frequency of amino acids in vertebrates (384).. For example, the frequency-of-occurrence Arg, Lys, Pro, Trp and Tyr, remain constant in inner LWI throughout the vertebrate evolution while Cys amino acid is completely excluded in inner LWI throughout the vertebrate evolution, suggesting that Cys residue is misfit there. Residues such as His, Glu, and Thr gradually declined and ultimately got excluded in mammals, suggesting that these amino acids are not suitable in the inner LWI regions, especially in warm blooded animals. While positively charged amino acids such as Arg and Lys are selected at high-frequency, exclusion of His in the inner LWI is highly suggestive. The observed frequency of Arg in the inner LWI region of TRPV1 is much higher than the natural frequency of Arg, suggesting a true enrichment of Arg in the LWI region. Interestingly, Tyr and Lys in the inner LWI region of TRPV1 just matches with the natural frequency of Tyr and Lys, which may suggest a very precise stabilization of inner LWI region of TRPV1 during the course of evolution. In contrary, though observed frequency of Trp is less than 5% in case of inner LWI of TRPV1, it is much higher than the natural frequency of Trp, suggesting that Trp is also enriched at the inner LWI region. Higher frequency of positively charged residues also accord well with the “positive inside rule” described before(277).

High-frequency of Arg and Lys accords well with their ability to snorkel as well as their ability to form bonds with membrane components (385) (270). For example, Arg and Lys are able to form bonds with the –OH group of cholesterol at the LWI region, while His residue is unable to form such bonds. Also, considering the protonation-deprotonation possibilities at physiological pH in the inner LWI, His appears to be a misfit

amino acid there (386). Reduction in frequencies of Phe, Asn, Ala, Leu, and increment in frequencies of Ile, Val, Gln in the LWI correlates with the transition from cold-blooded animals to warm blooded animals (reptiles to birds). Therefore, these changes are more-likely to accommodate the bio-physical changes that took place in lipid membrane during the transition from low body temperature to warm temperature. From these data it has also become evident that the amino acids that have retained a high frequency-of-occurrence (~10%, and at constant values) during vertebrate evolution in the inner LWI are Arg and Asp. In fact, Arg and Asp share 1:1 ratio at the inner LWI region, especially in higher vertebrates. Data suggests that Arg at 575th position may play important role in channel gating, possibly by altering the conformation of TM5 and thus the lower-gate of TRPV1. At physiological pH, most-likely the net neutral charge at inner LWI of TM5 [due to presence of a positive (Arg575) and negative charge (Asp576)] and ability of the Arg residue to interact with cholesterol may allow TM5 to be fixed in a conformation that is equivalent to “closed state”, yet flexible enough for opening in presence of proper stimuli. Considering that the inner surface of the lipid bilayer is intrinsically negatively charged (due to the presence of phospho-groups), when the inner LWI region of the TM5 is fixed with more negative charge, the TM5 may shift further down from the bilayer resulting in “locking of mutant channel” in either “open” or “open-like” or even a “dilated” state. This is more relevant, as TRPV1 become sensitized (equivalent to more spontaneous opening) upon phosphorylation in its Ser residues, which introduces more negative charge in its loop regions (387).

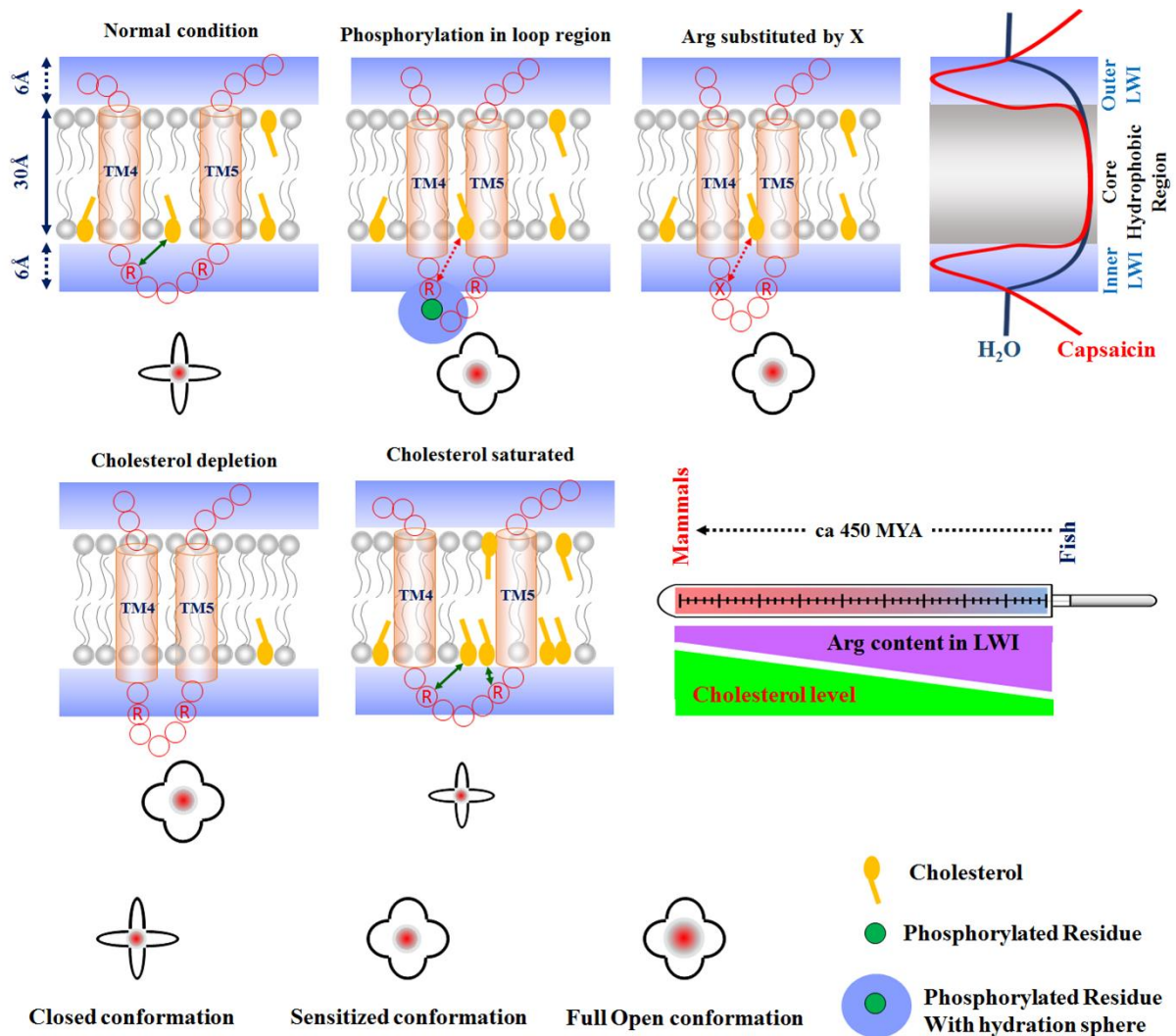


Figure 58. A plausible model depicting the importance of Arg-cholesterol interaction and loop hydration in TRPV1 channel gating. The transmembrane helices and unstructured loops are mostly occupied in the core hydrophobic lipid bilayer (~ thickness of 30Å) and both side lipid-water interface regions (~ thickness of 6Å) respectively. The relative amount of free water is much less in LWI regions. Arg-cholesterol interaction in LI region preferably stabilizes TRPV1 in closed conformation and loss of this interaction possibly decreases the activation energy and thus increases the open probability and spontaneous opening of TRPV1. Phosphorylation at the loop residues induces more hydration of the loop regions and thereby can sensitize TRPV1. Similarly, substitution of Arg with other amino acids or cholesterol depletion results in loss of this interaction resulting in unwanted spontaneous activation. Cholesterol saturation and/or presence of other sterols may strengthen this interaction and therefore stabilize the closed conformation resulting in requirement of more activation energy and/or delayed channel opening. Cold-blooded and warm-blooded animals share inverse relationship with the levels of Arg present in lipid-water interface and cholesterol in membrane. Such relationship might be crucial for thermo-gating behaviour of TRPV1 in cold-blooded and warm-blooded animals.

Importance of Arg-cholesterol interaction and loop hydration in TRPV1 channel gating has been demonstrated in this model (Figure 58).

3.2.6. Importance of maintenance of ratio of positive-negative and hydrophobic-hydrophilic amino acids at inner LWI of TRPV1

So far several diseases have been identified that are linked with the dysfunction of ion channels, collectively termed as “channelopathies”. The most common cause of such impairment is point mutation in genes encoding ion channels. Such mutations affect different properties such as channel folding, proper localization, relevant interactions with lipids and/or proteins, post-translational modifications, and often channel-gating behaviour (388). As TRPV1 is a non-selective cation channel and polymodal in nature (i.e. it gets activated by different chemicals and temperature), changes in TRPV1 sequence is indicative of suitability of amino acids in membranous micro-environments for proper channel functions including channel gating. As TRPV1 is involved in thermo-sensory functions and other physiological functions, improper channel gating, i.e. constitutive-opening or constitutive-closing is expected to provide either disadvantages or at least provide no adaptive advantages. Therefore, uncontrolled spontaneous opening of TRPV1 is expected to cause lethality at the level of cells, tissues and also in individual. The results obtained from this study confirms that TRPV1 retains a specific ratio of hydrophobic-hydrophilic residues (1:1.36) as well as positive-negative charged residues (1.67:1) in its inner LWI region throughout vertebrate evolution. In spite of the variation in frequency-of-occurrence in individual amino acids, the conservation in these ratio is highly significant and sheds important information about the structure-function relationship of TRPV1. Notably, these values remain constant in all vertebrates. In fact, there is no change in these ratio values in reptiles as well as in birds (indicating transition from cold-blooded animals to warm blooded animals), suggesting that these values indicate functions that are independent of body temperature. As this ratio is maintained in cold-blooded animals as well, it is proposed that these ratio values indicate suitability

of amino-acids in specialized micro-environments required for “channel-gating” and not for “thermo-gating” as such.

3.2.7. Does Arg575Asp mutation makes it as a constitutive open ion channel

The Arg residue at 575 position is mostly conserved throughout the vertebrate evolution. Notably Arg at 575 position seem to be very critical for proper localization of TRPV1 at lipid raft and also maintaining interaction with cholesterol, at least in the closed state. In case of TRPV1-Arg575Asp mutant (showing the ER retention and ER fragmentation phenotype), the localization of the mutant is predominantly at the perinuclear region. This suggests a general defect in “membrane trafficking”. Blockage of budding process from ER, a process which is cholesterol-dependent cannot be ruled out also. The lack in proper trafficking to the plasma membrane can also be compromised in case of this mutant. In fact, the surface labelling experiment also suggest so. However, the phenotype (ER-retention and ER fragmentation) observed in case of TRPV1-Arg575Asp mutant is not due to over expression as such. This is mainly due to the fact that such defects are “only observed in case of TRPV1-Arg575Asp”, and even in case of low expression levels and even at shorter time points. Such defects are not observed in case of very high expression levels of Wild type and some other mutants, even at later time points. As this residue gets changed during the transition from reptiles (cold blooded) to birds (warm blooded), it can be proposed that Arg575 is not involved in “thermo-gating” (equivalent to response in minute temperature differences) property *per se*, but is actually involved in “channel gating” (equivalent to channel function) in vertebrate membrane containing cholesterol. However, this is a crucial amino acid for overall channel gating and Arg575Asp mutation brings double negative charge to the end of TM5 located at LWI regions. Such strong negative charge is expected to place TM5 further

down from LWI region due to strong repulsion by negatively charged surface and lack of bond formation with membrane cholesterol. Such aspects may cause “permanent locking” of Arg575Asp mutant in a constitutive open conformation. Indeed, there are several reasons that lead to the consideration of TRPV1-Arg575Asp channel as a “constitutively open” channel. First, expression of Arg575Asp mutant leads to change in cellular morphology immediately after its expression in F11 cell (~24 hrs). The same phenotype is also observed in other cell types such as HaCaT and SaOS suggesting that Arg575Asp mutation is universally toxic for cells. Second, the basal level of cytosolic Ca^{2+} is relatively high in cells expressing Arg575Asp mutation compared to other non-transfected cells. Third, the cells that express Arg575Asp mutant is more permeable to large compounds such as Rhod-3 AM dye when compared to other non-transfected cells (Figure 60). Finally, the toxicity due to Arg575Asp can be mostly rescued by a TRPV1 specific blocker 5'-IRTX, suggesting that Arg575Asp is a constitutively open channel. Accordingly the relative comparison of TRPV1-WT with Arg575Asp suggests that the single mutant most likely takes more time to open, closes faster than wild type and thus conduct less amount of Ca^{2+} (at least in case of external stimulation by Capsaicin). Also TRPV1-Arg575Asp-Asp576Arg mutant rescues some of these properties to a large extent, but certainly differs from WT (Figure 59).

This possibility has been supported by the fact that introducing Asp576Arg mutation in the background of Arg575Asp rescue normal cellular morphology, though the double mutant show defects in the lipid raft localization. Therefore, it might be possible that Arg575Asp-Asp576Arg rescues normal channel functioning, but not the lipid raft localization. The surface expression of TRPV1-Arg575Asp-Asp576Arg is much reduced as compared to TRPV1-WT but is not totally absent at the membrane.

Condition	Average amount of Ca ²⁺ -influx (in relative scale)	Average time taken to reach highest intensity upon adding ligand (in arbitrary units)	Average time taken to reach lowest intensity from highest intensity (in arbitrary units)
TRPV1-WT	100	100	100
TRPV1-Arg575Asp	7.288467725	225.343694	65.58725263
TRPV1-Arg575Asp Asp576Arg	111.654139	163.6580992	87.76664097

Figure 59: Relative properties of TRPV1-WT, TRPV1-Arg575Asp and TRPV1-Arg575Asp/Asp576Arg channels*.

*All these properties are inferred indirectly from the Ca²⁺-imaging experiments done. The values may not indicate the “absolute/actual values of individual channels”.

In fact, immunostaining for surface expressed TRPV1 (using an antibody that recognizes the extracellular loop of TRPV1) in non-permeabilized cells confirm this. Accordingly, Ca²⁺-influx experiments were executed in presence of Thapsigargin (1μM). As observed, it seemed that the capsaicin sensitivity exhibited by TRPV1-Arg575Asp-Asp576Arg is mostly mediated by their expression on intracellular organelles, mainly in ER. That is why when the intracellular Ca²⁺ stores were depleted using Thapsigargin (1 μM for 12 hours), a delayed response of TRPV1-Arg575Asp-Asp576Arg to Capsaicin (10 μM) was observed. Whereas Thapsigargin treatment did not alter Capsaicin response in case of TRPV1-WT. Thus maintenance of the ratio of positive to negatively charged amino acids at the inner LWI of TRPV1 is crucial for its activity. In this context it is worth mentioning that TRPV1 is highly permeable to Ca²⁺ and it shows Ca²⁺-dependent desensitization, which effectively allows TRPV1 channel to become insensitive to stimuli when applied repetitively (389). Notably, intracellular Ca²⁺ can interact with phosphatidylserine in physiological concentration and cause physico-chemical changes, altered hydration in the lipid-water-interface. This in turn alters lipid packing and slow down interfacial dynamics (390). Such changes might be useful for the Ca²⁺-dependent desensitization event of wild-type TRPV1. However, Arg575Ap mutant may be different in that aspect also. Thus, the importance of the ratio of positive and negatively charged

amino acids at TRPV1 LWI and their interaction with membrane cholesterol to ensure appropriate channel activity can be summarized by the following plausible model (Figure 61).

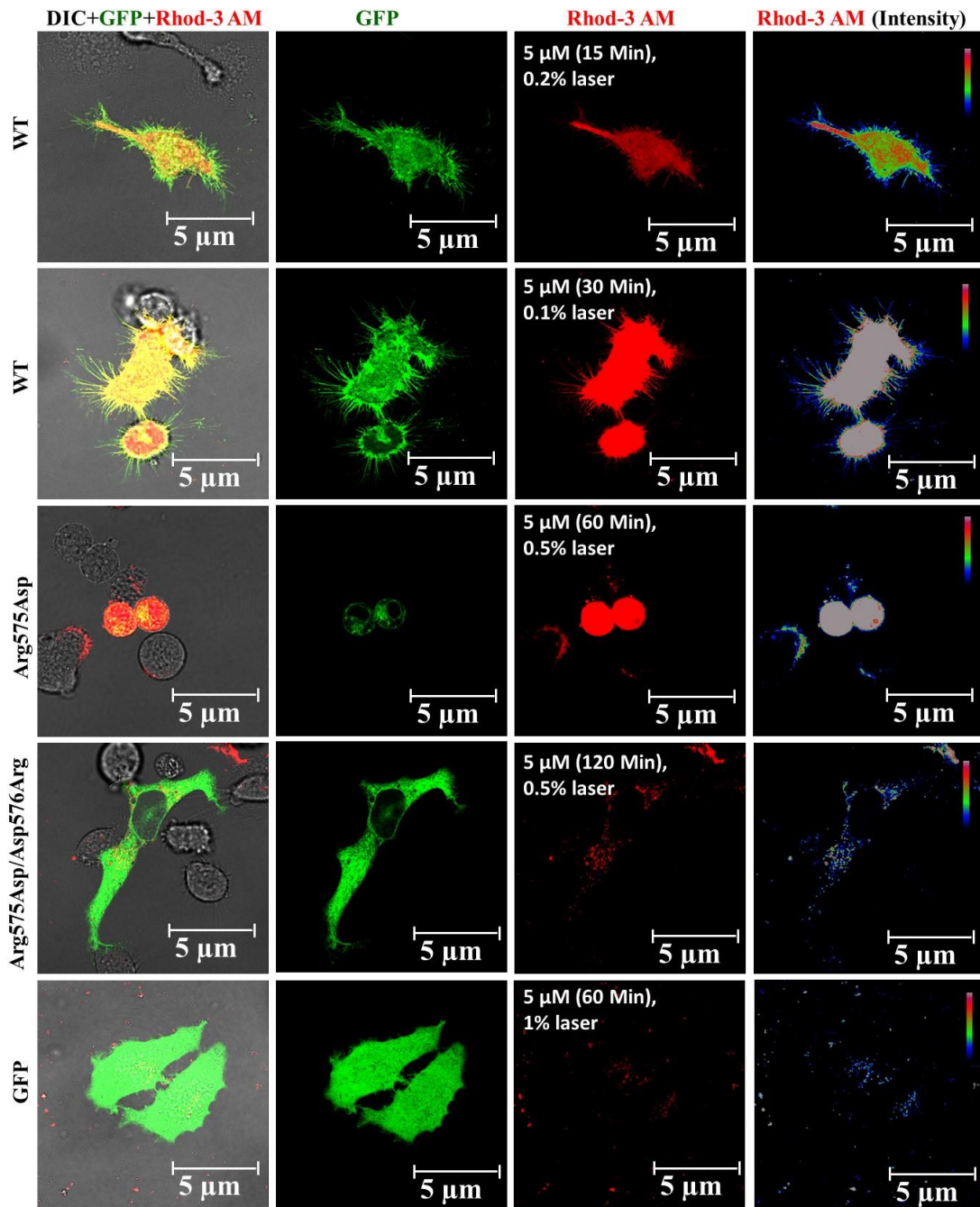


Figure 60. TRPV1-WT and TRPV1-Arg575Asp uptakes Ca^{2+} -sensor Rhod-3-AM dye in different extent. F-11 cells transiently transfected with TRPV1-WT, TRPV1-Arg575Asp, TRPV1-Arg575Asp/Asp576Arg (all in pSGFP2C1 vector) and pSGFP2C1 were incubated with 5 μM Rhod-3 AM dye for different time points (mentioned in the figure). The amount of fluorescence (red) is directly proportional to the amount of cytosolic calcium. The laser intensity required for visualization of Rhod-3 AM fluorescence varied according to the constructs with which they were transfected. TRPV1-WT was capable of rapid dye uptake even within 15 minutes of incubation and at extremely low laser intensity (0.2%), whereas TRPV1-Arg575Asp was capable of dye uptake only after 60 minutes of incubation.

TRPV1- Arg575Asp/Asp576Arg and pSGFP2C1 showed extremely low levels of dye uptake even after a longer incubation time and higher laser exposure percentage.

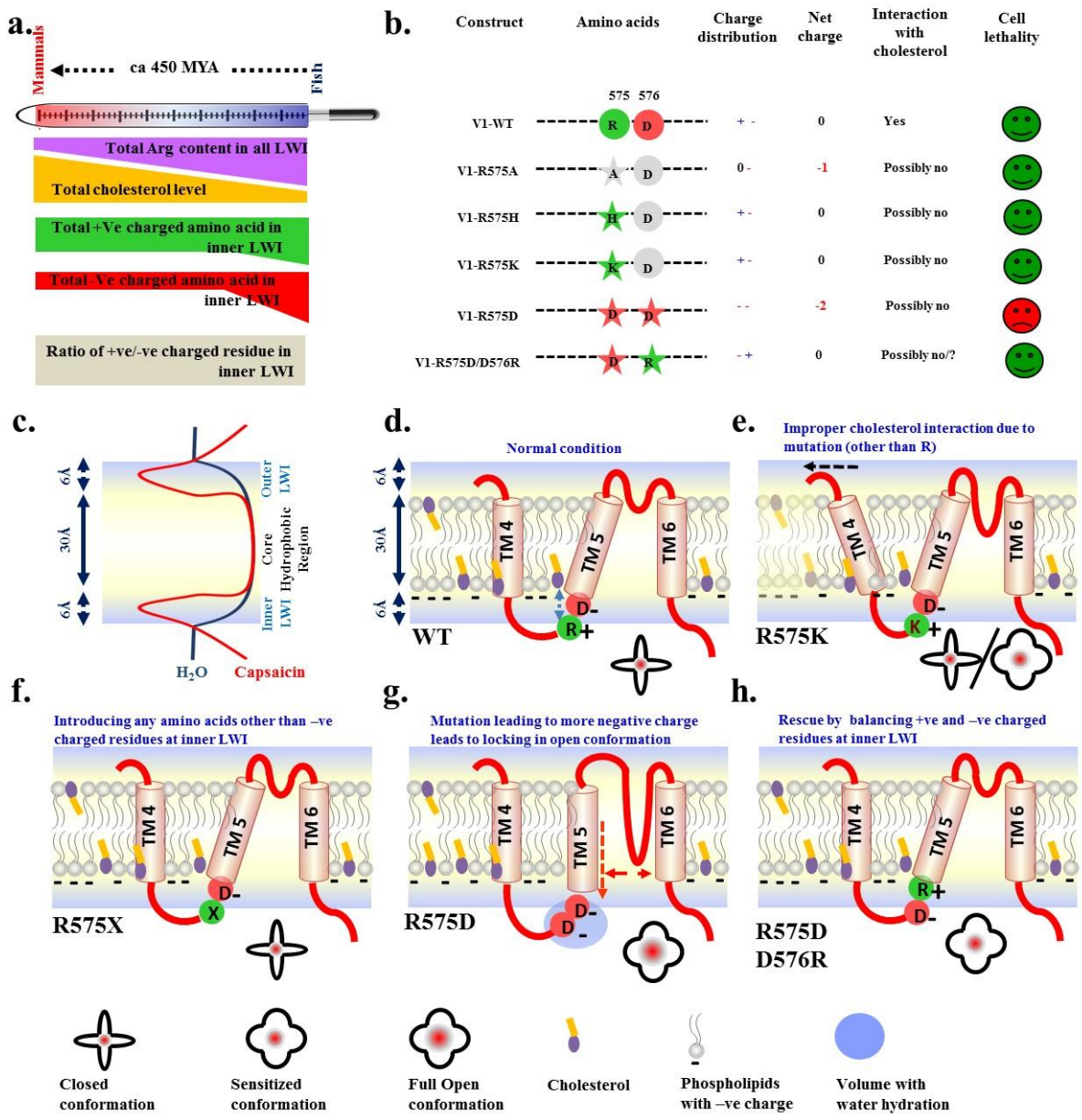


Figure 61. A plausible model depicting the importance of positive and negative charged amino acids in inner LWI region of TM5 in channel functions. **a.** During vertebrate evolution, average percentage of body cholesterol increases gradually while body temperature changed suddenly (warm-blooded animals evolved from cold-blooded animals). In spite of changes in the individual values of different amino acids, the ratio of total “positively-charged” to “total negatively-charged” residue remain constant in the inner LWI. **b.** Distribution of individual charged residues as well as net charge at the inner LWI region of TM5 for wild-type and different mutations are shown. **c.** The transmembrane helices and unstructured loops are mostly occupied in the core hydrophobic lipid bilayer (~ thickness of 30Å) and both side lipid-water interface regions (~ thickness of 6Å) respectively. **d-h.** Shown are the schematic representation of TM5-P-loop-TM6 of TRPV1 in different scenario. While R residues interact with -OH group of the cholesterol effectively, positive and negative charge at the inner LWI region of TM5 neutralize each other in order to position TM5 properly in an ideal confirmation suitable for channel gating. Alteration in negative-positive charge distribution there alters the positioning and conformation of TM5 as well as its possibility to interact with cholesterol. Introducing more negative charge in the inner LWI region of TM5 leads to “locking” of

the TM5 in a more open-like conformation and pore dilation resulting cell lethality. Introducing a positive charge next to 575th position rescue this lethality.

3.3. Regulation of TRP channels by microtubules

Microtubules form a dynamic and intricate network that is capable of shuttling vesicles containing ion channels to their destinations (391). Crosstalk between ion channels and tubulin/microtubules and its impact on each other's structure-function relationship has been a matter of extensive study from a considerable time. Cytoplasmic β -II tubulin, unassembled into microtubules, interacts with Voltage Dependent Anion Channel (VDAC) and this interaction is crucial for some bioenergetics in muscle cells. Whereas interaction of β -III tubulin with VDAC plays an important role in brain synaptosomes (392). Mitochondrial membrane is enriched with tyrosinated, acetylated and β -III tubulin but possess sparse amounts of the β -IV isotype. Mitochondrial tubulin is associated with Voltage-dependent Anion Channels (VDAC) (393). Thus each different type of tubulin exerts different functional role to the ion channel it is associated with. End-binding proteins (EB) are a class of microtubule plus end tracking proteins. There are 3 such proteins: EB1, EB2 and EB3 that are involved in regulating microtubule dynamics. Interaction of TRPM4 with EB1 and EB2 regulates its membrane trafficking and localization. Abolition of this interaction not only affected membrane localization but also diminished focal adhesion turnover, cell migration and invasion (394). NOMPC, a *Drosophila* TRP channel involved in touch and hearing sensation is regulated by microtubule acetylation in order to be gated by mechanical stimuli (395). Polycystin-2 (PC-2), a TRP-type (TRPP2) non-selective cation channel directly interacts with microtubules in human syncytiotrophoblast cells of placenta and this interaction plays an important role in the regulation of ion transport in placenta (396).

3.3.1. Importance of TRPV1-Microtubule interaction in channel functioning

In this work, the importance of TRPV1-TBS1 interaction with tubulin dimers and polymerised microtubules has been demonstrated and the impact this interaction (and also the subtle change in this interaction) has on channel functions has been studied using mutagenesis, biochemical and cell biological approaches. Biochemical analysis using only the C-terminus fragment of TRPV1 (TRPV1-Ct) showed that both WT and different point mutants in the TBS1 region were capable of retaining most of the interaction with tubulin dimers in presence or absence of 1 mM Ca^{2+} . The interaction with TRPV1-TBS1-Hexamutant is minimally reduced for some of the modified tubulins as compared to TRPV1-WT. Particularly in presence of Ca^{2+} ion, TRPV1-TBS1-Hexamutant showed a marked decrease in interaction with β -III tubulin (neuronal specific tubulin) and Tyrosinated Tubulin (marker for dynamic microtubules) with respect to WT. With acetylated tubulin, which is a marker of stable microtubules, the mutant exhibited significant reduction in interaction in presence as well as absence of Ca^{2+} . Soluble tubulin dimer and/or polymerized microtubule binding to the C-terminus of TRPV1 is observed in Ca^{2+} -free conditions also, but are more prominent in presence of Ca^{2+} . Such interaction is a “ Ca^{2+} -sensitive phenomenon” and not “exclusively Ca^{2+} -dependent” event. The C-terminus of TRPV1 interacts with tubulin (and different forms of post-translationally modified tubulins also) through two independent positions and multiple positively charged amino acids are involved in such interactions (122)(300). It was seen that most of these point mutations retained tubulin interaction, and in fact none of the mutations (that was tested so far) showed “complete loss” of tubulin interaction. In fact, there are subtle differences in the interaction (both in terms of binding extent as well as different types of tubulin) which can be very critical for channel functions. The band intensities

were quantified and normalized (considered as 100%) with control condition (Wild type in absence of Ca^{2+}).

Co-sedimentation of polymerised microtubules with TRPV1-WT and TRPV1-TBS1-Hexamutant yielded no such significant difference in presence and absence of Ca^{2+} ion. Both TRPV1-WT and TRPV1-TBS1-Hexamutant were also capable of forming high molecular weight complexes with tubulin dimers in presence of a specific chemical cross-linker, namely DMS. The mutant was only showing a meagre time lag in complex formation as compared to the WT. This retention in interaction can be explained by the presence of an intact TBS2 region in its vicinity that might be mediating the interaction between TRPV1 and tubulin/microtubule. Transient transfection of full-length TRPV1-WT-GFP and other mutants in DRG neuron derived F-11 cell line showed that in comparison to TRPV1-WT, which exhibited distinct membrane localization, TRPV1-TBS1-Hexamutant lack surface expression. However, some of the point mutants like Lys714Ala, Arg717Ala, Lys718Ala, and Lys724Ala were capable of being trafficked to the cell membrane properly. Two point mutants, namely Lys710Ala, Arg721Ala show prominent defects in surface localization. This membrane localization was conserved for both control and Taxol treated conditions (microtubule stabilized condition), but upon treatment with Nocodazole (microtubule depolymerised into soluble tubulin dimers) both TRPV1-WT and the membrane localized mutants failed to exhibit surface expression. TRPV1-TBS1-Hexamutant and the other point mutants (Lys710Ala, Arg721Ala) did not show membrane localization under control, Taxol as well Nocodazole-treated conditions. Taxol binds to the β subunit of tubulin dimers in a polymerised microtubule. There are seven different isotypes of this β tubulin and all of them differ in their C-terminal region. Out of these isotypes, increased levels of β -III tubulin renders microtubules insensitive to Taxol and thereby behaves as “Taxol resistant tubulin” population (397). Acetylated

microtubules are relatively more resistant to destabilization by Nocodazole application (398) Thus, microtubule dynamics seem to play an important role in precise localization of TRPV1 channels at the membrane and their disruption impairs their trafficking.

Status of microtubule dynamics can also be analysed by using a rat monoclonal antibody that is directed against the tyrosinated C-terminal end of α -tubulin. The monoclonal antibody YL1/2 is routinely used as a marker for newly synthesized and/or dynamic microtubules (399). Under the same conditions (control, Taxol- and Nocodazole-treated), the transfected cells were stained with YL1/2 antibody. TRPV1-WT, as well as the membrane localizing mutants Lys714Ala, Arg717Ala, Lys718Ala, and Lys724Ala exhibited an interspersed localization pattern with the dynamic microtubule population as labelled by YL1/2 under control as well as in Taxol treated conditions. However, disassembly of microtubules into tubulin dimers by Nocodazole disturbed this interspersed pattern and generated two distinct red (YL1/2) and green (TRPV1) population. The other point mutants and TRPV1-TBS1-Hexamutant demonstrated distinct areas enriched with red (representing tubulin) and green (representing TRPV1) indicating much lower probabilities for interaction under control as well as treated conditions.

While electrophysiological recordings are the best to characterize the channel properties, Ca^{2+} imaging (400)(401) with full-length Rat TRPV1-WT-pmCherryC1 and TRPV1-TBS1-Hexamutant-pmCherryC1 transiently transfected in F-11 cell line under control, Taxol and Nocodazole-treated conditions shed useful information about the importance of TRPV1-TBS1 interaction with dynamic microtubules in “Capsaicin sensitivity” i.e. ligand mediated activation of TRPV1. Quantification of average time points required by cells transfected with a particular construct and under the desired conditions (control, Taxol or Nocodazole) have shown that they have differential

responses to Ca^{2+} -influx upon Capsaicin addition. It is to be noted that all the Ca^{2+} -imaging experiments described in this work were conducted in a live cell chamber devoid of any inlet or outlet that would flush out the added drug and replenish it with fresh media. Thus the responses recorded by opening and closing of several overexpressed ion channels (both TRPV1-WT and TRPV1-TBS1-Hexamutant) under different conditions tested upon TRPV1 activation (or lack of it) by adding Capsaicin can be considered as the first step leading to “channel opening due to ligand responsiveness” and then cumulative channel functions over a reasonable long time period in a “desensitized environment” where the added drugs (Capsaicin and Taxol/Nocodazole) remained in the bath throughout the experiment. The “total area of the graph” is often considered as equivalent to “total amount of Ca^{2+} ” in arbitrary unit. The time taken to reach the maximum values after adding ligand is often taken as equivalent to the “opening probabilities”. Similarly, the time taken to reach the minimum values from the maximum value is often taken as equivalent to the “opening closing events”. The approximate values of each conditions are provided (Figure 62). These values indicate subtle changes in certain parameters and thus also sheds light on the channel properties. First, the “amount of Ca^{2+} -influx” allowed by this mutant channel upon Capsaicin activation is around 9.5 times less than TRPV1-Wt suggesting that the TRPV1-Hexa mutant has drastically low ability to respond against ligand. Next, the values also show that under control conditions, TRPV1-TBS1-Hexamutant requires almost twice as more time than that of TRPV1-WT to reach a time point of maximum response after adding Capsaicin as agonist. Third, the TRPV1-Hexa mutant also attains the time point of lowest intensity quicker as compared to TRPV1-WT.

Condition	Average amount of Ca ²⁺ -influx (In relative scale)	Average time taken to reach highest intensity upon adding ligand (In arbitrary units)	Average time taken to reach lowest intensity from highest intensity (In arbitrary units)
TRPV1-WT	100%	100	100
TRPV1-WT + Taxol	~ 126.36 %	~ 65.68	~ 106.02
TRPV1-WT + Nocodazole	~ 146.60 %	~ 120.57	~ 97.35
TRPV1-TBS1 - Hexamutant	~ 10.60 %	~ 186.67	~ 75.27
TRPV1-TBS1-Hexamutant + Taxol	~ 19.96 %	~ 165.68	~ 89.20
TRPV1-TBS1-Hexamutant + Nocodazole	~ 13.89 %	~ 178.58	~ 84.46

Figure 62. Relative properties of TRPV1 and TRPV1-Hexamutant channels*.

*All these properties are inferred indirectly from the Ca²⁺-imaging experiments done. The values may not indicate the “absolute/actual values of individual channels”.

In this case, it is important to note that TRPV1-Hexamutant does not show loss-of-tubulin interaction as it retains most of the tubulin interaction (mostly due to the intact TBS2), yet with slightly less capacity.

In case of TRPV1-WT, under Taxol-treated conditions, the average time taken to attain the point of highest intensity after ligand addition was 1.54 times faster than that of control conditions, suggesting that microtubule stabilization helps in the channel opening and/or a quick response against ligand. In the same context, the average time TRPV1-Wt expressing cells required to achieve the point of lowest intensity from the highest intensity was 1.06 times more than that of control cells, suggesting slightly delay in terms of channel closure. These differences can also be due to an “increased open probability” or “more number of open channels” facilitated by interaction with stabilized microtubule. The amount of total Ca²⁺-influx was also higher (1.26 times) as compared to control conditions. In contrast, Nocodazole-induced depolymerisation of microtubules into tubulin dimers resulted in a time lag (1.2 times more than control) to acquire the point of highest intensity after ligand addition, suggesting difficulties in channel opening in this

conditions. In the same line, under the influence of depolymerized microtubules (Nocodazole), the lowest intensity was reached from the higher intensity slightly quicker than that of control or Taxol-treated conditions, suggesting a slightly faster closure of ion channels.

Considering that though the channel opening and closing are relatively slower (in case of microtubule depolymerisation due to Nocodazole) and faster (in case of microtubule stabilization due to Taxol) conditions, the amount of total Ca^{2+} -influx is much higher in both cases, i.e. ~1.46 times more in Nocodazole treatment condition and ~1.26 times more in Taxol-treated condition than control.

Notably, in a Taxol-treated or microtubule stabilized condition, some of the cells expressing TRPV1-TBS1-Hexamutant were responsive towards Capsaicin activation and hence they were capable of attaining highest intensity at a reasonably lesser time than TRPV1-TBS1-Hexamutant under control conditions (1.12 times faster). Likewise, the amount of intracellular Ca^{2+} for TRPV1-TBS1-Hexamutant (Taxol-treated) was almost double that of TRPV1-TBS1-Hexamutant control. Even microtubule disassembly by Nocodazole was capable of triggering a higher Ca^{2+} -influx via the mutated channel upon Capsaicin activation (1.38 times more than V1-TBS1-Hexamutant control), but lesser than that of Taxol-treated conditions. However, the time point for acquisition of highest intensity is just one fold faster for TRPV1-TBS1-Hexamutant + Nocodazole in comparison to TRPV1-TBS1-Hexamutant Control. It seems that the Hexamutant requires a longer time to reach the lowest intensity point in presence of Nocodazole and an even longer time in presence of Taxol.

The above recordings show that under all conditions, TRPV1-TBS1-Hexamutant is several magnitudes less sensitive to Capsaicin activation as compared to TRPV1-WT. Microtubule stabilization and destabilization enables this mutant to be subtly sensitive to

Capsaicin application and henceforth a sparse Ca^{2+} -influx. However, it is possible that stabilization of microtubules increases the “open probability” of TRPV1-WT channels whereas destabilization of microtubules allows for “delayed opening” and “quicker closing”. This in general suggest that change in microtubule dynamics can modulate the intracellular Ca^{2+} -signalling via TRPV1, a concept that matches well with observed pain scores in animal models as well as Taxol-induced neuropathic pain conditions in patients.

Thus, it seems that under all circumstances, it is the dynamic behaviour of tubulin/microtubules that ensures a proper channel functioning when interacting with TRPV1-TBS1. The positively charged residues in TBS1 are crucial for mediating TRPV1-Tublin/MT interaction. Abrogation of this interaction probably renders the channel Capsaicin insensitive resulting in lack of Ca^{2+} -influx.

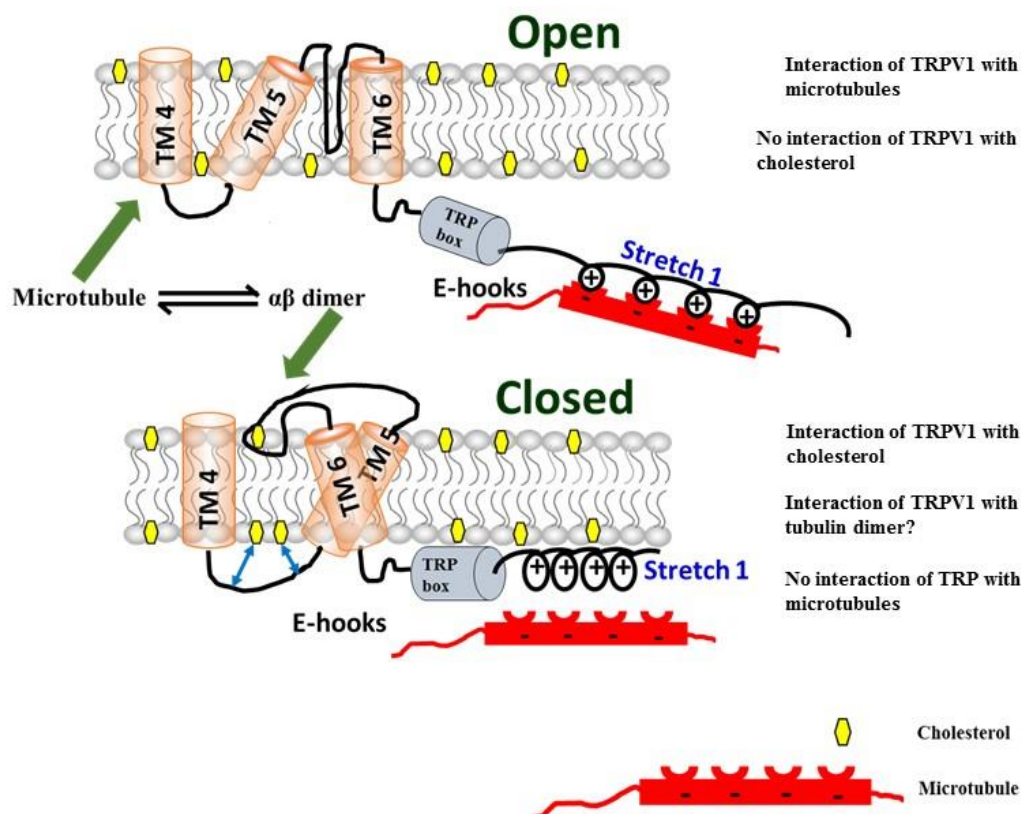


Figure 63. A tentative model: TRPV1 channel gating in response to tubulin, microtubule and cholesterol. The open conformation of TRPV1 is possibly triggered when the channel interacts with microtubules and not with cholesterol. Whereas interaction with cholesterol prevents spontaneous opening of the channel and also its loss of interaction with microtubules tends to keep the channel in a closed conformation. However, the role of tubulin dimers on TRPV1 gating mechanism needs further validation.

Microtubule stabilization might induce a conformational change that enables this mutant channel for transient Ca^{2+} -fluxes. Hence it can be inferred that the tubulin interaction is not only important for the TRPV1 channels' membrane localization but also serves as a regulator for channel activity. This is similar to other channels and receptors such as NMDA (N-methyl-D-aspartate) receptors also require microtubule integrity for their normal functionality. Microtubule depolymerisation significantly suppresses NMDAR mediated currents (402). Combined disruption of microtubules and microfilaments in Rat cerebellum granule cells impaired the subcellular localization as well as function of GABAA receptors (403). Microtubule disruption by Nocodazole or Colchicine improves the β -adrenoceptor-mediated relaxation of renal and mesenteric arteries by increased expression of membranous Kv7 voltage gated potassium channels (404).

Thus, the effect of tubulin dimers, microtubules and cholesterol on TRPV1 channel functioning (as observed in this study) has been summarised in this model ([Figure 63](#)).

3.4. Molecular evolution of TRPA1

The sperm physiology is tightly controlled by a set of ion channels. Given the fact that sperm cells are terminally differentiated, and have suppressed transcription and translation, the pool of ion channels present in mature sperm is expected to remain same as that obtained during final stages of sperm development. So far only few ion channels have been studied in sperm and majority of the ion channels present in the mature sperm cells and their respective functions remain undiscovered. The endogenous presence of temperature-sensitive ion channel TRPV1 in fish sperm, TRPV4 in different vertebrate and cold-sensitive ion channel TRPM8 in different vertebrates sperm cells have been previously reported (405)(406)(407). TRPV4 expression was found to be miss-localized

in immotile human sperm implicating that TRPV4 could be important for motility of the sperm in female reproductive tract. Consistent with this observation, TRPV4 has been recently shown to mediate the initial phase of membrane depolarization that is essential to initiate sperm hyper-activation (290). Activation of the cold-sensitive channel TRPM8 leads to decrease in sperm motility (405). However so far endogenous expression of TRPA1 hasn't been reported in the spermatozoa of any species, hence its functional significance has remained largely unexplored.

The *in silico* analysis indicate that TRPA1 is present as a single copy gene in most species with its origin dating back to around 900 MYA. This period coincides with the time when invertebrates started evolving and molecular machineries involving sexual reproduction started evolving through changes and subsequent natural selection process. Male gametes do not have transcriptional and translational machinery and have a predefined set of proteins that are critical for sperm functions. Therefore, expression and function of certain ion channels and other critical proteins in male gametes often correlates well with the survival and subsequent conservation or evolution of the species. Hence it is likely that TRPA1 had and still has relevance in reproduction since a long time. Notably, in Zebra fish (and possibly in some other fishes also), TRPA1 is present in two copies and both the TRPA1 homologs share 59.4% identity and 75.2 % similarity. It is noteworthy to mention that Zebra fish has lost several genes including TRPM8 (another TRP channel that respond to low temperature) due to its genome compaction (301). However, at the protein level, TRPA1 is not a conserved protein and its high-level of divergence actually indicates that TRPA1 probably is involved in processes that are conserved as a fundamental process (such as immunity, spermatogenesis, sperm motility, fertilization, sensory functions, etc. that need interaction with uncertain environmental factors) but have gone through molecular selection through diverged mechanisms. In this

context, the high-variability of extracellular loops of TRPA1, which is exposed to the outside and are in contact with the extracellular environments (at least for sperm cells) is an indicative of TRPA1 function. It strongly suggests that such exposed regions have changed rapidly in different species, possibly in order to cope up with the variable environments like exposure to environmental pollutants and irritants, ROS, electrophiles, reactive sulphur based molecules, etc. It is noteworthy to mention that such changes are critical for the species to survive and evolve further.

The conservation pattern of same genes including TRPA1 from fishes to mammals reveals that these gene products may be involved in similar functions at protein levels and have common functional relevance. Useful information can be derived from such strong linkages which retains these genes in same DNA locus for more than 400 million years. For example, TRAM1 (Translocating chain associating Membrane protein) is a mammalian ER resident transmembrane protein and is a component of the translocon. It can mediate the lateral movement of selected signal peptides and transmembrane segments from the translocon into the membrane bilayer (408) . This protein gets upregulated during ER stress and efficiently dislocates the ER- resident membrane proteins destined for degradation to the cytosol (409). Considering sperm cell is an ER-free system, TRAM1 and TRPA1 may share complex relationship. Similarly, LACTB2 (β -Lactamase-like protein 2) is a mitochondrial protein, at least in mammals. In humans it plays an important role in regulating mitochondrial functions and acts as an endoribonuclease that is involved in the turnover of mitochondrial RNA (410). As TRPA1 is located near mitochondrial region (at least in sperm cell), LACTB2 and TRPA1 may share similar functions. In addition, β -lactamase translocation is TRAM dependent suggesting that this genomic locus is actually involved in similar functions (411). The EYA1 gene present in humans is an orthologue of the eyes absent (*eya*) gene present in

Drosophila (412). Mutations in human EYA1 lead to BOR/BO syndrome, which mainly affects ear development (413). Mammalian inner ear hair cell development is also regulated by EYA1(414). Close proximity with EYA1 may suggest that TRPA1 is involved in sensory functions in such organs. Musculin (MSC) is a helix-loop-helix transcription factor whose expression was first reported in mouse embryonic skeletal muscle cells(415). This transcription factor promotes the development of induced Treg cells by silencing the TH2 developmental program (416). Considering the endogenous expression of TRPA1 in T cells and its involvement in T cell functions, close association of these two genes are extremely relevant for adaptation and evolution (266)(417)(240). Voltage-gated potassium channel, Shab related subfamily, member 2 (KCNB2) or Kv2.2 is a member of the voltage gated potassium channels and is related to the shab channels in *Drosophila* (418). It is a delayed rectifier that plays an important role in maintaining the membrane potential of myocytes (419). Sudden Cardiac Death (SCD) has been correlated with mutations in KCNB2 gene (420). In this context also, TRPA1 might be relevant in such tissues and functions. Sudden cardiac Repeat Binding Factor 1 (TERF1) is a protein that maintains and protects chromosome ends. A splice variant of TERF1 is abundantly and exclusively expressed in human testes. This splice variant with an extra 90 bp sequence might have a role in spermatogenesis, since telomeres execute special functions during meiosis (421). Eukaryotic RPL7 is a protein associated with the large subunit (60S) of ribosome (422). It is involved in translational regulation and interferes with the translation of proteins involved in cell cycle progression and/or initiation of apoptosis (423). In mammalian embryos and oocytes, RPL7 protein distribution was seen mostly throughout the cytoplasm with maximum intensity in oocyte nucleus as compared to nucleus of embryo (424). RDH10 (retinol dehydrogenase class 10) is a transmembrane protein and first cloned from bovine, mouse and human RPE (Retinal Pigment

Epithelium) belongs to a family of short-chain dehydrogenases/reductases (SDRs). The primary structure of RDH10 is highly conserved among different species across evolution (425). In mouse, RDH10 is indispensable for craniofacial, organ and limb development. During embryogenesis, its activity is necessary to mediate the first step of Vitamin A metabolism (426).

3.5. Chemical sensitivity of TRPA1

Temperature threshold for TRPA1 activation is highly variable across different vertebrates and invertebrates. However, unlike TRPV1 its chemical sensitivity to electrophilic compounds such as cinnamaldehyde and AITC are well conserved. Therefore; the physiological role of TRPA1 in detecting irritating chemicals seems to be well conserved across evolution. Nevertheless, ability of TRPA1 to detect non-electrophilic compounds displayed species specific difference. A-967079 acts as a TRPA1 specific blocker for mammalian TRPA1 but it acts as an agonist in chicken and tropical clawed frogs. L881 in TM5 of Human TRPA1 and an Isoleucine corresponding to this position in the other two species brings about this striking feature (427).

3.6. TRPA1 channel gating

There are several disputes regarding thermosensitivity of TRPA1. It was also reported that primate TRPA1 acts as a warm sensor whereas rodent TRPA1 functions as a sensor for noxious cold temperatures. Apparently, Val875 residue in primate TRPA1, corresponding to Gly878 in rodent TRPA1 was the single amino acid in the S5 region that was responsible for such discrepancy. Gly878Val change in mouse and rat TRPA1 abolished its cold sensitivity (428). However, a recent finding demonstrated that cold sensitivity of both mouse and human TRPA1 is triggered only after they have been

simultaneously exposed to noxiously warm temperatures and depolarizing voltage (429). TRPA1 is the only ion channel that can respond to both hot and cold temperature. Such bi-directionality in temperature gating was explained recently. According to this theory, opening of the channel induces a conformational change that causes transfer of specific residues between aqueous and hydrophobic environments, which leads to alterations in the heat capacity of the channel protein complex (430). The inner cavity formed by the lower part of the S1-S4 sensor domain encompassing the TRP-like domain, pre-S1 helix, S4-S5 linker contain critical amino acid residues that play an important role in channel gating. This is the region where activation signals are integrated and conveyed via the TRP-like domain to the channel gate. The charged residues lining this crevice are not only important for the channel's sensitivity towards voltage, electrophiles and Ca^{2+} but is also important for PIP_2 binding (431). The S1-S2 linker present on the extracellular side of TRPA1 plays an important role in voltage dependent gating of this channel. Critical residues lying in this region are also responsible for proper insertion of the channel in the lipid bilayer (432).

3.7. Role of TRPA1 in sperm functions and impact on reproductive fitness

Indeed, sperm membranes have detectable levels of TRPA1 (even in invertebrate sperm, [Figure 64](#)). The abundance of TRPA1 at the tail of fish, amphibian, avian and mammalian (bull) sperm indicated that TRPA1 might have a role in sperm motility, at least in flagellar beat regulation. Therefore; the motility parameters of freshly ejaculated bull sperm using CASA system was evaluated. Neither TRPA1 activation, nor its inhibition with specific agonist like AITC and specific inhibitor A967079 (both in 3 different log fold doses) had any significant effect on the “average values” on several

motility parameters. For example, neither TRPA1 activation nor inhibition alters average values for % of motile sperm, % of progressive sperm, % of rapid moving cells, % of slow moving cells, % of medium moving cells or % of static cells. Interestingly we observed decrease BCF, and increase VCL as well as ALH upon TRPA1 activation by AITC at 100 μ M concentration. These 3 parameters indicate that optimal activation of TRPA1 by natural agonists is itself sufficient to hyper-activate sperm cells, at least in case of bovine sperm. Hyperactivation is a part of the lengthy process of capacitation, which is marked by increase in global phosphotyrosination of sperm proteins (433). Neither TRPA1 activation, nor inhibition by pharmacological modulators is efficient in altering phosphotyrosination in bull sperm. This indicates that as such TRPA1 modulation doesn't drastically affect the kinases responsible for Tyrosine phosphorylation of sperm proteins. TRPA1 inhibition is not able to block heparin-induced phosphotyrosination, but is able to marginally reduce progesterone-induced phosphotyrosination. TRPA1 activation leads to nearly 10% increase in sperm cells that lose acrosome within 1 hour, while

TRPA1 inhibition fails to affect this process alone. TRPA1 inhibition isn't able to affect heparin induced in acrosomal reaction drastically, while TRPA1 inhibition is able to marginally decrease number of acrosome reacted sperm in Progesterone-treated sample. Phosphotyrosination and acrosome reaction data indicate that TRPA1 may not be relevant in these pathways triggered by Heparin, but it may be relevant in Progesterone-mediated capacitation and acrosome reaction. Further signalling studies will clarify the details of the mechanisms involved in this process.

Endogenous expression of TRPA1 in sperm cells is conserved in all vertebrates. On the other hand, neither TRPA1 activation nor inhibition altered the "average values" in most of the motility parameters. These contradictory aspects allowed us to explore if TRPA1 activation or inhibition can induce variability in sperm motility parameters. The

more variability in sperm parameters ensures better survival and other functions of a population, especially in unpredictable hostile environments. Indeed, the variability in certain motility parameters often fits well with a trend for dose-responsiveness, confirming that TRPA1 is able to induce “variations” in sperm motility parameters when compared to control condition. Therefore, triggering variability in sperm cell parameters due to TRPA1 modulation might have specific roles that can actually provide better reproductive fitness and thus adaptive benefits.

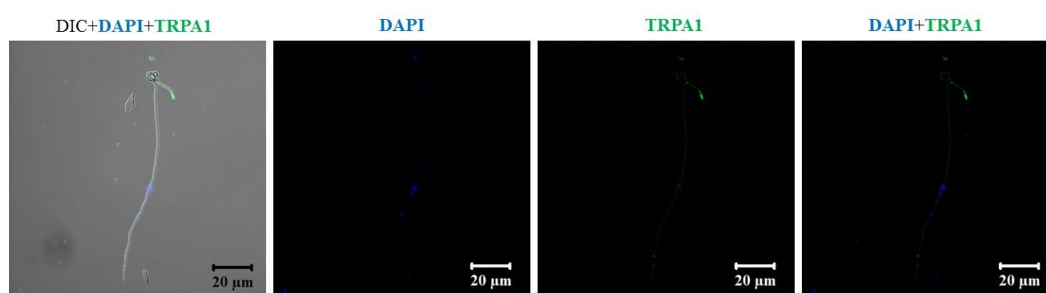


Figure 64. Endogenous expression of TRPA1 in butterfly sperm cells. Confocal image of Butterfly sperm cell stained with Anti-TRPA1 (extracellular loop) antibody (green) and DAPI (blue). Experiment performed and imaged by Dr. Rakesh Kumar Majhi.

3.8. Regulation of TRPA1 by tubulin/microtubules

The C-terminal fragment of Human TRPA1 is capable of interacting with tubulin dimers in presence as well as absence of Ca^{2+} , as observed biochemically from pull down experiments with various tubulin and modified tubulin antibodies (Figure 65). Thus, it was intriguing to explore its expression and function in vertebrate sperm cells.

Vertebrate sperm membranes have detectable levels of TRPA1. The significant expression of TRPA1 at the tail of fish, amphibian, avian and mammalian (bull) sperm indicated that TRPA1 might have a role in sperm motility, at least in the regulation of its flagellar beating pattern. Spermatogenesis or the formation of a structurally and functionally different sperm cell from primordial germ cells, is an excellent example of

cytoskeletal rearrangement modulating a developmental process. Tubulin dimers are subjected to various post-translational modifications like tyrosination, detyrosination, glutamylation, glycylation. These modifications may attribute different functions in microtubule structures, stability and properties. Male germ cells exhibit differential expression of modified tubulin which reflects the diversity in functions of the microtubules present in them (434). The flagellar beating of sperm tail is aided by the surge of Ca^{2+} -waves as well as by the activity of motor proteins that are regulated by microtubule cytoskeleton (435). Thus, bull sperm samples (control, AITC and A96 treated) were stained for both TRPA1 and various modified tubulin (tyrosinated, detyrosinated, polyglutamylated, polglycylation and acetylated). Tyrosinated tubulin showed co-localization with that of TRPA1 in the tail region indicating a plausible role in sperm motility. Taken together, these data present TRPA1 as a candidate ion channel that is expressed in all vertebrate sperm and have importance in regulation of sperm motility possibly by interacting and/or regulating with the axonemal microtubules. TRPA1 seems to induce more variability in motility parameters and thus can be critical for reproductive fitness of the species.

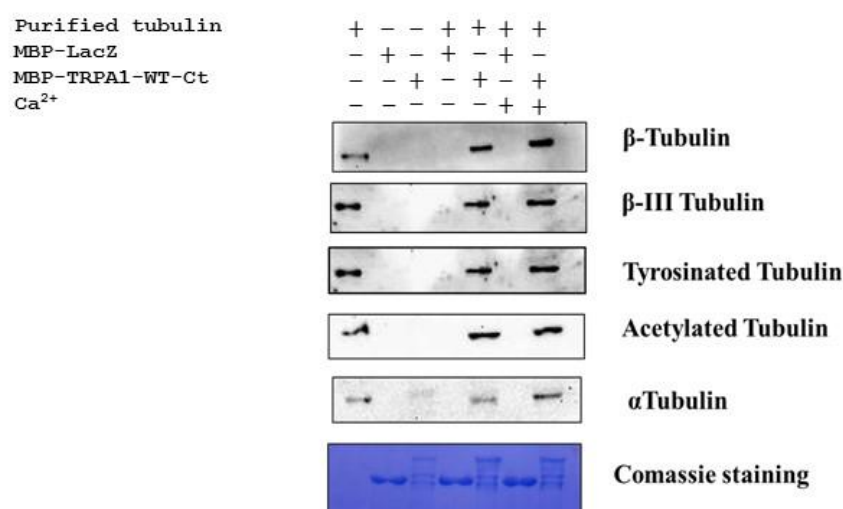


Figure 65. Human TRPA1-Ct interacts with various modified tubulin. The C-terminal fragment of Human TRPA1 (TRPA1-Ct) interacts with tubulin dimers in presence and absence of Ca^{2+} . Figure taken from Subhadra Majhi's M.Sc dissertation thesis work (NISER).

Such aspects may have huge impact on the selection as well molecular evolution of TRPA1 in vertebrates.

3.9. TRPA1-cholesterol crosstalk: implication in biological systems

TRPA1 is one of the most primitive TRP channels whose expression and function can be found in invertebrates also. For example, in *C. elegans* it functions as a warm sensor, in insects such as mosquito and honeybee it functions as warm sensor. There are 4 different TRP homolog splice variants in *Drosophila*, out of which some are heat sensitive and some are heat insensitive. It is also found in planarians where it acts as sensor for ROS (436). Interestingly, molecular origin of TRPA1 dates back even before the insertion of cholesterol in lipid bilayers. LWI regions are occupied by snorkelling amino acids i.e. amino acids having a flexible side chain that can stretch to keep the more hydrophilic part of its side chain at the more hydrophilic LWI interface and the hydrophobic hydrocarbon part within the lipid bilayer. Presence of such amino acids enable interaction with various membranous and sub-membranous components, ligands, agonists, antagonists that regulate channel gating. Lack of conservation of different amino acids at the LWI arises a speculation that such diversity might be an outcome of its ever-changing structure in order to comply with the desired functions. The inner LWI regions have a higher rate of conservation in terms of occurrence of certain amino acids throughout vertebrate evolution in comparison to outer LWI. A plausible explanation for this difference in distribution of amino acids in the outer and inner LWI might be a difference in lipid bilayer composition on either leaflets. Moreover, the residues on the inner leaflet are more prone to modifications by various enzymes, intracellular signalling molecules, etc. Identification of 14 CRAC and 6 CARC motifs indicate a probability of TRPA1's interaction with cholesterol. Global and local docking of Human TRPA1 with

cholesterol has resulted in identification of two residues Arg 852 and Asn 855 that can mediate interaction of TRPA1 with cholesterol. Recently it was seen that mouse TRPA1 co-localizes with lipid raft marker, namely with Cholera Toxin B in HEK293T cells. TRPA1 directly interacts with cholesterol via CRAC domains present in S2 and S4 segments (264). This is in accordance with the results obtained here which also shows that under endogenous as well as overexpression conditions, Human TRPA1-GFP co-localizes with lipid raft markers like Cholera-Toxin B, Flotillin-1-RFP and Caveolin-1-RFP in DRG neuron derived F-11 cells.

3.10. TRPA1, its mutants, genetic variants and diseases

Familial Episodic Pain Syndrome (FEPS) is an autosomal dominant syndrome caused by a gain-of-function mutation Asn855Ser in the S4-S5 linker region of Human TRPA1. This syndrome is characterised by episodes of severe pain particularly in the upper body region triggered by conditions of fasting, fatigue and cold (437). This mutation causes enhanced activity in response to TRPA1 specific activators and alters the gating behaviour of the channel to a Ca²⁺-independent mechanism. This is the first pain related TRP channelopathy that was reported in humans (437). The Arg852 residue lying in the loop region connecting S4 and S5 helix of TRPA1 is a highly conserved residue among all vertebrate TRPA1 is a crucial amino acid involved in transduction of chemical and voltage stimuli of TRPA1 and is involved in Ca²⁺ regulation of the channel. Its mutation Arg852Glu has not yet been associated with any channelopathy, but it is a gain-of-function mutation that is known to induce spontaneous channel opening and increased basal channel activity (438).

Thus, evolution of TRPV1 is relatively new when compared to TRPA1, whose orthologues have been traced in lower invertebrates as well, mostly as pseudogenes and

orphan genes. Thus, it seems that in ancestral vertebrates, heat sensitive TRPV1 emerged more recently and started co-expressing with the already existing TRPA1 in a subset of nociceptive neurons (317). A plausible phylogenetic tree of their evolution has been depicted (Figure 66).

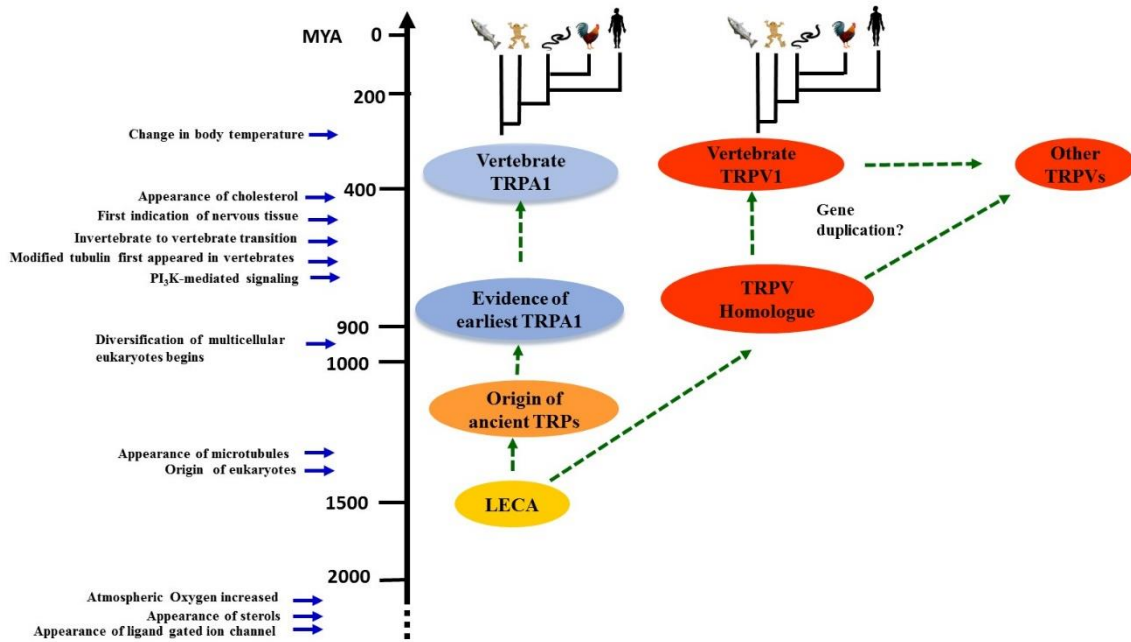


Figure 66. Possible molecular evolution of TRPV1 and TRPA1.

	TRPV1	TRPA1
Origin	~400 MYA	~900 MYA
Conservation	Fairly conserved	Highly diverged
Temperature-sensing ability	Noxious warm sensor	Species specific (Hot & cold)
Thermogating	Yes	Yes/debatable
Expression in nervous system		
a) Vertebrates	Yes	Yes
b) Invertebrates	Only functional homologues	Yes
Expression in reproductive system		
a) Vertebrates	Yes	Yes
b) Invertebrates	Not known	Yes
Expression in immune system		
a) Vertebrates	Yes	Yes
b) Invertebrates	Not known	Not known
LWI residues (total)		
a) hydrophobic amino acids	Not conserved	Not conserved
b) hydrophilic amino acids	Not conserved	Not conserved
c) ratio of hydrophobic: hydrophilic amino acids	Conserved	Not conserved
a) positively charged amino acids	Not conserved	Not conserved
b) negatively charged amino acids	Not conserved	Not conserved
c) ratio of positive: negatively charged amino acids	Not conserved	Not conserved
Cholesterol-interacting motifs	Present, fairly conserved	Present in vertebrate, but largely diverged
Tubulin/MT interaction	Yes	Yes
Cholesterol-mediated channel gating	Yes	Needs further study
Tubulin/MT-mediated channel gating	Yes	Needs further study

Table 4. Comparative analysis of TRPV1 and TRPA1 from this study

Chapter 4

Conclusion

Future prospects and conclusion

Thus from this study, cholesterol and tubulin/microtubules emerge to be important regulators of TRPV1 and TRPA1 channel gating. Critical residues lining the LWI regions of these channels' play an important role in mediating their interaction with membranous components. In higher animals, both TRPA1 and TRPV1 are expressed in nociceptive sensory neurons that are involved in pain transduction. Several agonists and antagonists of these channels have been tested in clinical trials for pain management. However, none of them has reached level 3 of these trials. Understanding the regulators and gating mechanisms of these channels will enable specific targeting of these channels to alleviate pain. Modulation of these TRP channels by cholesterol and microtubules provides a novel angle to drug discovery. In human population, a large number of TRP channel variants are present. These variants can shed important information on the thermal-sensitivity of different ethnic groups and also to other physiological processes and information about likelihood to have certain diseases.

The experimental system used here (Calcium imaging in a chamber slide) does not allow to explicitly talk on "channel gating" as such in milli-second time frame or faster, though the results primarily suggest more probability of channel opening and enhanced channel function, especially in case of certain mutants or vice versa. The experiments done in this study has been mostly restricted to a specific activator and inhibitor for both the channels. Hence, in order to have a conclusive idea about their gating mechanism, other chemical ligands and toxins need to be tested. In case of TRPV1, the effect of mutating TBS2 still remains to be investigated. The mechanism by which TRPA1-microtubule interaction modulates various cellular function is still sparsely clear. Role of cholesterol in mediating TRPA1 channel gating needs to be explored in further details. Ca²⁺-imaging has provided a comprehensive knowledge about the total cellular

behaviour, but the activity of individual channels could not be recorded. Electrophysiology experiments will enable analysis at the level of individual channels, whereby the conclusions can be more accurate.

Chapter 5

Materials and Methods

5.1. Materials

5.1.1. Reagents used

Chemical Used	Source
5'-IRTX	Tocris
A967079	Sigma-Aldrich
Acrylamide	Sigma-Aldrich
Adenosine-5'-Triphosphate Disodium Salt Trihydrate	MP Biomedicals
Agar agar, Type I	Himedia
Agarose	Lonza
AITC (Allyl isothiocyanate)	Sigma-Aldrich
Ammonium Persulphate	Sigma-Aldrich
Amphotericin B	MP Biomedicals
Ampicillin	Sigma-Aldrich
Amylose Resin Beads	NEB
Antibiotic Solution	Himedia
Bovine Serum Albumin	MP Biomedicals
Bradford Reagent	Sigma-Aldrich
Bromophenol Blue	Sigma-Aldrich
Calcium Chloride Dihydrate	Sigma-Aldrich
Capsaicin	Sigma-Aldrich
Cholera Toxin B-594	Invitrogen
Complete Protease Inhibitor Cocktail	Sigma-Aldrich
Coomassie Brilliant Blue G250	MP Biomedicals
Coverslips (12 mm and 18 mm)	Fisher Scientific
Coverslips (25 mm)	Himedia
DAPI	Invitrogen
Dimethyl Sulfoxide (DMSO)	Invitrogen and MP biomedical
Disodium hydrogen phosphate	MP Biomedicals
DMS (dimethyl suberimidate)	Thermo Scientific
dNTP's	NEB
EDTA	Sigma-Aldrich
EGTA	Sigma-Aldrich
Ethanol (Molecular Grade)	Merck Millipore
Ethidium bromide	Sigma-Aldrich
F-12 Ham's Media	Himedia
Fetal Bovine Serum(Australian Origin)	Himedia
FITC-PNA	Sigma
Fluoromount-G	Southern Biotech
Glacial Acetic Acid	MP Biomedicals
Glucose	MP Biomedicals
Glycerol	Sigma-Aldrich
Glycine	MP Biomedicals

GTP powder	MP Biomedicals
Heparin	Sigma
HEPES	MP Biomedicals
Hydrochloric Acid	Rankem
Kanamycin	Sigma-Aldrich
Lactic Acid	Himedia
L-Glutamine	Himedia
Lipofectamine	Invitrogen
Lysozyme	Amresco
Magnesium Chloride	MP Biomedicals
Maltose	Sigma-Aldrich
Manganese Chloride	Biocore LifeSciences
Methanol	MP Biomedicals
Methyl β -Cyclodextrin	Sigma-Aldrich
MOPS(3-(N-Morpholino)propanesulfonic acid)	Fluka
N,N'-Methylenebis(acrylamide)	Sigma-Aldrich
Nocodazole	Sigma
Phenylmethylsulfonyl fluoride	Sigma-Aldrich
Phosphate Buffer Saline (10X)	Himedia
PIPES	MP Biomedicals
Potassium Acetate	MP Biomedicals
Potassium Chloride	MP Biomedicals
Potassium Hydroxide	MP Biomedicals
Progesterone	Sigma
Rubidium Chloride	MP Biomedicals
Skimmed Milk Powder	Himedia
Sodium Bicarbonate	Sigma-Aldrich
Sodium Chloride	MP Biomedicals
Sodium Dodecyl Sulphate	MP Biomedicals
Sodium Hydroxide	MP Biomedicals
Sodium Pyruvate	Sigma-Aldrich
Sucrose	Sigma-Aldrich
Taxol	Sigma-Aldrich
TEMED (Tetramethylethylenediamine)	Sigma-Aldrich
Thapsigargin	Sigma-Aldrich
Triethanolamine	Himedia
Tris	MP Biomedicals
Triton X-100	Sigma-Aldrich
Trpytone	Himedia
Tween-20	Sigma-Aldrich
Yeast Extract	Himedia
β -Mercaptoethanol	Biocore Lifesciences

5.1.2. Kits, markers and enzymes

Kit name	Source
QIAprep Spin Miniprep Kit	Qiagen
QIAquick Gel Extraction Kit	Qiagen
Gel Extraction Kit	Qiagen
QuikChange Site-Directed Mutagenesis Kit	Agilent Technologies
PageRuler™ Plus Prestained Protein Ladder	Thermo Scientific
1 kb DNA ladder	Biosphere Corp.
100 bp DNA ladder	Biosphere Corp.
Q5 DNA Polymerase	NEB
EcoRI-HF	NEB
Sall-HF	NEB
T4-DNA Ligase	NEB

5.1.3. Cell lines and sperm samples used

Cell lines and primary cells	Source	IAEC number
F-11	Prof. F. Hucho (FU, Berlin)	
SaoS-2	Prof. F. Hucho (FU, Berlin)	
HaCaT	Prof. F. Hucho (FU, Berlin)	
Bovine sperm	FSB, Cuttack and Dr. Apratim Maity, West Bengal University of Animal & Fishery Sciences	NISER-IAEC/SBS-AH/07/13/10
Fish sperm	CIFA, Bhubaneswar	NISER-IAEC/SBS-AH/07/13/10
Avian sperm	CARI, Bhubaneswar	NISER-IAEC/SBS-AH/07/13/10
Amphibian sperm	NISER, Bhubaneswar	NISER-IAEC/SBS-AH/07/13/10
Reptile sperm	Dr. Apratim Maity, West Bengal University of Animal & Fishery Sciences	NISER-IAEC/SBS-AH/07/13/10

5.1.4. Bacterial strains

Strain name	Source
DH5 α	CG lab, NISER
DE3	CG lab, NISER

5.1.5. Primary Antibodies

Antibody	Host	Source	Application	Dilution
α -Tubulin	Mouse	Invitrogen	WB, IF	1:500
β -Tubulin	Mouse	Sigma	WB, IF	1:500
β -III-Tubulin	Mouse	Sigma	WB, IF	1:500
Acetylated Tubulin	Mouse	Sigma	WB, IF	1:500
Polyglutamylated Tubulin	Mouse	Sigma	WB, IF	1:500
Tyrosinated Tubulin	Mouse	Sigma	WB, IF	1:500
Detyrosinated Tubulin	Mouse	Sigma	WB, IF	1:500
Polyglycylated Tubulin	Mouse	Merck Millipore	WB, IF	1:500
YL1/2	Rat	Abcam	IF	1:500
TRPA1- Extracellular loop	Rabbit	Alomone	IF	1:300
TRPV1-Ct	Rabbit	Alomone	WB	1:300
MBP	Mouse	NEB	WB	1:30,000
Phosphotyrosine antibody (PY20)	Mouse	Abcam	WB	1:500
TRPV1- Extracellular- ATTO-488	Rat	Alomone	IF	1:100

5.1.6. Secondary Antibodies

Antibody	Host	Source	Application	Dilution
Alexa-488-labelled anti-rabbit	Chicken	Molecular Probes	IF	1:1000

Alexa-594-labelled anti-rat	Chicken	Molecular Probes	IF	1:1000
Alexa-594-labelled anti-mouse	Chicken	Molecular Probes	IF	1:1000
HRP labelled anti-mouse	Donkey	GE Healthcare	WB	1:10,000
HRP labelled anti-rabbit	Donkey	GE Healthcare	WB	1:10,000

5.1.7. Constructs used

Vector	Expression system	Source
pGP-CMV-GCaMP6f	Mammalian	Addgene
pSGFP2-C1	Mammalian	Addgene
pmCherry-C1	Mammalian	Takara
Flotillin-1-RFP	Mammalian	Dr. Bao-Liang Song, Wuhan University
Caveolin-1-RFP	Mammalian	Addgene
Rat TRPV1-WT-FL-pBF1	Xenopus	Dr. Soenke Cordeiro, Institute Of Physiology, Christian-Albrechts-Universität zu Kiel
Human TRPA1-pMO	Mammalian	Dr. David Julius, University Of California, San Francisco
pDsRed2-Bid	Mammalian	Clontech
MBP-TRPV1-WT-Ct	Bacterial	Dr. Chandan Goswami
MBP-TRPV1-K710A-Ct	Bacterial	Prepared in CG lab
MBP-TRPV1-K714A-Ct	Bacterial	Prepared in CG lab
MBP-TRPV1-R717A-Ct	Bacterial	Prepared in CG lab
MBP-TRPV1-K718A-Ct	Bacterial	Prepared in CG lab
MBP-TRPV1-R721A-Ct	Bacterial	Prepared in CG lab
MBP-TRPV1-K724A-Ct	Bacterial	Prepared in CG lab

MBP-TRPV1-TBS1-Hexamutant-Ct	Bacterial	Prepared in CG lab
TRPV1-FL-WT-pSGFP2C1	Mammalian	Prepared in CG lab
TRPV1-FL-WT-pmCherryC1	Mammalian	Prepared in CG lab
TRPV1-FL-K710A-pSGFP2C1	Mammalian	Prepared in CG lab
TRPV1-FL-K714A-pSGFP2C1	Mammalian	Prepared in CG lab
TRPV1-FL-R717A-pSGFP2C1	Mammalian	Prepared in CG lab
TRPV1-FL-K718A-pSGFP2C1	Mammalian	Prepared in CG lab
TRPV1-FL-R21A-pSGFP2C1	Mammalian	Prepared in CG lab
TRPV1-FL-K724A-pSGFP2C1	Mammalian	Prepared in CG lab
TRPV1-FL-TBS1-Hexamutant-pSGFP2C1	Mammalian	Prepared in CG lab
TRPV1-FL-TBS1-Hexamutant-pmCherryC1	Mammalian	Prepared in CG lab
TRPV1-FL-R557A-pSGFP2C1	Mammalian	Prepared in CG lab
TRPV1-FL-R557D-pSGFP2C1	Mammalian	Prepared in CG lab
TRPV1-FL-R557H-pSGFP2C1	Mammalian	Prepared in CG lab
TRPV1-FL-R557K-pSGFP2C1	Mammalian	Prepared in CG lab
TRPV1-FL-R575A-pSGFP2C1	Mammalian	Prepared in CG lab
TRPV1-FL-R575D-pSGFP2C1	Mammalian	Prepared in CG lab
TRPV1-FL-R575H-pSGFP2C1	Mammalian	Prepared in CG lab
TRPV1-FL-R575K-pSGFP2C1	Mammalian	Prepared in CG lab
TRPV1-FL-R575D/D576R-pSGFP2C1	Mammalian	Prepared in CG lab
TRPV1-FL-R575D/D576R-pmCherryC1	Mammalian	Prepared in CG lab
TRPV1-FL-R575D-pmCherryC1	Mammalian	Prepared in CG lab

TRPA1-FL- pSGFP2C1	Mammalian	Prepared in CG lab by Subhadra Majhi
-----------------------	-----------	---

5.2. Methods

5.2.1. Molecular biology techniques

5.2.1.1. Polymerase Chain Reaction (PCR)

In this study, PCR was mainly employed to incorporate specific regions or an entire gene into desired expression vectors. It was also used for generating mutants by site directed mutagenesis (SDM). The reaction conditions were different for both these purposes but the master mix contained the same components barring the polymerase enzyme. For cloning of a specific stretch or entire insert from one vector to another, primers were designed to have specific restriction sites, whereas for SDM purpose the primers harboured the desired mutations and not any restriction site. The basic components of a PCR master mix are DNA template, forward and reverse primer, 1X polymerase buffer, DNA polymerase enzyme, dNTP mix and MilliQ water. The reactions were carried out under the conditions that have been tabulated below. Use of different high-fidelity polymerases have also been mentioned under different conditions.

5.2.1.2. Site Directed Mutagenesis and Construct preparation

Full-length Rat TRPV1-WT in pBF1 vector was a kind gift from Dr. Soenke Cordeiro, Institute of Physiology, Christian-Albrechts-Universität zu Kiel. Using this as a template six point mutants namely: Lys710Ala, Lys714Ala, Arg717Ala, Lys718Ala, Arg721Ala, Lys724Ala were made. Using Lys710Ala as a template, 3 sets of primers were used to generate the TRPV1-TBS1-Hexamutant having all the above-mentioned mutations. Site Directed Mutagenesis (SDM) was performed using QuikChange Site-Directed Mutagenesis Kit from Agilent Technologies. The primers used for synthesizing

each mutant has been tabulated below. Once the mutants were generated, full-length Rat TRPV1-WT and these mutants were cloned into pSGFP2C1 vector (Addgene) and only the C-terminus of Rat TRPV1 (681-838 amino acid) harbouring all these mutations were cloned into pMAL-c2X vector (NEB). Both full-length and C-terminus of TRPV1 were cloned between EcoRI and Sall sites in both pSGFP2C1 vector and pMAL-c2X vector. Using the same primer sets, Full-length Rat TRPV1-WT and TRPV1-TBS1-Hexamutant were cloned into pmCherryC1 vector (Takara). Similarly, the TRPV1 Lipid Water Interface (LWI) mutants, Arg557Ala, Arg557Asp, Arg557Lys, Arg557His, Arg575Ala, Arg575Asp, Arg575Lys and Arg575His were generated taking TRPV1-WT-pBF1 as template. TRPV1-Arg575Asp/Asp576Arg mutant was generated using TRPV1-Arg575Asp as the template. All these full-length TRPV1-LWI mutants were cloned into pSGFP2C1 vector using the same set of primers as done for earlier constructs. TRPV1-Arg575Asp and TRPV1-Arg575Asp/Asp576Arg were cloned into pmCherryC1 vector also. The prepared constructs have been schematically represented in Annexure 3.

List of primers used for Site Directed Mutagenesis (SDM):

Name of Mutant	Primer sequence for SDM (5'-3')
TRPV1-Lys710Ala	Forward Primer: TGGATACAGAGGCGAGCTTCCTGAAGTG Reverse Primer: CACTTCAGGAAGCTCGCCTCTGTATCCA
TRPV1-Lys714Ala	Forward Primer: GAGAAGAGCTTCCTGGCGTGCATGAG Reverse Primer: CTCATGCACGCCAGGAAGCTCTTCTC
TRPV1Arg717Ala	Forward Primer: TGCATGGCTAAGGCCTTCCGCTCTG Reverse Primer: CAGAGCGGAAGGCCTTAGCCATGCA
TRPV1-Lys718Ala	Forward Primer: AGTGCATGAGGGCAGCCTTCCGCTC Reverse Primer: GAGCGGAAGGCTGCCCTCATGCACT
TRPV1-Arg721Ala	Forward Primer: AGGAAGGCCTTCGCATCTGGCAAGCTG Reverse Primer: CAGCTTGCCAGATGCGAAGGCCTTCCT
TRPV1-Lys724Ala	Forward Primer: TTCCGCTCTGGCGCACTGCTGCAGGTGGGG Reverse Primer: CCCACCTGCAGCAGTGCGCCAGAGCGGAA
TRPV1-TBS1-Hexamutant	Forward Primer: GATACAGAGGCGAGCTTCCTGGCGTGCATGAGGAAGGCCTT CCG Reverse Primer: CGGAAGGCCTTCCTCATGCACGCCAGGAAGCTCGCCTCTGT ATC

	<p>Forward Primer: GAGCTTCCTGGCGTGCATGGCGGCGGCCTTCCGCTCTGGCAAGC</p> <p>Reverse Primer: GCTTGCCAGAGCGGAAGGCCGCCATGCACGCCAGGAA GCTC</p>
	<p>Forward Primer: GCATGGCGGCGGCCTTCGCCTCTGGCGGCTGCTGCAGGTGGG</p> <p>Reverse Primer: CCCCACCTGCAGCAGCGCGCCAGAGGCGAAGGCCGCC ATGC</p>
TRPV1- Arg557Ala	<p>Forward Primer: CCAACATGCTCTACTATAACCGCAGGATTCCAGCAGATGGGC</p> <p>Reverse Primer: GCCCATCTGCTGGAATCCTGCGGTATAGTAGAGCATGTTGG</p>
TRPV1- Arg557Asp	<p>Forward Primer: CCAACATGCTCTACTATAACCGACGATTCCAGCAGATGGGC</p> <p>Reverse Primer: GCCCATCTGCTGGAATCCGTCGGTATAGTAGAGCATGTTGG</p>
TRPV1-Arg557His	<p>Forward Primer: CCAACATGCTCTACTATAACCCATGGATTCCAGCAGATGGGC</p> <p>Reverse Primer: GCCCATCTGCTGGAATCCATGGGTATAGTAGAGCATGTTGG</p>
TRPV1-Arg557Lys	<p>Forward Primer: CCAACATGCTCTACTATAACCAAAGGATTCCAGCAGATGGGC</p> <p>Reverse Primer: GCCCATCTGCTGGAATCCTTTGGTATAGTAGAGCATGTTGG</p>
TRPV1- Arg575Ala	<p>Forward Primer: GATTGAGAAGATGATCCTCGCAGACCTGTGCCGTTTATG</p> <p>Reverse Primer: CATAAACCGGCACAGGTCTGCGAGGATCATCTTCTCAATC</p>
TRPV1- Arg575Asp	<p>Forward Primer: GATTGAGAAGATGATCCTCGACGACCTGTGCCGTTTATG</p> <p>Reverse Primer: CATAAACCGGCACAGGTCTGCGAGGATCATCTTCTCAATC</p>
TRPV1-Arg575His	<p>Forward Primer: GATTGAGAAGATGATCCTCCACGACCTGTGCCGTTTATG</p> <p>Reverse Primer: CATAAACCGGCACAGGTCTGGAGGATCATCTTCTCAATC</p>
TRPV1-Arg575Lys	<p>Forward Primer: GATTGAGAAGATGATCCTCAAAGACCTGTGCCGTTTATG</p> <p>Reverse Primer: CATAAACCGGCACAGGTCTTTGAGGATCATCTTCTCAATC</p>
TRPV1-Arg575Asp/Asp576Arg	<p>Forward Primer: AAGATGATCCTCGACCGCCTGTGCCGTTTATG</p> <p>Reverse Primer: CATAAACCGGCACAGGCGGTCTGAGGATCATCTT</p>

PCR for Site-Directed Mutagenesis:

DNA template (100ng/μl)	0.5 μl
10X reaction buffer	2.5 μl

Forward Primer (25 μ M)	0.5 μ l
Reverse Primer (25 μ M)	0.5 μ l
dNTP mix	0.5 μ l
Pfu Turbo DNA polymerase(2.5U/ μ l)	0.5 μ l
Autoclaved MilliQ water	20 μ l
Total	25 μ l

PCR Reaction Conditions for SDM:

Segment	Cycles	Temperature	Time
1	1	95°C	30 seconds
2	16	95°C	30 seconds
		55°C	1 minute
		68°C	6 minutes
3	1	68°C	10 minutes
4	1	4°C	∞

4 μ l of the PCR product was run on 0.8% Agarose Gel in order to confirm the size of the product. Upon confirmation, remaining 21 μ l of PCR product was subjected to digestion by adding 0.5 μ l of Dpn1 enzyme (supplied in the kit) for 4 hours at 37°C. The digested product was then transformed into DH5 α competent cells to obtain colonies. These colonies were grown overnight in LB media and plasmid was isolated using Qiagen Miniprep Kit. The isolated DNA was verified for the desired mutations by Sanger sequencing.

List of primers used for cloning into pSGFP2C1, pmCherryC1 and MBP-LacZ vector

Forward primer: EcoRI Reverse primer: Sall	
Name of primer	Primer sequence
TRPV1-FL-GFP Forward Primer	5'-CCAGGAATTC TATGGAACAACGGGCTAGC-3'

TRPV1-FL-GFP Reverse Primer	5'-CCAG GTCGACTT ATTTCTCCCCTGGGACC-3'
TRPV1-Ct-MBP Forward Primer	5'-GCGC GAATTC ATGGGTGAGACCGTCAAC-3'
TRPV1-Ct-MBP Reverse Primer	5'-CGCC GTCGACTT ATTTCTCCCCTGGGACC-3'

PCR reaction for Cloning:

Autoclaved MilliQ water	31 μ l
5X Q5 buffer	10 μ l
10 mM dNTP	4 μ l
Forward Primer (25 μ M)	1.5 μ l
Reverse Primer (25 μ M)	1.5 μ l
DNA template (100 ng/ μ l)	1 μ l
Q5 Polymerase	1 μ l
Total	50 μ l

PCR Cycle for Cloning into pSGFP2C1 and pmCherryC1 vector:

Segment	Cycles	Temperature	Time
1	1	98°C	5 minutes
2	35	98°C	30 seconds
		55°C	30 seconds
		72°C	1 minute
3	1	72°C	5 minutes
4	1	4°C	∞

PCR Cycle for Cloning into pMAL-c2X vector:

Segment	Cycles	Temperature	Time
1	1	98°C	5 minutes
2	35	98°C	30 seconds
		55°C	30 seconds
		72°C	30 seconds
3	1	72°C	2 minutes
4	1	4°C	∞

5.2.1.3. Agarose Gel Electrophoresis

Double stranded DNA (dsDNA) was separated by horizontal agarose gel electrophoresis in 0.8% or 1% agarose gel placed in a tank of 1X TAE. The gel of desired percentage was prepared by mixing agarose powder in 1X TAE buffer, microwaved for 2-3 minutes until the agarose powder dissolved to give a clear solution. The gel percentage depends upon the length of dsDNA that needs to be resolved. EtBr (Ethidium Bromide) solution at a final concentration of 0.1-0.5 $\mu\text{g/ml}$ was added to the gel solution for visualization of DNA. The casting tray was set on the workbench by proper levelling and a comb of desired thickness and well number was inserted in it. The molten agarose gel containing EtBr (0.01%) was poured onto it and was allowed to solidify at room temperature (25°C). Upon solidification, the comb was gently removed without tampering the bases of wells and the gel was transferred into a tank filled with 1X TAE (electrophoresis buffer). DNA samples were mixed with DNA loading dye (final concentration 1X) and added to individual wells. The gel should be completely immersed into the electrophoretic buffer. The apparatus was connected to an electric supply and a value for voltage and current was set. The tracking dyes present in loading buffer enable visualization of dye front. Electrophoresis was stopped and the DNA bands were visualized by using an UV transilluminator.

50X TAE buffer recipe (for 1 litre)		
Tris	242 gm	The volume was adjusted till 1 litre with double distilled water
EDTA	18.61 gm	
Glacial Acetic Acid	57.1 ml	

5.2.1.4. Restriction digestion

For cloning purposes, the entire PCR product as well as the desired vector was run on 0.8% or 1% Agarose gel. The bands at correct size were excised out using a clean scalpel. Using Qiagen Gel Extraction kit, the DNA fragment was extracted and the whole of it was subjected to restriction digestion using EcoRI and SalI enzymes (NEB) for 3 hours at 37°C. The reaction was set up using the extracted DNA, restriction enzymes, 1X CutSmart Buffer (NEB) and Autoclaved MilliQ water. The minimum amount of DNA that was used for restriction digestion was 1µg. Depending upon the concentration of DNA, the reaction volume varied between 10-20 µl.

5.2.1.5. Ligation of insert and vector

The digested product was run on a 0.8% Agarose gel, the fragment was cut out using a scalpel and then extracted from the gel using Qiagen Gel Extraction Kit. The concentrations of both insert and vector DNA were measured using Nanodrop (Thermo Scientific). A ligation mix was prepared in which insert: vector ratio was kept at 3:1. Depending upon the volumes of the insert and vector DNA the reaction volume was set to either 10-15 µl. Apart from that the ligation mix contained 1X T4 Ligation buffer (NEB), T4 DNA Ligase enzyme (NEB) and autoclaved MilliQ water. The ligation reaction was set at 16°C for 12 hours.

5.2.1.6. Transformation

For transformation, 3.5-4 µl of the ligated product was added to 50 µl of DH5α competent cells kept in ice. Addition of DNA was followed by a 15-20 minute of incubation in ice. This was followed by a heat shock at 42°C for 45 seconds. The vial was then immediately placed back into ice and kept for 5 minutes. Around 900 µl of LB media

was then added to the vial and incubated for 1 hour at 37°C and 220 RPM. Post incubation, the bacterial cells were pelleted down at 13000 RPM for 1 minute. Around 800 µl of the supernatant was discarded and the bacterial pellet was re-suspended in the remaining media. Antibiotic containing LB plates (50mg/ml for Kanamycin or 100mg/ml for Ampicillin) were pre-incubated at 37°C and to these plates the bacterial suspension was added. The culture was spread all over the plate using glass beads (MP Biomedicals). The plates were incubated at 37°C for 12-14 hours for the appearance of bacterial colonies.

LB Media composition (for 1 litre)		
Yeast extract	5 gm	The components were dissolved by adding around 700 ml double distilled water and the volume was made upto 1 litre
Tryptone	10 gm	
Sodium Chloride	10 gm	

5.2.1.7. Competent Cell Preparation by RbCl method

Competent cells of two different bacterial strains were made: DH5α and DE3. In both cases the same protocol were followed using the Rubidium Chloride method. A single bacterial colony was inoculated into an LB tube from a freshly streaked plate of either of the two strains. The culture was allowed to grow overnight at 37°C at 220 RPM. 1-2ml of the fully grown culture was then added to 100 ml of fresh LB media and it was allowed to grow at 37°C at 220 RPM until the culture reached an OD at 600 nm between 0.4-0.6. Once the optimum OD was reached the 100 ml bacterial culture was kept in ice for 15 minutes. The entire culture was then pelleted at 4500 RPM at 4°C for 10 minutes. The supernatant was discarded and the pellet was re-suspended in 40 ml of TFB1 buffer. The suspension was incubated in ice for 15 minutes and then centrifuged at 4000 RPM at 4°C for 5 minutes. The supernatant was discarded and the pellet was re-suspended in 4 ml of TFB2 buffer while keeping the tube in ice. This bacterial suspension was then

distributed in small volumes of 50-100 μ l in pre-chilled micro centrifuge tubes. These aliquots were then snap-chilled in liquid nitrogen and stored in -80°C for long term use.

Composition of TFBI buffer:

	For 50 ml	
RbCl (100 mM)	0.725 gm	pH was adjusted to 5.8 with acetic acid, filter sterilized and stored at 4°C away from light.
MnCl ₂ -4H ₂ O (50 mM)	0.5 gm	
Potassium acetate (30 mM)	0.147 gm	
CaCl ₂ -2H ₂ O (10mM)	0.075 gm	
Glycerol (15% final)	7.5 ml	
Autoclaved MilliQ water	42.5 ml	

Composition of TFBII buffer:

	For 15 ml	
MOPS (10mM)	0.031 gm	pH was adjusted to 6.5 with KOH, filter sterilized and stored at 4°C away from light.
RbCl (10mM)	0.018 gm	
CaCl ₂ -2H ₂ O (75mM)	0.165 gm	
Glycerol (15% final)	2.25 ml	
Autoclaved MilliQ water	12 ml	

5.2.1.8. Instant screening

In order to differentiate a self-ligated colony from a true one, screening of a large number of transformed colonies is necessary. So whenever an insert of >1 Kb was cloned into a vector, the transformed colonies post ligation were subjected to instant screening. In this technique, 20-30 colonies were streaked into another LB plate (having the same antibiotic as that of the master plate). Apart from the ligated colonies, a colony containing the empty vector only was also streaked in the same plate. The streaked plate was

incubated at 37°C for about 12 hours. A small amount of each streaked colony was mixed into 40 µl of 1X Instant Screening Lysis Buffer, incubated at 37°C for 7 minutes. The tubes were then incubated in ice for 5 minutes after which they were centrifuged at 13000 RPM for 10 minutes at 4°C. Around 20 µl of supernatant from each tube was loaded in a previously made 0.8 % agarose gel.

Composition of 1X Lysis buffer for Instant Screening:

	Stock	For 10 ml
10% w/v sucrose		1 gm
100 mM NaOH	10 N	100 µl
60 mM KCl	1M	600 µl
5 mM EDTA	0.5M	100 µl
0.25% SDS	10%	250 µl
Bromophenol Blue		6 mg
Autoclaved MilliQ water		8.95 ml

Only the lanes that show a shift with respect to the empty vector by a size corresponding to the size of the insert were considered. Out of the selected lanes, 1 or 2 streaked colonies were cultured overnight at 37°C/220 RPM. The plasmid was isolated using Qiagen MiniPrep Kit. The isolated plasmids were verified for the correct insert by double digestion and eventually Sanger sequencing.

5.2.2. Biochemical techniques

5.2.2.1. SDS-PAGE

Proteins were separated on the basis of their molecular weight by SDS-PAGE by resolving them on polyacrylamide gels (8% or 12%). Sodium Dodecyl Sulphate (SDS) is an anionic detergent that is used to impart a uniform negative charge to the proteins, so that the proteins separate only on the basis of the molecular weight and not charge. U.K. Laemmli introduced this technique for separation of proteins (439). Laemmli buffer was added to protein samples (final concentration 1X) and then boiled at 95°C for 5-7 minutes

to ensure complete denaturation of the protein. Resolving and stacking gel for the desired percentage of polyacrylamide gels was prepared according to the composition tabulated below. Two glass plates (10 cm wide and 7 cm high) separated by spacer were set up in the cassette. Around 5 ml of resolving gel was poured in between the glass plates. 1 ml of water was slowly added to form a thin layer on this gel in order to provide a smooth surface. The resolving gel was allowed to polymerise at room temperature (25°C). After polymerisation, the water was decanted in order to pour the stacking gel. Around 2 ml of stacking gel was added and 10 or 15 well comb was inserted into it for well formation. After polymerisation of stacking gel, the comb was slowly removed. The cassette was then inserted vertically into a tank containing 1X SDS running buffer. The protein samples were loaded into wells using a Hamilton syringe. After loading the tank was connected to a power pack and the gel was run at constant current 10 mAmp. Bromophenol blue present in Laemmli buffer acts as a tracking dye and enables visualization of protein movement along the gel. When the dye front almost reached the end of the gel, electrophoresis was stopped. Subsequently the gel was taken out and the separated proteins were visualized by Coomassie blue staining and followed by destaining. For Western blot analysis, the gel containing separate proteins was processed differently.

12% SDS-PAGE gel composition			
		Resolving	Stacking
30% Acrylamide Solution		1.9 ml	30% Acrylamide Solution 500 µl
Autoclaved MilliQ water		1.7 ml	Autoclaved MilliQ water 2.1 ml
Tris (pH=8.8)		1.3 ml	Tris (pH=6.8) 380 µl
10% SDS		50 µl	10% SDS 30 µl
APS		50 µl	APS 30 µl
TEMED		8 µl	TEMED 4 µl

Composition of 10X SDS Running buffer (500 ml)	
Tris Base	15.1 gm
Glycine	94 gm
SDS	5 gm
The volume was made up to 500 ml by addition of double distilled water	
5X Laemmli buffer (for 10 ml)	
0.5 M Tris HCl (pH=6.8)	1.25 ml
β -Mercaptoethanol	0.5 ml
Glycerol	5 ml
20% SDS	1 ml
Bromophenol Blue	0.01 gm
Autoclaved Milli Q water	2.6 ml

5.2.2.2. Coomassie staining

The staining and destaining solutions were prepared as mentioned below. The SDS-PAGE gels were stained overnight in staining solution on a rocker. Constant agitation allows proper circulation of dyes and uniform staining. The dye stains the entire gel but permanently sticks to the proteins present in the gel. The stained gels were destained for around 2 hours in destaining solution by constant agitation. Methanol present in solution causes shrinkage of gels which can be restored back to its normal size by placing it in distilled water.

Composition of staining solution (for 500 ml)	
Coomassie Brilliant Blue G-250	0.5 gm
Methanol	250 ml
Glacial Acetic Acid	50 ml
Autoclaved milli Q water	200 ml

Composition of de-staining solution (for 500 ml)	
Methanol	250 ml
Glacial Acetic Acid	50 ml
Autoclaved milli Q water	200 ml

5.2.2.3. Western blot analysis

After the proteins were separated by SDS-PAGE, the proteins were transferred onto a PVDF membrane by semi-dry method. In this method, a Whatman paper pad

soaked in Western Transfer buffer was placed on the semi-dry transfer apparatus. A glass rod was rolled on it to remove any bubble. A PVDF membrane pre-soaked in methanol and then soaked in Western Transfer buffer was laid on it and rolled with a glass rod for uniform spreading and avoiding air bubbles that hinders proper transfer. The polyacrylamide gel containing proteins was also dipped in the same buffer and laid on the membrane. Another Whatman paper pad soaked in Western Blot Transfer buffer was placed on this gel and the entire set up was gently rolled on with a glass rod. The semi dry transfer unit was closed and connected to a power supply and the transfer was allowed to continue at 25 volts for 35 minutes. After transfer, the PVDF membrane was immersed in blocking solution (either 5% NFDM or 5% BSA made in 1X TBS-T). After blocking for an hour the membrane was incubated with primary antibody overnight at 4°C. After that it was washed thrice with 1X TBS-T and then incubated with secondary antibody for 1 hour at room temperature. The blot was then washed thrice with 1X TBST and developed by chemiluminescence using a detection reagent (Super Signal™ West Femto Maximum Sensitivity Substrate, Thermo Scientific) and detected by ChemiDoc apparatus (BioRad).

Composition of TBS (5X) for 500 ml	
20 mM Tris Base	6.05 gm
150 mM NaCl	21.915 gm
Adjust volume to 500 ml with MilliQ water	

Composition of Western Blot Transfer Buffer (for 1 litre)	
Tris	3.04 gm
Glycine	14.42 gm
Methanol	200 ml
SDS	0.373 gm
The volume was made up to 1 litre by addition of autoclaved Milli Q water	

5.2.2.4. Protein expression

All the TRPV1-TBS1 mutants and TRPV1-WT constructs were cloned in pMAL-c2X, which is a protein expression vector. After verification of the right clones by restriction digestion and sequencing, the plasmids were transformed into DE3 competent cells. The fully grown cultures were stored as glycerol stocks in -80°C. For expressing the desired proteins, the glycerol stocks were revived by adding a small volume of it to 50 ml of sterile LB containing 100 mg/ml Ampicillin. This starter culture was grown overnight at 37°C/220 RPM. The fully grown culture was then transferred to another flask containing 250 ml of sterile LB and 100 mg/ml Ampicillin. The culture was allowed to grow until it reached an OD of 0.6-0.8 at 600 nm. After that 0.5M IPTG was added to the culture for induction of protein expression at 37°C/220 RPM. IPTG induction was continued for 2 hours after which the culture was kept at 4°C for an hour. This enabled halting of the translational machinery. The bacteria were pelleted down from the culture by centrifuging at 10,000 RPM for 5 minutes in a Sorvall Centrifuge (Thermo Scientific). In order to recover the overexpressed protein, the bacterial cells were lysed by addition of Lysis Buffer and incubated for an hour in ice. In order to ensure complete lysis, the suspension was frozen in liquid nitrogen and then thawed in water bath kept at 37°C. After three rounds of freeze thaw cycle, the tubes were subjected to centrifugation at 25,000 RPM for 2 hours. The supernatant containing a mixture of the protein of interest as well as other proteins was collected and the pellet was discarded.

Composition of Lysis buffer (50 ml)	
1X PBS	50 ml
Protease Inhibitor (2X)	2 ml
Lysozyme	500 µl
PMSF	500 µl

5.2.2.5. Isolation of MBP-tagged proteins

In order to isolate the MBP-tagged overexpressed protein of interest from a cocktail of different bacterial proteins, the extracted lysate was incubated with Amylose Resin Beads (NEB) overnight at 4°C in a nutating mixer. The beads were washed thrice with PEMS buffer (composition given below) to remove unbound proteins. Finally, the MBP tagged protein was eluted by addition of 20mM Maltose. The eluted proteins were denatured by addition of 5X Laemmli buffer so that the final concentration was 1X and then boiled at 95°C for 5-7 minutes. These samples were analysed by 12% SDS-PAGE.

PEMS buffer composition	For 500 ml	
PIPES (50 mM)	7.55 gm	The pH was adjusted to 6.8 and the volume was made up to 500ml by adding Autoclaved MilliQ water.
MgCl ₂ (0.2 mM)	9.52 mg	
NaCl (150 mM)	4.38 gm	
EGTA (1 mM)	1 ml	

5.2.2.6. Protein quantification by Bradford estimation

The concentration of protein was estimated by Bradford assay (440). BSA solutions of the following concentrations (20, 40, 60, 80, 100 µg) were made in 100 µl of 1X PBS and added to 1 ml cuvettes. 900 µl of Bradford reagent was added to each of these tubes, mixed well by pipetting and allowed to incubate for 5 minutes in dark. For the blank solution, Bradford reagent was added to only 1X PBS. After incubation, the absorbance of individual samples were measured at 595 nm in a spectrophotometer. BSA solution (company name) was used as a Protein standard.

5.2.2.7. Pull-down assay

In order to check the extent of interaction of TRPV1-WT, TRPV1-TBS1 mutants and only MBP with $\alpha\beta$ -tubulin dimers in presence and absence of calcium, only MBP or

MBP-tagged proteins were expressed and bacterial lysates containing these proteins were passed through Amylose Resin beads in different columns. After washing thrice with PEMS buffer, the beads were incubated at room temperature (25°C) with 90 µg of purified $\alpha\beta$ -tubulin dimers in a nutating mixer for 2 hours. In order to see the effect of calcium on this interaction, 1mM CaCl₂ was also along with tubulin dimers. Post incubation, the beads were washed with PEMS buffer thrice to remove unbound proteins. The MBP-tagged proteins along with their interacting partners were eluted using 20mM Maltose. The eluted proteins were denatured by addition of 5X Laemmli buffer and then boiled at 95°C for 5-7 minutes. They were analysed by Western blotting and probed with α and β -tubulin antibody as well as different modified tubulin antibodies.

5.2.2.8. Co-sedimentation assay

In order to check the extent of interaction of TRPV1-WT, TRPV1-TBS1 mutants and only MBP with polymerised microtubules in presence and absence of Ca²⁺, the proteins were expressed and eluted using 20 mM maltose as described earlier. The proteins were quantified by Bradford Assay. These were then centrifuged at 40,000 RPM for 15 minutes at 30°C in order to sediment the protein aggregates. Tubulin dimers were incubated with 5 mM GTP and 1 µM Taxol at room temperature (RT, ~25°C) for 30 minutes in order to facilitate polymerisation of tubulin dimers to microtubules. After incubation these were centrifuged at 40,000 RPM for 30 minutes at 30°C in a table-top Ultracentrifuge (Beckmann Coulter). The supernatant was discarded. The desired proteins (TRPV1-WT, TRPV1-TBS1 mutants and MBP only) were allowed to incubate with this microtubule pellet in absence and presence of 1 mM CaCl₂ for 30 minutes at RT in a buffer that contains 5 mM GTP and 1 µM Taxol. After incubation the tubes were centrifuged at 40,000 RPM for 30 minutes at 30°C. The supernatant was collected and

denatured by addition of 5X Laemmli buffer and then boiled at 95°C for 5-7 minutes. PEMS buffer was added to the pellet fraction in order to dissolve the pellet in it. The same amount of PEMS buffer was added to the pellet fraction in order to make the gel sample so that the protein present in pellet fraction can be compared (by volume) with the protein present in supernatant fraction (by volume). The supernatant and pellet fractions were analysed by Western blotting using anti-MBP antibody.

5.2.2.9. Cross-linking assay

The C-terminus fragment of TRPV1-WT and TRPV1-Hexamutant was purified as explained earlier. Bradford estimation was done to assess the concentration of TRPV1-WT-Ct, TRPV1-TBS1-Hexamutant-Ct and purified tubulin from goat brain. Prior to the start of this experiment, 8 tubes were labelled as 0', 1', 3', 6', 10', 20', 40' and 60' and to each of them 20 µl of 5X Laemmli buffer was added. Two separate 1.5 ml microcentrifuge tubes were taken and to each equal volumes having equal concentrations of either TRPV1-WT-Ct or TRPV1-TBS1-Hexa and purified tubulin were added (150 µl protein+ 150 µl purified tubulin+ 25µl water+ 25µl Triethanolamine). Each of the tubes were supplemented with 0.2M Triethanolamine (Himedia) and autoclaved MilliQ water to achieve a final volume of 300 µl. The tubes were vortexed vigorously and from these tubes 40 µl of the mixture was added to the tube labelled 0' and heated at 95°C for 5-7 minutes. This tube was devoid any cross linker. 20 µg of the chemical cross-linker DMS (Thermo Scientific) was added to the mix and vortexed vigorously. 1 min post addition of crosslinker, 40 µl of the mixture was added to the tube labelled 1' and it was subjected to heating at 95°C. The added Laemmli buffer halted the progression of further crosslinking reaction. In this way, crosslinking was stopped at 3, 6, 10, 20, 40 and 60 minutes. The gel samples for TRPV1-WT and TRPV1-TBS1-Hexa were run separately

on 8% SDS-PAGE gel, subjected to Western blotting using different tubulin and modified tubulin antibodies to assess which of the two proteins formed higher molecular weight complexes with tubulin in presence of cross-linker and at which time point. Band intensities at different molecular weights and at different time points were quantified using ImageLab software and then these intensities were plotted with respect to time for both TRPV1-WT-Ct and TRPV1-TBS1-Hexamutant-Ct.

5.2.2.10. Tubulin purification

Tubulin dimers were purified from cattle brain with slight modifications in protocol as described in (441). Four brains were collected from freshly slaughtered goats in ice cold PBS during transportation from slaughterhouse to the lab. Meninges, blood vessels and brain stem were removed manually and the remaining brain tissue was homogenised in ice cold PEMS buffer (50 mM PIPES: pH 6.8, 1mM EGTA, 0.2 mM MgCl₂) in a mixer in presence of complete protease inhibitor cocktail tablets (Sigma). The homogenate was then distributed into 6 Sorvall centrifuge tubes and centrifuged for 1 hour at 12,000 RPM at 4°C (Rotor: F14-6X250y, Thermo Scientific). The supernatants were subjected to re-centrifugation in an ultracentrifuge (Beckman Coulter) at 40,000 RPM for 30 minutes at 4°C to get a clear supernatant. The supernatant was collected in a conical flask and equal volumes of Glycerol was added to it. Powdered GTP at a final concentration of 0.1 mM, 3.5 mM MgCl₂ and 1µM Taxol was also added to this mixture. The conical flask was swirled gently to mix all the components and it was incubated in water bath set at 37°C for 30 minutes. The solution started turning turbid indicating polymerization of microtubules. This solution of polymerised microtubules was then centrifuged at 40,000 RPM for 1 hour at 37°C. The supernatant was discarded and the gelatinous pellet of polymerised microtubules was re-suspended in ice cold PEMS buffer

to induce depolymerisation, homogenised with glass douncer and incubated in ice for 30 minutes. This mixture of depolymerised microtubule was then centrifuged at 40,000 RPM for 30 minutes at 4°C in order to remove the chunky pellet. The collected supernatant containing recyclable tubulin and associated proteins was measured, powdered GTP at a final concentration of 0.5 mM, 3.5 mM MgCl₂ and 1 μM Taxol was added to it to allow another cycle of polymerisation. All the components were mixed by swirling and incubated at 37°C for 30 minutes. This polymerised mixture was again centrifuged at 40,000 RPM for 30 minutes at 37°C. The resulting pellet was again subjected to cold-induced depolymerisation by application of ice cold PEMS buffer and homogenisation with a glass douncer. The depolymerisation was allowed to proceed by incubating the solution in ice for 30 minutes. This was followed by centrifugation at 40,000 RPM at 4°C for 30 minutes in order to obtain a clear supernatant enriched in tubulin dimer having sparse populations of MAP's. This supernatant was collected and passed through a phosphocellulose packed column. Different fractions were eluted that varied in their concentration of tubulin. The enriched fractions were pooled together, the concentration was measured by Bradford assay and were aliquoted into small tubes. These tubes were snap chilled in liquid nitrogen and then stored at -80°C for long term use. The purified tubulin was analysed by SDS-PAGE for its quality and it represents phosphocellulose-purified tubulin (having traces of MAPs, ~98-99% pure tubulin).

5.2.3. Cell Biology techniques

5.2.3.1. Cell culture and transfection

F-11 cells were cultured in nutrient mixture F-12 Ham media supplemented with 10% Fetal Bovine Serum, L-glutamine (2 mM), Streptomycin and Penicillin (100 mg/ml each, HiMedia, Bangalore, India). Cells were maintained in a humidified

atmosphere at 5% CO₂ and 37°C. Lipofectamine was used for transient transfection according to manufacturer's protocol.

For TRPV1-tubulin studies, full-length Rat TRPV1-WT-GFP as well as TRPV1-Lys710Ala, TRPV1-Lys714Ala, TRPV1-Arg717Ala, TRPV1-Lys718Ala, TRPV1-Arg721Ala, TRPV1-Lys724Ala and TRPV1-TBS1-Hexamutant in GFP construct were transiently transfected in F-11 cells grown in 12 mm coverslips. 36 hours post transfection the cells were fixed with 4% PFA and subsequently stained with YL1/2 (1:500) antibody and DAPI (1:1000).

For TRPV1-cholesterol interaction studies, F-11 cells were transiently transfected with TRPV1-WT-GFP, all eight LWI mutants and Flotillin-RFP (for co-localization studies). Co-localization experiments were repeated with Caveolin 1-RFP also. Cells were fixed with 4% PFA 36 hours post transfection. Fixed cells were then washed twice with 1X PBS (Himedia), treated with DAPI and then mounted using Fluoromount-G. In some experiments, F-11 cells expressing TRPV1-WT-GFP or LWI mutants were treated with 5mM Methyl β -Cyclodextrin (Sigma) for 30 mins for cholesterol depletion (442) and subsequently fixed with 4% PFA. Untreated or β -MCD-treated cells were stained with Cholera Toxin-B-594 (Invitrogen, 1:200 dilution). The B subunit of Cholera Toxin derived from *Vibrio cholera* binds to the GM1 ganglioside present in plasma membrane and is considered as a bona fide lipid raft marker (443) .

5.2.3.2. Imaging and Image analysis

Imaging of all transiently transfected neuronal cells and sperm cells were done using LSM-780 (Zeiss), LSM-800 (Zeiss) and FV3000 (Olympus) confocal microscopes. Imaging of constructs tagged with GFP and RFP was done using 488nm and 561 nm lasers. DAPI was imaged using 405 nm laser with a 63X objective.

Similarly, cells stained with AF-488 and AF-594 were also visualized using 488nm and 561 nm laser line. Laser intensity was adjusted according to the HiLo module of signal saturation. Acquired images were either processed in LSM image analysis software or Fiji software.

All the confocal images have been acquired using 63X objective (Zeiss LSM 780 and Zeiss LSM 800) or 60X objective (Olympus FV3000) with an image size of 512X512 pixels. Fixed cell images have been represented at 1X and/or 4X Zoom where needed. All 1X images are 3D representations, whereas the zoomed images represent single plane image with best morphological clarity and projections. The pinhole size has been maintained at 1AU in all imaging. All live cell imaging has been performed at 2X zoom. The 3 laser lines (solid state laser) employed in this study were 405nm, 488 nm and 561 nm. Most images were acquired with a laser power ranging from 0.1%-2.5% (to reduce the photo-toxicity as low as possible without compromising the imaging) and a gain value ranging from 550-850 V was mostly used for imaging. In experiments where fluorescence intensity was compared among different conditions, all imaging conditions including the laser power and gain value were maintained at a constant value.

5.2.3.3. Estimation of cellular dimensions of transfected F-11 cells

Length, breadth, area and perimeter of F-11 cells transiently transfected with TRPV1-WT-, TRPV1-Arg575Asp and TRPV1-Arg575Asp-Asp576Arg (all in pSGFP2C1) was measured using Fiji Software. The images were opened in this software; an ROI was drawn demarcating the periphery of the transfected cells only. Using the tools of this software, a line was drawn longitudinally to assign the length of the cell and another line was drawn along the latitude to determine its breadth. Depending upon the ROI, length and breadth assigned to each cell, the software

calculated the area and perimeter for each. The same was performed for F-11 cells transiently transfected with TRPV1-WT-pSGFP2C1 and TRPV1-Arg575Asp-pSGFP2C1 with and without 5'I-RTX (1 μ M, Tocris).

5.2.3.4. Calcium-sensor based imaging

F-11 cells were transiently transfected with TRPV1-WT, TRPV1-Arg575Asp, TRPV1-Arg575Asp/Asp576Arg (all in pmCherryC1) and pmCherryC1. Each of these were co-transfected with ultrasensitive protein calcium sensor pGP-CMV-GCaMP6f (Addgene). 24 hours after transfection, doubly transfected cells were imaged for 200 frames whereby cells were activated by adding 10 μ M Capsaicin at the 30th frame and 2 μ M Ionomycin at the 120th frame (in some cases). The same experimental setup was also executed for TRPV1-WT and TRPV1-Arg575Asp-Asp576Arg in pmCherryC1 vector. In some experiments aimed to observe the effect of intracellular Ca²⁺-depletion, 24 hours post transfection, the cells were treated with 1 μ M Thapsigargin to deplete Ca²⁺ from intracellular calcium stores for 12 hours after which they were subjected to live cell imaging. Snaps of doubly transfected cells were acquired using 488 nm and 561 nm laser and then time series of live cells were conducted by only using 0.4% 488 nm laser.

Similar experiment was performed with TRPV1-WT and TRPV1-TBS1-Hexamutant constructs (both in pmCherryC1 vector). However, F-11 cells transfected with both these constructs were also subjected to 30 minutes of Taxol (1 μ M) and 20 minutes of Nocodazole (1 μ M) pre-treatment in order to facilitate microtubule stabilization and disassembly respectively. All these live cell experiments were done in a live cell chamber that is devoid of any inlet and outlet. So the drugs that are added to the chamber during pre-treatment or during the experiment remained in the bath until the completion of experiment.

5.2.3.5. Quantification of Ca²⁺-imaging

Change in intensity of the ultrasensitive protein calcium sensor pGP-CMV-GCaMP6f was quantified over time throughout 200 frames. Each cell was considered to be a single ROI and then the change in intensity was quantified using Fiji software. The initial intensity at Frame 1 was considered to be 1 and accordingly the changes were calculated relative to it. These relative intensities of 200 frames were plotted using GraphPad Prism 7 software. Live cell imaging was done using Olympus FV3000 Confocal microscope.

5.2.3.6. Immunocytochemistry for F-11 cells

F-11 cells were grown on coverslips. 36 hours post transient transfection the cells were fixed with 4% PFA. The cells were washed thrice with 1X PBS in order to remove the PFA. Then they were permeabilized with 0.1% Triton X-100 for 5 minutes. This was followed by a mild wash with 1X PBS in order to remove traces of Triton X-100. Non-specific sites were blocked with 5% BSA for about 1 hour. Primary antibody (YL1/2 at a dilution of 1:500) was added to a solution composed of 0.1% PBS-T and 5% BSA (1:1). Primary antibody incubation was executed overnight at 4°C. It was then washed thrice with 0.1% PBS-T and incubated with secondary antibody (AF-594 at a dilution of 1:1000) prepared in a solution of 0.1% PBS-T and 5% BSA (1:1) for 1 hour at room temperature. This was followed by washing for 3 times with 0.1% PBS-T. DAPI (1:1000) was added and incubated for 15 minutes. The coverslips were washed twice with 1X PBS and mounted using Fluoromount G.

To understand the surface expression of TRPV1-Wt and different mutants, F-11 cells were grown on coverslips and transiently transfected with full length Rat TRPV1-WT, TRPV1-Arg575Asp, TRPV1-Arg575Asp-Asp576Arg and TRPV1-TBS1-

Hexamutant (all in pmCherryC1 vector). Approximately, 36 hours post transient transfection the cells were fixed with 4% PFA. The cells were washed thrice with 1X PBS in order to remove the PFA. Without permeabilizing the cells, they were treated with 5% BSA for about 1 hour to block non-specific sites. Primary antibody (TRPV1-extracellular-ATTO-488) was added to a solution composed of 1X PBS and 5% BSA (1:1). Primary antibody (1:100) incubation was executed for 6 hours at room temperature. It was then washed thrice with 1X PBS and treated with DAPI (1:1000) for 15 minutes. The coverslips were washed twice with 1X PBS and mounted using Fluoromount G.

5.2.4. Sperm cell techniques

5.2.4.1. Collection and isolation of sperm cells

Freshly ejaculated sperms were collected from healthy bulls after at least 48 hours of sexual abstinence by trained professionals (at the Frozen Semen Bank, Cuttack) by means of artificial vagina. For collection of avian sperm, we used chicken (*Gallus gallus domesticus*) testis. The testis were collected (n = 4) from the slaughter house and bought to the laboratory within 15 minutes. After removing the tunica albuginea (outer covering membrane of testis), the testis was chopped into pieces, smeared and then immediately fixed in 4% PFA. The testis was then centrifuged at 1000 RPM for 10 min to pellet down the tissue debris. The supernatant containing the sperm cells was taken for further analysis. Sperm pellet was obtained by centrifugation at 6000 RPM for 5 min. For collection of sperm from reptiles, we used house lizard (*Hemidactylus leschenaultii*). Sexually mature males (n = 3) were collected from institutional campus and sacrificed by cervical dislocation. Testes was dissected out and immediately fixed in 4% PFA. The testis was then smeared and tissue debris removed by centrifuging the testis at 1000 RPM for 1min. The supernatant containing the sperm cells was collected for further analysis

and sperm pellet was obtained by centrifugation at 6000 RPM for 5min. For collection of sperm from amphibians, we used a common toad (*Duttaphrynus melanostictus*). Sexually mature male toads (n = 3) were collected from institutional campus and sacrificed by cervical dislocation. Testes were dissected out and immediately fixed in 4% PFA. The testis was then smeared and centrifuged at 1000 RPM for 30s. The supernatant containing the sperm cells was collected for further analysis. Sperm pellet was obtained by centrifuging at 6000 RPM for 5min. Matured male brood fish of rohu (*Labeo rohita*) were collected from the experimental ponds of Aquaculture Production and Environment Division, ICAR-Central Institute of Freshwater Aquaculture (CIFA), Kausalyaganga, Bhubaneswar, India. Milers were induced with a synthetic gonadotropin (Ovaprim) at the rate of 0.2 - 0.3 ml/kg body weight of the fish during peak breeding season (in the month of July). Milers were stripped into separate plastic tubes held over ice. Care was taken to avoid contamination of water, blood, urine, faeces etc. After that milt samples were processed for further analysis. In all cases, extreme care was taken to minimize the sufferings of these animals. All experiments were done according to the approval from Institutional Animal Ethics Committee of NISER (NISER-IAEC/SBS-AH/07/13/10).

5.2.4.2. Computer Assisted Sperm Analysis (CASA)

Freshly ejaculated bull semen from 8 different bulls was diluted in TALP buffer (pH 6.8) and was distributed in different tubes for treatment. Samples were taken 1 hr and 2 hr post incubation with TRPA1 specific activator and inhibitor. A Hamilton Thorne IVOS, model 10 sperm analyzer with the slide chamber set at 37°C was used. Chambered slides containing 2µl of each sample were analyzed by the machine. For each chamber/sample 4 frames were selected and the different motility parameters were acquired. CASA defines sperm movement characteristics via various parameters like

curvilinear velocity (VCL), Straight-line (rectilinear) velocity (VSL), Average path velocity (VAP), Amplitude of lateral head displacement (ALH), Linearity of a curvilinear path (LIN), Wobble (WOB), Straightness (STR), Beat-cross frequency (BCF), Mean angular displacement (MAD). ALH, expressed in μm , is the magnitude of lateral head displacement of a sperm in while traversing its average path. VCL, expressed in $\mu\text{m/s}$, is defined as time-averaged velocity of a sperm head along its actual curvilinear path. BCF is the average rate at which the curvilinear path crosses the average path, and is expressed in Hz.

5.2.4.3. Immunofluorescence analysis and microscopy for sperm cells

Control as well as drug treated sperm cells were fixed with 4% PFA. They were washed thrice with 1X PBS to remove PFA and then permeabilized with 0.1% PBST for 5 minutes. This was followed by blocking with 5% BSA for an hour at room temperature. Rabbit polyclonal anti-TRPA1 antibody (Alomone Lab, ACC-037) directed against the 1st extracellular loop (747-760aa) of human TRPA1 was used in this study. Dual staining of both TRPA1 and modified tubulin antibodies was also performed in the same way. Primary antibody dilution was mostly kept at 1:500. All primary antibodies were incubated for overnight at 4°C in 0.1% PBST: 5% BSA. AlexaFluor-488 labelled anti rabbit (Molecular probes, 1:1000) was used as secondary antibody in case of single staining and for dual staining it was clubbed with Alexa Flour-594 labelled anti mouse (Molecular Probes, 1:1000). All images were taken on a confocal laser-scanning microscope (LSM-780, LSM-800 Zeiss) with a 63Xobjective and analyzed with the Zeiss LSM image examiner software or Fiji software. For acrosomal reaction studies, paraformaldehyde-fixed bull spermatozoa were washed thrice with PBS (pH 7.4) by centrifuging at 3000 RPM for 3 min each time and then incubated with FITC-PNA (Sigma

Aldrich and used at 1 : 200 v/v dilution) for 1 h and washed thrice with PBS to remove unincorporated FITC-PNA. Acrosome status of more than 100 sperm cells of 4 different bulls was visualized using fluorescence microscope (Olympus, IX83) and was subsequently quantified manually.

5.2.5. *In silico* techniques

5.2.5.1. Sequence retrieval, alignment and structure retrieval for TRPA1 and TRPV1

The full-length sequences of both TRPV1 and TRPA1 were retrieved from National Centre for Biotechnology Information (NCBI) database (444) (445), tables of which have been provided in Annexure 1 and Annexure 2. Details of each gene and protein have been tabulated below. The sequence alignment was done by using MUSCLE alignment software with its default values (446)(447). The working structures of rTRPV1 and hTRPA1 were downloaded from the PDB (<https://www.rcsb.org/pdb>). 3J5P was used as closed conformation of rTRPV1 and 3J5R was used as the open conformation. 3J9P was used as the 3D structure for Human TRPA1.

5.2.5.2. Embedding the TRPV1 structures in PEA or POPC membrane and determining the LWI residues

Lipid bilayer made of PEA or POPC without any cholesterol or with 30% cholesterol were prepared *in silico* separately. The closed structure (3J5P) was imported into YASARA and was ‘cleaned’, hydrogen bonding network was optimized and force field parameters were added (197). The open and closed conformation of TRPV1 was inserted in to these lipid bilayers separately. *In silico* membrane with different compositions of required size was built and the protein structure was embedded within it

followed by a 250ps equilibration simulation was run, during which the membrane is artificially stabilized while it adapts to the protein. For all analysis, the temperature of the *in silico* system was maintained at 298 K. From the embedded structure, the lipid-water interface (LWI) residues were determined as the 5 residues (both in the N- and in the C-terminal regions) of all the 6 transmembrane helices of the closed structure of rTRPV1. Homologous regions were identified in the human TRPV1 sequence by aligning with MUSCLE alignment tool. LWI stretches for TRPA1 were determined by embedding the Human TRPA1 sequence (derived from Uniprot, ID: O75762) in the membrane generated by Protter and analysed according to its default algorithm.

5.2.5.3. Membrane representation and SeqLogo generation for TRPV1 and TRPA1

Graphical representation of hTRPV1 and hTRPA1 with the determined LWI residues used in this study was prepared with *Protter-visualize proteoforms* (448). SeqLogos were generated with the Weblogo webserver (<http://weblogo.berkeley.edu/>) (449)(450).

5.2.5.4. Boxplot of TRPA1 and TRPV1

Distance Matrix was generated using MEGA 5. The alignments of all domains of TRPA1 in vertebrates and invertebrates, the lipid-water interface regions and different CRAC and CARC motifs of both the channels (TRPA1 and TRPV1) were saved and then analysed with MEGA 5 software package (451)(300). The pairwise matrices were generated to measure the pairwise distance between two different amino acid sequences in a group of aligned sequences. In distance estimation analysis method, Bootstrap method was chosen for variance estimation (Bootstrap value = 1000), amino acid substitution method was set to p-distance model, to treat the gaps or missing data, pairwise

deletion model was chosen. The distance matrices thus generated showed the respective pairwise distance of all sequences in a group.

Domains and motifs of TRPV1:

Domains/Motifs	Amino acid positions	Species
Transmembrane1	429-454	Rat
Loop1	455-468	Rat
Transmembrane2	469-497	Rat
Loop2	498-510	Rat
Transmembrane3	511-532	Rat
Loop3	533-534	Rat
Transmembrane4	535-556	Rat
Loop4	557-569	Rat
Transmembrane5	570-598	Rat
Loop5	599-629	Rat
Pore loop	630-642	Rat
Loop6	643-655	Rat
Transmembrane6	656-686	Rat
N Terminal	1-428	Rat
C Terminal	687-838	Rat

Domains and motifs of TRPA1:

Name of domain of TRPA1	Amino acids involved	Species
Ankyrin repeat-1	62-96	Human
Ankyrin repeat-2	97-129	Human
Ankyrin repeat-3	130-163	Human
Ankyrin repeat-4	164-196	Human
Ankyrin repeat-5	197-237	Human
Ankyrin repeat-6	238-270	Human
Ankyrin repeat-7	271-307	Human
Ankyrin repeat-8	308-340	Human
Ankyrin repeat-9	341-373	Human
Ankyrin repeat-10	374-411	Human
Ankyrin repeat-11	412-444	Human
Ankyrin repeat-12	445-480	Human
EF-hand like motif	468-480	Human
Ankyrin repeat-13	481-512	Human
Ankyrin repeat-14	513-546	Human
Ankyrin repeat-15	547-578	Human
Ankyrin repeat-16	579-616	Human

Ankyrin repeat-17	617-649	Human
TM-1	718-738	Human
L1	739-774	Human
TM-2	775-794	Human
L2	795-805	Human
TM-3	806-825	Human
L3	826-829	Human
TM-4	830-850	Human
L4	851-869	Human
TM-5	870-892	Human
Pore	893-934	Human
TM-6	935-959	Human
N-terminus	1-717	Human
TM and loop region	718-959	Human
C-terminus	960-1119	Human

5.2.5.5. Statistical tests for TRPA1 and TRPV1

The pairwise distance values from the matrices generated were imported in “R” software package and box-plots were generated for different regions and motifs of TRPV1 and TRPA1 to evaluate the evolutionary relationship and differential selection pressure between these regions. To check the reliability and significance of the data generated, the Kruskal-Wallis test of variance was performed in “R” for all groups. The median values of each group were also calculated using “R” and outliers denoted subsequently and represented in the box plots. The graphical representation (box plots) depicts divergence of a particular domain or motif and the Y-axis represents the divergence of those regions, so lower values in the Y-axis represents higher level of conservation of the proteins.

5.2.5.6. Identification of CRAC, CARC and CCM motifs for TRPA1 and TRPV1

To identify the presence of cholesterol binding motifs in hTRPV1 and hTRPA1, a sequence wide search of the protein was done manually for CRAC, CARC and CCM motifs for TRPV1 and CRAC and CARC for TRPA1, the well-studied motifs responsible for binding of cholesterol. CRAC was characterized by the consensus motif (L/V-X (1-

5)-Y-X (1-5)-R/K) and CARC is inverted CRAC. CCM was characterized by considering one helix containing the sequence motif (W/Y) (I/V/L) (K/R), whereby all residues are facing the same side of the helix. In addition, another aromatic amino acid, either phenylalanine or tyrosine is needed on a second helix to bind cholesterol from the other side (452).

5.2.5.7. Docking of cholesterol on closed and open structures of rTRPV1 and hTRPA1

Docking was performed using VINA using default parameters (453). The setup was done with the YASARA molecular modeling program (272), the best hit of 25 runs was manually chosen. A flexible docking was performed, i.e. the ligand's internal degrees of freedom were taken into account. Cholesterol interaction with both the channels as revealed by docking experiments were excluded if the interactions are either with very low binding energy, or with thermodynamically unfavourable orientations (such as OH group located at the middle of the membrane), or binds in areas which does not have apparently any specific target motifs or TM-Loop regions. A local docking of Cholesterol was performed with TRPV1 whereby its hydrophobic interactions with the CCM motif formed between TM1 and TM2 of TRPV1 was evaluated.

5.2.5.8. Structural alignment and mutation of Arg residues in TRPV1

Structural alignment of the cholesterol docked closed rTRPV1 with the open conformation was done with MUSTANG multiple structural alignment algorithm included in the YASARA (454). The default MUSTANGPP method is a YASARA-specific extension to MUSTANG with additional Post-Processing. Starting from the initial MUSTANG superposition, YASARA extracts those residues that can be

considered structurally aligned according to the current parameters and superposes on these residues only. This procedure is iterated until the number of aligned residues converges to a maximum. The resulting superposition is more focused on structurally equivalent residues. Mutating Arg557 and Arg575 to Ala, Asp or His was done with the ‘SwapRes’ command in YASARA. The mutated side chains were optimized with a rotamer library in the SCWALL method in YASARA. This approach optimizes Side-Chain conformations With ALL available methods (272)(454)(273)(455).

5.2.5.9. Frequency calculation of different amino acids at the lipid water interface of both TRPV1 and TRPA1

Complete TRPV1 and TRPA1 sequences from different mammals, birds, reptiles, amphibians and fishes were taken. LWI residues were determined and the percentage content of all twenty amino acids at the inner, outer and total LWI was calculated. In addition to this, calculations were made for the following groups: Positively charged, negatively charged, hydrophobic and hydrophilic amino acids. In each LWI region a total 5 amino acids as a stretch was considered. Frequency calculations were done for LWI on the inside (cytoplasmic side, for 6 positions; total 30 amino acids), outside (extracellular side, for 6 positions; total 30 amino acids) as well as for the overall (i.e. for a total of 60 amino acids) residues for each species. The different values of each amino acid were plotted and statistical significance derived (non-parametric student’s T test or one-way ANNOVA, wherever applicable) in Graphpad Prism 6 (www.graphpad.com/).

5.2.5.10. Construction of phylogenetic tree for TRPA1

The evolutionary history was inferred by using the Maximum Likelihood method based on the JTT matrix-based model (456). The analysis involved 39 amino acid

sequences. All positions containing gaps and missing data were eliminated. Evolutionary analyses were conducted in MEGA5 (451).

5.2.5.11. Calculation of evolutionary time for TRPA1

The sequences among different classes were compared and number of changes of amino acids/100 amino acids was calculated by comparing birds with reptiles, fish with reptiles and reptiles with mammals for available TRPA1 sequences. The hTRPA1 is considered as the most recent one (considered as 0 MY). The average changes were calculated and radiations of mammalian TRPA1 sequences were plotted against million years.

Chapter 6

Bibliography

1. Miura RM. Analysis of excitable cell models. *J Comput Appl Math.* 2002; 144: 29–47.
2. Abdul Kadir L, Stacey M and Barrett-Jolley R. Emerging Roles of the Membrane Potential: Action beyond the Action Potential. *Front. Physiol.* 2018; 9: 1661.
3. Brenowitz S, Duguid I, Kammermeier PJ. Ion Channels: History, Diversity, and Impact. *Cold Spring Harb Protoc.* 2017; 7: 509-513.
4. Neher E, Sakmann B. The patch clamp technique. *Sci Am.* 1992; 266: 44–51.
5. Resting Potentials and Action Potentials Neuroscience Online: An Electronic Textbook for the Neurosciences (<https://nba.uth.tmc.edu/neuroscience/m/s1/chapter01.html>)
6. Gadsby DC. Ion channels versus ion pumps: the principal difference, in principle. *Nat Rev Mol Cell Biol.* 2009, 10: 344–52.
7. Hubner CA, Jentsch TJ. Ion channel diseases. *Hum Mol Genet.* 2002; 11: 2435–45.
8. Zhou H-X, McCammon JA. The gates of ion channels and enzymes. *Trends Biochem Sci.* 2010; 35: 179-85.
9. Goldschen-Ohm MP, Chanda B. SnapShot: Channel Gating Mechanisms. *Cell.* 2017; 170: 594–594
10. Clapham DE. Calcium Signaling. *Cell.* 2007; 131: 1047–58.
11. Minke B. The history of the *Drosophila* TRP channel: the birth of a new channel superfamily. *J Neurogenet.* 2010; 24: 216–33.
12. Fowler MA, Montell C. *Drosophila* TRP channels and animal behavior. *Life Sci.* 2013; 92: 394–403.
13. Purves D, Augustine GJ, Fitzpatrick D, Katz LC, LaMantia A-S, McNamara JO, et al. 2nd edition, Phototransduction (Chapter 11). 2001.
14. Cosens DJ, Manning A. Abnormal electroretinogram from a *Drosophila* mutant. *Nature.* 1969; 224: 285–7.
15. Minke B, Wu CF, Pak WL. Induction of photoreceptor voltage noise in the dark in *Drosophila* mutant. *Nature.* 1975; 258: 84-7.
16. Montell C, Rubin GM. Molecular characterization of the *Drosophila* trp locus: a putative integral membrane protein required for phototransduction. *Neuron.* 1989; 2: 1313–23.
17. Phillips AM, Bull A, Kelly LE. Identification of a *Drosophila* gene encoding a calmodulin-binding protein with homology to the trp phototransduction gene. *Neuron.* 1992; 8: 631-42.
18. Yoon J, Ben-Ami HC, Hong YS, Park S, Strong LLR, Bowman J, et al. Novel mechanism of massive photoreceptor degeneration caused by mutations in the trp gene of *Drosophila*. *J Neurosci.* 2000; 20: 649-659.
19. Clapham DE, Runnels LW, Strübing C. The TRP ion channel family. *Nature Reviews Neuroscience.* 2001. 2: 387-96.
20. Clapham DE. TRP channels as cellular sensors. *Nature.* 2003; 426: 517-24.
21. Ferreira G, Raddatz N, Lorenzo Y, González C, Latorre R. Biophysical and molecular features of thermosensitive TRP channels involved in sensory transduction. In: *TRP Channels in Sensory Transduction.* 2015; (DOI: 10.1007/978-3-319-18705-1_1.)
22. Venkatachalam K, Montell C. TRP channels. *Annu Rev Biochem.* 2007; 76: 387–417.

23. Dhakal S, Lee Y. Transient Receptor Potential Channels and Metabolism. *Molecules and cells*. 2019; 42: 569-578.
24. White JPM, Cibelli M, Urban L, Nilius B, McGeown JG, Nagy I. TRPV4: Molecular conductor of a diverse orchestra. *Physiol Rev*. 2016; 96: 911-73.
25. Peng J-B, Suzuki Y, Gyimesi G, Hediger MA. TRPV5 and TRPV6 Calcium-Selective Channels. In: *Calcium Entry Channels in Non-Excitable Cells*. CRC Press; 2018. 241–74.
26. Abramowitz J, Birnbaumer L. Physiology and pathophysiology of canonical transient receptor potential channels. *FASEB J*. 2009; 23: 297-328.
27. Harteneck C. Function and pharmacology of TRPM cation channels. *Naunyn Schmiedebergs Arch Pharmacol*. 2005; 371: 307-14.
28. Fonfria E, Murdock PR, Cusdin FS, Benham CD, Kelsell RE, McNulty S. Tissue distribution profiles of the human TRPM cation channel family. *J Recept Signal Transduct*. 2006; 26: 159-78.
29. Ong AC. Polycystin expression in the kidney and other tissues: Complexity, consensus and controversy. *Experimental Nephrology*. 2000;8: 208-14.
30. Busch T, Köttgen M, Hofherr A. TRPP2 ion channels: Critical regulators of organ morphogenesis in health and disease. *Cell Calcium*. 2017; 66: 25-32.
31. Zheng W, Yang JW, Beauchamp E, Cai R, Hussein S, Hofmann L, et al. Regulation of TRPP3 channel function by N-terminal domain palmitoylation and phosphorylation. *J Biol Chem*. 2016; 291: 25678-25691.
32. Watanabe H, Murakami M, Ohba T, Ono K, Ito H. The pathological role of transient receptor potential channels in heart disease. *Circ J*. 2009; 73: 419-27.
33. Yamaguchi S, Jha A, Li Q, Soyombo AA, Dickinson GD, Churamani D, et al. Transient receptor potential mucolipin 1 (TRPML1) and two-pore channels are functionally independent organellar ion channels. *J Biol Chem*. 2011;286:22934–42.
34. Cuajungco MP, Silva J, Habibi A, Valadez JA. The mucolipin-2 (TRPML2) ion channel: a tissue-specific protein crucial to normal cell function. *Pflugers Arch*. 2016; 468: 177-92.
35. Schmiege P, Fine M, Li X. The regulatory mechanism of mammalian TRPMLs revealed by cryo-EM. *FEBS J*. 2018; 285: 2579-2585.
36. Ramsey IS, Delling M, Clapham DE. An introduction to TRP channels. *Annu Rev Physiol*. 2006; 68: 619-47.
37. Gaudet R. Structural Insights into the Function of TRP Channels. *TRP Ion Channel Function in Sensory Transduction and Cellular Signaling Cascades*. CRC Press/Taylor & Francis; 2007, Chapter 25.
38. Madej MG, Ziegler CM. Dawning of a new era in TRP channel structural biology by cryo-electron microscopy. *Pflugers Arch*. 2018; 470: 213-225.
39. Nilius B, Owsianik G, Voets T. Transient receptor potential channels meet phosphoinositides. *EMBO J*. 2008; 27: 2809-16.
40. Rohacs T. Phosphoinositide regulation of TRP channels. *Handb Exp Pharmacol*. 2014; 223: 1143-

76.

41. Tóth B, Csanády L. Pore collapse underlies irreversible inactivation of TRPM2 cation channel currents. *Proc Natl Acad Sci U S A*. 2012; 109: 13440-5.
42. Zhang Z, Okawa H, Wang Y, Liman ER. Phosphatidylinositol 4,5-bisphosphate rescues TRPM4 channels from desensitization. *J Biol Chem*. 2005; 280: 39185-92.
43. Nilius B, Mahieu F, Prenen J, Janssens A, Owsianik G, Vennekens R, et al. The Ca²⁺-activated cation channel TRPM4 is regulated by phosphatidylinositol 4,5-bisphosphate. *EMBO J*. 2006;25:467–78.
44. Liu D, Liman ER. Intracellular Ca²⁺ and the phospholipid PIP₂ regulate the taste transduction ion channel TRPM5. *Proc Natl Acad Sci U S A*. 2003; 100: 15160-5.
45. Xie J, Sun B, Du J, Yang W, Chen HC, Overton JD, et al. Phosphatidylinositol 4,5-bisphosphate (PIP₂) controls magnesium gatekeeper TRPM6 activity. *Sci Rep*. 2011;146: 1-11.
46. Runnels LW, Yue L, Clapham DE. The TRPM7 channel is inactivated by PIP₂ hydrolysis. *Nat Cell Biol*. 2002; 4: 329-36.
47. Gwanyanya A, Sipido KR, Vereecke J, Mubagwa K. ATP and PIP₂ dependence of the magnesium-inhibited, TRPM7-like cation channel in cardiac myocytes. *Am J Physiol Cell Physiol*. 2006; 291: C627-35.
48. Takezawa R, Schmitz C, Demeuse P, Scharenberg AM, Penner R, Fleig A. Receptor-mediated regulation of the TRPM7 channel through its endogenous protein kinase domain. *Proc Natl Acad Sci U S A*. 2004; 101: 6009-14.
49. Langeslag M, Clark K, Moolenaar WH, van Leeuwen FN, Jalink K. Activation of TRPM7 channels by phospholipase C-coupled receptor agonists. *J Biol Chem*. 2007; 282: 232-9.
50. Liu B, Qin F. Functional control of cold- and menthol-sensitive TRPM8 ion channels by phosphatidylinositol 4,5-bisphosphate. *J Neurosci*. 2005; 25: 1674-81.
51. Rohács T, Lopes CMB, Michailidis I, Logothetis DE. PI(4,5)P₂ regulates the activation and desensitization of TRPM8 channels through the TRP domain. *Nat Neurosci*. 2005; 8: 626-34.
52. Yudin Y, Lukacs V, Cao C, Rohacs T. Decrease in phosphatidylinositol 4,5-bisphosphate levels mediates desensitization of the cold sensor TRPM8 channels. *J Physiol*. 2011; 589: 6007-27.
53. Daniels RL, Takashima Y, McKemy DD. Activity of the neuronal cold sensor TRPM8 is regulated by phospholipase C via the phospholipid phosphoinositol 4,5-bisphosphate. *J Biol Chem*. 2009; 284: 1570-82.
54. Zakharian E, Thyagarajan B, French RJ, Pavlov E, Rohacs T. Inorganic polyphosphate modulates TRPM8 channels. *PLoS One*. 2009; 4: e5404
55. Zakharian E, Cao C, Rohacs T. Gating of transient receptor potential melastatin 8 (TRPM8) channels activated by cold and chemical agonists in planar lipid bilayers. *J Neurosci*. 2010; 30: 12526-34.
56. Fujita F, Uchida K, Takaishi M, Sokabe T, Tominaga M. Ambient temperature affects the temperature threshold for TRPM8 activation through interaction of phosphatidylinositol 4,5-bisphosphate. *J Neurosci*. 2013; 33: 6154-9.
57. Stein AT, Ufret-Vincenty CA, Hua L, Santana LF, Gordon SE. Phosphoinositide 3-kinase binds to

- TRPV1 and mediates NGF-stimulated TRPV1 trafficking to the plasma membrane. *J Gen Physiol.* 2006; 128: 509-22.
58. Lukacs V, Thyagarajan B, Varnai P, Balla A, Balla T, Rohacs T. Dual regulation of TRPV1 by phosphoinositides. *J Neurosci.* 2007; 27: 7070-80.
 59. Kim D, Cavanaugh EJ, Simkin D. Inhibition of transient receptor potential A1 channel by phosphatidylinositol-4,5-bisphosphate. *Am J Physiol Cell Physiol.* 2008; 295: C92-99.
 60. Klein R, Ufret-Vincenty C, Hua L, Gordon S. Determinants of molecular specificity in phosphoinositide regulation: PI (4, 5) P2 is the endogenous lipid regulating TRPV1. *J Biol Chem.* 2008; 283: 26208-16.
 61. Ufret-Vincenty CA, Klein RM, Hua L, Angueyra J, Gordon SE. Localization of the PIP2 sensor of TRPV1 ion channels. *J Biol Chem.* 2011; 286: 9688-98.
 62. Lukacs V, Rives JM, Sun X, Zakharian E, Rohacs T. Promiscuous Activation of Transient Receptor Potential Vanilloid 1 (TRPV1) channels by negatively charged intracellular lipids: The key role of endogenous phosphoinositides in maintaining channel activity. *J Biol Chem.* 2013; 288: 35003-13.
 63. Lishko P V, Procko E, Jin X, Phelps CB, Gaudet R. The Ankyrin Repeats of TRPV1 Bind Multiple Ligands and Modulate Channel Sensitivity. *Neuron.* 2007; 54: 905-18
 64. Lukacs V, Yudin Y, Hammond GR, Sharma E, Fukami K, Rohacs T. Distinctive changes in plasma membrane phosphoinositides underlie differential regulation of TRPV1 in nociceptive neurons. *J Neurosci.* 2013; 33: 11451-63.
 65. Hammond GRV, *et al.* PI4P and PI(4,5)P2 are essential but independent lipid determinants of membrane identity. *Science.* 2012; 337: 727-30.
 66. Yao J, Qin F. Interaction with phosphoinositides confers adaptation onto the TRPV1 pain receptor. *PLoS Biol.* 2009; 7: e46
 67. Sowa NA, Street SE, Vihko P, Zylka MJ. Prostatic acid phosphatase reduces thermal sensitivity and chronic pain sensitization by depleting phosphatidylinositol 4,5-bisphosphate. *J Neurosci.* 2010; 30: 10282-93.
 68. Kim AY, Tang Z, Liu Q, Patel KN, Maag D, Geng Y, *et al.* Pirt, a Phosphoinositide-Binding Protein, Functions as a Regulatory Subunit of TRPV1. *Cell.* 2008; 133: 475-85.
 69. Chuang HH, Prescott ED, Kong H, Shields S, Jordt SE, Basbaum AI, *et al.* Bradykinin and nerve growth factor release the capsaicin receptor from PtdIns(4,5)P2-mediated inhibition. *Nature.* 2001; 411: 957-62.
 70. Prescott ED, Julius D. A modular PIP2 binding site as a determinant of capsaicin receptor sensitivity. *Science.* 2003; 300: 1284-8.
 71. Patil MJ, Belugin S, Akopian AN. Chronic alteration in phosphatidylinositol 4,5-bisphosphate levels regulates capsaicin and mustard oil responses. *J Neurosci Res.* 2011; 89: 945-54.
 72. Cao E, Cordero-Morales JF, Liu B, Qin F, Julius D. TRPV1 Channels Are Intrinsically Heat Sensitive and Negatively Regulated by Phosphoinositide Lipids. *Neuron.* 2013; 77: 667-79.
 73. Jeske NA, Por ED, Belugin S, Chaudhury S, Berg KA, Akopian AN, *et al.* A-kinase anchoring protein 150 mediates transient receptor potential family V type 1 sensitivity to phosphatidylinositol-4,5-bisphosphate. *J Neurosci.* 2011; 31: 8681-8.

74. Mercado J, Gordon-Shaag A, Zagotta WN, Gordon SE. Ca²⁺-dependent desensitization of TRPV2 channels is mediated by hydrolysis of phosphatidylinositol 4,5-bisphosphate. *J Neurosci.* 2010;30:13338–47.
75. Doerner JF, Hatt H, Ramsey IS. Voltage-and temperature-dependent activation of TRPV3 channels is potentiated by receptor-mediated PI(4,5)P₂ hydrolysis. *J Gen Physiol.* 2011; 137: 271-88.
76. Garcia-Elias A, Mrkonjić S, Pardo-Pastor C, Inada H, Hellmich UA, Rubio-Moscardó F, et al. Phosphatidylinositol-4,5-bisphosphate-dependent rearrangement of TRPV4 cytosolic tails enables channel activation by physiological stimuli. *Proc Natl Acad Sci U S A.* 2013; 110: 9553-8.
77. Lee J, Cha SK, Sun TJ, Huang CL. PIP₂ activates TRPV5 and releases its inhibition by intracellular Mg²⁺. *J Gen Physiol.* 2005; 126: 439-51.
78. Thyagarajan B, Lukacs V, Rohacs T. Hydrolysis of phosphatidylinositol 4,5-bisphosphate mediates calcium-induced inactivation of TRPV6 channels. *J Biol Chem.* 2008; 283: 14980-7.
79. Zakharian E, Cao C, Rohacs T. Intracellular ATP supports TRPV6 activity via lipid kinases and the generation of PtdIns(4,5)P₂. *FASEB J.* 2011; 25: 3915-28. 80. Cao C, Zakharian E, Borbiri I, Rohacs T. Interplay between calmodulin and phosphatidylinositol 4,5-bisphosphate in Ca²⁺-induced inactivation of transient receptor potential vanilloid 6 channels. *J Biol Chem.* 2013; 288: 5278–90.
81. Saleh SN, Albert AP, Large WA. Activation of native TRPC1/C5/C6 channels by endothelin-1 is mediated by both PIP₃ and PIP₂ in rabbit coronary artery myocytes. *J Physiol.* 2009; 587: 5361-75.
82. Saleh SN, Albert AP, Large WA. Obligatory role for phosphatidylinositol 4,5-bisphosphate in activation of native TRPC1 store-operated channels in vascular myocytes. *J Physiol.* 2009; 587: 531-40.
83. Shi J, Ju M, Abramowitz J, Large WA, Birnbaumer L, Albert AP. TRPC1 proteins confer PKC and phosphoinositol activation on native heteromeric TRPC1/C5 channels in vascular smooth muscle: comparative study of wild-type and TRPC1 ^{-/-} mice. *FASEB J.* 2012; 26: 409-19.
84. Lemonnier L, Trebak M, Putney JW. Complex regulation of the TRPC3, 6 and 7 channel subfamily by diacylglycerol and phosphatidylinositol-4,5-bisphosphate. *Cell Calcium.* 2008; 43: 506-14.
85. Imai Y, Itsuki K, Okamura Y, Inoue R, Mori MX. A self-limiting regulation of vasoconstrictor-activated TRPC3/C6/C7 channels coupled to PI(4,5)P₂-diacylglycerol signalling. *J Physiol.* 2012; 590: 1101-19.
86. Itsuki K, Imai Y, Okamura Y, Abe K, Inoue R, Mori MX. Voltage-sensing phosphatase reveals temporal regulation of TRPC3/C6/C7 channels by membrane phosphoinositides. *Channels.* 2012; 6: 206-9.
87. Otsuguro KI, Tang J, Tang Y, Xiao R, Freichel M, Tsvilovskyy V, et al. Isoform-specific inhibition of TRPC4 channel by phosphatidylinositol 4,5-bisphosphate. *J Biol Chem.* 2008; 283: 10026-36.
88. Kim H, Jeon JP, Hong C, Kim J, Myeong J, Jeon JH, et al. An essential role of PI(4,5)P₂ for maintaining the activity of the transient receptor potential canonical (TRPC)4 β . *Pflugers Arch Eur J Physiol.* 2013; 465: 1011-21.
89. Trebak M, Lemonnier L, Dehaven WI, Wedel BJ, Bird GS, Putney JW. Complex functions of

- phosphatidylinositol 4,5-bisphosphate in regulation of TRPC5 cation channels. *Pflugers Arch Eur J Physiol.* 2009; 457: 757-69.
90. Kim BJ, Kim MT, Jeon JH, Kim SJ, So I. Involvement of phosphatidylinositol 4,5-bisphosphate in the desensitization of canonical transient receptor potential 5. *Biol Pharm Bull.* 2008; 31: 1733-8.
 91. Albert AP, Saleh SN, Large WA. Inhibition of native TRPC6 channel activity by phosphatidylinositol 4,5-bisphosphate in mesenteric artery myocytes. *J Physiol.* 2008; 586: 3087-95.
 92. Ju M, Shi J, Saleh SN, Albert AP, Large WA. Ins(1,4,5)P3 interacts with PIP2 to regulate activation of TRPC6/C7 channels by diacylglycerol in native vascular myocytes. *J Physiol.* 2010; 588: 1419–33.
 93. Jardín I, Redondo PC, Salido GM, Rosado JA. Phosphatidylinositol 4,5-bisphosphate enhances store-operated calcium entry through hTRPC6 channel in human platelets. *Biochim Biophys Acta - Mol Cell Res.* 2008; 1783: 84-97
 94. Kwon Y, Hofmann T, Montell C. Integration of Phosphoinositide- and Calmodulin-Mediated Regulation of TRPC6. *Mol Cell.* 2007; 25: 491-503.
 95. Akopian AN, Ruparel NB, Jeske NA, Hargreaves KM. Transient receptor potential TRPA1 channel desensitization in sensory neurons is agonist dependent and regulated by TRPV1-directed internalization. *J Physiol.* 2007; 583: 175-93.
 96. Karashima Y, Prenen J, Meseguer V, Owsianik G, Voets T, Nilius B. Modulation of the transient receptor potential channel TRPA1 by phosphatidylinositol 4,5-bisphosphate manipulators. *Pflugers Arch Eur J Physiol.* 2008; 457: 77-89.
 97. Dai Y, Wang S, Tominaga M, Yamamoto S, Fukuoka T, Higashi T, et al. Sensitization of TRPA1 by PAR2 contributes to the sensation of inflammatory pain. *J Clin Invest.* 2007; 117: 1979-87.
 98. Kim D, Cavanaugh EJ. Requirement of a soluble intracellular factor for activation of transient receptor potential A1 by pungent chemicals: Role of inorganic polyphosphates. *J Neurosci.* 2007; 27: 6500-9.
 99. Wang YY, Chang RB, Waters HN, McKemy DD, Liman ER. The nociceptor ion channel TRPA1 is potentiated and inactivated by permeating calcium ions. *J Biol Chem.* 2008; 283: 32691-703.
 100. Dong XP, Shen D, Wang X, Dawson T, Li X, Zhang Q, et al. PI(3,5)P2 controls membrane trafficking by direct activation of mucolipin Ca²⁺ release channels in the endolysosome. *Nat Commun.* 2010; 1: 1-21.
 101. Zhang X, Li X, Xu H. Phosphoinositide isoforms determine compartment-specific ion channel activity. *Proc Natl Acad Sci U S A.* 2012; 109: 11384-9.
 102. Ma R, Li W-P, Rundle D, Kong J, Akbarali HI, Tsiokas L. PKD2 Functions as an Epidermal Growth Factor-Activated Plasma Membrane Channel. *Mol Cell Biol.* 2005; 25: 8285-98.
 103. Karve TM, Cheema AK. Small changes huge impact: the role of protein posttranslational modifications in cellular homeostasis and disease. *J Amino Acids.* 2011; 2011: 1-13.
 104. Chang Q, Hoefs S, van der Kemp AW, Topala CN, Bindels RJ, Hoenderop JG. The beta-glucuronidase klotho hydrolyzes and activates the TRPV5 channel. *Science.* 2005;310:490–3.
 105. Dietrich A, Mederos y Schnitzler M, Emmel J, Kalwa H, Hofmann T, Gudermann T. *N*-Linked

- Protein Glycosylation Is a Major Determinant for Basal TRPC3 and TRPC6 Channel Activity. *J Biol Chem.* 2003;278:47842–52.
106. Pertusa M, Madrid R. Modulation of TRP Channels by N-glycosylation and Phosphorylation. In: *TRP Channels in Sensory Transduction.* Cham: Springer International Publishing; 2015;73–96.
 107. Xu H, Fu Y, Tian W, Cohen DM. Glycosylation of the osmoresponsive transient receptor potential channel TRPV4 on Asn-651 influences membrane trafficking. *Am J Physiol Physiol.* 2006;290:F1103–9.
 108. Voolstra O, Huber A. Post-Translational Modifications of TRP Channels. *Cells.* 2014;3:258–87.
 109. Yao X, Kwan H-Y, Huang Y. Regulation of TRP Channels by Phosphorylation. *Neurosignals.* 2005;14:273–80.
 110. Goswami C, Kuhn J, Dina OA, Fernández-Ballester G, Levine JD, Ferrer-Montiel A, et al. Estrogen destabilizes microtubules through an ion-conductivity-independent TRPV1 pathway. *J Neurochem.* 2011;117:995–1008.
 111. Takahashi N, Mori Y. TRP Channels as Sensors and Signal Integrators of Redox Status Changes. *Front Pharmacol.* 2011;2:1-11.
 112. Clark K, Middelbeek J, Vanleeuwen F. Interplay between TRP channels and the cytoskeleton in health and disease. *Eur J Cell Biol.* 2008; 87: 631–40.
 113. Smani T, Dionisio N, López JJ, Berna-Erro A, Rosado JA. Cytoskeletal and scaffolding proteins as structural and functional determinants of TRP channels. *Biochim Biophys Acta - Biomembr.* 2014;1838:658–64.
 114. Shimizu S, Yoshida T, Wakamori M, Ishii M, Okada T, Takahashi M, et al. Ca²⁺-calmodulin-dependent myosin light chain kinase is essential for activation of TRPC5 channels expressed in HEK293 cells. *J Physiol.* 2006; 570: 219-35.
 115. Goswami C, Kuhn J, Heppenstall PA, Hucho T. Importance of non-selective cation channel TRPV4 interaction with cytoskeleton and their reciprocal regulations in cultured cells. *PLoS One.* 2010;5:e11654.
 116. Li Q, Montalbetti N, Shen PY, Dai XQ, Cheeseman CI, Karpinski E, et al. Alpha-actinin associates with polycystin-2 and regulates its channel activity. *Hum Mol Genet.* 2005;14:1587–603.
 117. Li Q, Dai X-Q, Shen PY, Wu Y, Long W, Chen CX, et al. Direct binding of alpha-actinin enhances TRPP3 channel activity. *J Neurochem.* 2007;103:2391–400.
 118. Putney JW, Broad LM, Braun FJ, Lievreumont JP, Bird GSJ. Mechanisms of capacitative calcium entry. *J Cell Sci.* 2001; 114: 2223-9.
 119. Vandebrouck A, Sabourin J, Rivet J, Balghi H, Sebille S, Kitzis A, et al. Regulation of capacitative calcium entries by alpha1-syntrophin: association of TRPC1 with dystrophin complex and the PDZ domain of alpha1-syntrophin. *FASEB J.* 2007;21:608–17.
 120. Shin SH, Lee EJ, Hyun S, Chun J, Kim Y, Kang SS. Phosphorylation on the Ser 824 residue of TRPV4 prefers to bind with F-actin than with microtubules to expand the cell surface area. *Cell Signal.* 2012;24:641–51.
 121. Goswami C, Dreger M, Jahnel R, Bogen O, Gillen C, Hucho F. Ca²⁺ -sensitive interaction of the vanilloid receptor TRPV1 with tubulin. Identification and characterization of a. *J Neurochem.*

- 2004;91:1092–103.
122. Goswami C, Hucho TB, Hucho F. Identification and characterisation of novel tubulin-binding motifs located within the C-terminus of TRPV1. *J Neurochem.* 2007;101:250–62.
 123. Goswami C, Dreger M, Jahnel R, Bogen O, Gillen C, Hucho F. Identification and characterization of a Ca²⁺-sensitive interaction of the vanilloid receptor TRPV1 with tubulin. *J Neurochem.* 2004;91:1092–103.
 124. Goswami C, Dreger M, Otto H, Schwappach B, Hucho F. Rapid disassembly of dynamic microtubules upon activation of the capsaicin receptor TRPV1. *J Neurochem.* 2006;96:254–66.
 125. Goswami C, Schmidt H, Hucho F. TRPV1 at nerve endings regulates growth cone morphology and movement through cytoskeleton reorganization. *FEBS J.* 2007;274:760–72.
 126. Goswami C, Hucho T. TRPV1 expression-dependent initiation and regulation of filopodia. *J Neurochem.* 2007;103:1319–33.
 127. Andrés M, Göpfert MC. Neuronal osmotransduction: Push-activating TRPV1 with microtubules. *Developmental Cell.* 2014; 30: 363-4.
 128. Morales-Lázaro SL, Rosenbaum T. Cholesterol as a Key Molecule That Regulates TRPV1 Channel Function. *Adv Exp Med Biol.* 2019;1135:105–17.
 129. Liu M, Huang W, Wu D, Priestley J V. TRPV1, but not P2X, requires cholesterol for its function and membrane expression in rat nociceptors. *Eur J Neurosci.* 2006; 24:1-6.
 130. Szoke É, Börzsei R, Tóth DM, Lengl O, Helyes Z, Sándor Z, et al. Effect of lipid raft disruption on TRPV1 receptor activation of trigeminal sensory neurons and transfected cell line. *Eur J Pharmacol.* 2010; 628: 67-74.
 131. Saha S, Ghosh A, Tiwari N, Kumar A, Kumar A, Goswami C. Preferential selection of Arginine at the lipid-water-interface of TRPV1 during vertebrate evolution correlates with its snorkeling behaviour and cholesterol interaction. *Sci Rep.* 2017;7:1-21.
 132. Jansson ET, Trkulja CL, Ahemaiti A, Millingen M, Jeffries GDM, Jardemark K, et al. Effect of cholesterol depletion on the pore dilation of TRPV1. *Mol Pain.* 2013; 9:1-9.
 133. Morales-Lázaro SL, Rosenbaum T. Multiple Mechanisms of Regulation of Transient Receptor Potential Ion Channels by Cholesterol. In: *Current Topics in Membranes.* 2017; 80: 139-161.
 134. Naylor J, Li J, Milligan CJ, Zeng F, Sukumar P, Hou B, et al. Pregnenolone sulphate-and cholesterol-regulated TRPM3 channels coupled to vascular smooth muscle secretion and contraction. *Circ Res.* 2010; 106: 1507-15.
 135. Sun Y, Sukumaran P, Varma A, Derry S, Sahnoun AE, Singh BB. Cholesterol-induced activation of TRPM7 regulates cell proliferation, migration, and viability of human prostate cells. *Biochim Biophys Acta - Mol Cell Res.* 2014; 1843: 1839-50.
 136. Morenilla-Palao C, Pertusa M, Meseguer V, Cabedo H, Viana F. Lipid raft segregation modulates TRPM8 channel activity. *J Biol Chem.* 2009;284:9215–24.
 137. Veliz LA, Toro CA, Vivar JP, Arias LA, Villegas J, Castro MA, et al. Near-membrane dynamics and capture of TRPM8 channels within transient confinement domains. *PLoS One.* 2010; 5: e13290.
 138. Klein AS, Tannert A, Schaefer M. Cholesterol sensitises the transient receptor potential channel

- TRPV3 to lower temperatures and activator concentrations. *Cell Calcium*. 2014; 55: 59-68.
139. Kumari S, Kumar A, Sardar P, Yadav M, Majhi RK, Kumar A, et al. Influence of membrane cholesterol in the molecular evolution and functional regulation of TRPV4. *Biochem Biophys Res Commun*. 2015;456:312–319.
 140. Das R, Goswami C. TRPV4 expresses in bone cell lineages and TRPV4-R616Q mutant causing Brachyolmia in human reveals “loss-of-interaction” with cholesterol. *Biochem Biophys Res Commun*. 2019; 517: 566-574.
 141. Morales-Lázaro SL, Lemus L, Rosenbaum T. Regulation of thermoTRPs by lipids. *Temperature*. 2017; 4: 24-40.
 142. Yadav M, Saha S, Kumar A, Goswami C. Biological Research and Reviews Plant and natural products as modulators of TRP channels. 2019; 1: e1363.
 143. Fattori V, Hohmann MSN, Rossaneis AC, Pinho-Ribeiro FA, Verri WA. Capsaicin: Current understanding of its mechanisms and therapy of pain and other pre-clinical and clinical uses. *Molecules*. 2016; 21:1-33.
 144. Caterina MJ, Schumacher MA, Tominaga M, Rosen TA, Levine JD, Julius D. The capsaicin receptor: A heat-activated ion channel in the pain pathway. *Nature*. 1997; 389: 816–24.
 145. Yang F, Zheng J. Understand spiciness: mechanism of TRPV1 channel activation by capsaicin. *Protein and Cell*. 2017; 8: 169-177.
 146. Caterina MJ, Schumacher MA, Tominaga M, Rosen TA, Levine JD, Julius D. The capsaicin receptor: a heat-activated ion channel in the pain pathway. *Nature*. 1997;389:816–24.
 147. Muller C, Morales P, Reggio PH. Cannabinoid ligands targeting TRP channels. *Frontiers in Molecular Neuroscience*. 2019; 11: 1-15.
 148. Siemens J, Zhou S, Piskorowski R, Nikai T, Lumpkin EA, Basbaum AI, et al. Spider toxins activate the capsaicin receptor to produce inflammatory pain. *Nature*. 2006; 444: 208-12.
 149. Monastyrnaya M, Peigneur S, Zelepuga E, Sintsova O, Gladkikh I, Leychenko E, et al. Kunitz-Type peptide HCRG21 from the sea anemone *heteractis crispa* is a full antagonist of the TRPV1 receptor. *Mar Drugs*. 2016; 14: 1-20.
 150. Bohlen CJ, Priel A, Zhou S, King D, Siemens J, Julius D. A bivalent tarantula toxin activates the capsaicin receptor, TRPV1, by targeting the outer pore domain. *Cell*. 2010; 141: 834-45.
 151. Yang S, Yang F, Wei N, Hong J, Li B, Luo L, et al. A pain-inducing centipede toxin targets the heat activation machinery of nociceptor TRPV1. *Nat Commun*. 2015;6: 1-11.
 152. Geron M, Hazan A, Priel A. Animal toxins providing insights into TRPV1 activation mechanism. *Toxins*. 2017; 9: 1-19.
 153. Kitaguchi T, Swartz KJ. An inhibitor of TRPV1 channels isolated from funnel web spider venom. *Biochemistry*. 2005; 44: 15544-49.
 154. Bowen C V., DeBay D, Ewart HS, Gallant P, Gormley S, Ilenchuk TT, et al. In Vivo Detection of Human TRPV6-Rich Tumors with Anti-Cancer Peptides Derived from Soricidin. *PLoS One*. 2013; 8: e58866.
 155. Siemens J, Hanack C. Modulation of TRP ion channels by venomous toxins. *Handb Exp Pharmacol*. 2014; 223: 1119-42.

156. Lin King J V., Emrick JJ, Kelly MJS, Herzig V, King GF, Medzihradzky KF, et al. A Cell-Penetrating Scorpion Toxin Enables Mode-Specific Modulation of TRPA1 and Pain. *Cell*. 2019; 178: 1362-1374.
157. Togashi K, Inada H, Tominaga M. Inhibition of the transient receptor potential cation channel TRPM2 by 2-aminoethoxydiphenyl borate (2-APB). *Br J Pharmacol*. 2008; 153: 1324-30.
158. Harteneck C, Klose C, Krautwurst D. Synthetic modulators of TRP channel activity. *Adv Exp Med Biol*. 2011;704:87–106.
159. Numata T, Kiyonaka S, Kato K, Takahashi N, Mori Y. Activation of TRP Channels in Mammalian Systems 2014; 1–28..
160. Holzer P. Acid-sensitive ion channels and receptors. *Handbook of Experimental Pharmacology*. 2009; 194: 283-332.
161. Pattison LA, Callejo G, St John Smith E. Evolution of acid nociception: ion channels and receptors for detecting acid. *Philos Trans R Soc B Biol Sci*. 2019;374:1-16.
162. Chang RB, Waters H, Liman ER. A proton current drives action potentials in genetically identified sour taste cells. *Proc Natl Acad Sci U S A*. 2010; 107: 22320-5.
163. Jiang J, Li M, Yue L. Potentiation of TRPM7 inward currents by protons. *J Gen Physiol*. 2005;126:137–50.
164. De La Roche J, Eberhardt MJ, Klinger AB, Stanslowsky N, Wegner F, Koppert W, et al. The molecular basis for species-specific activation of human TRPA1 protein by protons involves poorly conserved residues within transmembrane domains 5 and 6. *J Biol Chem*. 2013;288:20280–92.
165. Startek JB, Boonen B, Talavera K, Meseguer V. TRP channels as sensors of chemically-induced changes in cell membrane mechanical properties. *International Journal of Molecular Sciences*. 2019; 20: 1-20.
166. Liu C, Montell C. Forcing open TRP channels: Mechanical gating as a unifying activation mechanism. *Biochemical and Biophysical Research Communications*. 2015. 460: 22-25.
167. Liedtke W, Tobin DM, Bargmann CI, Friedman JM. Mammalian TRPV4 (VR-OAC) directs behavioral responses to osmotic and mechanical stimuli in *Caenorhabditis elegans*. *Proc Natl Acad Sci U S A*. 2003; 100: 14531-14536.
168. Ranade SS, Syeda R, Patapoutian A. Mechanically Activated Ion Channels. *Neuron*. 2015;87:1162–79.
169. Prager-Khoutorsky M, Khoutorsky A, Bourque CW. Unique Interweaved Microtubule Scaffold Mediates Osmosensory Transduction via Physical Interaction with TRPV1. *Neuron*. 2014; 83: 866-78.
170. Dhaka A, Viswanath V, Patapoutian A. TRP ion channels and temperature sensation. *Annu Rev Neurosci*. 2006; 29: 135-61.
171. Katanosaka K, Takatsu S, Mizumura K, Naruse K, Katanosaka Y. TRPV2 is required for mechanical nociception and the stretch-evoked response of primary sensory neurons. *Sci Rep*. 2018;8: 1-10.
172. Park U, Vastani N, Guan Y, Raja SN, Koltzenburg M, Caterina MJ. TRP vanilloid 2 knock-out mice are susceptible to perinatal lethality but display normal thermal and mechanical nociception.

- J Neurosci. 2011; 31: 11425-36.
173. Moqrich A, Hwang SW, Earley TJ, Petrus MJ, Murray AN, Spencer KSR, et al. Impaired thermosensation in mice lacking TRPV3, a heat and camphor sensor in the skin. *Science* 2005; 307: 1468-72.
 174. Lamas JA, Rueda-Ruzafa L, Herrera-Pérez S. Ion Channels and Thermosensitivity: TRP, TREK, or Both? *International journal of molecular sciences*. 2019; 20: 1-16.
 175. Wang H, Siemens J. TRP ion channels in thermosensation, thermoregulation and metabolism. *Temperature*. 2015; 2: 178–187.
 176. Parra A, Madrid R, Echevarria D, Del Olmo S, Morenilla-Palao C, Acosta MC, et al. Ocular surface wetness is regulated by TRPM8-dependent cold thermoreceptors of the cornea. *Nat Med*. 2010; 16: 1396-9.
 177. Story GM, Peier AM, Reeve AJ, Eid SR, Mosbacher J, Hricik TR, et al. ANKTM1, a TRP-like channel expressed in nociceptive neurons, is activated by cold temperatures. *Cell*. 2003; 112: 819-29.
 178. Kwan KY, Allchorne AJ, Vollrath MA, Christensen AP, Zhang DS, Woolf CJ, et al. TRPA1 Contributes to Cold, Mechanical, and Chemical Nociception but Is Not Essential for Hair-Cell Transduction. *Neuron*. 2006; 50: 277-89.
 179. Vandewauw I, De Clercq K, Mulier M, Held K, Pinto S, Van Ranst N, et al. Correction: A TRP channel trio mediates acute noxious heat sensing. *Nature*. 2018; 555: 662-666.
 180. Moparathi L, Kichko TI, Eberhardt M, Högestätt ED, Kjellbom P, Johanson U, et al. Human TRPA1 is a heat sensor displaying intrinsic U-shaped thermosensitivity. *Sci Rep*. 2016;6: 1-10.
 181. Laursen WJ, Anderson EO, Hoffstaetter LJ, Bagriantsev SN, Gracheva EO. Species-specific temperature sensitivity of TRPA1. *Temperature*. 2015; 2: 214-26.
 182. Gordon-Shaag A, Zagotta WN, Gordon SE. Channels Mechanism of Ca²⁺-dependent desensitization in TRP channels. 2008; 2: 125-9.
 183. Hasan R, Zhang X. Ca²⁺ Regulation of TRP Ion Channels. *Int J Mol Sci*. 2018;19: 1-16.
 184. Hemenway CS, Heitman J. Calcineurin. Structure, function, and inhibition. *Cell Biochem Biophys*. 1999;30:115–51.
 185. Numazaki M, Tominaga T, Takeuchi K, Murayama N, Toyooka H, Tominaga M. Structural determinant of TRPV1 desensitization interacts with calmodulin. *Proc Natl Acad Sci U S A*. 2003; 100: 8002-6.
 186. Xiao R, Tang J, Wang C, Colton CK, Tian J, Zhu MX. Calcium plays a central role in the sensitization of TRPV3 channel to repetitive stimulations. *J Biol Chem*. 2008; 283: 6162-74.
 187. Plant TD, Strotmann R. TRPV4: A Multifunctional Nonselective Cation Channel with Complex Regulation. *TRP Ion Channel Function in Sensory Transduction and Cellular Signaling Cascades*. 2007; Chapter 9.
 188. Kim J-B. Channelopathies. *Korean J Pediatr*. 2014;57:1.
 189. Nilius B, Szallasi A. Transient receptor potential channels as drug targets: From the science of basic research to the art of medicine. *Pharmacol Rev*. 2014;66:676–814.
 190. Nilius B, Owsianik G. Transient receptor potential channelopathies. *Pflugers Archiv European*

- Journal of Physiology. 2010; 460: 437-450.
191. Canales J, Morales D, Blanco C, Rivas J, Diaz N, Angelopoulos I, et al. A tr(i)p to cell migration: New roles of trp channels in mechanotransduction and cancer. *Front Physiol.* 2019;10:1-14.
 192. Lee WH, Choong LY, Mon NN, Lu S, Lin Q, Pang B, et al. TRPV4 regulates breast cancer cell extravasation, stiffness and actin cortex. *Sci Rep.* 2016; 6:1-16.
 193. Monet M, Lehen'kyi V, Gackiere F, Firlej V, Vandenberghe M, Roudbaraki M, et al. Role of cationic channel TRPV2 in promoting prostate cancer migration and progression to androgen resistance. *Cancer Res.* 2010; 70: 1225-35.
 194. Chen Z, Zhu Y, Dong Y, Zhang P, Han X, Jin J, et al. Overexpression of TrpC5 promotes tumor metastasis via the HIF-1 α -Twist signaling pathway in colon cancer. *Clin Sci.* 2017; 131: 2439-2450.
 195. Parenti A, De Logu F, Geppetti P, Benemei S. What is the evidence for the role of TRP channels in inflammatory and immune cells? *British Journal of Pharmacology.* 2016; 173: 953-69.
 196. Moiseenkova-Bell VY, Stanciu LA, Serysheva II, Tobe BJ, Wensel TG. Structure of TRPV1 channel revealed by electron cryomicroscopy. *Proc Natl Acad Sci U S A.* 2008;105:7451-5.
 197. Liao M, Cao E, Julius D, Cheng Y. Structure of the TRPV1 ion channel determined by electron cryo-microscopy. *Nature.* 2013; 504: 107-12.
 198. Cao E, Liao M, Cheng Y, Julius D. TRPV1 structures in distinct conformations reveal activation mechanisms. *Nature.* 2013;504:113-8.
 199. Gao Y, Cao E, Julius D, Cheng Y. TRPV1 structures in nanodiscs reveal mechanisms of ligand and lipid action. *Nature.* 2016;534:347-51.
 200. Du Q, Liao Q, Chen C, Yang X, Xie R, Xu J. The Role of Transient Receptor Potential Vanilloid 1 in Common Diseases of the Digestive Tract and the Cardiovascular and Respiratory System. *Frontiers in Physiology.* Frontiers Media S.A. 2019; 10: 1-17.
 201. Reinach PS, Mergler S, Okada Y, Saika S. Ocular transient receptor potential channel function in health and disease. *BMC Ophthalmol.* 2015;15: 29-40..
 202. Ramírez-Barrantes R, Cordova C, Poblete H, Muñoz P, Marchant I, Wianny F, et al. Perspectives of TRPV1 Function on the Neurogenesis and Neural Plasticity. Vol. 2016, *Neural Plasticity.* Hindawi Publishing Corporation; 2016; 2016: 1-12.
 203. El Karim IA, Linden GJ, Curtis TM, About I, McGahon MK, Irwin CR, et al. Human odontoblasts express functional thermo-sensitive TRP channels: Implications for dentin sensitivity. *Pain.* 2011;152:2211-23.
 204. Frias B, Merighi A. Capsaicin, nociception and pain. *Molecules.* 2016; 21: 1-33.
 205. Morenilla-Palao C, Planells-Cases R, García-Sanz N, Ferrer-Montiel A. Regulated exocytosis contributes to protein kinase C potentiation of vanilloid receptor activity. *J Biol Chem.* 2004;279:25665-72.
 206. Turner H, Fleig A, Stokes A, Kinet JP, Penner R. Discrimination of intracellular calcium store sub-compartments using TRPV1 release channel activity. *Biochem J.* 2003; 371, 341-350.
 207. Haustrate, Prevarskaya, Lehen'kyi. Role of the TRPV Channels in the Endoplasmic Reticulum Calcium Homeostasis. *Cells.* 2020;9: 1-8..

208. Miyake T, Shirakawa H, Nakagawa T, Kaneko S. Activation of mitochondrial transient receptor potential vanilloid 1 channel contributes to microglial migration. *Glia*. 2015;63:1870–82.
209. Caterina MJ, Leffler A, Malmberg AB, Martin WJ, Trafton J, Petersen-Zeitl KR, et al. Impaired nociception and pain sensation in mice lacking the capsaicin receptor. *Science*. 2000; 288: 306-313.
210. Zhao R, Tsang SY. Versatile Roles of Intracellularly Located TRPV1 Channel. Vol. 232, *Journal of Cellular Physiology*. Wiley-Liss Inc.; 2017; 232: 1957-1965.
211. Wick EC, Hoge SG, Grahn SW, Kim E, Divino LA, Grady EF, et al. Transient receptor potential vanilloid 1, calcitonin gene-related peptide, and substance P mediate nociception in acute pancreatitis. *Am J Physiol - Gastrointest Liver Physiol*. 2006;290:G959-69.
212. Takahashi N, Matsuda Y, Sato K, De Jong PR, Bertin S, Tabeta K, et al. Neuronal TRPV1 activation regulates alveolar bone resorption by suppressing osteoclastogenesis via CGRP. *Sci Rep*. 2016;6:1–11.
213. Zhong B, Ma S, Wang DH. TRPV1 mediates glucose-induced insulin secretion through releasing neuropeptides. *In Vivo (Brooklyn)*. 2019;33:1431–7.
214. Fernandes ES, Fernandes MA, Keeble JE. The functions of TRPA1 and TRPV1: Moving away from sensory nerves. Vol. 166, *British Journal of Pharmacology*. John Wiley and Sons Inc.; 2012; 166: 510–21.
215. Jiang M, Li H, Johnson A, Karasawa T, Zhang Y, Meier WB, et al. Inflammation up-regulates cochlear expression of TRPV1 to potentiate drug-induced hearing loss. *Sci Adv*. 2019;5:1-14.
216. Brito R, Sheth S, Mukherjea D, Rybak L, Ramkumar V. TRPV1: A Potential Drug Target for Treating Various Diseases. *Cells*. 2014; 3: 517-45.
217. Storozhuk M V., Moroz OF, Zholos A V. Multifunctional TRPV1 Ion Channels in Physiology and Pathology with Focus on the Brain, Vasculature, and Some Visceral Systems. *BioMed Research International*. 2019; 2019: 1-13.
218. Martins D, Tavares I, Morgado C. “hotheaded”: The role of TRPV1 in brain functions. *Neuropharmacology*. 2014; 85:151-157.
219. Storti B, Bizzarri R, Cardarelli F, Beltrami F. Intact microtubules preserve transient receptor potential vanilloid 1 (TRPV1) functionality through receptor binding. *J Biol Chem*. 2012;287:7803–11.
220. Wong CO, Chen K, Lin YQ, Chao Y, Duraine L, Lu Z, et al. A TRPV channel in drosophila motor neurons regulates presynaptic resting Ca²⁺ levels, synapse growth, and synaptic transmission. *Neuron*. 2014;84:764–77.
221. Picazo-Juárez G, Romero-Suárez S, Nieto-Posadas AS, Llorente I, Jara-Oseguera AS, Briggs M, et al. Identification of a binding motif in the S5 helix that confers cholesterol sensitivity to the TRPV1 ion channel. *J Biol Chem*. 2011; 286: 24966-76.
222. Liu B, Hui K, Qin F. Thermodynamics of Heat Activation of Single Capsaicin Ion Channels VR1. *Biophys J*. 2003;85:2988–3006.
223. Iwasaki Y, Tamura Y, Inayoshi K, Narukawa M, Kobata K, Chiba H, et al. TRPV1 agonist monoacylglycerol increases UCP1 content in brown adipose tissue and suppresses accumulation of visceral fat in mice fed a high-fat and high-sucrose diet. *Biosci Biotechnol Biochem*. 2011;75:904–

9.

224. Ma L, Zhong J, Zhao Z, Luo Z, Ma S, Sun J, et al. Activation of TRPV1 reduces vascular lipid accumulation and attenuates atherosclerosis. *Cardiovasc Res.* 2011;92:504–13.
225. Wang GY, Wang LL, Xu B, Zhang J Bin, Jiang JF. Effects of moxibustion temperature on blood cholesterol level in a mice model of acute hyperlipidemia: Role of TRPV1. *Evidence-based Complement Altern Med.* 2013; 2013: 1-8.
226. Harb AA, Bustanji YK, Almasri IM, Abdalla SS. Eugenol Reduces LDL Cholesterol and Hepatic Steatosis in Hypercholesterolemic Rats by Modulating TRPV1 Receptor. *Sci Rep.* 2019;9:1–10.
227. Paulsen CE, Armache JP, Gao Y, Cheng Y, Julius D. Structure of the TRPA1 ion channel suggests regulatory mechanisms. *Nature.* 2015;520:511–7.
228. Nilius B, Prenen J, Owsianik G. Irritating channels: The case of TRPA1. *Journal of Physiology.* 2011; 589: 1543–1549.
229. Cvetkov TL, Huynh KW, Cohen MR, Moiseenkova-Bell VY. Molecular architecture and subunit organization of TRPA1 ion channel revealed by electron microscopy. *J Biol Chem.* 2011;286:38168–76.
230. Wang L, Cvetkov TL, Chance MR, Moiseenkova-Bell VY. Identification of in vivo disulfide conformation of TRPA1 ion channel. *J Biol Chem.* 2012; 287: 6169-76.
231. Ye W, Tu YH, Cooper AJ, Zhang Z, Katritch V, Liman ER. Activation Stoichiometry and Pore Architecture of TRPA1 Probed with Channel Concatemers. *Sci Rep.* 2018;8: 1-12..
232. Zurborg S, Yurgionas B, Jira JA, Caspani O, Heppenstall PA. Direct activation of the ion channel TRPA1 by Ca²⁺. *Nat Neurosci.* 2007; 10: 277-9.
233. Okada Y, Shirai K, Reinach PS, Kitano-Izutani A, Miyajima M, Flanders KC, et al. TRPA1 is required for TGF- β signaling and its loss blocks inflammatory fibrosis in mouse corneal stroma. *Lab Invest.* 2014;94:1030–41.
234. Gratzke C, Streng T, Waldkirch E, Sigl K, Stief C, Andersson KE, et al. Transient Receptor Potential A1 (TRPA1) Activity in the Human Urethra-Evidence for a Functional Role for TRPA1 in the Outflow Region. *Eur Urol.* 2009; 55: 696-704.
235. Kaji I, Yasuoka Y, Karaki SI, Kuwahara A. Activation of TRPA1 by luminal stimuli induces EP 4-mediated anion secretion in human and rat colon. *Am J Physiol - Gastrointest Liver Physiol.* 2012; 302: G690-701.
236. Nassini R, Pedretti P, Moretto N, Fusi C, Carnini C, Facchinetti F, et al. Transient receptor potential ankyrin 1 channel localized to non-neuronal airway cells promotes non-neurogenic inflammation. *PLoS One.* 2012;7:e42454.
237. Cao DS, Zhong L, Hsieh T han, Abooj M, Bishnoi M, Hughes L, et al. Expression of transient receptor potential ankyrin 1 (TRPA1) and its role in insulin release from rat pancreatic beta cells. *PLoS One.* 2012;7 e38005.
238. Shigetomi E, Tong X, Kwan KY, Corey DP, Khakh BS. TRPA1 channels regulate astrocyte resting calcium and inhibitory synapse efficacy through GAT-3. *Nat Neurosci.* 2012;15:70–80.
239. Viana F. TRPA1 channels: molecular sentinels of cellular stress and tissue damage. *J Physiol.* 2016; 594: 4151-69.

240. Sahoo SS, Majhi RK, Tiwari A, Acharya T, Kumar PS, Saha S, et al. Transient receptor potential ankyrin1 channel is endogenously expressed in T cells and is involved in immune functions. *Biosci Rep*. 2019;391-16.
241. Macpherson LJ, Dubin AE, Evans MJ, Marr F, Schultz PG, Cravatt BF, et al. Noxious compounds activate TRPA1 ion channels through covalent modification of cysteines. *Nature*. 2007;445:541–5.
242. Takahashi N, Kuwaki T, Kiyonaka S, Numata T, Kozai D, Mizuno Y, et al. TRPA1 underlies a sensing mechanism for O₂. *Nat Chem Biol*. 2011; 7: 701-11.
243. Takahashi N, Chen HY, Harris IS, Stover DG, Selfors LM, Bronson RT, et al. Cancer Cells Co-opt the Neuronal Redox-Sensing Channel TRPA1 to Promote Oxidative-Stress Tolerance. *Cancer Cell*. 2018; 33: 985-1003.
244. Andersson DA, Gentry C, Bevan S. TRPA1 Has a Key Role in the Somatic Pro-Nociceptive Actions of Hydrogen Sulfide. *PLoS One*. 2012; 7: e46917.
245. Guntur AR, Gu P, Takle K, Chen J, Xiang Y, Yang CH. Drosophila TRPA1 isoforms detect UV light via photochemical production of H₂O₂. *Proc Natl Acad Sci U S A*. 2015; 112: E5753–61.
246. Nesuashvili L, Hadley SH, Bahia PK, Taylor-Clark TE. Sensory nerve terminal mitochondrial dysfunction activates airway sensory nerves via transient receptor potential (TRP) channels. *Mol Pharmacol*. 2013;83:1007–19.
247. Wang YY, Chang RB, Liman ER. TRPA1 is a component of the nociceptive response to CO₂. *J Neurosci*. 2010;30:12958–63.
248. Nassini R, Materazzi S, Benemei S, Geppetti P. The TRPA1 channel in inflammatory and Neuropathic pain and migraine. *Rev Physiol Biochem Pharmacol*. 2014;167:1–44.
249. Bandell M, Story GM, Hwang SW, Viswanath V, Eid SR, Petrus MJ, et al. Noxious cold ion channel TRPA1 is activated by pungent compounds and bradykinin. *Neuron*. 2004; 41: 849-57.
250. Jordt SE, Bautista DM, Chuang HH, McKemy DD, Zygmunt PM, Högestätt ED, et al. Mustard oils and cannabinoids excite sensory nerve fibres through the TRP channel ANKTM1. *Nature*. 2004; 427: 260-5.
251. Nagata K. Nociceptor and Hair Cell Transducer Properties of TRPA1, a Channel for Pain and Hearing. *J Neurosci*. 2005; 25: 4052-61.
252. Saito S, Nakatsuka K, Takahashi K, Fukuta N, Imagawa T, Ohta T, et al. Analysis of transient receptor potential ankyrin 1 (TRPA1) in frogs and lizards illuminates both nociceptive heat and chemical sensitivities and coexpression with TRP vanilloid 1 (TRPV1) in ancestral vertebrates. *J Biol Chem*. 2012; 287: 30743-54.
253. Viswanath V, Story GM, Peier AM, Petrus MJ, Lee VM, Hwang SW, et al. Opposite thermosensor in fruitfly and mouse. *Nature*. 2003; 423: 822-3.
254. Gracheva EO, Ingolia NT, Kelly YM, Cordero-Morales JF, Hollopeter G, Chesler AT, et al. Molecular basis of infrared detection by snakes. *Nature*. 2010; 464: 1006-11.
255. Prober DA, Zimmerman S, Myers BR, McDermott BM, Kim SH, Caron S, et al. Zebrafish TRPA1 channels are required for chemosensation but not for thermosensation or mechanosensory hair cell function. *J Neurosci*. 2008;28:10102–10.
256. Motter AL, Ahern GP. TRPA1 is a polyunsaturated fatty acid sensor in mammals. *PLoS One*. 2012;

7: e38439.

257. Kindt KS, Viswanath V, Macpherson L, Quast K, Hu H, Patapoutian A, et al. Caenorhabditis elegans TRPA-1 functions in mechanosensation. *Nat Neurosci.* 2007; 10: 568-77.
258. Wang S, Lee J, Ro JY, Chung MK. Warmth suppresses and desensitizes damage-sensing ion channel TRPA1. *Mol Pain.* 2012;8: 1-9.
259. Meseguer V, Alpizar YA, Luis E, Tajada S, Denlinger B, Fajardo O, et al. TRPA1 channels mediate acute neurogenic inflammation and pain produced by bacterial endotoxins. *Nat Commun.* 2014;5:1-14.
260. Moilanen LJ, Hämäläinen M, Nummenmaa E, Ilmarinen P, Vuolteenaho K, Nieminen RM, et al. Monosodium iodoacetate-induced inflammation and joint pain are reduced in TRPA1 deficient mice - potential role of TRPA1 in osteoarthritis. *Osteoarthr Cartil.* 2015; 23: 2017-26.
261. Benemei S, Dussor G. TRP channels and migraine: Recent developments and new therapeutic opportunities. *Pharmaceuticals.* 2019; 12:1-17.
262. Sághy É, Szoke É, Payrits M, Helyes Z, Börzsei R, Erostyák J, et al. Evidence for the role of lipid rafts and sphingomyelin in Ca²⁺-gating of Transient Receptor Potential channels in trigeminal sensory neurons and peripheral nerve terminals. *Pharmacol Res.* 2015;100:101-16.
263. Zhao JF, Shyue SK, Kou YR, Lu TM, Lee TS. Transient receptor potential ankyrin 1 channel involved in atherosclerosis and macrophage-foam cell formation. *Int J Biol Sci.* 2016;12:812-23.
264. Startek JB, Boonen B, López-Requena A, Talavera A, Alpizar YA, Ghosh D, et al. Mouse TRPA1 function and membrane localization are modulated by direct interactions with cholesterol. *Elife.* 2019;8: 1-24.
265. Yue Z, Xie J, Yu AS, Stock J, Du J, Yue L. Role of trp channels in the cardiovascular system. *Am J Physiol - Hear Circ Physiol.* 2015; 308: H157-H182.
266. Bertin S, Aoki-Nonaka Y, Lee J, De Jong PR, Kim P, Han T, et al. The TRPA1 ion channel is expressed in CD4⁺ t cells and restrains T-cell-mediated colitis through inhibition of TRPV1. *Gut.* 2017; 66:1584-1596.
267. Staruschenko A, Jeske NA, Akopian AN. Contribution of TRPV1-TRPA1 interaction to the single channel properties of the TRPA1 channel. *J Biol Chem.* 2010; 285: 15167-15177.
268. Salas MM, Hargreaves KM, Akopian AN. TRPA1-mediated responses in trigeminal sensory neurons: Interaction between TRPA1 and TRPV1. *Eur J Neurosci.* 2009; 29:1568-1578.
269. Chen TW, Wardill TJ, Sun Y, Pulver SR, Renninger SL, Baohan A, et al. Ultrasensitive fluorescent proteins for imaging neuronal activity. *Nature.* 2013;499:295-300.
270. Killian JA, Von Heijne G. How proteins adapt to a membrane-water interface. *Trends in Biochemical Sciences.* 2000; 25: 429-34.
271. Hübner W, Blume A. Interactions at the lipid-water interface. *Chem Phys Lipids.* 1998; 96, 1-164.
272. Krieger E, Joo K, Lee J, Lee J, Raman S, Thompson J, et al. Improving physical realism, stereochemistry, and side-chain accuracy in homology modeling: Four approaches that performed well in CASP8. *Proteins: Structure, Function and Bioinformatics.* 2009; 77: 114-22.
273. Canutescu AA, Shelenkov AA, Dunbrack RL. A graph-theory algorithm for rapid protein side-chain prediction. *Protein Sci.* 2003;12:2001-14.

274. Granseth E, Von Heijne G, Elofsson A. A study of the membrane-water interface region of membrane proteins. *J Mol Biol.* 2005; 346: 377-85.
275. Yoo J, Cui Q. Does arginine remain protonated in the lipid membrane? Insights from microscopic pKa calculations. *Biophys J.* 2008; 94: L61-3.
276. Rothman JE, Lenard J. Membrane asymmetry. *Science.* 1977; 195: 743-53.
277. Baker JA, Wong WC, Eisenhaber B, Warwicker J, Eisenhaber F. Charged residues next to transmembrane regions revisited: “Positive-inside rule” is complemented by the “negative inside depletion/outside enrichment rule.” *BMC Biol.* 2017;15:1-29.
278. Wimley WC, White SH. Experimentally determined hydrophobicity scale for proteins at membrane interfaces. *Nature Structural Biology.* 1996; 3: 842-848.
279. Eaton SB. Evolution and cholesterol. *World Rev Nutr Diet.* 2009; 100: 46-54.
280. Alexander C, Day CE. Distribution of serum lipoproteins of selected vertebrates. *Comp Biochem Physiol -- Part B Biochem.* 1973; 46: 295-312.
281. Miao L, Nielsen M, Thewalt J, Ipsen JH, Bloom M, Zuckermann MJ, et al. From lanosterol to cholesterol: Structural evolution and differential effects on lipid bilayers. *Biophys J.* 2002; 82: 1429-44.
282. Yoshida A, Furube E, Mannari T, Takayama Y, Kittaka H, Tominaga M, et al. TRPV1 is crucial for proinflammatory STAT3 signaling and thermoregulation-associated pathways in the brain during inflammation. *Sci Rep.* 2016; 6: 1-11.
283. Alawi KM, Aubdool AA, Liang L, Wilde E, Vepa A, Psefteli MP, et al. The sympathetic nervous system is controlled by transient receptor potential vanilloid 1 in the regulation of body temperature. *FASEB J.* 2015; 29: 4285-98.
284. Billen LP, Shamas-Din A, Andrews DW. Bid: A Bax-like BH3 protein. *Oncogene.* 2008; 27: S93–S104.
285. Sehgal P, Szalai P, Olesen C, Praetorius HA, Nissen P, Christensen SB, et al. Inhibition of the sarco/endoplasmic reticulum (ER) Ca²⁺-ATPase by thapsigargin analogs induces cell death via ER Ca²⁺ depletion and the unfolded protein response. *J Biol Chem.* 2017; 292: 19656–19673.
286. Pastor-Soler N. Role of Acid/Base Transporters in the Male Reproductive Tract and Potential Consequences of Their Malfunction. *Physiology.* 2005; 20: 417-28.
287. Kavanagh JP. Sodium, potassium, calcium, magnesium, zinc, citrate and chloride content of human prostatic and seminal fluid. *J Reprod Fertil.* 1985; 75: 35-41.
288. Suarez SS, Pacey AA. Sperm transport in the female reproductive tract. *Human Reproduction Update.* 2006; 12: 23–37.
289. Hamamah S, Gatti JL. Role of the ionic environment and internal pH on sperm activity. In: *Human Reproduction.* 1998; 13: 20–30.
290. Mundt N, Spehr M, Lishko P V. TRPV4 is the temperature-sensitive ion channel of human sperm. *Elife.* 2018;7: 1-20.
291. Lishko P V., Botchkina IL, Fedorenko A, Kirichok Y. Acid Extrusion from Human Spermatozoa Is Mediated by Flagellar Voltage-Gated Proton Channel. *Cell.* 2010; 140: 327-37.
292. Wang D, Hu J, Bobulescu IA, Quill T a, McLeroy P, Moe OW, et al. A sperm-specific Na⁺/H⁺

- exchanger (sNHE) is critical for expression and in vivo bicarbonate regulation of the soluble adenylyl cyclase (sAC). *Proc Natl Acad Sci U S A*. 2007; 104: 9325-30.
293. Demarco IA, Espinosa F, Edwards J, Sosnik J, De La Vega-Beltrá L, Hockensmith JW, et al. Involvement of a Na⁺/HCO₃⁻ Cotransporter in Mouse Sperm Capacitation*. *J Biol Chem*. 2002; 278: 7001-9.
 294. Lishko P V., Botchkina IL, Kirichok Y. Progesterone activates the principal Ca²⁺ channel of human sperm. *Nature*. 2011; 471: 387-91.
 295. Strünker T, Goodwin N, Brenker C, Kashikar ND, Weyand I, Seifert R, et al. The CatSper channel mediates progesterone-induced Ca²⁺ influx in human sperm. *Nature*. 2011; 471: 382–386.
 296. Zeng X-H, Navarro B, Xia X-M, Clapham DE, Lingle CJ. Simultaneous knockout of *Slo3* and *CatSper1* abolishes all alkalization- and voltage-activated current in mouse spermatozoa. *J Gen Physiol*. 2013; 142: 305–313.
 297. De Toni L, Garolla A, Menegazzo M, Magagna S, Nisio A Di, Šabović I, et al. Heat sensing receptor TRPV1 is a mediator of thermotaxis in human spermatozoa. *PLoS One*. 2016; 11: e0167622.
 298. Hamano K-I, Kawanishi T, Mizuno A, Suzuki M, Takagi Y. Involvement of Transient Receptor Potential Vanilloid (TRPV) 4 in mouse sperm thermotaxis. *J Reprod Dev*. 2016; 62: 415-22.
 299. Whelan S, Goldman N. A general empirical model of protein evolution derived from multiple protein families using a maximum-likelihood approach. *Mol Biol Evol*. 2001; 18: 691-9.
 300. Sardar P, Kumar A, Bhandari A, Goswami C. Conservation of tubulin-binding sequences in TRPV1 throughout evolution. *PLoS One*. 2012;7:e31448.
 301. Majhi RK, Saha S, Kumar A, Swain N, Goswami L, Mohapatra PP, et al. Expression of temperature-sensitive ion channel TRPM8 in sperm cells correlates with vertebrate evolution. *PeerJ*. 2014; 3: e1310..
 302. P. B. Farrell, R. H. Foote, M. M. McArdle VLT-TAALT. Media and dilution procedures tested to minimize handling effects on human, rabbit, and bull sperm for computer-assisted sperm analysis (CASA). *J Androl*. 1996; 17: 293-300.
 303. Kathiravan P, Kalatharan J, Karthikeya G, Rengarajan K, Kadirvel G. Objective Sperm Motion Analysis to Assess Dairy Bull Fertility Using Computer-Aided System - A Review. *Reproduction in Domestic Animals*. 2011; 46: 165-72.
 304. Ickowicz D, Finkelstein M, Breitbart H. Mechanism of sperm capacitation and the acrosome reaction: role of protein kinases. *Asian J Androl*. 2012; 14: 816–821.
 305. Ahluwalia B, Farshori P, Jamuar M, Baccetti B, Anderson WA. Specific localization of lectins in boar and bull spermatozoa. *J Submicrosc Cytol Pathol*. 1990;22:53–62.
 306. Parrish JJ, Susko-Parrish JL, First NL. Effect of heparin and chondroitin sulfate on the acrosome reaction and fertility of bovine sperm in vitro. *Theriogenology*. 1985; 24: 537-49.
 307. Thérien I, Manjunath P. Effect of progesterone on bovine sperm capacitation and acrosome reaction. *Biol Reprod*. 2003; 69: 1408-15.
 308. Lehti MS, Sironen A. Formation and function of sperm tail structures in association with sperm motility defects. *Biology of Reproduction*. 2017; 97: 522–536.
 309. Parrish JJ, Susko-Parrish J, Winer MA, First NL. Capacitation of Bovine Sperm by Heparin1. *Biol*

- Reprod. 1988; 41: 683-99.
310. Calogero AE, Burrello N, Barone N, Palermo I, Grasso U, D'Agata R. Effects of progesterone on sperm function: Mechanisms of action. *Human Reproduction*. 2000; 15: 28-45.
 311. Hill K, Schaefer M. TRPA1 is differentially modulated by the amphipathic molecules trinitrophenol and chlorpromazine. *J Biol Chem*. 2007; 282: 7145-53.
 312. Startek JB, Talavera K, Voets T, Alpizar YA. Differential interactions of bacterial lipopolysaccharides with lipid membranes: implications for TRPA1-mediated chemosensation. *Sci Rep*. 2018;8: 1-11.
 313. Green DP, Ruparel S, Gao X, Ruparel N, Patil M, Akopian A, et al. Central activation of TRPV1 and TRPA1 by novel endogenous agonists contributes to mechanical and thermal allodynia after burn injury. *Mol Pain*. 2016 Jul 1;12:1-9.
 314. Franciolini A, Petris. Evolution of ionic channels of biological membranes. *Molecular Biology and Evolution*. 1989; 6:503–513.
 315. Pohorille A, Schweighofer K, Wilson MA. The origin and early evolution of membrane channels. *Astrobiology*. 2005; 5:1-17.
 316. Brehm P, Okamura Y, Mandel G. Ion channel evolution. *Semin Neurosci*. 1991;3:355–67.
 317. Saito S, Tominaga M. Evolutionary tuning of TRPA1 and TRPV1 thermal and chemical sensitivity in vertebrates. *Temperature*. 2017; 4: 141-152.
 318. Bandell M, Macpherson LJ, Patapoutian A. From chills to chilis: mechanisms for thermosensation and chemesthesis via thermoTRPs. *Current Opinion in Neurobiology*. 2007; 17: 490-7.
 319. Liedtke WB, Heller S. TRP Ion Channel Function in Sensory Transduction and Cellular Signaling Cascades. *TRP Ion Channel Function in Sensory Transduction and Cellular Signaling Cascades*. CRC Press/Taylor & Francis; 2007.
 320. Patapoutian A, Peier AM, Story GM, Viswanath V. Thermotrp channels and beyond: Mechanisms of temperature sensation. *Nat Rev Neurosci*. 2003;4:529–39.
 321. Saito S, Shingai R. Evolution of thermoTRP ion channel homologs in vertebrates. *Physiol Genomics*. 2006; 27: 219-30.
 322. Saito S, Tominaga M. Functional diversity and evolutionary dynamics of thermoTRP channels. *Cell Calcium*. 2015; 57: 214-21.
 323. Ohkita M, Saito S, Imagawa T, Takahashi K, Tominaga M, Ohta T. Molecular cloning and functional characterization of *Xenopus tropicalis* frog transient receptor potential vanilloid 1 reveal its functional evolution for heat, acid, and capsaicin sensitivities in terrestrial vertebrates. *J Biol Chem*. 2012; 287: 2388–97.
 324. Saito S, Ohkita M, Saito CT, Takahashi K, Tominaga M, Ohta T. Evolution of heat sensors drove shifts in thermosensation between *Xenopus* species adapted to different thermal niches. *J Biol Chem*. 2016; 291: 11446-59.
 325. Jara-Oseguera A, Huffer KE, Swartz KJ. The ion selectivity filter is not an activation gate in TRPV1-3 channels. *Elife*. 2019;8:1-27.
 326. Sánchez-Moreno A, Guevara-Hernández E, Contreras-Cervera R, Rangel-Yescas G, Ladrón-De-Guevara E, Rosenbaum T, et al. Irreversible temperature gating in *trpv1* sheds light on channel

- activation. *Elife*. 2018;7:1-11.
327. Zubcevic L, Lee SY. The role of π -helices in TRP channel gating. *Current Opinion in Structural Biology*. 2019; 58: 314-323.
 328. Mouritsen OG, Zuckermann MJ. What's so special about cholesterol? In: *Lipids*. 2004; 39: 1101-1113.
 329. Alonso MA, Millán J. The role of lipid rafts in signalling and membrane trafficking in T lymphocytes. *Journal of Cell Science*. 2001; 114: 3957-3965.
 330. Head BP, Patel HH, Insel PA. Interaction of membrane/lipid rafts with the cytoskeleton: Impact on signaling and function: Membrane/lipid rafts, mediators of cytoskeletal arrangement and cell signaling., *Biochimica et Biophysica Acta - Biomembranes*. Elsevier B.V. 2014; 1838: 532-545.
 331. Martinac B. The ion channels to cytoskeleton connection as potential mechanism of mechanosensitivity. *Biochimica et Biophysica Acta - Biomembranes*. 2014; 1838: 682-691.
 332. Chalfie M. Neurosensory mechanotransduction. *Nature Reviews Molecular Cell Biology*. 2009; 10: 44-52.
 333. Kelkar DA, Chattopadhyay A. Membrane interfacial localization of aromatic amino acids and membrane protein function. *Journal of Biosciences*. 2006; 31: 297-302.
 334. Simons K, Gerl MJ. Revitalizing membrane rafts: New tools and insights. *Nature Reviews Molecular Cell Biology*. 2010; 11: 688-99.
 335. Op den Kamp JAF. Lipid Asymmetry in Membranes. *Annu Rev Biochem*. 1979; 48: 47-71.
 336. Bergelson LD, Barsukov LI. Topological asymmetry of phospholipids in membranes. *Science*. 1977; 197: 224-30.
 337. Bretscher MS. Asymmetrical lipid bilayer structure for biological membranes. *Nat New Biol*. 1972; 236: 11-12.
 338. Nagle JF, Tristram-Nagle S. Structure of lipid bilayers. *Biochimica et Biophysica Acta - Reviews on Biomembranes*. 2000; 1469: 159-95.
 339. Tieleman DP, Marrink SJ, Berendsen HJC. A computer perspective of membranes: Molecular dynamics studies of lipid bilayer systems. *Biochimica et Biophysica Acta - Reviews on Biomembranes*. 1997; 1331: 235-70.
 340. Nagle JF. Lipid bilayer phase transition: density measurements and theory. *Proc Natl Acad Sci U S A*. 1973; 70: 3443-3444.
 341. Gawrisch K, Barry JA, Holte LL, Sinnwell T, Bergelson LD, Ferretti JA. Role of interactions at the lipid-water interface for domain formation. *Mol Membr Biol*. 1995; 12: 83-8.
 342. Kiessling V, Wan C, Tamm LK. Domain coupling in asymmetric lipid bilayers. *Biochimica et Biophysica Acta - Biomembranes*. 2009; 1788: 64-71.
 343. Needham D, Nunn RS. Elastic deformation and failure of lipid bilayer membranes containing cholesterol. *Biophys J*. 1990; 58: 997-1009.
 344. Seddon JM, Templer RH. Polymorphism of lipid-water systems. In: *Handbook of Biological Physics*. North-Holland; 1995; 1:97-160.
 345. Phillips R, Ursell T, Wiggins P, Sens P. Emerging roles for lipids in shaping membrane-protein function. *Nature*. 2009; 459: 379-85.

346. Bachur NR, Masek K, Melmon KL, Udenfriend S. Fatty acid amides of ethanolamine in mammalian tissues. *J Biol Chem.* 1965; 240: 1019-24.
347. Vance JE. Phospholipid Synthesis and Transport in Mammalian Cells. *Traffic.* 2015; 16: 1-18.
348. van der Veen JN, Kennelly JP, Wan S, Vance JE, Vance DE, Jacobs RL. The critical role of phosphatidylcholine and phosphatidylethanolamine metabolism in health and disease. *Biochimica et Biophysica Acta - Biomembranes.* 2017; 1859: 1558-1572.
349. Exton JH. Signaling through phosphatidylcholine breakdown. *Journal of Biological Chemistry.* 1990;265:1-4.
350. Fagone P, Jackowski S. Phosphatidylcholine and the CDP-choline cycle. *Biochimica et Biophysica Acta - Molecular and Cell Biology of Lipids.* 2013;1831: 523-532.
351. Vance JE. Phosphatidylserine and phosphatidylethanolamine in mammalian cells: Two metabolically related aminophospholipids. *Journal of Lipid Research.* 2008; 49:1377-87.
352. Li Z, Vance DE. Phosphatidylcholine and choline homeostasis. *Journal of Lipid Research.* 2008; 49:1187-94.
353. Lenzi A, Picardo M, Gandini L, Dondero F. Lipids of the sperm plasma membrane: From polyunsaturated fatty acids considered as markers of sperm function to possible scavenger therapy. *Human Reproduction Update.* 1996; 2:246-56.
354. Chamberlain AK, Bowie JU. Asymmetric amino acid compositions of transmembrane β -strands. *Protein Sci.* 2004; 13: 2270-4.
355. Wu Z, Cui Q, Yethiraj A. Why Do Arginine and Lysine Organize Lipids Differently? Insights from Coarse-Grained and Atomistic Simulations. *J Phys Chem B.* 2013;117:12145–56.
356. Li L, Vorobyov I, Allen TW. The different interactions of lysine and arginine side chains with lipid membranes. *J Phys Chem B.* 2013; 117: 11906-20.
357. Li B, Vorobyov I, MacKerell AD, Allen TW. Is arginine charged in a membrane? *Biophys J.* 2008; 94:L11-3.
358. Kim C, Schmidt T, Cho EG, Ye F, Ulmer TS, Ginsberg MH. Basic amino-acid side chains regulate transmembrane integrin signalling. *Nature.* 2012; 481: 209-13.
359. Green ME. Consequences of phosphate-arginine complexes in voltage-gated ion channels. *Channels.* 2008; 2: 395-400.
360. Gebhardt M, Henkes LM, Tayefeh S, Hertel B, Greiner T, Van Etten JL, et al. Relevance of lysine snorkeling in the outer transmembrane domain of small viral potassium ion channels. *Biochemistry.* 2012; 51: 5571-9.
361. Pfrieger FW. Role of cholesterol in synapse formation and function. *Biochimica et Biophysica Acta - Biomembranes.* 2003; 1610: 271-80.
362. Wood WG, Igbavboa U, Müller WE, Eckert GP. Cholesterol asymmetry in synaptic plasma membranes. *Journal of Neurochemistry.* 2011; 116: 684-9.
363. Pfrieger FW, Ungerer N. Cholesterol metabolism in neurons and astrocytes. *Progress in Lipid Research.* 2011; 50: 357-71.
364. Orth M, Bellosta S. Cholesterol: Its regulation and role in central nervous system disorders. *Cholesterol.* 2012; 2012: 1-20.

365. Brauchi S, Orta G, Mascayano C, Salazar M, Raddatz N, Urbina H, et al. Dissection of the components for PIP2 activation and thermosensation in TRP channels. *Proc Natl Acad Sci U S A*. 2007; 104: 10246-10251.
366. Schroeder F, Nemezc G, Gibson Wood W, Joiner C, Morrot G, Ayrault-Jarrier M, et al. Transmembrane distribution of sterol in the human erythrocyte. *BBA - Biomembr*. 1991; 1066: 183-192.
367. Devaux PF, Morris R. Transmembrane asymmetry and lateral domains in biological membranes. *Traffic*. 2004; 5: 241-246.
368. Edidin M. The state of lipid rafts: From model membranes to cells. *Annual Review of Biophysics and Biomolecular Structure*. 2003; 32: 257-283.
369. Wood WG, Schroeder F, Avdulov NA, Chochina S V., Igbavboa U. Recent advances in brain cholesterol dynamics: Transport, domains, and Alzheimer's disease. *Lipids*. 1999; 34: 225-234.
370. Pucadyil TJ, Chattopadhyay A. Role of cholesterol in the function and organization of G-protein coupled receptors. *Progress in Lipid Research*. 2006; 45: 295-333.
371. Prasanna X, Chattopadhyay A, Sengupta D. Cholesterol modulates the dimer interface of the β 2-adrenergic receptor via cholesterol occupancy sites. *Biophys J*. 2014; 106: 1290-1300.
372. Fantini J, Barrantes FJ. How cholesterol interacts with membrane proteins: An exploration of cholesterol-binding sites including CRAC, CARC, and tilted domains. *Frontiers in Physiology*. 2013; 4: 1-9.
373. Baier CJ, Fantini J, Barrantes FJ. Disclosure of cholesterol recognition motifs in transmembrane domains of the human nicotinic acetylcholine receptor. *Sci Rep*. 2011; 1:1-7.
374. Yoo J, Cui Q. Chemical versus mechanical perturbations on the protonation state of Arginine in complex lipid membranes: Insights from microscopic pKa calculations. *Biophys J*. 2010; 99: 1529-1538.
375. Crockett EL. Cholesterol function in plasma membranes from ectotherms: membrane-specific roles in adaptation to temperature. *American Zoologist*. 1998; 38: 291-304.
376. Botto L, Bernabò N, Palestini P, Barboni B. Bicarbonate induces membrane reorganization and CBR1 and TRPV1 endocannabinoid receptor migration in lipid microdomains in capacitating boar spermatozoa. *J Membr Biol*. 2010; 238: 33-41.
377. Petrov AM, Yakovleva AA, Zefirov AL. Role of membrane cholesterol in spontaneous exocytosis at frog neuromuscular synapses: Reactive oxygen species-calcium interplay. *J Physiol*. 2014; 592: 4995-5009.
378. Petrov AM, Kasimov MR, Giniatullin AR, Zefirov AL. Effects of Oxidation of Membrane Cholesterol on the Vesicle Cycle in Motor Nerve Terminals in the Frog *Rana Ridibunda*. *Neurosci Behav Physiol*. 2014; 44: 1020-1030.
379. Klein AH, Joe CL, Davoodi A, Takechi K, Carstens MI, Carstens E. Eugenol and carvacrol excite first- and second-order trigeminal neurons and enhance their heat-evoked responses. *Neuroscience*. 2014; 271: 45-55.
380. Nilius B, Flockerzi V. Mammalian transient receptor potential (TRP) cation channels. Preface. *Handbook of experimental pharmacology*. 2014;1.

381. Winter Z, Buhala A, Ötvös F, Jósvay K, Vizler C, Dombi G, et al. Functionally important amino acid residues in the transient receptor potential vanilloid 1 (TRPV1) ion channel - an overview of the current mutational data. *Molecular Pain*. 2013; 9: 1-29.
382. Boukalova S, Marsakova L, Teisinger J, Vlachova V. Conserved residues within the putative S4-S5 region serve distinct functions among thermosensitive vanilloid transient receptor potential (TRPV) channels. *J Biol Chem*. 2010; 285: 41455-41462.
383. Vetter I, Cheng W, Peiris M, Wyse BD, Roberts-Thomson SJ, Zheng J, et al. Rapid, opioid-sensitive mechanisms involved in transient receptor potential vanilloid 1 sensitization. *J Biol Chem*. 2008; 283: 19540-19550.
384. King JL, Jukes TH. Non-Darwinian evolution. *Science*. 1969;164: 788-798.
385. Caputo GA, London E. Cumulative effects of amino acid substitutions and hydrophobic mismatch upon the transmembrane stability and conformation of hydrophobic α -helices. *Biochemistry*. 2003; 42: 3275-3285.
386. Ulmschneider MB, Sansom MSP. Amino acid distributions in integral membrane protein structures. *Biochim Biophys Acta - Biomembr*. 2001; 1512: 1-4.
387. Studer M, McNaughton PA. Modulation of single-channel properties of TRPV1 by phosphorylation. *J Physiol*. 2010; 588: 3743-3756.
388. Verma P, Kumar A, Goswami C. TRPV4-mediated channelopathies. *Channels (Austin)*. 4:319–28.
389. Vyklický L, Nováková-Toušová K, Benedikt J, Samad A, Touška F, Vlachova V. Calcium-dependent desensitization of vanilloid receptor TRPV1: A mechanism possibly involved in analgesia induced by topical application of capsaicin. *Physiological Research*. 2008; 57: S59-S68.
390. Valentine ML, Cardenas AE, Elber R, Baiz CR. Physiological Calcium Concentrations Slow Dynamics at the Lipid-Water Interface. *Biophys J*. 2018; 115: 1541-1551.
391. Smyth JW, Shaw RM. Forward trafficking of ion channels: What the clinician needs to know. *Hear Rhythm*. 2010; 7: 1135-1140.
392. Binarová P, Tuszyński J. Tubulin: Structure, Functions and Roles in Disease. *Cells*. 2019;8: 1-7..
393. Carré M, André N, Carles G, Borghi H, Bricchese L, Briand C, et al. Tubulin is an inherent component of mitochondrial membranes that interacts with the voltage-dependent anion channel. *J Biol Chem*. 2002; 277: 33664-33669.
394. Blanco C, Morales D, Mogollones I, Vergara-Jaque A, Vargas C, Álvarez A, et al. EB1- and EB2-dependent anterograde trafficking of TRPM4 regulates focal adhesion turnover and cell invasion. *FASEB J*. 2019; 33: 9434-9452.
395. Yan C, Wang F, Peng Y, Williams CR, Jenkins B, Wildonger J, et al. Microtubule Acetylation Is Required for Mechanosensation in *Drosophila*. *Cell Rep*. 2018; 25: 1051-1065.
396. Montalbetti N, Li Q, Wu Y, Chen XZ, Cantiello HF. Polycystin-2 cation channel function in the human syncytiotrophoblast is regulated by microtubular structures. *J Physiol*. 2007; 579: 717-728.
397. Kamath K, Wilson L, Cabral F, Jordan MA. β III-tubulin induces paclitaxel resistance in association with reduced effects on microtubule dynamic instability. *J Biol Chem*. 2005; 280: 12902-12907.
398. Włoga D, Joachimiak E, Fabczak H. Tubulin post-translational modifications and microtubule dynamics. *International Journal of Molecular Sciences*. 2017; 18: 1-18.

399. Sheriff O, Lim LF, He CY. Tracking the biogenesis and inheritance of subpellicular microtubule in *trypanosoma brucei* with inducible YFP- α -tubulin. *Biomed Res Int.* 2014;2014:1-13.
400. Anderson M, Zheng Q, Dong X. Investigation of Pain Mechanisms by Calcium Imaging Approaches. *Neuroscience Bulletin.* 2018; 34: 194-199.
401. Yu HB, Li M, Wang WP, Wang XL. High throughput screening technologies for ion channels. *Acta Pharmacologica Sinica.* 2016; 37: 34-43.
402. Yuen EY, Jiang Q, Feng J, Yan Z. Microtubule regulation of N-Methyl-D-aspartate receptor channels in neurons. *J Biol Chem.* 2005; 280: 29420-29427.
403. Luccardini C, Casagrande S, Cupello A, Pellistri F, Ramoino P, Robello M. The combined disruption of microfilaments and microtubules affects the distribution and function of GABAA receptors in rat cerebellum granule cells in culture. *Neurosci Lett.* 2004; 359: 25-28.
404. Lindman J, Khammy MM, Lundegaard PR, Aalkjær C, Jepps TA. Microtubule Regulation of Kv7 Channels Orchestrates cAMP-Mediated Vasorelaxations in Rat Arterial Smooth Muscle. *Hypertension.* 2018; 71: 336-345.
405. Majhi RK, Sahoo SS, Yadav M, Pratheek BM, Chattopadhyay S, Goswami C. Functional expression of TRPV channels in T cells and their implications in immune regulation. *FEBS J.* 2015; 282: 2661-2681.
406. Majhi RK, Kumar A, Yadav M, Swain N, Kumari S, Saha A, et al. Thermosensitive ion channel TRPV1 is endogenously expressed in the sperm of a fresh water teleost fish (*Labeo rohita*) and regulates sperm motility. *Channels.* 2013; 7: 483-492.
407. Kumar A, Majhi RK, Swain N, Giri SC, Kar S, Samanta L, et al. TRPV4 is endogenously expressed in vertebrate spermatozoa and regulates intracellular calcium in human sperm. *Biochem Biophys Res Commun.* 2016; 473: 781-788.
408. Rapoport TA, Goder V, Heinrich SU, Matlack KES. Membrane-protein integration and the role of the translocation channel. *Trends in Cell Biology.* 2004; 14: 568-575.
409. Ng CL, Oresic K, Tortorella D. TRAM1 is involved in disposal of ER membrane degradation substrates. *Exp Cell Res.* 2010; 316: 2113-2122.
410. Levy S, Allerston CK, Liveanu V, Habib MR, Gileadi O, Schuster G. Identification of LACTB2, a metallo- β -lactamase protein, as a human mitochondrial endoribonuclease. *Nucleic Acids Res.* 2016; 44: 1813-1832.
411. Hegde RS, Voigt S, Lingappa VR. Regulation of protein topology by trans-acting factors at the endoplasmic reticulum. *Mol Cell.* 1998; 2: 85-91.
412. Bonini NM, Leiserson WM, Benzer S. The eyes absent gene: genetic control of cell survival and differentiation in the developing *Drosophila* eye. *Cell.* 1993; 72: 379-395.
413. Landgraf K, Bollig F, Trowe M-O, Besenbeck B, Ebert C, Kruspe D, et al. Sipl1 and Rbck1 Are Novel Eya1-Binding Proteins with a Role in Craniofacial Development. *Mol Cell Biol.* 2010; 30: 5764-5775.
414. Zou D, Erickson C, Kim EH, Jin D, Fritsch B, Xu PX. Eya1 gene dosage critically affects the development of sensory epithelia in the mammalian inner ear. *Hum Mol Genet.* 2008; 17: 3340-3356.

415. Robb L, Hartley L, Wang CC, Harvey RP, Begley CG. musculin: a murine basic helix-loop-helix transcription factor gene expressed in embryonic skeletal muscle. *Mech Dev.* 1998;76:197–201.
416. Wu C, Chen Z, Dardalhon V, Xiao S, Thalhamer T, Liao M, et al. The transcription factor musculin promotes the unidirectional development of peripheral Treg cells by suppressing the TH2 transcriptional program. *Nat Immunol.* 2017; 18:344-353.
417. Cevikbas F, Wang X, Akiyama T, Kempkes C, Savinko T, Antal A, et al. A sensory neuron-expressed IL-31 receptor mediates T helper cell-dependent itch: Involvement of TRPV1 and TRPA1. *J Allergy Clin Immunol.* 2014; 133: 448-460.
418. Schmalz F, Kinsella J, Koh SD, Vogalis F, Schneider A, Flynn ER, et al. Molecular identification of a component of delayed rectifier current in gastrointestinal smooth muscles. *Am J Physiol.* 1998; 274: G901-911.
419. MALYSZ J, FARRUGIA G, OU Y, SZURSZIEWSKI JH, NEHRA A, GIBBONS SJ. The Kv2.2 α Subunit Contributes to Delayed Rectifier K⁺ Currents in Myocytes From Rabbit Corpus Cavernosum. *J Androl.* 2002;23:899–910.
420. Juang MJ, Lu TP, Lai LC, Ho CC, Liu Y Bin, Tsai CT, et al. Disease-targeted sequencing of ion channel genes identifies de novo mutations in patients with non-familial Brugada syndrome. *Sci Rep.* 2014;4: 1-7.
421. Hartmann N, Scherthan H. Characterization of the telomere complex, TERF1 and TERF2 genes in muntjac species with fusion karyotypes. *Exp Cell Res.* 2005; 306: 64-74.
422. Hadjiolov A. The Nucleolus and Ribosome Biogenesis. *Cell Biology Monographs.* 1985.
423. Neumann F, Hemmerich P, Von Mikecz A, Peter H hatmut, Krawinkel U. Human ribosomal protein L7 inhibits cell-free translation in reticulocyte lysates and affects the expression of nuclear proteins upon stable transfection into jurkat T-lymphoma cells. *Nucleic Acids Res.* 1995; 23: 195-202.
424. Jansova D, Tetkova A, Koncicka M, Kubelka M, Susor A. Localization of RNA and translation in the mammalian oocyte and embryo. *PLoS One.* 2018;13: 1-25.
425. Wu BX, Chen Y, Chen Y, Fan J, Rohrer B, Crouch RK. Cloning and Characterization of a Novel all- trans from the RPE. *Invest Ophthalmol Vis Sci.* 2002; 43: 3365-3372.
426. Sandell LL, Sanderson BW, Moiseyev G, Johnson T, Mushegian A, Young K, et al. RDH10 is essential for synthesis of embryonic retinoic acid and is required for limb, craniofacial, and organ development. *Genes Dev.* 2007; 21: 1113-1124.
427. Banzawa N, Saito S, Imagawa T, Kashio M, Takahashi K, Tominaga M, et al. Molecular basis determining inhibition/activation of nociceptive receptor TRPA1 protein: A single amino acid dictates species-specific actions of the most potent mammalian TRPA1 antagonist. *J Biol Chem.* 2014;289:31927–39.
428. Chen J, Kang D, Xu J, Lake M, Hogan JO, Sun C, et al. Species differences and molecular determinant of TRPA1 cold sensitivity. *Nat Commun.* 2013; 4: 1-7.
429. Sinica V, Zimova L, Barvikova K, Macikova L, Barvik I, Vlachova V. Human and Mouse TRPA1 Are Heat and Cold Sensors Differentially Tuned by Voltage. *Cells.* 2019;9:1-24.
430. Chowdhury S, Jarecki BW, Chanda B. A molecular framework for temperature-dependent gating of ion channels. *Cell.* 2014; 158: 1148-1158.

431. Zimova L, Sinica V, Kadkova A, Vyklicka L, Zima V, Barvik I, et al. Intracellular cavity of sensor domain controls allosteric gating of TRPA1 channel. *Sci Signal*. 2018;11: 1-13.
432. Marsakova L, Barvik I, Zima V, Zimova L, Vlachova V. The first extracellular linker is important for several aspects of the gating mechanism of human TRPA1 channel. *Front Mol Neurosci*. 2017;10:1-19.
433. Bravo MM, Aparicio IM, Garcia-Herreros M, Gil MC, Peña FJ, Garcia-Marin LJ. Changes in tyrosine phosphorylation associated with true capacitation and capacitation-like state in boar spermatozoa. *Mol Reprod Dev*. 2005; 71: 88-96.
434. Sperry AO. The dynamic cytoskeleton of the developing male germ cell. *Biol Cell*. 2012;104:297–305.
435. Corkidi G, Montoya F, Hernández-Herrera P, Ríos-Herrera WA, Müller MF, Treviño CL, et al. Are there intracellular Ca²⁺ oscillations correlated with flagellar beating in human sperm? A three vs. two-dimensional analysis. *Mol Hum Reprod*. 2017; 23: 583-593.
436. Arenas OM, Zaharieva EE, Para A, Vásquez-Doorman C, Petersen CP, Gallio M. Activation of planarian TRPA1 by reactive oxygen species reveals a conserved mechanism for animal nociception. *Nat Neurosci*. 2017; 20: 1686-1693.
437. Kremeyer B, Lopera F, Cox JJ, Momin A, Rugiero F, Marsh S, et al. A Gain-of-Function Mutation in TRPA1 Causes Familial Episodic Pain Syndrome. *Neuron*. 2010;66:671–80.
438. Zíma V, Witschas K, Hynkova A, Zímová L, Barvík I, Vlachova V. Structural modeling and patch-clamp analysis of pain-related mutation TRPA1-N855S reveal inter-subunit salt bridges stabilizing the channel open state. *Neuropharmacology*. 2015; 93: 294-307.
439. Laemmli UK. Cleavage of structural proteins during the assembly of the head of bacteriophage T4. *Nature*. 1970;227:680–5.
440. Bradford MM. A rapid and sensitive method for the quantitation of microgram quantities of protein utilizing the principle of protein-dye binding. *Anal Biochem*. 1976;72:248–54.
441. Shelanski ML, Gaskin F, Cantor CR. Microtubule assembly in the absence of added nucleotides. *Proc Natl Acad Sci U S A*. 1973;70:765–8.
442. Smith AJ, Sugita S, Charlton MP. Cholesterol-dependent kinase activity regulates transmitter release from cerebellar synapses. *J Neurosci*. 2010; 30: 6116-6121.
443. Day CA, Kenworthy AK. Functions of cholera toxin B-subunit as a raft cross-linker. *Essays Biochem*. 2015; 57: 135-145
444. Wheeler DL, Barrett T, Benson DA, Bryant SH, Canese K, Chetvernin V, et al. Database resources of the National Center for Biotechnology Information. *Nucleic Acids Res*. 2006; 34: D173-D180.
445. Wheeler DL, Barrett T, Benson DA, Bryant SH, Canese K, Chetvernin V, et al. Database resources of the National Center for Biotechnology Information. *Nucleic Acids Res*. 2007; 36: D13-D21.
446. Edgar RC. MUSCLE: A multiple sequence alignment method with reduced time and space complexity. *BMC Bioinformatics*. 2004; 5: 1-19.
447. Edgar RC. MUSCLE: Multiple sequence alignment with high accuracy and high throughput. *Nucleic Acids Res*. 2004; 32: 1792-1797.
448. Omasits U, Ahrens CH, Müller S, Wollscheid B. Protter: Interactive protein feature visualization

- and integration with experimental proteomic data. *Bioinformatics*. 2014;30:884–6.
449. Schneider TD, Stephens RM. Sequence logos: A new way to display consensus sequences. *Nucleic Acids Res*. 1990;18:6097–100.
 450. Crooks G, Hon G, Chandonia J, Brenner S. NCBI GenBank FTP Site\nWebLogo: a sequence logo generator. *Genome Res*. 2004;14:1188–90.
 451. Tamura K, Peterson D, Peterson N, Stecher G, Nei M, Kumar S. MEGA5: Molecular evolutionary genetics analysis using maximum likelihood, evolutionary distance, and maximum parsimony methods. *Mol Biol Evol*. 2011; 28: 2731-2739.
 452. De Vries M, Herrmann A, Veit M. A cholesterol consensus motif is required for efficient intracellular transport and raft association of a group 2 HA from influenza virus. *Biochem J*. 2015; 465:305-14.
 453. Trott O, Olson AJ. Software news and update AutoDock Vina: Improving the speed and accuracy of docking with a new scoring function, efficient optimization, and multithreading. *J Comput Chem*. 2010;31:455–61.
 454. Konagurthu AS, Whisstock JC, Stuckey PJ, Lesk AM. MUSTANG: A multiple structural alignment algorithm. *Proteins Struct Funct Genet*. 2006;64:559–74.
 455. Dunbrack RL, Cohen FE. Bayesian statistical analysis of protein side-chain rotamer preferences. *Protein Sci*. 1997;6:1661–81.
 456. Jones DT, Taylor WR, Thornton JM. The rapid generation of mutation data matrices from protein sequences. *Bioinformatics*. 1992; 8: 275-282.

Annexure

Annexure 1. List of TRPV1 sequences used:

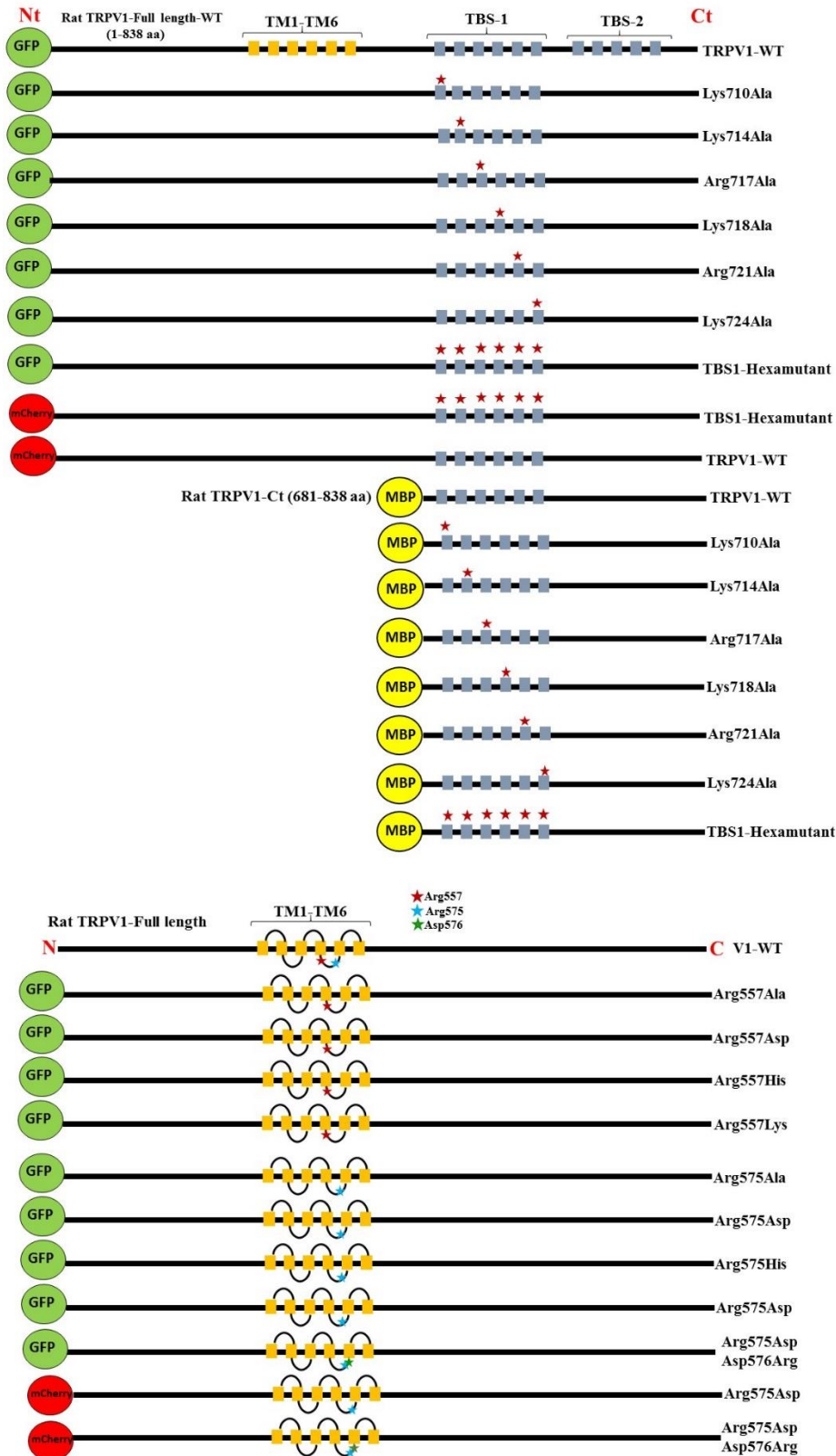
Species	Accession no.	Length(aa)
Human	NP_542437.2	839
Rat	NP_114188.1	838
Mouse	NP_001001445.1	839
Dog	NP_001003970.1	840
Western clawed frog	NP_001243521.1	840
Domestic guinea pig	NP_001166123.1	839
White-tufted-ear marmoset	JAB43279.1	839
Crab-eating macaque	XP_005582574.1	839
Golden snub-nosed monkey	XP_010380508.1	839
Minke whale	XP_007177510.1	837
Polar bear	XP_008693474.1	841
Golden hamster	XP_005067483.1	840
Prairie vole	XP_005349658.1	842
Thirteen-lined ground squirrel	XP_005337354.1	840
Mouse-eared bats	XP_006761554.1	840
Northern white-cheeked gibbon	XP_003277885.1	839
Bolivian squirrel monkey	XP_010341958.1	839
Lesser Egyptian jerboa	XP_004672443.1	838
Ostrich	XP_009671260.1	843
Green anole	XP_003230583.2	839
Goat	XP_005693465.1	843
Chiru	XP_005975783.1	843
Killer whale	XP_004267082.1	837
Yangtze River dolphin	XP_007454246.1	837
Wild Bactrian camel	XP_006172598.1	838
Alpaca	XP_006213403.1	838
Domestic cat	XP_003996439.1	841
Amur tiger	XP_007076214.1	841
Pacific walrus	XP_004412178.1	841
Southern white rhinoceros	XP_004433330.1	841
Philippine tarsier	XP_008058943.1	840
Small-eared galago	XP_003799103.1	840
Naked mole-rat	NP_001266788.1	840
Chinese hamster	XP_007615297.1	840
Prairie deer mouse	XP_006992283.1	840
Star-nosed mole	XP_004684824.1	841
Big brown bat	XP_008154990.1	840
Black flying fox	XP_006922257.1	840
African savanna elephant	XP_003417052.1	840
Cape golden mole	XP_006863326.1	837
Chicken	NP_989903.1	843
Northern fulmar	XP_009577944.1	844

Collared flycatcher	XP_005056751.1	840
Cuckoo roller	XP_009948710.1	844
African clawed frog	NP_001177322.1	838
White-throated tinamou	XP_010223284.1	841
Tibetan ground-tit	XP_005525785.1	844
Western diamondback rattlesnake	ADD82931.1	822
Elephant shark	XP_007894726.1	847
Western painted turtle	XP_005298235.1	843

Annexure 2. List of TRPA1 sequences used:

Name of species	Protein ID	Length of amino acid
Human	ENSP00000262209	1119
Chimpanzee	XP_519806.2	1119
Orangutan	XP_002819221.1	1119
Monkey	XP_001083172.1	1119
Common marmoset	XP_002759054.1	1119
Vampire bat	AEL30803.1	1116
Silky short tailed bat	AEL30802.1	1116
Mouse eared bat	ELK27489.1	1251
Wild pig	XP_001926150.1	1120
Dog	XP_544123.2	1118
Panda	NSAMEP00000006318	1120
Rabbit	ENSOCUP00000019628	1122
Guinea pig	NP_001185699.1	1111
Mouse	NP_808449.1	1125
Rat	NP_997491.1	1125
Tasmanian devil	ENSSHAP00000000587	1122
Opossum	ENSMODP00000008943	1123
Turkey	ENSMGAP00000012117	1102
Chicken	BAO51998.1	1126
Anole lizard	BAM42681.1	1112
Python	ADD82928.1	1114
Amazon tree boa	ADD82932.1	1111
Western diamondback rattlesnake	ADD82930.1	1111
Xenopus	NP_001121434.1	1144
Zebrafish	NP_001007066.1	1115
Tilapia	ENSMGAP00000012118	1118
Stickleback	ENSMGAP00000012122	1129
Japanese oyster	EKC35184.1	1029
Drosophila	NP_648263.4	1296
Drosophila	ADG84994.1	1200
Drosophila	ADG84993.1	1193
Mosquito	KFB46925.1	1234
Mosquito	ACC86138.1	1248
Silkworm	BAO53211.1	1156
Cotton ballworm	AHV83756.1	1220
Zootermopsis	KDR08794.1	1145
Worm	A5HJZ7	1206
Chinese Liver fluke	GAA49883.1	1197

Annexure 3. Schematic representation of constructs prepared in this study:



Annexure 4. Enrichment of different snorkeling amino acids in Lipid Water

Interface region of other ion channels:

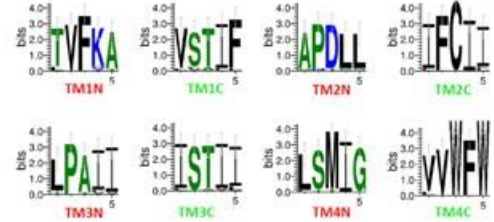
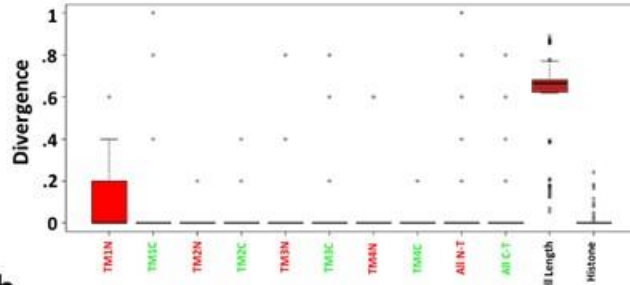
Mu		TRPV6		TRPV2		TREK1					
FL	LWI	FL	LWI	FL	LWI	FL	LWI				
Arg	4.75	7.142857	Arg	7.172413793	5	Arg	4.581151832	11.66667	Arg	4.225352113	0
Tyr	3.75	7.142857	Tyr	3.448275862	3.333333	Tyr	3.403141361	5	Tyr	2.34741784	0
Phe	5	1.428571	Phe	4.689655172	10	Phe	4.712041885	6.666667	Phe	5.868544601	10
Lys	3	4.285714	Lys	3.310344828	1.666667	Lys	4.057591623	3.333333	Lys	5.399061033	2.5
His	1.75	0	His	2.344827586	0	His	2.094240838	0	His	1.877934272	0
Ala	6.5	5.714286	Ala	6.896551724	5	Ala	6.806282723	5	Ala	7.981220657	7.5
Cys	4.25	2.857143	Cys	2.068965517	1.666667	Cys	2.094240838	0	Cys	1.17370892	2.5
Asp	3.75	2.857143	Asp	4.551724138	3.333333	Asp	4.319371728	3.333333	Asp	3.286384977	2.5
Glu	2.25	2.857143	Glu	5.793103448	3.333333	Glu	6.413612565	6.666667	Glu	5.633802817	0
Gly	3.75	4.285714	Gly	5.793103448	6.666667	Gly	6.67539267	1.666667	Gly	7.042253521	2.5
Ile	8.75	10	Ile	6.344827586	5	Ile	4.45026178	5	Ile	10.79812207	25
Leu	9.25	7.142857	Leu	13.37931034	15	Leu	14.65968586	18.33333	Leu	9.389671362	10
Met	3.5	4.285714	Met	4.137931034	1.666667	Met	2.094240838	5	Met	0.704225352	2.5
Asn	6	2.857143	Asn	3.310344828	3.333333	Asn	3.926701571	1.666667	Asn	3.286384977	0
Pro	5.75	7.142857	Pro	4.275862069	5	Pro	4.842931937	5	Pro	3.755868545	5
Gln	1.75	1.428571	Gln	4.689655172	3.333333	Gln	4.97382199	1.666667	Gln	3.051643192	0
Ser	8	2.857143	Ser	5.103448276	5	Ser	6.806282723	6.666667	Ser	7.042253521	7.5
Thr	9.25	11.42857	Thr	5.379310345	11.66667	Thr	4.45026178	1.666667	Thr	7.746478873	7.5
Val	7.25	10	Val	5.379310345	6.666667	Val	6.544502618	5	Val	7.511737089	10
Trp	1.75	4.285714	Trp	1.931034483	3.333333	Trp	2.094240838	6.666667	Trp	1.877934272	5
Total	400 AA	70 AA	Total	725 AA	60 AA	Total	764 AA	60 AA	Total	426 AA	40 AA

Annexure 5. Boxplot and sequence logo of lipid water interface region amino acids

present in different ion channels:

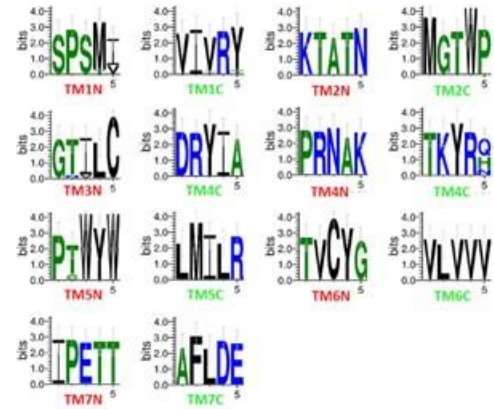
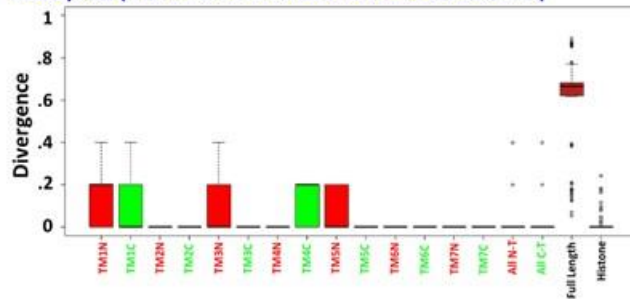
a.

TREK1 (Thermo sensitive multi-pass NON-TRP ion channel)



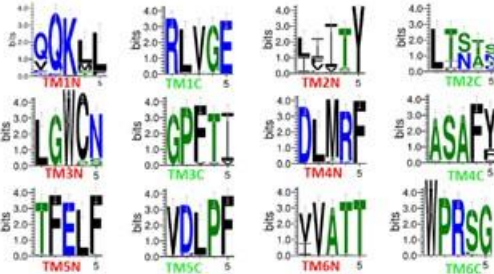
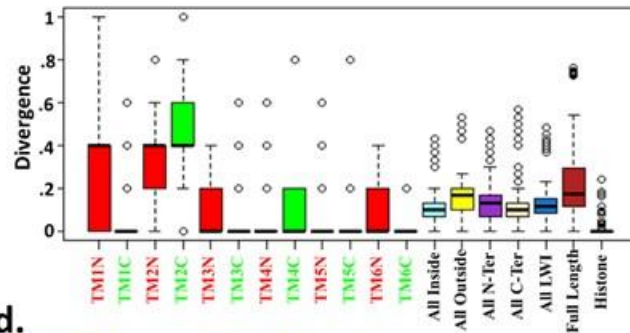
b.

Mu Opioid (Non Thermosensitive NON-TRP ion channel)



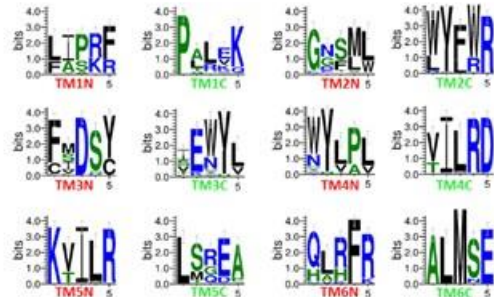
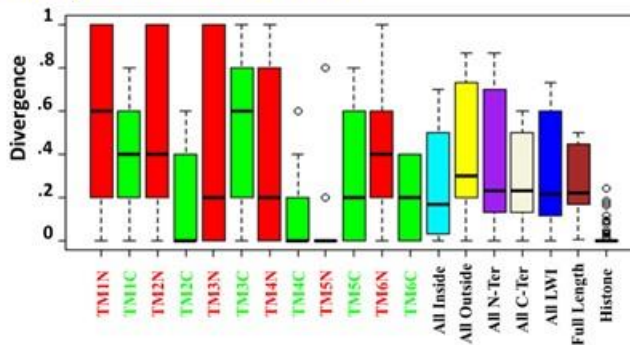
c.

TRPV6 (Non-Thermosensitive TRP channel)



d.

TRPV2 (Thermosensitive TRP Channel)



a. TREK1, example of thermosensitive multi-pass non-TRP ion channel. **b.** Mu Opioid receptor, example of non-thermosensitive non-TRP ion channel. **c.** TRPV6, example of non-thermosensitive TRP ion channel. **d.** TRPV2, example of thermosensitive TRP ion channel.